Mechanism and Function of Dendritic Self-Avoidance and Self/non-Self Discrimination in the Mammalian Nervous System

Mechanism and function of dendritic self-avoidance and self/non-self discrimination in the mammalian nervous system

A dissertation presented

by

Dimitar Vladimirov Kostadinov

to

The Division of Medical Sciences

in partial fulfillment of the requirements

for the degree of

Doctor of Philosophy

in the subject of

Neurobiology

Harvard University

Cambridge, Massachusetts

May, 2015

Dissertation Advisor: Professor Joshua R. Sanes Dimitar Vladimirov Kostadinov

Mechanism and function of dendritic self-avoidance and self/non-self discrimination in the mammalian nervous system

Abstract

Dendritic and axonal arbors of many neuronal types exhibit self-avoidance, a phenomenon in which branches repel each other. This process ensures that individual neurons cover all parts of their territory uniformly. Some neurons that self-avoid overlap with neighbors of the same type, suggesting that nominally identical neurons are immune to each other's repellent forces, a phenomenon called self/non-self discrimination. Here, I describe the roles of the 22 clustered gamma-Protocadherin (Pcdhg) recognition molecules in dendritic self-avoidance and self/non-self discrimination of mammalian neurons, and the roles of these phenomena in a retinal circuit.

First, I present studies showing that Pcdhgs are necessary for dendritic self-avoidance and self/non-self discrimination of retinal starburst amacrine cells (SACs) and cerebellar Purkinje cells. Using loss and gain of function experiments, we showed that no single Pcdhg isoform is necessary and any Pcdhg isoform is sufficient to mediate self-avoidance. However, forcing neighboring SACs to express a single Pcdhg decreases their overlap. Thus, Pcdhg diversity is necessary for SACs to avoid their own dendrites, but interact with their neighbors (self/non-self discrimination).

Second, I describe the roles of self-avoidance and self/non-self discrimination in the function of a retinal direction-selective circuit that depends on SACs. Dendrites of SACs compute directional motion and endow classes of retinal ganglion cells with this property by inhibiting them asymmetrically during visual motion. In addition, SACs form inhibitory synapses in order to sharpen each other's direction-selectivity. I present findings that elucidate the roles self-avoidance and self/non-self discrimination in the function of this direction-selective circuit: (1) In the absence of self-avoidance, SACs form synapses with

their own dendrites. (2) In the absence of self/non-self discrimination, SACs form few synapses with each other, (3) Loss of either self-avoidance or self/non-self discrimination degrades directional responses of ganglion cells.

Lastly, I describe initial efforts to understand the combinatorial roles of all clustered Pcdh family members, which also include 14 alpha- and 22 beta-Protocadherins (Pcdhas and Pcdhbs, respectively). We used CRISPR-mediated genome engineering to generate Pcdha/Pcdhg double mutants. Initial analysis shows that their defects are more striking than those of either Pcdha or Pcdhg mutants, suggesting redundancy between these two subclusters.

Acknowledgements

I must begin by thanking my parents, Vladimir Kostadinov and Guergana Kostadinova for their care and support. The choices that you have made in your lives have given me the opportunity to achieve what I have, and I hope to repay the favor someday. I would also like to thank alex for being a pretty awesome brother and the most loyal person in the world. I must also acknowledge my whole family for their love. We have rarely been in the same place, but we have always been together. Обичам ви!

Next, I must thank my wife, Megan Klarenbach, who has displayed more grace, patience, and acceptance throughout our relationship than I deserve. A future with you looks like a bright and exciting place, and I cannot wait to get there.

I must also give my most sincere thanks to the many people in the lab for their support and advice. First and foremost, I would like to thank Josh Sanes for his support and mentorship throughout my graduate career. Your intelligence and dedication have and will continue to inspire me to be the best scientist that I can be. You have given me every opportunity to succeed, and I will be forever grateful. Next, I would like to thank two others who have been instrumental in my successes over the past few years. First, I would like to thank my early mentor in the Sanes lab, Julie Lefebvre. Working with you was a great period of learning for me, and I will always be appreciative of your guidance. I would also like to thank Arjun Krishnaswamy. You have been both a great mentor and friend throughout the years, and I can truly say that meeting you was the luckiest thing that ever happened to me as a scientist but is less important to me than our friendship. I will always be indebted to you and your family for the generosity and support that you have shown me. I have had the privilege of working next to many great people in the Sanes lab: Jin, Jeremy, Greg, Xin, Masa, Brendan, Melanie, Dave, Sumeet, Yi-Rong, Mu, Tomek, Irene, Nick, Mariah, Daisy, Mallory, Jasmine, and others. You have made coming to work every day a real pleasure.

I would also like to thank my classmates: Stan, Tim, Anna, Allison, Dave, and the rest. I feel tremendously lucky to have gotten to be a part of such a wonderful group.

Finally, I would like to acknowledge the many great friends that are not already listed above. Mattye, Jake, Kevin, Eric, Kotaro, Shay, Laura, Evan, Max, Bobby, and others, you have been a great group to be around. I would also like to thank Sarah Parker, Caitlin Klarenbach, and Nick Falla for being so good to the people that are dearest to me.

While this list is long, I am sure it could be much longer. I am sorry to the people I have forgotten, but thank you anyway!

Dimitar

April, 2015

Table of Contents

List of Figures

List of Tables

Chapter 1: Introduction

Understanding the relationship between the structure and function of neural circuits is one of the fundamental problems in neuroscience. This relationship is important at all scales – from the arrangement of individual synaptic contacts to the projection patterns of the whole brain. The work presented in this thesis is focused on understanding this relationship at the level of the branches of individual neurons, focusing on dendrites. Individual neurons display tremendous variety in the shapes and sizes of their dendritic arborizations, and this variety in morphology is the most common, and perhaps easiest, way to classify groups of neurons into 'cell types' (**Figure 1.1**). Implicit in this assumption of cell types is the idea that neurons with a given dendritic geometry will have similar functions within neural circuits and systems.

The diversity of these morphologies has at least two broad implications for information processing. First, the location and density of dendritic arborizations determines the number, position, and types of synaptic connections that a neuron makes. Second, the electrical properties of dendrites, in combination with the location of synaptic connections, endow individual neurons with tremendous computational power. While dendrites have, historically, been treated as passive integrators of synaptic inputs, individual dendritic branches are likely to be the fundamental processing units of the nervous system (Branco and Hausser, 2010). Thus, morphological diversity across neuronal types allows each of these types to perform unique computational roles within neural circuits.

The adoption of particular morphologies is an active developmental process. Understanding the mechanisms that instruct the adoption of neuronal morphologies and the roles that these morphologies play in the function of neural circuits are the focus of my work. The approach that my colleagues and I have taken is to (1) target particular neuronal populations within a neural circuit genetically, (2) identify candidate mediators of aspects of their morphology and function, (3) use loss- and gain-of-function experiments to assess the structural and functional roles of these candidates in our cells of interest, and (4) assess how the adoption of particular morphologies relates to the function of neurons within a circuit.

Figure 1.1: The diversity of neuronal morphologies

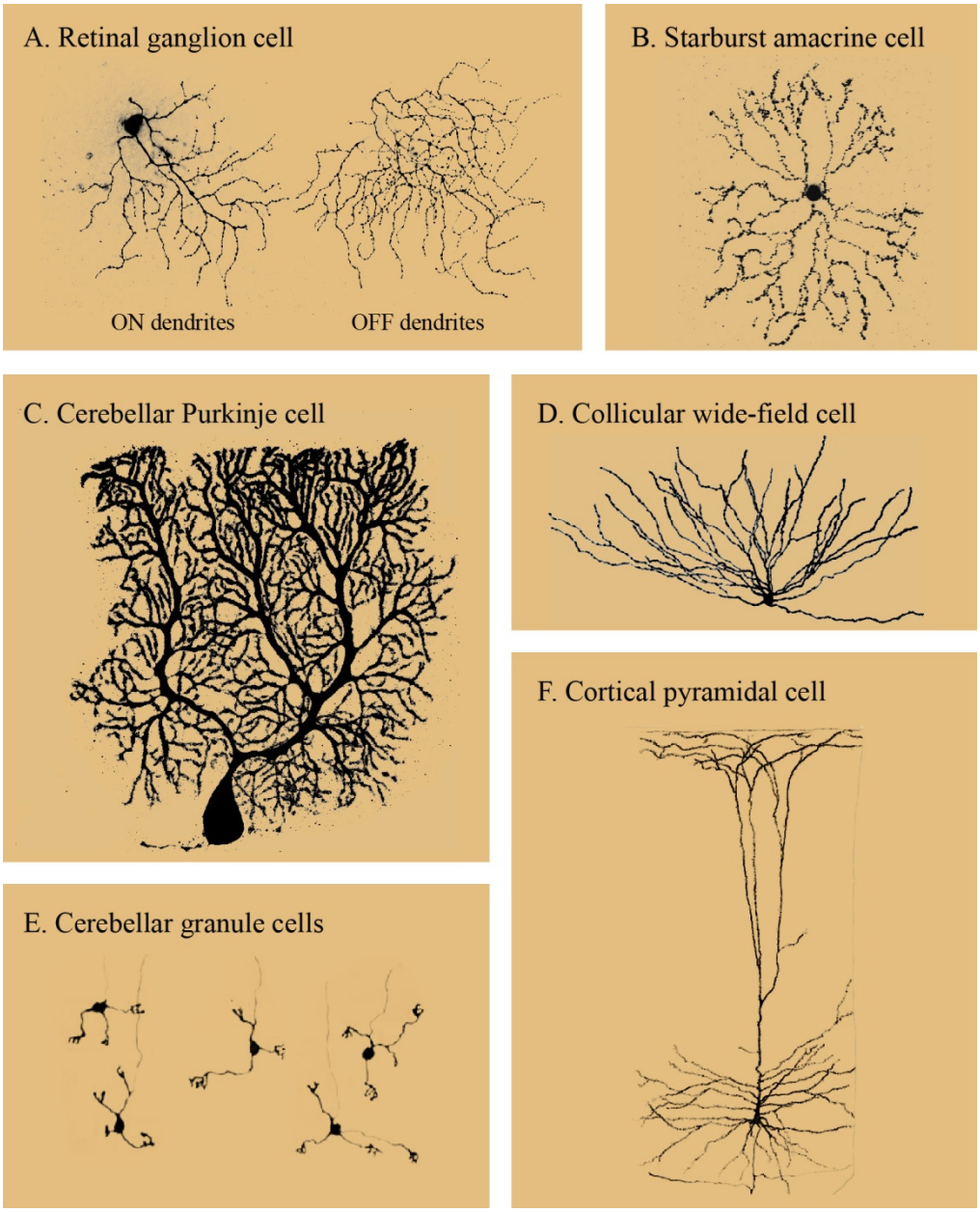

Image in panel D provided by 'Diamond' David L. Rousso. Images in E and F adapted from original drawings by Santiago Ramon y Cajal.

Specifically, my work focuses on the dendritic patterning and function of a retinal cell type called starburst amacrine cells (SACs). As their name implies, these retinal interneurons have a striking radial morphology, and this morphology is intimately related to their function – to detect directional motion. Individual SAC dendrites are direction-selective subunits that are activated by visual motion presented along their proximo-distal axis. SACs transmit this directional information to each other to direction-selective retinal ganglion cells (DSGCs), which in turn relay this information to the rest of the brain for further processing. Previous to the work I present here, several studies had documented the ability of SAC dendrites to detect directional motion, form connections with each other and DSGCs, and shown that the presence of these cells is necessary for directional motion detection (Euler et al., 2002; Fried et al., 2002; Lee and Zhou, 2006; Yoshida et al., 2001); however, little was known about how SACs adopt this particular morphology and what role this morphology plays in the synaptic connections they form with each other and with DSGCs. In collaboration with a Julie Lefebvre, I showed that SACs require a family of cellular recognition molecules, the clustered gamma-Protocadherins (Pcdhgs), to adopt their characteristic dendritic morphology. I then went on to elucidate the roles of this dendritic patterning in the function of the retinal direction-selective circuit. Finally, I have also begun to extend this work to study the combinatorial roles of gamma-Protocadherins and their relatives, the alpha-Protocadherins, in the nervous system.

In this chapter, I will introduce several concepts that are necessary to understand the motivation of this work. Specifically, I will discuss: (1) The retina as a system to study circuit development and function; (2) general mechanisms of dendritic development; (3) specific mechanisms of dendritic development, focusing on the phenomena of self-avoidance and self/non-self discrimination and parallels between invertebrate *Dscam1* and the clustered *Protocadherins*; and (4) the development and function of retina circuits, focusing on starburst amacrine cells and direction-selective circuitry.

1.1 Organization of the retina

The vertebrate retina is an excellent system for studies of functional circuit development due to its accessibility, pleasing regularity, segregation of cell bodies from neuropil, and generally known function. This brain structure contains five principal neuronal classes: photoreceptors (principal light detectors), retinal ganglion cells (RGCs; the projection neurons out of the retina), and 3 classes of interneurons (horizontal cells, bipolar cells, and amacrine cells). These general neuronal classes can be broken down into subclasses, so the true number of 'neuronal types' in the mammalian retina is more than 80. The somata of these cells are segregated into three nuclear layers, and their dendritic and axonal processes and synaptic contacts reside in two plexiform layers (outer and inner – OPL and IPL, respectively) (**Figure 1.2**). The plexiform layers are each comprised of sublaminae (2-3 in the OPL and ~10 in the IPL) where distinct classes of cells make synaptic connections.

1.1.1 Functional architecture

Vision begins with the absorption of light by photoreceptors – rods and cones. Rods are sensitive to very low light levels and are therefore used predominately during night (scotopic) vision, while cones are much less sensitive and are used mainly during day (photopic) vision. In both photoreceptor types, photon absorption causes hyperpolarization and a decrease in the release of glutamate from nerve terminals. These photoreceptors make synapses in the OPL with horizontal cells and bipolar cells.

Bipolar cells can be divided into two groups: "ON bipolar cells" are depolarized at light onset and hyperpolarized at light offset, while "OFF bipolar cells" are hyperpolarized by light onset and depolarized by light offset. Transmission from photoreceptors onto OFF bipolar cells is sign conserving and mediated through an ionotropic glutamatergic synapse which causes depolarization upon glutamate binding. Transmission onto ON bipolar cells, meanwhile, is sign inverting, and mediated through a metabotropic glutamate receptor that causes hyperpolarization upon glutamate binding. Thus, bipolar cells split photoreceptor signals into ON and OFF visual channels that they convey via their axons into the IPL (Werblin and Dowling, 1969). These channels are physically segregated at the outputs of bipolar

Figure 1.2: Organization of the vertebrate retina

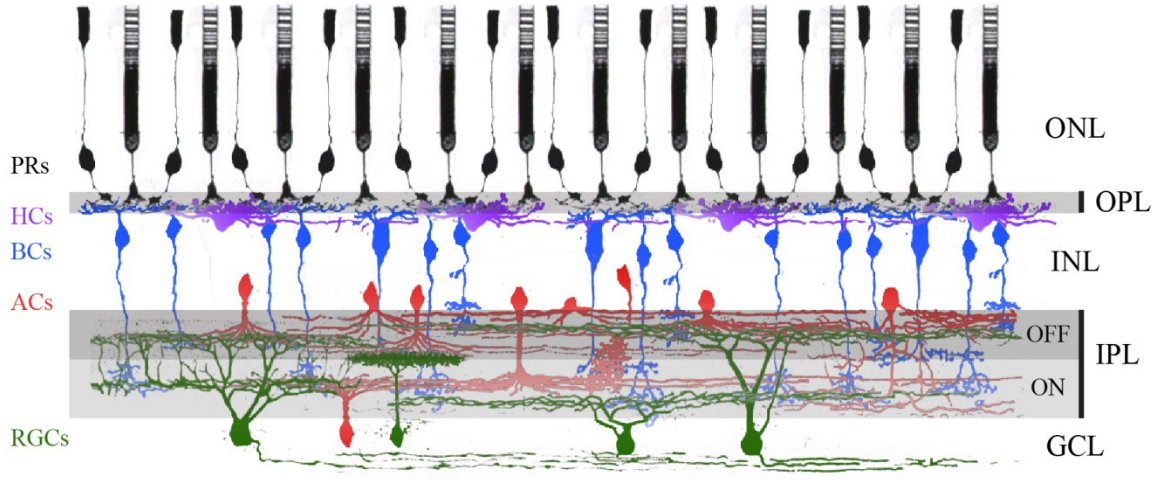

Cell classes and layers in the retina are shown. Cell classes: photoreceptors (PRs) shown in black, horizontal cells (HCs) shown in purple, bipolar cells (BCs) shown in blue, amacrine cells (ACs) shown in red, and retinal ganglion cells (RGCs) shown in green. Cellular layers: outer nuclear layer (ONL) contains photoreceptors, inner nuclear layer (INL) contains horizontal cells, bipolar cells, and amacrine cells, and ganglion cell layer (GCL) contains retinal ganglion cells and displaced amacrine cells. Synaptic layer: outer plexiform layer (OPL) contains synapses between photoreceptors, horizontal cells, and bipolar cells and inner plexiform layer (IPL) contains synapses between bipolar cells, amacrine cells, and ganglion cells. Original drawing by Santiago Ramon y Cajal, pseudocolored by Arjun Krishnaswamy.

cells, with terminals of OFF cells occupying the outer half and terminals of ON cells occupying the inner half of the IPL (**Figure 1.2**) (Famiglietti and Kolb, 1976).

Excitatory signals from bipolar cells are transmitted directly to RGCs and also indirectly via amacrine cells, which are predominately inhibitory. Amacrine cells filter and transform these bipolar signals and transmit these altered signals to RGCs, allowing these neurons to extract salient features of visual space in their receptive fields. Thus, the ~30 classes of RGCs, which each tessellate visual space independently, report on different features of the visual world. This selective feature detection is made possible by specific neuronal morphologies and motifs of connectivity between subsets of bipolar cells (~14 types), amacrine cells (~40 types), and a given RGC type.

While the response of the different bipolar cell classes do differ – there are fast, slow, transient, and sustained ON and OFF cells (Baden et al., 2013), these cells perform a limited amount of filtering of visual information. The major transformation of visual signals from luminance detection by photoreceptors to feature detection by RGCs is dependent on amacrine cells (Werblin, 2011). The diversity of morphologies and functional properties of amacrine cells enrich the diversity of ganglion cell responses, allowing RGCs to respond specifically to features such as edges, color, luminance, and several types of motion – directional, local, and looming. Many amacrine cells classes have processes that lack a clear distinction between axon and dendrite because they both receive input synapses and transmit output synapses [an exception to this are wide-field polyaxonal amacrine cells, which have true axons and fire action potentials (Volgyi et al., 2001)]. This peculiar morphological property allows for compartmentalization that substantially increases the computational power of any given amacrine cell and underlies their specialized functions (Masland, 2012). One of the best examples of compartmentalized dendritic function in individual amacrine cell processes is SACs, each of whose dendrites computes radial motion independently from other dendrites of the same cell (Euler et al., 2002). SACs come in an OFF and an ON type that reside in the INL and GCL and laminate in the outer and inner half of the IPL, respectively. While the processes of these amacrine cells have mixed inputs and outputs, I will consider

them as dendrites here, due to their generally local projection patterns and processing, as well as their lack of sodium-dependent action potentials (Masland, 2012; Werblin, 2011).

1.1.2 Principles of specificity

In the retina, bipolar, amacrine, and ganglion cell processes and connections converge in the IPL, exhibiting at least three forms of specificity: (1) laminar specificity – each neuronal type extends processes into one or a few of the sublaminae of the IPL, (2) intralaminar specificity – a given neuronal type is not equally likely to make synapses with other neurons in its own layer, and (3) lateral specificity – individual neuronal types extend dendrites of a given size and overlap with neighbors of the same type to different extents within a lamina, ensuring uniform coverage of visual space, appropriate receptive field size, and feature detection that requires comparisons across space, such as motion detection. Together, these processes ensure that at any given position of visual space, all 30 types of RGCs are poised to detect their dedicated trigger feature.

1.1.3 Why the retina?

Studying the retina offers several advantages. The neurons comprising a given cell class in the retina not only share functional properties, but also have anatomical and molecular similarities, which facilitate marking, identification, and manipulation of specific types and circuit motifs over development and across animals. Furthermore, unlike many parts of the nervous system, retinal neurons in the mouse extend processes and assemble into functional circuits after birth, allowing for developmental studies in postnatal animals. Lastly, because we know what features are computed by many retinal circuits, and because we have specific access to manipulate specific molecules in specific cell types, we can make and test very specific predictions about how structural and functional elements construct the response properties of retinal neurons. This distinguishes retina from other areas such as cerebellum and cortex, whose overall role in mental activities remain incompletely understood.

Despite these differences, mechanisms of retinal specificity are not unique to retinal circuits. Through nervous systems of both vertebrates and invertebrates, neurons and the processes show tremendous stereotypy in their laminar, intralaminar, lateral organization, and projection patterns at every spatial scale examined (Hubel and Wiesel, 1962; Mountcastle, 1957; Ohki and Reid, 2007; Pfeffer et al., 2013; Sanes and Zipursky, 2010; Spruston, 2008). Thus, the organizing principles we infer from the study of the retina are likely to generalize to almost any circuit throughout the brain.

The retina is also fascinating in its own right. Humans are visual creatures, so understanding how this structure works will give insights into human perception. Furthermore, the retina is important for the regulation of many adaptive behaviors, such as setting circadian rhythms and mediating optokinetic nystagmus (Berson, 2003; Simpson, 1984).

1.2 Mechanisms of dendritic development

The developmental trajectories of individual neurons that ultimately lead to particular morphologies and synaptic connections are diverse and likely dictated by the differing needs and ultimate functions that individual neurons will have in a circuit. It is useful, however, to group these processes in order to extract principles that govern circuit development throughout the nervous system.

Generally, I will discuss how developing neurons segregate their processes into different compartments (dendrites and axons), grow out their processes to particular locations where they may receive input synapses or form output synapses, elaborate processes of a particular size in order to receive input from or transmit output to an appropriate volume of the brain, and refine their neurites to adopt particular geometries that influence how densely they receive inputs or make outputs in their arborization fields. While these topics are discussed separately for clarity, they are likely happening simultaneously as brains develop. The adoption of mature neuronal morphologies is a dynamic process that relies on the interplay of cell-intrinsic cues and influences of a neuron's local environment. The relative contributions of intrinsic versus extrinsic cues, how these cues are integrated by individual neurons, and how these choices influence neuronal function are active areas of research. The focus of my discussion here, as that of my thesis, is on the choices made by developing dendrites that lead to the assembly of functional circuits.

1.2.1 Initial neuronal polarization

Cell biology of polarization. For many neurons, morphological development begins with an initial polarization into dendritic and axonal compartments (for reviews, see Barnes and Polleux, 2009; Cheng and Poo, 2012). Many aspects of neuronal polarization were first studied in cultured neurons, where neurons initially grow out several neurites, one of which becomes the axon and the rest of which become dendrites. Segregation of axons and dendrites in culture is therefore possible without extrinsic cues (Craig and Banker, 1994). Dendritic and axonal compartments can be distinguished readily based on orientation of cytoskeletal proteins and localization of organelles. While the plus-ends of microtubules are

almost exclusively directed away from the cell body in axons, the polarity of these structures in dendrites is mixed – with about an equal proportion of plus-ends directed towards and away from the cell body (Baas et al., 1988). This difference underlies the ability of different types of cargo to be trafficked to these different cellular compartments; different classes of motor proteins – kinesins and dyneins – move preferentially towards the plus-ends and minus-ends of microtubules, respectively (Conde and Caceres, 2009; Huang and Banker, 2012). These cytoskeletal differences likely underlie the preferential placement of organelles that are trafficked by minus-end-directed transport, such as ribosomes, secretory endoplasmic reticulum, and Golgi apparatus, in dendrites, where they can locally influence branching and insertion of specific proteins into the plasma membrane (Cui-Wang et al., 2012; Horton et al., 2005; Puram and Bonni, 2013; Zheng et al., 2008).

Polarization in vivo. While cultured neurons do not necessarily require extrinsic factors to polarize into axons and dendrites, these types of cues are present as neurons develop *in vivo*. Much of the work on environmental cues that are necessary for neuronal polarization have been studied in the retinas of zebrafish, whose genetic accessibility and transparency make it a perfect model system for time-lapse studies of developing neurons. In the zebrafish retina, Harris and colleagues have shown that axons emerge directly from RGCs without a prolonged 'choice' phase and require extrinsic adhesive interactions with laminin derived from the retinal inner limiting membrane (Randlett et al., 2011; Zolessi et al., 2006). These interactions may be mediated through integrin signaling in RGCs themselves, since this molecule is crucial for ganglion cell layer development in mice (Riccomagno et al., 2014).

Another extrinsic mechanism by which neurons may acquire their polarized morphologies is to inherit them from their progenitors. For example, retinal bipolar cells dendrites and axons emerge directly from apical and basal neuroepithelial processes, respectively (Morgan et al., 2006). In the cerebellum, meanwhile, migrating granule cell progenitors grow through the molecular layer to reach and form the granule cell layer, leaving behind processes that become their axons as they grow. A similar mechanism is used by migrating pyramidal neurons in the neocortex and hippocampus (Barnes and Polleux, 2009). Many retinal amacrine cells, including SACs, do not have strict polarization of processes into axons and

dendrites. Instead, their processes serve as a combination of axons and dendrites, containing both pre- and post-synaptic machinery. These cells, therefore, do not rely on polarizing cues of their progenitors to target their separate compartments to different regions of the brain. Instead, they target all of their processes to the IPL, where they receive connections from and form connections with bipolar cells, RGCs, and other amacrine cells. To accomplish this task, amacrine cells initially grow out neurites that are untargeted, but quickly stabilize branches that are directed towards to IPL (Galli-Resta, 2000; Godinho et al., 2005). Because these cells are the first to extend processes into the IPL, it has been suggested that they lay down the scaffold that assembles all the layers of the IPL (Kay et al., 2004). The formation of the IPL is an excellent system for the study of targeted outgrowth, and I will discuss this topic in detail in the next section.

1.2.2 Directed dendritic outgrowth

After polarization, neurons must place processes in locations that allow them to process information properly. In this regard, dendrites and axons initially encounter vastly different problems to find their arborization fields. Many axons must grow over long distances in order to find the appropriate termination fields before they can make local choices, while dendrites face relatively local decisions about where to grow since dendrites generally reside close the cell bodies of neurons (Sanes and Yamagata, 2009). Axon guidance is a fascinating field but not discussed here (for reviews, see Tessier-Lavigne and Goodman, 1996 and Dickson, 2002). Once axons reach their target zones, their task is, in principle, similar to that of dendrites. In both cases, finding appropriate targets requires local cues, which may include cell-type specific interactions or sensing of gradients; in both of these cases, these local cues can be either attractive or repulsive.

1.2.2.1 Roles of neuronal recognition molecules

Laminar targeting in the retina. In the vertebrate retina, the formation of the multilayered inner plexiform layer (IPL) that allows for the processing of distinct visual features in parallel is initiated by

amacrine cells. As mentioned above, these cells initially grow out dendrites in all directions as they are migrating into the inner nuclear layer (INL) and ganglion cell layer (GCL), but selectively stabilize processes located between these two cellular strata (Godinho et al., 2005; Hinds and Hinds, 1978). Amacrine cell processes are soon joined in the IPL by dendrites of RGCs, which are localized to this structure through a similar process of unbiased outgrowth followed by selective stabilization of processes residing in the IPL (Choi et al., 2010). Amacrine cells are not only the initiators of IPL formation, they are also sufficient to form and maintain this structure. While deletion of RGCs delays IPL formation and causes some amacrine cells to form disorganized arborizations initially, the majority of these errors are eventually corrected, and the remaining IPL eventually looks remarkably normal without RGCs (Kay et al., 2004). Thus although RGC dendrites can be used to stabilize IPL formation, they are not required for this process to occur.

The molecular mechanism of this initial stabilization of amacrine cell processes is not completely understood. However, the atypical cadherin FAT3 is one mediator of this process. FAT3 is expressed by developing amacrine cells and retinal ganglion cells but is required only in amacrine cells for proper IPL formation (Deans et al., 2011; Nagae et al., 2007). In the absence of FAT3, amacrine cells fail to stabilize processes localized between the INL and GCL, resulting in the formation of 3 separate plexiform layers in the middle of the INL, between the INL and GCL (as in wild type mice), and below the GCL at the level of RGC axons (Deans et al., 2011). FAT3 protein is localized to the nascent IPL even before amacrine cells have removed processes not directed towards this structure, suggesting that the homophilic interactions of amacrine cell dendrites that initiate IPL formation rely on FAT3.

While it is attractive to speculate that homotypic FAT3 interactions mediate the dendritic contact that stabilizes IPL formation between the INL and GCL, it is unclear how amacrine cells choose this location. Recent studies by Kolodkin and colleagues have shown that a pair of transmembrane semaphorins, Sema5A and Sema5B are selectively expressed by progenitor neurons in the outer retinal neuroblast layer and restrict the processes of bipolar cells, amacrine cells, and RGCs to the future location

of the IPL. Removal of Sema5A and Sema5B, or their receptors PlexinA1 and A3, causes ectopic IPL formation similar to that seen in FAT3 mutants (Matsuoka et al., 2011a).

Once the location of the IPL is established, amacrine cells and RGCs elaborate dendrites into specific layers of the IPL, a process that limits synaptic partner choices and allows for the parallel processing of visual information described above. Time lapse studies in zebrafish and careful single cell labelling in mice have shown that laminar targeting is initiated by amacrine cells, and that RGCs follow the processes of these interneurons (Mumm et al., 2006; Stacy and Wong, 2003). Bipolar cells, the latest-born neurons that innervate the IPL, elaborate their axons after the laminar structure of the IPL has been established.

Directed dendritic outgrowth to particular sublaminae of the IPL has been studied best in the chick retina. In this system, individual homophilic adhesion molecules of the immunoglobulin superfamily (IgSF) – Dscam, DscamL, Sidekick1, Sidekick2, and Contactin1-5 – are expressed by non-overlapping subsets of bipolar, amacrine, and ganglion cells. Knockdown of these molecules disrupts specific targeting to particular sublaminae and overexpression of these molecules is sufficient to target neuronal processes to sublaminae containing the processes of cells with endogenous expression of these molecules (Yamagata and Sanes, 2008, 2012a; Yamagata et al., 2002). Thus, this 'IgSF code' provides a genetic address book, allowing synaptic partners to choose each other by selective homophilic adhesion.

How the relative positions of these sublaminae within the IPL are established is also beginning to be understood. The most simple laminar separation of the IPL can be made by dividing it into OFF (outer) and ON (inner) sublaminae that roughly divide the IPL in half (Famiglietti and Kolb, 1976). In the mammalian retina, selective expression of another semaphorin, Sema6A, and its plexin receptors, PlexA2 and PlexA4, divide the IPL into its OFF and ON portions. Sema6A is expressed selectively by displaced amacrine cells and RGCs in the GCL, with protein localized to the ON portion of the IPL. Meanwhile, PlexA2 and PlexA4 are expressed by OFF interneurons whose cell bodies reside in the INL. Specifically, Sema6A-PlexA4 interactions are crucial for the restriction of tyrosine-hydroxylase (TH)-positive dopaminergic amacrine cells to the outer boundary of IPL, as well as some calbindin-positive amacrine

and ganglion cells (Matsuoka et al., 2011b). When this interaction is disrupted, TH amacrine cells still target their correct lamina but also place dendrites in ON sublaminae. Remarkably, these misprojecting neurons recruit dendrites of their synaptic partners, melanopsin-expressing intrinsically photosensitive RGCs, into their new locations, likely because synaptic partners still express homophilic adhesion molecules like the IgSFs describe above. It remains to be tested whether the additional dendritic arborizations of OFF cells in the ON layers are due to a lack of elimination of ON projections by OFF neurons or excessive outgrowth into incorrect laminae, which would result in more total dendritic territory for individual cells, or a redistribution of existing dendrites, which would result in the same total amount of dendrite.

Meanwhile, interactions between Sema6A and PlexA2 are specifically required for the laminar restriction of starburst amacrine cells (SACs). As mentioned above, SACs come in an OFF and ON type whose cell bodies and dendrites are reflected vertically across the middle of the IPL. However, during the early stages of IPL formation, SAC dendrites occupy a single layer and separate as the sublaminae of the IPL are established during the first two postnatal weeks in mice (Stacy and Wong, 2003). While PlexA2 is expressed by both OFF and ON SACs, Sema6A is only found in ON SACs. Thus, repulsive interactions between OFF and ON SACs are thought to segregate OFF and ON SAC dendrites into the outer and inner half of the IPL during development. Single cell labeling of SACs in mutant mice shows that individual OFF SACs still establish their radial morphology, but portions of their dendrites are found in the ON SAC layer (Sun et al., 2013).

The last neurons to elaborate processes in the IPL, bipolar cells, choose appropriate laminae after the layers of the IPL have already been established. Studies of bipolar cells that innervate the two SAC layers have shown that these cells express specific cadherin recognition molecules, Cdh8 and Cdh9, to find the OFF and ON SAC layers, respectively (Duan et al., 2014). Interestingly, removal of Cdh8 in the OFF bipolar subtype or removal of Cdh8 in the ON bipolar subtype do not cause a general mistargeting of bipolar axons to all layers of the IPL. Instead, removal of these molecules causes a redistribution of bipolar cell axons from their appropriate layer into an approximately even distribution into the two SAC

layers, suggested that the target choice of these axons is limited by the existing structure of the IPL. OFF bipolar cells that redistribute into ON laminae fail to connect with ON SACs in this lamina. This finding highlights how even if neurons place processes in a location (laminar specificity), they may still require additional factors to form connections in that location (intralaminar specificity).

In summary, developing neuronal processes find their proper locations in the IPL through a combination of partner matching and restriction from incorrect locations. Interestingly, developing RGCs exhibit several different modes of choosing their appropriate sublaminae, with some types of cells showing specific targeting to particular sublaminae early in development and others initially occupying several sublaminae before refining to a single layer (Kim et al., 2010; Mumm et al., 2006). Time lapse studies of developing dendrites in the mutant mice described above, like the ones performed in zebrafish, would shed light on this issue.

Molecular mechanisms of neurite targeting outside the retina. The precise targeting of dendritic processes is not a unique property of retinal neurons. Throughout the nervous system of both vertebrates and invertebrates, the molecular mechanisms that direct dendrites to their proper locations and also specify their connectivity within those locations exist (Lefebvre et al., 2015). Here, I highlight a few examples from other parts of the brain and draw parallels to the vertebrate retina.

Perhaps the best known example of an attractive positional cue that establishes dendritic organization comes from the study of developing mammalian cortical neurons. These cells grow dendrites towards the apical surface of cortex in respond to a gradient of the secreted semaphorin, Sema3A, which is an attractive cue in this case (Polleux et al., 2000). Such gradients are a useful strategy for targeting of neuronal processes to particular regions of large arborization fields and can be either attractive or repulsive. RGC axons also rely on gradients to innervate distinct regions of their target regions, such as the optic tectum/superior colliculus. This topography is established by expression gradients of Eph receptors and ephrins in the retina and tectum/colliculus, respectively. Because Eph receptor-ephrin

interactions lead to repulsion, RGC axons expressing high levels of Eph-receptors are excluded from regions of the tectum/colliculus that express high levels of ephrins (McLaughlin and O'Leary, 2005).

Olfactory projection neurons (PNs) in the adult Drosophila antennal lobe establish dendritic territories before incoming excitatory afferents arrive, organizing into ~50 discrete glomeruli that carry distinct channels of olfactory information (Jefferis et al., 2004), in a system analogous to the discrete sublaminae of the vertebrate IPL. This coarse glomerular map is established by antiparallel gradients of Wnt5 and Sema2A/2B that are sensed by incoming PN dendrites through mechanisms that include another semaphorin, Sema1A (Komiyama et al., 2007; Sweeney et al., 2011; Wu et al., 2014). Further targeting to specific glomeruli in this system happens through dendro-dendritic adhesion that is specified for some glomeruli by the expression of the transmembrane protein Capricious (Hong et al., 2009), and also through specific partner matching with incoming afferents mediated by expression of the transmembrane teneurin proteins, Ten-m and Ten-a (Hong et al., 2012).

1.2.2.2 Positional cues derived from non-neuronal cells

Mechanisms that specify where neurons should elaborate processes are sometimes not even neuronal in origin. In the autonomic nervous system of mammals, sympathetic neurons are directed to innervate distinct targets by vascular-derived endothelins (Makita et al., 2008). In Drosophila larvae, somatosensory neurons require integrin-dependent interactions to remain in the 2-dimensional plane of the epidermis (Han et al., 2012; Kim et al., 2012). A loss of this interaction produces defects that resemble dendritic self-avoidance at the light-microscopic level (see section 1.3) but are in fact just projections out of the plane of the skin. In C. elegans, PVD sensory neurons also receive positional cues from factors in the skin. Here, the adhesion molecules SAX-7 and MNR-1 found at particular locations in the skin specify locations where PVD cells should branch (Dong et al., 2013). I will describe these classes of invertebrate neurons in much detail in a subsequent portion of this chapter while discussing dendritic field size (section 1.2.3) and orderly arrangement of dendrites within arborization fields (section 1.2.4 and 1.3).

1.2.2.3 Transcriptional mechanisms that underlie distinct patterns of targeting

The factors that regulate the selective expression of different recognition molecules and the differential expression of the same recognition molecules that generate the gradients described above remain a mystery. In the fly antennal lobe, PNs of different cell lineage and birth order project to different locations and express different POU domain transcription factors (Jefferis et al., 2001; Komiyama et al., 2003). It is likely that these cell-intrinsic mechanisms generate the diverse expression of cellular recognition molecules (described above) that act as effectors of dendritic position and synaptic specificity (Sweeney et al., 2011). In the mouse retina, RGCs also express the POU domain transcription factors Brn3a and Brn3b differentially, and the expression of Brn3a is required for proper laminar stratification of RGC dendrites (Badea et al., 2009). Due to the intimate relationship between dendritic targeting and function in both the visual and olfactory systems, it is perhaps unsurprising that these mechanisms are, at least in part, hard-wired.

1.2.3 Mechanisms that increase and limit dendritic size

Within their appropriate target locations, neurons must elaborate processes with size and complexity that are tailored to their particular function. In sensory systems, the extent of outgrowth of a given cell's dendritic arborization directly influences the portion of sensory space that it will sample. This is most obvious in the retina and somatosensory system, where sensory space is defined in spatial coordinates of visual field area and the dermatome, respectively, but also true elsewhere, such as the mammalian olfactory bulb. In this system, the main projection neurons, mitral and tufted (M/T) cells, send a main dendritic projection into single glomeruli but have dendritic collaterals that span hundreds of microns across several glomeruli. These lateral dendrites make connections with local circuits in different glomeruli. Thus, the lateral extent of this outgrowth may influence parallel olfactory processing (Murthy, 2011). Within a given sensory neuron's territory, the complexity of its branching patterns determines how densely it will sample its receptive field and therefore determine its spatial resolution or fidelity of response to any particular stimulus. Similar considerations apply throughout the brain, despite the

encoded features of these areas being less obvious. This is a multifaceted process that involves a combination of secreted growth cues, cell intrinsic transcriptional programs, and specific cues derived from afferents or homotypic neighbors, and can be influenced by network activity.

Neurotrophin signaling and activity. For many neurons, neurotrophin signaling has been demonstrated to play a central role in promoting dendritic outgrowth, without necessarily determining *where* dendrites should grow. While cultured neurons exhibit specific outgrowth towards a source of neurotrophins (Gundersen and Barrett, 1979), these molecules generally increase dendritic size and branch complexity *in vivo*, likely due to a lack of a singular target source (Lom and Cohen-Cory, 1999; Purves et al., 1988; Snider, 1988). Interestingly, different neurotrophins can promote dendritic outgrowth in different compartments of the same neuron (McAllister et al., 1995). Furthermore, these growth-promoting effects are blocked by application of activity blockers, suggesting that neurotrophin signaling may play a permissive role in dendritic outgrowth in the context of other molecular cues or network activity (McAllister et al., 1996). While the source of neurotrophins in many of the examples above is unclear, a neural circuit where afferent neurotrophins directly influence the dendritic size of target neurons is in the developing cerebellum, where granule cell-derived Neurotrophin-3 directly affects the dendritic arbor size of Purkinje cells (Joo et al., 2014).

How neurotrophin signaling and activity are integrated to cause changes in dendritic shape remains unclear, but afferent activity can have profound influences on dendritic outgrowth. For example, in the visual system of Xenopus, excitatory drive from the retina affects branching preferentially while inhibitory drive from local circuitry affects dendritic size (Cline and Haas, 2008; Shen et al., 2009). Dendritic outgrowth and branching of cells in some parts of the brain are less influenced by activity, and these circuits can be thought of as more 'hard-wired.' In the retina, excitatory input from bipolar cells is necessary to tune circuits locally but does not affect the general outgrowth of RGCs (Kerschensteiner et al., 2009). These cells, therefore, likely rely on cell intrinsic mechanisms or interactions with homotypic neighbors to establish their dendritic territories.

Cell intrinsic mechanism controlling arbor size. While a mechanistic understanding of these processes remains somewhat elusive in vertebrate systems, the ability to use rapid genetic screens has made Drosophila and C. elegans invaluable systems for these types of studies. In particular, the four classes of somatosensory neurons in Drosophila larvae, termed dendritic arborization (da) neurons, have been used extensively to identify such mediators. These four classes, denoted by Roman numerals I-IV, have overlapping dendritic arborizations but distinct dendritic field sizes and morphologies and encode distinct sensory modalities (Grueber et al., 2002). A recent RNA interference screen for transcriptional mediators of dendritic morphology identified over 70 such factors in class I neurons alone (Parrish et al., 2006). One such transcription factor, *abrupt*, is expressed exclusively by the class I neurons, which have small dendritic arborizations and simple branching patterns, but not by other classes. Expression of *abrupt* in other da neurons confers class I-like properties to their dendrites, suggesting that activation of *abrupt* signaling is sufficient to establish this particular dendritic morphology in any class of da neurons (Li et al., 2004; Sugimura et al., 2004). While *abrupt* is expressed specifically a single da class, the transcription factor *cut* is expressed at increasing levels in class II, IV, and III da neurons and its expression levels determine class-specific growth (Grueber et al., 2003a). Pairs of transcription factors can act in concert to confer class-specific morphologies. For example, while both class III and IV da neurons express relatively high levels of *cut*, only class IV neurons express another transcription factor, *knot*. This factor specifies class IV morphology by suppressing the formation of anatomical 'dendritic spikes' (not to be confused with dendritic action potentials), a characteristic morphology of class III da neurons (Jinushi-Nakao et al., 2007). Thus, combinatorial expression of these molecules can act as a switch between two similarly shaped neuronal types. While the transcriptional mechanisms that pattern vertebrate dendrites are not very well understood, one possibly fruitful approach is to look at mammalian homologues of these Drosophila genes. Indeed, the mammalian homologues of *cut*, called *Cux1 and Cux2*, promote dendritic branching in cortical neurons (Cubelos et al., 2010).

Interactions with homotypic neighbors. Another way that developing neurons control the size of their dendritic arbors is through interactions with homotypic neighbors. Many neurons exhibit a

phenomenon known as dendritic or axonal tiling. This process refers to the tendency of cells to minimize the overlap between their own processes and those of other cells of the same type; it is likely mediated by homotypic inhibitory interactions (Lohmann and Wong, 2001). Both RGCs and single da neuron classes exhibit dendritic tiling, and this is thought to ensure complete, but non-redundant, coverage of sensory space by these neurons. I will discuss this process in next section.

1.2.4 Mechanisms that establish appropriate dendritic and axonal territories

As neurons place their processes in appropriate locations, they use additional cues to determine local sampling and overlap with neighbors. These processes are often governed through interactions with neurons of the same type, or even dendrites of the same neuron. In the retina and elsewhere in the brain, three such mechanisms are mosaicism of cell bodies, dendritic tiling, and dendritic self-avoidance (**Figure 1.3**). A unifying feature of these three phenomena is that they are all mediated through contact-dependent repulsive interactions that are initiated at dendrites and axons of individual cell classes.

Mosaicism. In many parts of the nervous system, cell bodies of individual neuronal classes are found at non-random, regular intervals, forming what are called mosaics. This phenomenon establishes regular arrays of neurons across neural tissues and is one of the defining features of retinal cell types (Wassle and Riemann, 1978). Studies of retinal horizontal cells and SACs have shown that their cell body position is initially random, but mosaics organize as cells migrate to their target regions, extend neurites, and contact their neighbors (Galli-Resta et al., 2002; Huckfeldt et al., 2009; Poche et al., 2008). Thus, the formation of these mosaics likely relies on interactions among their dendrites of neighboring neurons. This hypothesis is supported by a recent study demonstrated that two related cell surface molecules, MEGF10 and MEGF11, are required for formation of these mosaics (Kay et al., 2012). Interestingly, horizontal cells, OFF SACs and ON SACs place their processes in distinct locations, and this is likely why they are capable of using the same molecules to organize their somata into mosaics. Different neuronal classes that share dendritic laminae but form mosaics independently are likely,

Figure 1.3: Mosaics, tiling, self-avoidance, and self/non-self discrimination

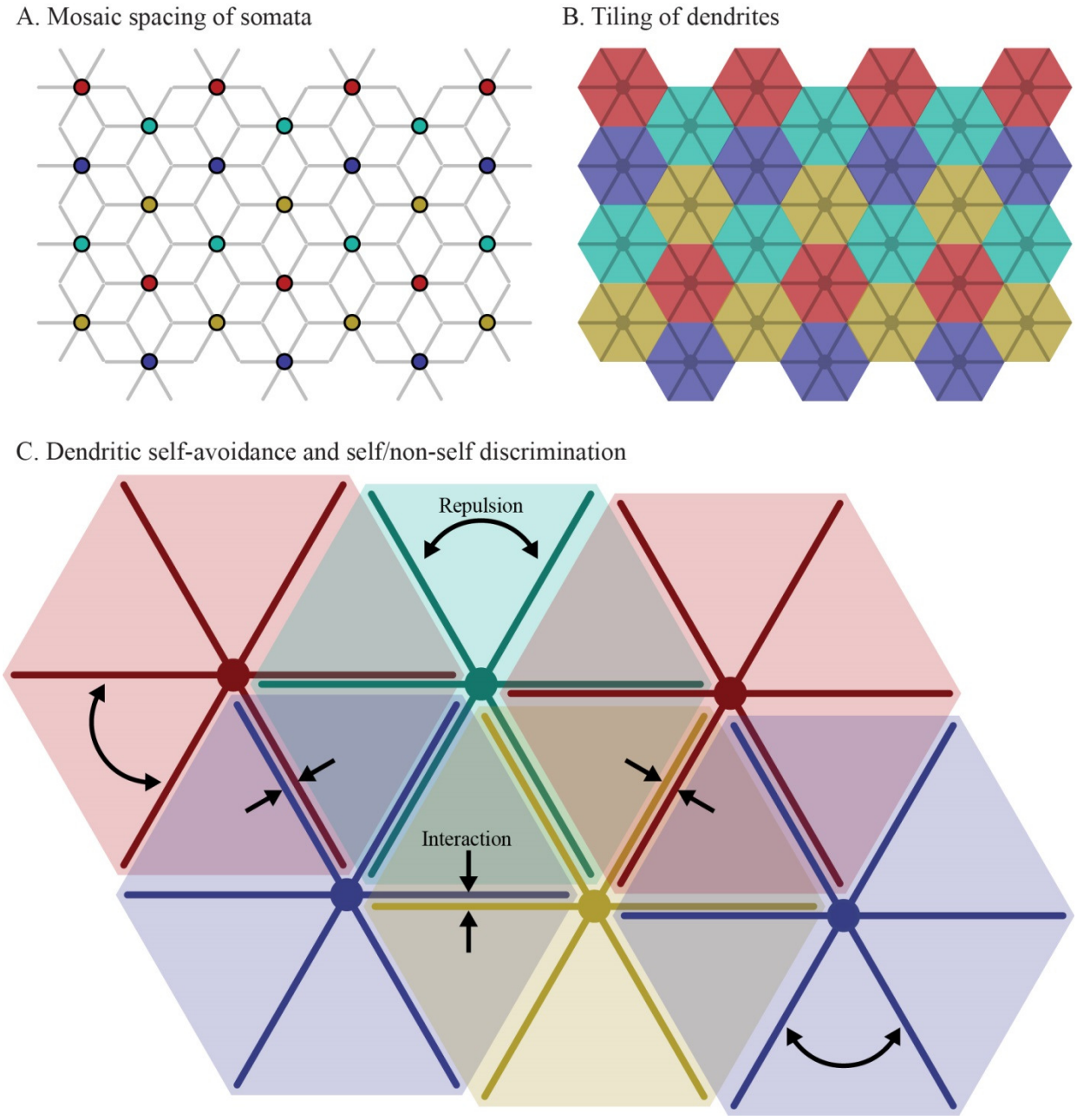

A. Mosaic spacing of individual neuronal somata (shown in different colors).

B. Dendritic tiling of neuronal processes (shown in different colors).

C. Self-avoidance and self/non-self discrimination allow for *repulsion* between a single neuron's sister dendrites and *interaction* between dendrites of neighboring cells.

therefore, to either use independent molecular mediators to form mosaics or have a different strategy for mosaic formation altogether.

Tiling. Processes of many neuronal cell types throughout invertebrates and vertebrates exhibit tiling of dendrites and axons (Grueber and Sagasti, 2010). The utility of tiling is most intuitive in sensory systems: if a given cell class tiles its processes, it ensures complete but not redundant coverage of sensory space by itself and its sister neurons. In the vertebrate retina, the dendrites and axons of many neuronal classes, including most bipolar and RGCs classes, exhibit tiling (Helmstaedter et al., 2013; Wassle et al., 1981; Wassle et al., 2009). The degree of overlap between neighboring cells of a given class is referred to as the 'coverage factor' of this cell class, and neuronal classes that exhibit tiling will have a coverage factor close to one. For example, cat alpha-RGCs exhibit a coverage factor of about 1.4 (Wassle et al., 1981). In contrast, few RGC types tile the mouse retina, with most exhibiting a coverage factor substantially greater than one. For example, direction-selective RGCs have more lenient boundaries, with a coverage factor between 2 and 3 (Rivlin-Etzion et al., 2011).

Similar to mosaic formation, the establishment of dendritic territories happens independently within a cell class, and this process is likely due to homotypic repulsion that terminates dendritic outgrowth when cells contact their neighbors. This hypothesis is supported by several lines of evidence. First, as mentioned above, neighboring neurons of a given type exhibit transient contacts with each other (Grueber et al., 2002; Grueber et al., 2003b; Huckfeldt et al., 2009; Lohmann and Wong, 2001). Second, while dendritic diameter of a given cell type may vary across the retinal surface, this change is accompanied by an inversely proportional variation in neuronal density, leading to a minor differences in coverage factors (Bleckert et al., 2014). Finally, local ablation of subsets of neurons that exhibit tiling causes neighboring cells' dendrites to grow towards the ablated region (Blackshaw et al., 1982; Okawa et al., 2014; Perry and Linden, 1982; Sagasti et al., 2005). Thus, as mentioned above, dendritic tiling is a mechanism that is capable of limiting dendritic field size.

The molecular mechanisms that generate tiling behavior of retinal neurons remain elusive; however, these processes have been studied in other systems. In the Drosophila visual system, axon

terminals of L1 neurons (roughly comparable to a single class of vertebrate retinal bipolar cells) tile by expressing a single repulsive isoform of the recognition molecule Dscam2 (Lah et al., 2014).

Tiling and mosaic formation are related but distinct processes. For neurons that exhibit low coverage factors, the same molecular mediators could, in principle, mediate both processes. However, cells need not tile to form mosaics. In fact, many neurons exhibit very high coverage factors while maintaining mosaics. For example, SACs have a coverage factor of about 40 and do not increase their dendritic field size in response to local ablation of the sister SACs (Farajian et al., 2004), so it is likely that they use different strategies to acquire proper morphologies (see next section).

Self-avoidance. The notion of self-avoidance arose from functional studies of the receptive fields of sensory neurons in leech by Nicholls and his students (Nicholls and Baylor, 1968; Yau, 1976). These authors observed that while the receptive fields of neighboring neurons often overlapped extensively, the subfields of a given cell's receptive field rarely overlapped. From these studies, they proposed that branches of the same neuron contain recognition cues that allow them to recognize and repel their own branches, but not those of their neighbors. The first experimental evidence for specific repulsion between branches of the same neuron was provided by Kramer and Stent (1985). These authors ablated individual branches of leech sensory neurons and observed that neighboring branches of the same neuron grew into the vacated territory of the missing branch.

The dendritic and axonal processes of many neurons exhibit self-avoidance, and this processes is thought to ensure uniform coverage within a cell's receptive field, minimizing gaps and clumps of processes that would receive or transmit redundant information. As noted above, the processes of neurons that exhibit self-avoidance can overlap with the dendrites of other neurons that also exhibit this phenomenon. This puzzling observation suggests individual neurons are immune to the repellent forces that act within each other's arbors, a phenomenon called self/non-self discrimination (Zipursky and Grueber, 2013).

Over the last 15 years, the molecular mechanisms that mediated self-avoidance and self/non-self discrimination have been studied extensively in both invertebrates and vertebrates. In the next section, I will discuss these mechanisms in more detail, as they are central to the studies presented in this thesis.

1.3 Dendritic self-avoidance and self/non-self discrimination

Self-avoidance of neuronal dendrites and axons is a pervasive phenomenon in the nervous systems of both invertebrates and vertebrates. Examples of neuronal classes that exhibit this phenomenon in non-mammalian species are: leech sensory neuron dendrites (in which, as noted above, the process was first described), C. elegans PVD neurons, moth larval sensory neurons, Drosophila da sensory neuron dendrites, Drosophila olfactory neurons, and Zebrafish sensory neurons (Grueber and Truman, 1999; Grueber et al., 2003b; Sagasti et al., 2005; Smith et al., 2012; Wang et al., 2002a). The sensory neurons of the leech, moth, and Drosophila are, in fact, analogous neuronal classes. In the mammalian nervous system, self-avoidance has been documented for cerebellar Purkinje cells and some classes of retinal horizontal, bipolar, amacrine, and ganglion cells (Lefebvre et al., 2012; Matsuoka et al., 2012; Montague and Friedlander, 1991; Wassle et al., 2009). Many of the neuronal classes above have relatively planar arborizations, which has facilitated documentation of their self-avoidance. However, it is likely that many other neuronal classes also exhibit self-avoidance, but their three-dimensional arborizations render phenotypic analysis less straightforward.

1.3.1 Differing requirements for self-avoidance and self/non-self discrimination

The molecular mechanisms that mediate self-avoidance at the level of cell surface recognition can be divided into two broad classes: (1) those that do not require self/non-self discrimination and can be accomplished by a single molecule, and (2) those that do require self/non-self discrimination and therefore require molecular diversity. For example, a neuronal class that exhibits both self-avoidance and tiling could, in principle, use the same molecule to avoid its own processes and those of its neighbors. One such example are the bilaterally symmetric PVD neurons described above, whose dendrites form unilateral menorah-like arborizations on each side of the worm. Because these neurons do not encounter homotypic neighbors within their own dendritic fields, they use a single signaling complex, for self-avoidance. In these neurons, the secreted protein UNC-6 (Netrin) is captured by the membrane tethered protein UNC-40 (DCC), allowing for binding to UNC-5 on sister branches and signaling that leads to

repulsion (Smith et al., 2012). Thus, PVD neurons use a single, albeit complicated, ligand-receptor combination to mediate self-avoidance. A similar ligand-receptor handshake is also necessary for the self-avoidance of Purkinje cell dendrites, in this case mediated by Slit-Robo interactions (Gibson et al., 2014). In the mammalian retina, the typical homophilic cell surface recognition molecules, DSCAM and DSCAML1 are required to prevent adhesion of both cell bodies (mosaics) and neuronal processes (self-avoidance) for a variety of neuronal classes (Fuerst et al., 2009; Fuerst et al., 2008), highlighting how single molecules can mediate multiple repulsive processes if neurons do not normally overlap substantially. On the other hand, the dendrites of the four classes of Drosophila da neurons and the dendrites of retinal SACs overlap extensively, and therefore require molecularly diverse families of recognition molecules – Dscam1 and clustered gamma-Protocadherins (Pcdhgs), respectively – to mediate both self-avoidance and self/non-self discrimination (**Figure 1.4**) (Zipursky and Grueber, 2013).

1.3.2 Self-avoidance and self/non-self discrimination are mediated by *Dscam1* in Drosophila

The molecular mechanism of self-avoidance and self/non-self discrimination have been studied most extensively in Drosophila da neurons. Each class of da neurons exhibits self-avoidance and overlap rarely with their neighbors. However, different classes of da neurons overlap extensively with each other. Thus, self-avoidance within the dendrites of a given neuron facilitate complete coverage within a neuron's receptive field, and self/non-self discrimination allows for coexistence of the dendrites of different da neuron classes. Together, these processes allow for complete detection of different somatosensory modalities over the body wall of these animals.

The diverse family of cellular recognition molecules, encoded by alternative splicing of the *Dscam1* gene, mediates this process. In *Dscam1* mutants, dendrites of individual da neurons often cross over each other and form clumps (Hughes et al., 2007; Matthews et al., 2007; Soba et al., 2007). A series of studies have revealed the three principles that allow Dscam isoforms to promote this process – molecular diversity, isoform-specific binding, and differential expression in neighboring neurons.

Figure 1.4: Similarity between Drosophila *Dscam1* and mammalian clustered *Protocadherins*

A. The *Dscam1* gene contains four cassettes of alternative exons that encode alternative variants of three extracellular immunoglobulin (Ig) domains and the transmembrane domain (TM). The clustered *Protocadherins* are separated into three subclusters – alpha (Pcdha), beta (Pcdhb), and gamma (Pcdhg). Individual isoforms are transcribed by alternative promoter choice. Variable extracellular exons are comprised of 6 extracellular cadherin (EC) domains, the transmembrane domain, and a small intracellular domain. For Pcdhas and Pcdhgs, these variable exons are spliced onto three common exons within each subcluster that encode additional intracellular domains.

B. Binding specificity of Dscam proteins is determined by matching of the three alternatively spliced extracellular Ig domains. Specificity of Pcdhs relies on matching of the EC2 and EC3 domains.

C. Neurons within individual classes express distinct subsets of Dscam1 and Pcdh proteins.

(Figure continues on next page)

Figure 1.4 (continued)

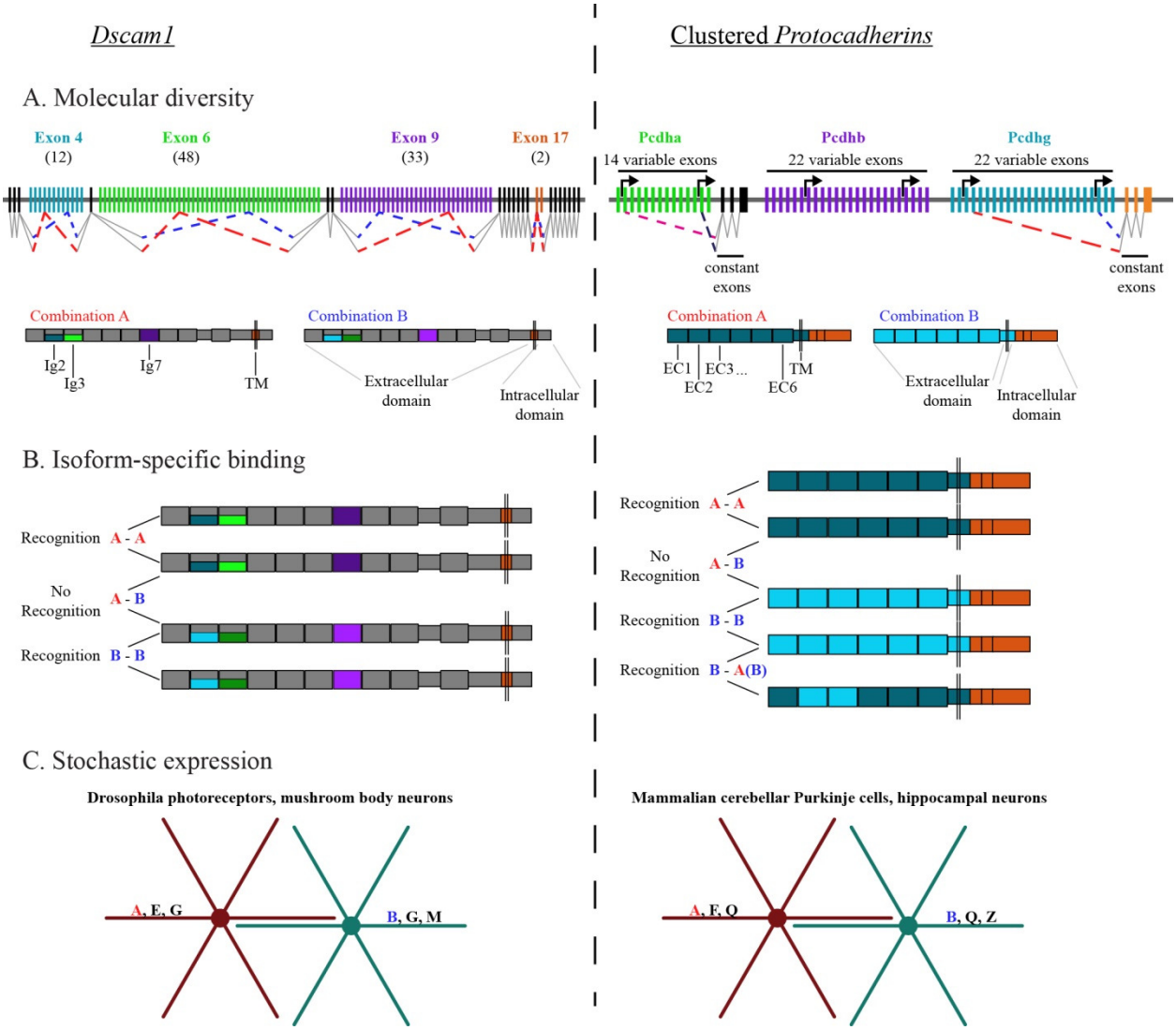

1.3.2.1 Three principles required to mediate self-avoidance and self/non-self discrimination

Molecular diversity. Dscam1 encodes a large family of cell surface receptors of the immunoglobulin superfamily generated from a single *Dscam1* gene. Alternative splicing at three locations of this gene, in exon 4 (12 variants), exon 6 (48 variants), and exon 9 (33 variants), which encode portions of Immunoglobulin (Ig) domains 2, 3, and 7, respectively, generate the possibility of 19,008 (12 x 48 x 33) different extracellular domains (Schmucker et al., 2000). The transmembrane domain of the protein also has 2 versions encoded by alternative exon 17 variants, and while these alternative exons do not contribute to the extracellular diversity of the protein, they do dictate the localization of Dscam1 proteins (Wang et al., 2004).

Isoform-specific binding. Each Dscam1 protein generated through the alternative splicing mechanism described above shows isoform-specific binding (Wojtowicz et al., 2004; Wojtowicz et al., 2007). This specificity is binding is possible because *trans* interactions between Dscam1 proteins happens at the very three Ig domains, 2, 3, and 7, that are alternatively spliced. Importantly, matching between all three Ig domains is necessary for binding in vitro, and self-avoidance in vivo (Meijers et al., 2007; Sawaya et al., 2008; Wu et al., 2012).

Stochastic expression. If all neurons expressed the same set of Dscam1 isoforms, they would not be able to distinguish self neurites from non-self neurites, and all branches would repel each other. However, expression profiling of individual neurons in the visual system and mushroom body, which require Dscam1 for self-avoidance (see next section), express unique subsets of Dscam1s, between 10-50 isoforms (Neves et al., 2004; Zhan et al., 2004). Furthermore, splicing choices happen in a probabilistic manner, so individual neurons continuously change the cohort of Dscam1 isoforms that they express (Miura et al., 2013).

Together, these three properties of Dscam1 proteins have led to a model of how these recognition molecules mediate self-avoidance: Individual neurons produce a subset of Dscam1 isoforms and display them on their surface. These proteins act as a 'molecular barcode' on a given neuron's surface, allowing it to recognize its own processes but not the processes of its neighbors. Finally, signals downstream of

homophilic *trans* interactions between matching Dscam1 isoforms on neighboring branches of the same cell leads to repulsion. Because neighboring cells are unlikely to express the same set of Dscam1 isoforms on their surface, they are unlikely to repel each other (review by Zipursky and Grueber, 2013). This model is supported by several studies that have documented the function of *Dscam1* in dendritic and axonal patterning *in vivo*.

1.3.2.2 Self-avoidance defects in *Dscam1* mutants

The role of Dscam1 in dendritic self-avoidance has been studied best in da neurons in the Drosophila body wall. In Dscam1 null mutant da neurons (of any class), individual dendritic branches often cross over each other and clump, exhibiting defects in self-avoidance (Hughes et al., 2007; Matthews et al., 2007; Soba et al., 2007). Interestingly, heteroneuronal tiling within individual classes of da neurons is not perturbed in these mutants, reinforcing the model that dendritic branches must display the same cohort of isoforms to repel each other. Furthermore, forcing da neurons of different classes, which normally share receptive fields, to express the same single Dscam1 isoform induces repulsion between neighboring neurons. Thus, Dscam1 is necessary for self-avoidance of sister dendrites of single da neurons for all classes, and self/non-self discrimination between dendrites of different da neuron classes.

The diversity of Dscam1 is also required for proper segregation of axonal projections in the mushroom body in the Drosophila olfactory system. In this structure, mushroom body neurons normally extend axons into a region known as the peduncle, where they bifurcate and send projections into medial and lateral lobes of the mushroom body. While axon bifurcation itself does not require Dscam1, the faithful targeting of individual axons into the two lobes does. Axons of mushroom body neurons in Dscam1 null mutants still bifurcate, but then choose a lobe to grow into at random (Hattori et al., 2007; Wang et al., 2002a; Zhan et al., 2004). In this system, reducing Dscam1 diversity to a single isoform in single cells is sufficient for sister axonal branches to repel each other and grow into the medial and lateral lobes. However, expressing a single Dscam1 in a group of neurons causes many axons to target both of

their branches to the same lobe, likely because neighboring axons are unable to distinguish neighboring axons that express the same Dscam1 isoform from their own.

It is clear from these studies that a single arbitrarily chosen Dscam1 isoform is sufficient to induce self-avoidance of both da neurons and mushroom body neuron axons. What remained a mystery was how many isoforms were necessary to guarantee enough molecular diversity to mediate robust self/non-self discrimination between neighboring cells. Zipursky and colleagues addressed this question directly by systematically reducing the diversity of Dscam1 isoforms and assessing how well neurons were able to discriminate self from non-self. These studies led to the conclusion that thousands of Dscam1 isoforms are necessary for this process to occur reliably (Hattori et al., 2009).

1.3.3 Mammalian Pcdhs as candidate mediators of self-avoidance and self/non-self discrimination

In the mammalian nervous system, several neuronal classes including retinal starburst amacrine cells exhibit self-avoidance and self/non-self discrimination. What molecules may mediate these processes in mammals? Mammalian Dscam1 does not undergo extensive alternative splicing like its Drosophila homologue, suggesting that these molecules are ill-suited to mediate both self-avoidance and self/non-self discrimination. However, the mammalian genome contains another family of recognition molecules – the clustered Protocadherins (Pcdhs) – that are well suited to mediate this process. As described in chapter two of this thesis, these Pcdhs do indeed mediate self-avoidance and self/non-self discrimination in mammals in a manner very similar to the way Dscam1 proteins do in Drosophila.

1.3.3.1 Discovery and characterization of the clustered Protocadherins

Just two years prior to the discovery of the diverse Drosophila *Dscam1* locus, two groups identified and characterized the organization of a large family of cadherin-related molecules in vertebrates that are now known as the clustered Protocadherins. The initial discovery of clustered Pcdhs was made by Yagi and colleagues, who identified a subset of Pcdh isoforms and showed that they were expressed in the developing nervous system and localize to synapses (Kohmura et al., 1998). The entirety of the Pcdh

locus was described in the next year by Wu and Maniatis (1999). These authors showed that the Protocadherins discovered by Kohmura and Yagi belonged to a larger family of recognition molecules that contain around 50 isoforms that are arrayed in tandem on a single chromosome in both mice and humans (Wu and Maniatis, 1999; Wu et al., 2001). The large family of clustered Protocadherins can be subdivided further into subclusters – in mice, for example, the 58 isoforms are divided into 14 alpha-, 22 beta-, and 22 gamma-Protocadherins (Pcdha, Pcdhb, and Pcdhg, respectively). These subclusters can be subdivided even further: the 14 Pcdhas are divided into two groups – Pcdha1-12 and PcdhaC1 and C2, and the 22 Pcdhgs are divided into three groups – PcdhgA1-12, PcdhgB1-2 and B4-8, and PcdhgC3-C5. Interestingly, PcdhaC1-2 and PcdhgC3-5 are more similar to each other than to the other variable regions with their own clusters, and may have specialized functions. Each Pcdh is encoded by a single exon containing multiple alternative extracellular, transmembrane, and intracellular juxtamembrane domains which, for Pcdhas and Pcdhgs, is spliced to exons encoding a single common intracellular domain. Thus, the Pcdh proteins exhibit extracellular diversity but mostly identical intracellular components that can engage common signaling mechanisms. It is likely that the three Pcdh subclusters interact with one another in single cells, since they are co-expressed by individual neurons, and Pcdhgs may be necessary to bring Pcdhas to cell membranes (Kaneko et al., 2006; Murata et al., 2004). Unlike Dscam1 isoforms, which are generated through alternative splicing of a single transcript, expression of specific Pcdh isoforms is accomplished through alternative promoter choice: each Pcdh extracellular variable exon is preceded by its own promoter region. Transcription leads to the creation of a long pre-mRNA containing a variable exon immediately downstream of the chosen promoter, all subsequent variable exons, and the constant exons. Cis-splicing downstream of the first transcribed variable exon leads to generation of single Pcdh protein products (Tasic et al., 2002; Wang et al., 2002b).

1.3.3.2 Initial studies of Pcdh function in the nervous system

Before the studies documented in this thesis, the roles of Pcdhs in promoting dendritic or axonal self-avoidance in vertebrate neurons had not been recognized. Roles of these molecules in other

neurodevelopmental contexts, such as promoting axonal targeting, neuron survival, synapse formation, and dendritic branching, had been documented. This situation is analogous to that of Drosophila Dscam1, which also has other roles in neural development.

Pcdhas are required for axonal targeting. Genetic analysis of Pcdha mutant mice has revealed that these proteins are required for proper innervation of the olfactory bulb by olfactory sensory neurons and of various brain regions by serotonergic neurons (Hasegawa et al., 2008; Katori et al., 2009). These serotonergic neurons lack Pcdhg expression, so perhaps in these neurons, Pcdha delivery to neuronal membranes is done by Pcdhbs. This would create a symbiotic relationship between Pcdhas, which are incapable of trafficking to cell membranes alone, and Pcdhbs, which lack intracellular domains necessary for signaling.

Pcdhgs are required for neuronal survival, synaptic development, and dendritic branching. Of the three subcluster of Pcdhs, the best studied group is the Pcdhgs. Initial studies of Pcdhgs demonstrated that these molecules are crucially important for survival of both individual neurons and animals as a whole (Wang et al., 2002c). In Pcdhg mutant mice, neurons are generated, differentiate, and initially mature, but die subsequently, likely through activation of apoptotic pathways. This cell death occurs in a cell-type specific manner: while sensory and motor neurons in the spinal cord are spared in Pcdh mutants, many interneuron classes require Pcdhgs specifically for their survival (Prasad et al., 2008). Pcdhg-deficient animals probably die at birth is likely due to defects in spinal cord, but this is not the only brain region that requires Pcdhgs for survival. In the retina, which develops predominately after mice are born, many neuronal classes require Pcdhgs for survival during the first postnatal week (Lefebvre et al., 2008). The survival defects in retinal neurons are specific to populations that are born in supernumerary quantities: these neurons exhibit accentuated cell death in Pcdhg mutant retinas while neurons born in their correct numbers, such as SACs, are spared (Lefebvre et al., 2012). The survival-promoting function of Pcdhgs likely works through a common mechanism in the retina and spinal cord, as cell death is prevented in both regions in mice where apoptosis is genetically blocked (Lefebvre et al., 2008; Weiner et al., 2005). Not all Pcdhgs have an equal role in survival – the ubiquitously expressed PcdhgC3-5 isoforms

are preferentially required to mediate survival in both retina and spinal cord, while the differentially expressed PcdhgA1-3 are not (Chen et al., 2012).

Interestingly, while Pcdhgs have similar survival-promoting effects in retina and spinal cord, they are differentially required for synapse formation in these different regions. In retina, general aspects of circuit function are preserved in Pcdhg mutants (Lefebvre et al., 2008). In spinal cord, meanwhile, Pcdhgs promote synaptic development independently from their role in survival (Weiner et al., 2005).

In addition to survival and synapse formation, Pcdhgs are also important for dendritic arborization of cortical neurons and olfactory bulb granule cells. Recent studies have demonstrated that in the absence these molecules, layer 5 pyramidal neurons and olfactory granule cells exhibit reductions of dendritic complexity (Garrett et al., 2012; Ledderose et al., 2013).

The relationships between these different phenotypic roles of Pcdhgs remain mysterious. One possibility is that different intracellular signaling mechanisms within different neuronal classes allow for this diversity of function. However, it is rather puzzling that none of the phenomena described above critically require isoform diversity. It is possible, therefore, that all of the functions described above can be accomplished solely by the ubiquitous expression of a single Pcdhg or a small subset of redundant isoforms such as PcdhgC3-5. Individual variable Pcdhg exons contain a short intracellular juxtamembrane region, and it is possible that this intracellular region endows individual isoforms with differential functions such that some Pcdhgs are necessary for survival while others are not.

1.3.3.3 Pcdhs exhibit the three principles necessary for self-avoidance and self/non-self discrimination

Molecular diversity. As described above, the Pcdh locus encodes a relatively large family of recognition molecules. Variable extracellular, transmembrane, and juxtacellular Pcdhg domains are spliced onto common intracellular domains, suggesting that at least some of the signaling mechanisms downstream of Pcdhg activation are common. However, the diversity of Dscam1 is seemingly orders of magnitude larger than that of Pcdhs. How, then, could Pcdhs serve a function similar to Dscam1 with so few isoforms? The answer comes from studying interactions between neighboring Pcdhs. Biochemical

and expression studies have shown Pcdhs form cis-tetramers on the surface of individual cells, both within subclusters and across them (Murata et al., 2004; Schreiner and Weiner, 2010; Thu et al., 2014), and that this has implications for trans binding (see below). This multimerization increases the potential diversity of Pcdhs into the range of Dscam1 (Zipursky and Sanes, 2010).

Isoform specific binding. The homophilic binding specificity of Pcdhs has recently been described and expanded using cellular adhesion assays in two recent studies (Schreiner and Weiner, 2010; Thu et al., 2014). These adhesion studies have elucidated both the combinatorial logic and molecular domains required for Pcdh interactions. Each Pcdh variable exon encodes six unique extracellular cadherin-like (EC) repeats, a transmembrane domain. Unlike classical cadherins, whose binding relies on the most distal repeat, EC1, homophilic binding of Pcdhs in *trans* requires matching of EC2 and EC3. EC1 is still required for binding per se, but not for the specificity of the interactions. The specificity of Pcdh interactions is further increased by their ability to multimerize in *cis*. Thu et al. (2014) found that even mismatch of a single Pcdh isoform in cells transfected with five different Pcdhs led to substantial reduction in their ability to recognize each other. This additional level of specificity increases the potential Pcdh isoform modules substantially. It is important to note, however, that not all Pcdh isoforms behave in the same way. For example, several studies have argued that while Pcdha, Pcdhb, and Pcdhg proteins can multimerize, it appears the majority of Pcdha isoforms require co-expression of a Pcdhb or Pcdhg to reach the cell surface in heterologous systems (Murata et al., 2004; Thu et al., 2014). It remains to be seen whether this requirement holds *in vivo*, but this may explain why the most striking phenotypes of Pcdh mutant mice have been described for the Pcdhg locus.

Stochastic expression. As noted in the sections above, molecular diversity and homophilic binding are not useful for the acquisition of cellular individuality if all cells express the same set of binding modules. A series of studies by Yagi and colleagues have demonstrated that Pcdhs are indeed differentially expressed within seemingly homogeneous cell types. This has been described best in cerebellar Purkinje cells, which exhibit differential expression of Pcdhas, Pcdhbs, and Pcdhgs (Esumi et al., 2005; Hirano et al., 2012; Kaneko et al., 2006). While the majority of Pcdhs were shown to be

expressed stochastically and monoallelically in these studies, five isoforms – PcdhaC1-C2 and PcdhgC3-C5 were shown to be expressed biallelically by all Purkinje cells. As noted above, this subset of Pcdh isoforms are more inter-related than any of the other Pcdhs, and they may subserve functions different from the diversity-generating Pcdh isoforms. Extrapolating from the subsampling expression in these studies, the authors estimated that an individual Purkinje cell expresses around 7 unique Pcdh isoforms in addition to the commonly expressed isoforms. Thus, in a cell type that exhibits striking dendritic self-avoidance, individual neurons express unique subsets of Pcdh isoforms. How this cell-type specific expression occurs is still not completely understood but likely relies on DNA methylation of individual Pcdh promoters during embryonic development by the DNA methyltransferase Dnmt3b (Toyoda et al., 2014), preventing expression of the majority of Pcdh isoforms in any particular cell.

These three principles make mammalian Pcdhgs proteins well suited to generate molecular barcodes displayed on neuronal membranes to mediate self-avoidance and self/non-discrimination in vertebrate neurons with overlapping dendrites, just as Dscam1 proteins do in invertebrates (Zipursky and Grueber, 2013)**.** In chapters 2 and 3 of this thesis, I will describe the mechanism by which Pcdhgs mediate self-avoidance and self/non-self discrimination in mammalian retinal starburst amacrine cells and cerebellar Purkinje cells. The dendritic patterning of starburst amacrine cells is thought to be crucially related to their function – to detect directional motion. Starburst amacrine cells are not unique in their requirement of specific morphological characteristics to generate complex functional properties – this in fact a general principle in neurons. In the next section, I will discuss the implications and the diversity of dendritic processing and give an overview of the retinal direction-selective circuit and the roles of starburst amacrine cells therein.

1.4 Starburst amacrine cells and the retinal direction-selective circuit

Why do neurons go to great lengths to acquire specific morphological and functional characteristics? The answer is that the myriad shapes and sizes of neuronal dendrites offer an array of advantages for neuronal computations on a single-cell and network level (London and Hausser, 2005; Spruston, 2008). First, as discussed previously, outgrowth and uniform coverage of a neuron's territory by its processes allows it to maximize the potential number of different inputs it can receive or transmit (Zipursky and Grueber, 2013). Second, the arrangement of these processes permits compartmentalized processing of these different inputs, allowing individual branches to act as subunits of computation (Branco and Hausser, 2010; Euler and Denk, 2001). Third, the location of excitatory and inhibitory synaptic inputs within dendritic trees and the spatio-temporal sequence of their activation determines neuronal dynamics, network information processing, and even behavioral output (Branco et al., 2010; Gidon and Segev, 2012; Xu et al., 2012). All of these processes are accomplished by non-uniformities in both the morphology and the passive and active properties of dendrites that are set up by specific developmental mechanisms (Lefebvre et al., 2015; Vetter et al., 2001).

Thus, understanding how these structures are constructed during developmental will likely inform us about how and why neurons and circuits are capable of processing sensory information and guiding adaptive behavior. In the retina, the circuit that detects directional motion is perhaps the best understood of all and relies critically on starburst amacrine cell function (**Figure 1.5**) (Yoshida et al., 2001). Here, I will discuss our current understanding of how this fundamental computation is accomplished.

1.4.1 Discovery of direction-selective computation in the retina

From the earliest retinal recordings, it has been clear that this structure is not just taking a photograph of visual space (Gollisch and Meister, 2010; Hartline, 1938; Kuffler, 1953). Rather, the retina extracts salient features from the visual world and transmits this information to subsequent brain regions. Perhaps the best-described retinal computation is the directional spiking of retinal ganglion cells in response to visual motion (Vaney et al., 2012). This property refers to the tendency of some ganglion

Figure 1.5: The retinal direction-selective circuit

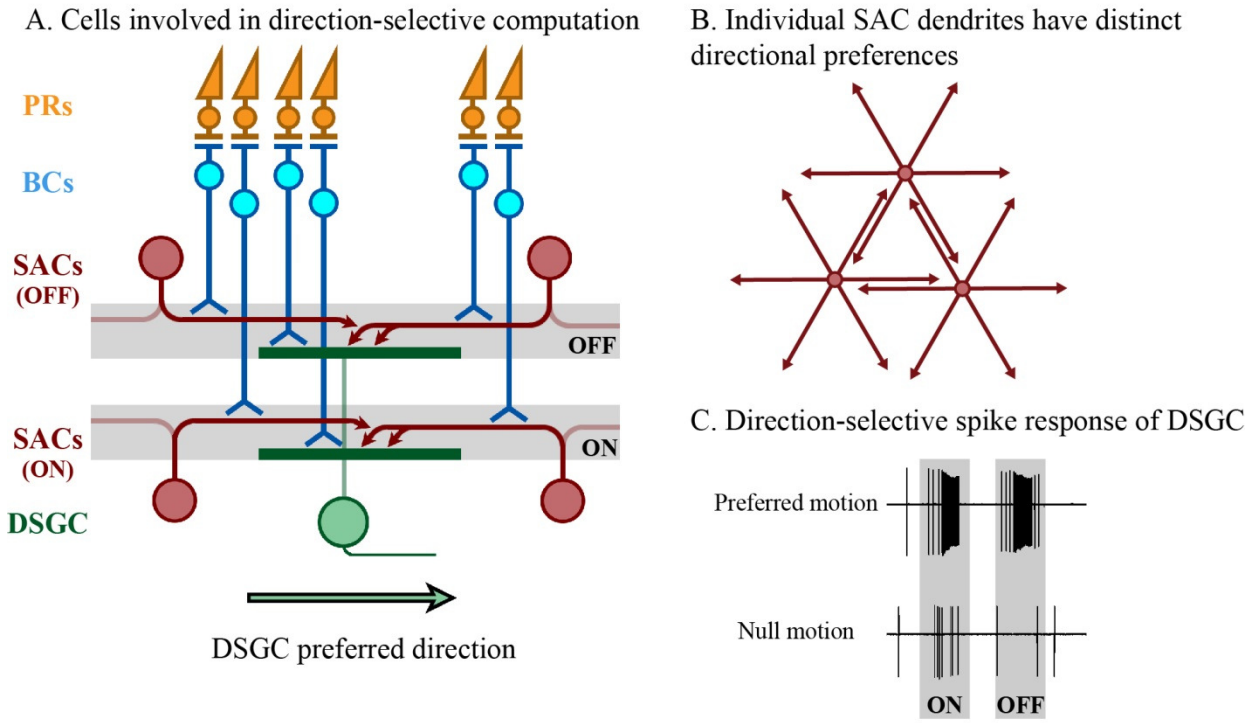

A. Directional responses of ON-OFF direction-selective ganglion cells (DSGCs) rely on integration of symmetrical excitation from bipolar cells (BCs) and asymmetric inhibition from starburst amacrine cells (SACs). This SAC-mediated inhibition sets the *null* direction of the DSGCs and is opposite to its *preferred* direction. SACs also exhibit mutual inhibition. Arrows denote direction of preference of individual cells.

B. Individual SAC dendrites compute directional motion independently. Dendrites of neighboring cells overlap extensively and can have opposing directional preferences.

C. DSGCs fire action potentials (spikes) in response to a bright bar entering (ON) and exiting (OFF) their receptive field when it is moving in their preferred direction, but not when it is moving in their null direction.

cells to fire many action potentials in response to a moving visual stimulus in one direction (defined as the *preferred* direction), but fire few action potentials to the same stimulus moving in the opposite direction (defined as the *null* direction). The discovery that such complex receptive fields exist just two synapses from photoreceptors was the first to challenge the conventional view that such computations are emergent properties of 'higher' visual centers.

Direction-selective retinal ganglion cells (DSGCs) were discovered and initially described in a series of studies by Barlow and colleagues in the rabbit retina (Barlow and Hill, 1963; Barlow and Levick, 1965). These authors documented several important functional properties of these cells and showed that they come in several different subtypes. Some cells were found to fire action potentials (spikes) to both the entrance and exit of bright objects moving through their receptive fields (called ON-OFF DSGCs), while other cells responded only to bright edges in this stimulus paradigm (called ON DSGCs) (Barlow et al., 1964). The directional preferences and speed tuning responses of these ON-OFF DSGCs and ON DSGCs were different. ON DSGCs were direction-selective for slow image motion and had large receptive fields, while ON-OFF DSGCs were selective over a large range of image speeds and had smaller receptive fields (Oyster, 1968; Oyster and Barlow, 1967; Wyatt and Daw, 1975). Furthermore, ON-OFF DSGCs come in four types that each responded preferentially to one of the four cardinal body axes, superior, inferior, anterior, and posterior, while ON DSGCs respond to three directions, sharing superior and splitting the rest into thirds. These differences in spatial selectivity and speed tuning may be related to the differing roles of ON-OFF and ON DSGCs in visual function. While ON-OFF DSGC axons project to image forming visual areas (Hong et al., 2011), ON DSGC axons project mainly to the accessory optic system that mediates visual reflexes (Simpson, 1984; Yonehara et al., 2009). Throughout the rest of this chapter, I will mainly discuss ON-OFF DSGCs and refer to these cells just as DSGCs.

1.4.1.1 Insights into the mechanism of retinal direction-selectivity from initial spike recordings

In addition to characterizing the nature of the directional responses of DSGCs, Barlow and Levick (1965) also gained fundamental insights into the cellular and synaptic mechanism of this computation. Using small probing spots, these authors discovered two aspects of directional responses that are fundamental to this retinal computation. First, DSGCs are capable of detecting directional motion over small portions of their total receptive fields, suggesting that the presynaptic circuitry that mediates direction selectivity is composed of small repeating 'subunits' that are independent from one another. Second, when two spots are shown in a spatio-temporal sequence that mimics preferred motion, the response of DSGCs is only slightly greater than the response to each stimulus shown independently. However, when a sequence that mimics null motion is shown, the cumulative response is substantially smaller than the response to these two stimuli in isolation. Thus, these authors inferred that direction-selectivity of DSGCs results from an inhibitory mechanism that vetoes excitation specifically for null motion. The mechanism and circuitry of retinal direction-selectivity has been a topic of study ever since these initial discoveries. We now know that this computation relies specifically on excitatory inputs from bipolar cells and inhibitory inputs from starburst amacrine cells (SACs).

1.4.2 Starburst amacrine cells mediate directional inhibition of direction-selective ganglion cells

The cellular source of the asymmetric inhibition that mediates the direction-selective responses of DSGCs was not obvious from these initial action potential recordings. However, the role of SACs in this computation has been documented through a series of anatomical, functional, and ablation studies (**Figure 1.5**).

1.4.2.1 SACs and DSGCs laminate and fasciculate together

In the 1980s, Masland and colleagues discovered that a subset of retinal amacrine cells expressed acetylcholine (ACh) (Hayden et al., 1980). The cell bodies of these amacrine cells were found in a mirror symmetric arrangement on either side of the IPL (in the INL and GCL) and their processes were arranged in a mirror symmetric arrangement in the upper and lower portions of the IPL, representing an OFF and

ON populations of neurons (Masland et al., 1984a; Masland et al., 1984b; Vaney et al., 1981). Anatomical studied of individual showed that these cholinergic neurons are a single neuronal class that exhibit 'starburst' morphology, hence their name (Famiglietti, 1983; Vaney, 1984). As a population, these neurons formed a highly non-random plexus of processes with areas of denser coverage and holes on the order of 20 µm (Tauchi and Masland, 1985).

Concurrent with these studies, the laminar restriction of DSGCs was also described. The dendrites of DSGCs are bistratified, with a set of dendrites each in the OFF and ON portions of the IPL that accounts for their ON-OFF responses (Amthor et al., 1984). Subsequently, several studies demonstrated that the laminae of the IPL occupied they OFF and ON SACs and the two sets of DSGC dendrites were in fact the same (Famiglietti, 1987, 1992; Vaney and Pow, 2000). Furthermore, within each of these laminae, the dendrites of DSGCs fasciculated on the plexus formed by SAC dendrites. The close association between SACs and DSGCs suggested that these amacrine cells may be the key cells that endow DSGCs with their selectivity. However, this hypothesis was perplexing for several reasons. First, how could a neuron that synthesizes and presumably releases an excitatory neurotransmitter, ACh, mediate a function that clearly requires inhibition? Second, how could this same neuron, which shows no obvious morphological asymmetry, mediate a function that is inherently asymmetric? Finally, if SACs did compute directional motion and transmit this information to DSGCs, how did they perform this computation?

1.4.2.2 SACs co-release ACh and GABA

The answer to how cholinergic neurons could be inhibitory is simple. Like many neurons throughout the nervous system, SACs are dual-transmitter neurons that release both ACh and GABA (O'Malley and Masland, 1989; O'Malley et al., 1992). This co-release happens from the same neurons (meaning there are not multiple populations of SACs) and can happen onto the same postsynaptic DSGC (Lee et al., 2010).

1.4.2.3 The geometry of connections between SACs and DSGCs is specific

Like many amacrine cells in the retina, there is not a clear distinction between the axons and dendrites of SACs. These cells receive excitatory inputs over their whole dendritic arbor, and release neurotransmitter from the distal portion of these same dendrites (Famiglietti, 1991), so the overlap between the distal dendrites of a given SAC and DSGCs are potentially predictive of where they may form synaptic connections. However, several physiological and anatomical studies have shown that, at the level of light microscopy, dendritic overlap is not predictive of connectivity between these two cell classes. To understand these findings, it is necessary to understand that individual SAC dendrites are independent direction-selective subunits that prefer motion moving along their proximo-distal axis (towards their output synapses). I will elaborate on this point in the next section.

Analysis of SAC-DSGC connectivity using paired electrophysiological recordings demonstrated that SACs make GABAergic connections with DSGCs in specific geometric arrangements. The size of synaptic conductances between a SAC whose soma is on the preferred side of a DSGC is substantially smaller than that of an equidistant SAC whose soma is on the null side of a DSGC (Fried et al., 2002). Interestingly, this asymmetric inhibition is not present in the first postnatal week in mice, but the size of inhibition from SACs on the null side of a DSGC increase substantially in the second postnatal week (Wei et al., 2011; Yonehara et al., 2011). This increased inhibitory synaptic conductance could be due to a strengthening of connections or an addition of many new connections.

The more likely explanation is the latter, as demonstrated by Briggman et al., (2011). In this comprehensive study, the authors identified DSGCs and their preferred directions in retinal explants using a combination of visual stimulation and calcium imaging of neural activity then used serial section electron microscopy to identify putative presynaptic partners of the same DSGCs. They demonstrated in full detail that there is a geometric rule of connectivity between SACs and DSGCs. From the DSGC's perspective, if it prefers a particular direction (for example superior), then the putative synaptic contacts that it receives from SAC dendrites that point in the opposite direction (in this case inferior). Thus, the dendritic orientation (proximo-distal axis) of a SAC dendrite is the same as the DSGC's null direction,

consistent with inhibitory input from SACs setting this null direction. These data are also consistent with the initial paired recordings described above, because the SAC dendrites that connect in this arrangement are most often going to have somata displaced to the null side of the DSGCs with which they connect. Furthermore, these data provide a cellular substrate for the 'subunits' of direction selectivity described in the initial reports of this phenomenon (Barlow and Levick, 1965). From the SAC's perspective, each quadrant of a cell's dendrites makes connections preferentially with DSGCs that prefer the opposite direction. Thus, the connectivity from SAC dendrites of particular orientations sets the inhibitory null direction of each particular class of DSGCs (Briggman et al., 2011).

1.4.2.4 Individual SAC dendrites are direction-selective subunits

The independent computation of directional motion in SAC dendrites was first demonstrated by Euler et al., (2002). Using a combination of visual stimulation and two-photon calcium imaging, these authors recorded directional signals at the tips of individual SAC dendrites that were aligned to the proximo-distal axis of each branch. Because this is the location of synaptic outputs of SACs, it suggested that transmitter release from SACs is directional. This finding, combined with the asymmetry of SAC-DSGC connectivity described above, have yielded a comprehensive understanding of the cellular and synaptic mechanisms than generate the asymmetric inhibitory receptive field of DSGCs. Importantly, ablation of SACs completely abolishes directional responses in DSGCs and reflexive behaviors that are thought to depend on directional motion detection (Yoshida et al., 2001). Despite this initial characterization of these directional responses in SAC dendrites, it is still not totally clear how individual SAC dendrite acquire their response specificity. Recent studies have tried to address this question and found evidence for both intrinsic and synaptic mechanisms that isolate individual SAC dendritic branches and endow them with direction-selective responses.

Passive properties of SAC dendrites. The direction-selective output in SACs can be explained at least in part by the continuous distribution of excitatory synaptic inputs and distal localization of synaptic outputs on SAC dendrites (Famiglietti, 1991). This specificity results in summation of depolarization in

distal dendrites (where release sites reside) for proximo-distal motion and summation in proximal dendrites (which have no release sites) for disto-proximal motion. An important feature of this mechanism is its implicit requirement for SAC dendrites to be radial, so that excitation from bipolar cells is able to activate successive dendritic segments sequentially.

Active properties of SAC dendrites. In addition to this passive cable property, there is evidence that SAC dendrites also have active conductances – voltage-gated calcium and sodium channels – that amplify these passive properties (Hausselt et al., 2007; Oesch and Taylor, 2010). SACs may also have differential sensitivity to inhibition along the proximo-distal axis of individual dendrites due to asymmetric distribution of chloride co-transporters (Gavrikov et al., 2006). The independent computation of individual SAC dendrites is possibly facilitated by specific localization of inwardly rectifying potassium channels to their proximal dendritic branches (Ozaita et al., 2004). This process is thought to act an electrical shunt for signals moving in the disto-proximal axis of individual SAC dendrites and also explain the disparity between direction-selective calcium signals in SAC dendritic tips and the lack of voltage-dependent calcium signals in SAC somata (Euler et al., 2002; Ozaita et al., 2004). While there is good evidence that these active mechanisms are present in SACs, a clear demonstration that they are required for some aspect of retinal direction-selectivity computation is lacking.

Excitatory inputs onto SACs. The temporal properties of different bipolar cell classes differ systematically with terminal depth in the IPL. Faster bipolar cells terminate their axonal projections in the middle of the IPL and slower bipolar cells terminate closer to the borders of the INL and GCL (Baden et al., 2013). Thus, bipolar cells have mirror-symmetric response properties that could be used by OFF and ON SACs to sum excitation in their distal processes. While the distal summation of depolarization in SAC dendrites does not require differences in the timing of excitatory inputs, recent connectomic reconstruction of such excitatory inputs and SAC dendrites have hinted at such an arrangement. SAC dendrites show a small but significant tilt towards the middle of the IPL, such that their proximal terminals overlap more with slower classes of bipolar cells and their distal processes overlap more with faster classes of bipolar cells (Kim et al., 2014). This arrangement could, in principle amplify the passive

propagation of excitation in SAC dendrites and lead to preferential summing in distal dendrites. However, these reconstructions were done using an electron-microscopic preparation that lacked intracellular detail so synaptic terminals were not evident. The correlation between membrane appositions and synaptic contacts is a tenuous one, so further functional measurements of the bipolar cell transmission onto SAC dendrites will be necessary to show that this mechanism is actually employed in SACs.

Inhibitory inputs onto SACs. The predominant source of inhibition onto SAC dendrites is thought to come from other SACs (Helmstaedter et al., 2013; Vaney et al., 2012). This evidence comes from paired recordings between SACs that have demonstrated that monosynaptic GABAergic connections are present between these cells (Lee and Zhou, 2006), and receptive field mapping of visually-evoked inhibition on SACs, which has the correct size characteristics to originate from other SACs (Taylor and Wassle, 1995). Interestingly, while connections between SACs and DGCs are both cholinergic and GABAergic, SAC-SAC connections are exclusively GABAergic in adult animals (Zheng et al., 2004).

For SAC-SAC inhibition to enhance the direction-selectivity of SAC dendrites, these connections would have to have specific dendritic geometries. Connections between SACs with closely-spaced somata, whose dendrites would be parallel to each other, would be counter-productive for the generation of directional signals, since dendrites with similar preferences would inhibit each other. Conversely, connections between SACs whose somata are further away from each other would boost directional responses because inhibition would occur between dendrites with antiparallel preferences (Taylor and Smith, 2012). Initial paired recordings between SACs did not document any distance-dependence to these connections (Lee and Zhou, 2006); however, the studies described in chapter 3 argue that SAC-SAC connections in adult mice are specifically antiparallel. A likely explanation for the disparity between these results is the age at which these experiments were done and possible differences between rabbit retinas used for these initial studies and mouse retinas used in my studies.

1.4.2.5 Integration of excitatory and inhibitory inputs in DSGCs

The mechanisms by which excitation and inhibition are integrated in DSGCs to generate direction-selective spiking responses have been studied extensively. While it has been debated whether DSGCs receive both asymmetric excitatory and inhibitory inputs or just asymmetric inhibitory inputs, recent direct measurements of excitatory neurotransmitter release onto DSGCs has demonstrated that this input is not directional (Park et al., 2014; Yonehara et al., 2013). The discrepancy between these recordings and earlier recordings of DSGCs may be due to voltage-clamp errors resulting in these initial studies (Vaney et al., 2012). This hypothesis is further substantiated by action-potential recordings from DSGCs that have shown that cholinergic excitation facilitates spiking responses in all directions equally (Chiao and Masland, 2002). Thus, the predominant mechanism that generates direction-selective spiking in DSGCs is integration of non-directional excitation and directional inhibition.

As described earlier in this chapter, directional motion is computed in small subfields within a DSGCs whole receptive field (Barlow and Levick, 1965). From this initial finding, we may infer two things about the responses of DSGCs that have been subsequently shown to be true. First, the ON and OFF dendrites of DSGCs are computed independently. Older pharmacological and more recent genetic studies have shown that this is indeed the case (Duan et al., 2014; Kittila and Massey, 1995). Secondly, DSGCs may have active conductances that generate dendritic spikes at the scale of individual 'subunits' described by Barlow and Levick. This has also been confirmed using a combination of pharmacology, calcium imaging, and direct dendritic recordings (Oesch et al., 2005; Sivyer and Williams, 2013). Thus, DSGCs likely use the asymmetric inputs they receive from SAC dendrites to veto bipolar cell excitation and spike generation locally in their dendrites.

1.4.3 Functional direction-selective circuitry is assembled during the first two postnatal weeks in mice

The establishment of this multilayered direction-selective circuit in the retina requires a series of active developmental processes. This circuit is already functional at eye opening, but this depends on a rapid maturation of this circuit in the second postnatal week (eye opening is around postnatal day [P]14 in mice). Connections between SACs and DSGCs are present by P4, but they lack the asymmetry of

adulthood at this stage (Wei et al., 2011). Furthermore, the role of SACs before eye opening is fundamentally different than that in adulthood. At these earlier stages, SACs are responsible for the initiation and propagation of retinal waves and transmit non-selective excitatory signals to each other and RGCs (Feller et al., 1996; Zheng et al., 2006). These retinal waves have a fundamental role in the segregation and refinement of visual outputs in retinorecipient areas (Ackman and Crair, 2014). The termination of SAC-mediated cholinergic retinal waves in this second postnatal week corresponds with two other important changes in SACs. First, SAC dendrites undergo substantial dendritic outgrowth and remodeling during this week, transforming from small bushy branches lacking self-avoidance to their adult form (Stacy and Wong, 2003). Second, this time period is when the chloride gradient that makes GABAergic transmission inhibitory is established (Barkis et al., 2010). Thus, at eye opening in mice, SACs have acquired their adult morphology and connectivity to DSGCs and are ready to inhibit them during null motion (Wei et al., 2011; Yonehara et al., 2011). SAC-SAC connections also go through a transformation during in the week prior to eye opening. While SAC-SAC connections are excitatory during retinal waves and propagated through both cholinergic and GABAergic transmission, as described above, these connections are exclusively GABAergic at eye opening (Zheng et al., 2004).

In summary, direction-selective responses in the retina arise through a combination of morphological maturation and synaptic specificity. Understanding the developmental processes that assemble this circuitry is therefore of utmost importance for understanding how SAC dendrites and DSGCs perform this computation.

1.4.4 Direction-selectivity is a universal neural computation

Perception of motion and direction are fundamental neural computations (Maunsell and Newsome, 1987). It is likely that the retinal inputs to higher visual areas form the basis of this perception; direction-selective visual responses have been described throughout the visual system and likely depend on retinal direction-selective computation (Cruz-Martin et al., 2014; Rochefort et al., 2011). The

fundamental nature of these computations is made evident by their existence across sensory areas, such as the auditory and somatosensory systems (Kuo and Wu, 2012; Rutlin et al., 2014) in vertebrates and across phyla (Borst and Euler, 2011). It is likely that the principles that organize this computation in the mammalian retina will teach us about how this computation occurs and is used in these other systems.

1.5 Description of research

The focus of the research presented here is to understand the mechanisms that organize cell classes into functional circuits. Specifically, I have addressed the molecular mechanisms by which neuronal dendrites in the mammalian brain exhibit self-avoidance and self/non-self discrimination and how these morphological phenomena mediated neuronal computation.

In Chapter 2 of this thesis, I will describe how the clustered gamma-Protocadherin family of cellular recognition molecules mediates dendritic self-avoidance and self/non-self discrimination in mammalian retinal starburst amacrine cells and cerebellar Purkinje cells.

In Chapter 3, I will describe the roles of dendritic self-avoidance and self/non-self discrimination in these starburst amacrine cells for the function of the retinal direction-selective circuit. I will show that both of these phenomena are required for this neural computation, but that they are required in different ways. Self-avoidance is necessary for strong directional tuning and proper directional tuning, while self/non-self discrimination

In Chapter 4, I will describe our initial efforts to understand the interactions between the alpha and gamma-Protocadherins in the nervous system using novel genomic modification techniques.

Chapter 2: Protocadherins mediate dendritic self-avoidance in the mammalian nervous system

Preface:

The work presented in this chapter was a collaboration between Julie Lefebvre, a former postdoctoral fellow in the Sanes lab, and me. Julie Lefebvre made the initial discovery that Protocadherins mediate dendritic self-avoidance in retinal starburst amacrine cells. I joined this project soon after this initial discovery and validation. Julie performed the viral histology of adult starburst amacrines, cell culture experiments, expression profiling of Protocadherins in retinal neurons, and made the Protocadherin single isoform mice. I performed the developmental studies of starburst amacrine cells, dye-filling of starburst amacrine cells, and analysis of heteroneuronal interactions between neighboring cells. Julie and I performed the cerebellar Purkinje cell experiments and analysis together. Weisheng Chen and Tom Maniatis provided two strains of mutant mice with decreased Protocadherin diversity. The studies presented here resulted in a publication:

Lefebvre, J.L., Kostadinov, D., Chen, W.V., Maniatis, T., and Sanes, J.R. (2012). Protocadherins mediate dendritic self-avoidance in the mammalian nervous system. Nature *488*, 517-521.

This manuscript was written and prepared by Julie Lefebvre, Josh Sanes (our supervisor), and me. This chapter appears much as the paper looks in press with a few minor changes. I have broken up the main text into sections and modified the presentation of figure panels slightly. I have also combined the main and supplementary figures so that they appear in the same sequence as they are referred to in the text. These changes do not alter the publication in any substantive way and are done for stylistic consistency throughout this thesis.

2.1 Abstract

Dendritic arborizations of many neurons are patterned by a process called self-avoidance, in which branches arising from a single neuron repel each other (Grueber and Sagasti, 2010; Hughes et al., 2007; Kramer and Kuwada, 1983; Matthews et al., 2007; Montague and Friedlander, 1989; Soba et al., 2007; Zipursky and Sanes, 2010). By minimizing gaps and overlaps within the arborization, self-avoidance facilitates complete coverage of a neuron's territory by its neurites (Grueber and Sagasti, 2010; Kramer and Kuwada, 1983; Montague and Friedlander, 1989). Remarkably, some neurons that display self-avoidance interact freely with other neurons of the same subtype, implying that they discriminate self from non-self. Here, we demonstrate roles for the clustered protocadherins (Pcdhs) in dendritic self-avoidance and self/non-self discrimination. The *Pcdh* locus encodes 58 related cadherin-like transmembrane proteins, at least some of which exhibit isoform-specific homophilic adhesion in heterologous cells and are expressed stochastically and combinatorially in single neurons (Kaneko et al., 2006; Kohmura et al., 1998; Schreiner and Weiner, 2010; Wu and Maniatis, 1999; Zipursky and Sanes, 2010). Deletion of all 22 *Pcdh* genes in the mouse γ-subcluster (*Pcdhg* genes) disrupts self-avoidance of dendrites in retinal starburst amacrine cells (SACs) and cerebellar Purkinje cells. Further genetic analysis of SACs showed that Pcdhg proteins act cell-autonomously during development, and that replacement of the 22 Pcdhg proteins with a single isoform restores self-avoidance. Moreover, expression of the same single isoform in all SACs decreases interactions among dendrites of neighboring SACs (heteroneuronal interactions). These results suggest that homophilic Pcdhg interactions between sibling neurites (isoneuronal interactions) generate a repulsive signal that leads to self-avoidance. In this model, heteroneuronal interactions are normally permitted because dendrites seldom encounter a matched set of Pcdhg proteins unless they emanate from the same soma. In many respects, our results mirror those reported for *Dscam1* (*Down syndrome cell adhesion molecule*) in *Drosophila*: this complex gene encodes thousands of recognition molecules that exhibit stochastic expression and isoform-specific interactions, and mediate both self-avoidance and self/non-self discrimination (Hattori et al., 2009; Hughes et al., 2007; Matthews et al., 2007; Neves et al., 2004; Soba et al., 2007; Wojtowicz et al., 2004; Zhan et al.,

2004; Zipursky and Sanes, 2010). Thus, although insect Dscam and vertebrate Pcdh proteins share no sequence homology, they seem to underlie similar strategies for endowing neurons with distinct molecular identities and patterning their arborizations.

2.2 Introduction

The 58 genes of the mouse *Pcdh* locus are tandemly arranged in α-, β- and γ-subclusters, called *Pcdha, Pcdhb* and *Pcdhg*, which encode 14, 22 and 22 cadherin-like proteins, respectively (Wu and Maniatis, 1999) (**Figure 2.1A**). In the *Pcdha* and *Pcdhg* subclusters, single variable exons encoding extracellular, transmembrane and juxtamembrane domains are spliced to three constant exons, generating proteins with unique extracellular but common intracellular domains (Wu and Maniatis, 1999). The complexity of this locus is reminiscent of that of *Dscam1*, which mediates self-avoidance in *Drosophila* (Hattori et al., 2009; Hughes et al., 2007; Matthews et al., 2007; Soba et al., 2007; Zipursky and Sanes, 2010). Moreover, *Pcdh* genes, like *Dscam1*, exhibit stochastic expression, and both Pcdhg and Dscam proteins exhibit isoform-specific homotypic recognition (Neves et al., 2004; Wojtowicz et al., 2004). In contrast, the two vertebrate *Dscam*s are not complex genes, so although they mediate both repulsive and attractive interactions among neurons (Fuerst et al., 2009; Fuerst et al., 2008; Sanes and Zipursky, 2010; Yamagata and Sanes, 2008), they are unlikely to underlie self/non-self discrimination. We therefore investigated roles of *Pcdh* genes in these processes.

Previous studies of mouse mutants lacking all 22 *Pcdhg* genes revealed that they are required for survival of multiple neuronal types (Lefebvre et al., 2008; Prasad et al., 2008; Wang et al., 2002c; Weiner et al., 2005). To seek roles of Pcdhgs in self-avoidance, we focused on a retinal interneuron, the SAC, which expresses *Pcdhg* genes (Lefebvre et al., 2008) and exhibits marked dendritic self-avoidance (Stacy and Wong, 2003). Radially symmetric SAC dendritic arborizations are confined to narrow planes within the inner plexiform (synaptic) layer; SACs have no axons. Dendrites of a single SAC seldom cross one another, yet dendrites of neighboring SACs cross freely (**Figures 2.1A-B and Figure 2.2**) and even form synapses with each other (Lee and Zhou, 2006; Stacy and Wong, 2003), suggesting that they can distinguish ‘self’ from ‘non-self’.

Figure 2.1: Pcdhgs are required for self-avoidance of SAC dendrites

A. *Pcdh* locus comprises *Pcdha, Pcdhb* and *Pcdhg* subclusters. *Pcdha* and *Pcdhg* isoforms are assembled by splicing of one variable exon encoding extracellular (ECD) and transmembrane domains to three constant exons encoding the intracellular domain (ICD).

B. SACs are present in both the inner nuclear layer (INL) and the ganglion cell layer (GCL) and extend dendrites that form radially symmetrical arborizations confined to thin sublaminae in the inner plexiform layer (IPL).

C. SAC dendrites avoid isoneuronal dendrites (red) but interact heteroneuronally with other SACs (blue), forming synapses on their dendrites.

D-I. Morphology of a single SAC, labelled with membrane-Cherry, in the GCL in control and *Pcdhg* mutant retinas. Wild-type SAC dendrites self-avoid. In *Pcdhg* mutants, self-avoidance defects include self-crossing and bundling of dendrites. Crossings are detected at 0.2 μm *x–y* resolution in single 0.8-μm optical sections (E, G, I show magnified views of boxed areas in D, F, H). Images with 0.2 μm *z* resolution are shown in **Figure 2.2**.

J. SAC dendritic self-crossings in first–fifth order branches per SAC. Graph underestimates difference between genotypes because the most severely affected mutant SACs could not be scored. $^{**}P < 0.01$.

K-L. Number of terminal branches (K) and dendritic field diameter (L) do not differ between wild-type and mutant SACs.

Panels J-L show means ± s.e.m.; $n = 8$ cells from 5–6 animals per genotype. Scale bars, 50 μm (D, F, H) and 10 μm (E, G, I).

(Figure continues on next page)

Figure 2.1 (continued)

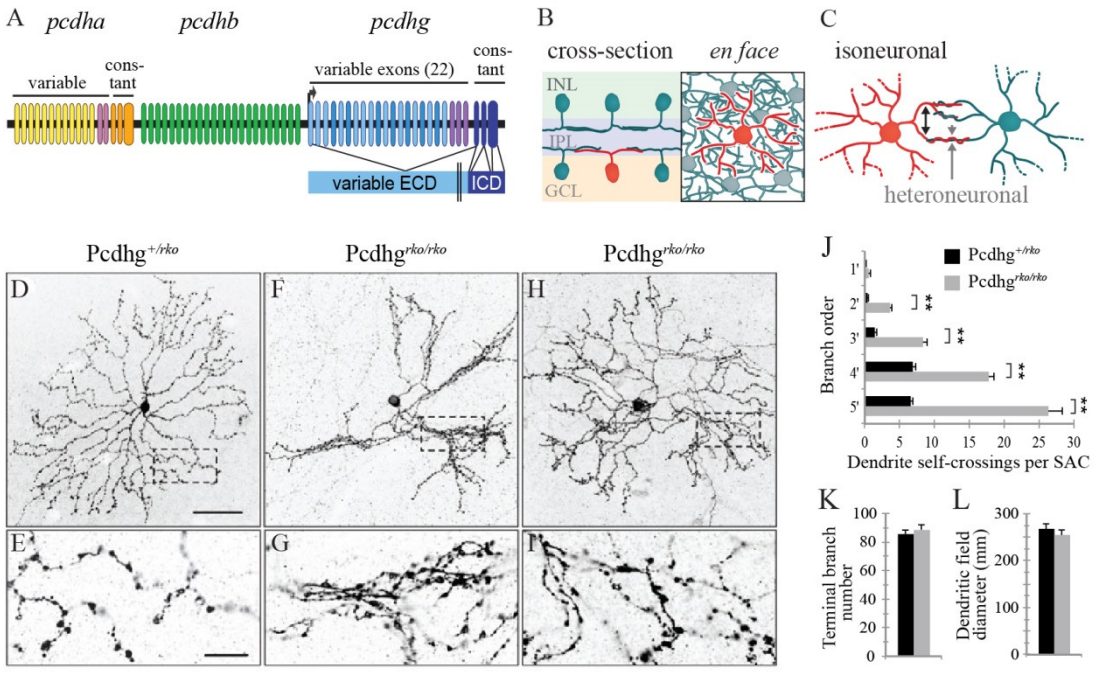

Figure 2.2: Heteroneuronal association between neighboring SAC dendrites

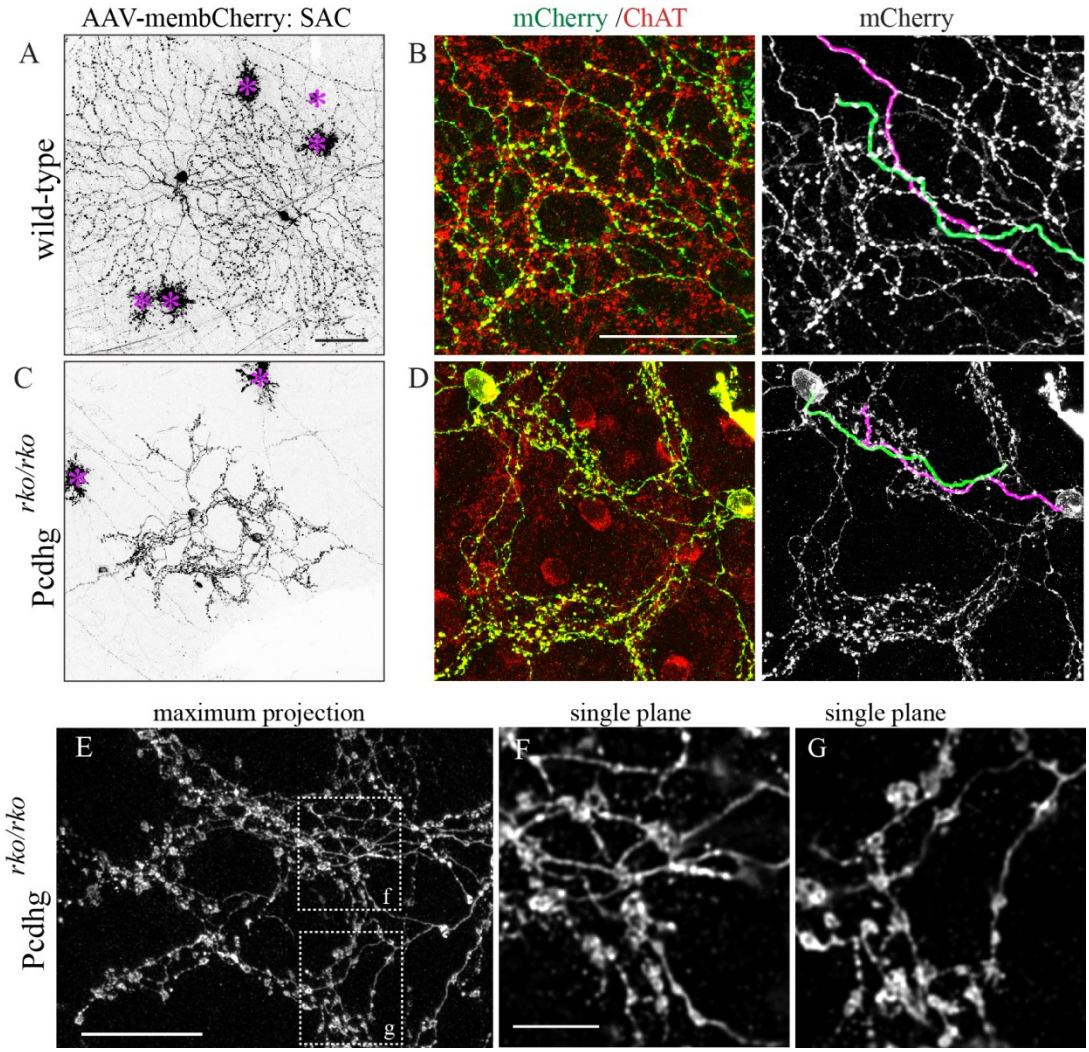

A. Dendrites of two labeled neighboring sacs that overlap extensively in wild-type retina.

B. Distal dendrites of two labeled sacs (green) freely overlap and associate with the chat labeled SAC plexus (red). Right panel, tracing of single distal dendrites arising from 2 SACs (green for one and magenta for the other) demonstrates overlap between heteroneuronal dendrites.

C-D. s in **A and B**, but in mutant *Pcdhgrko/rko* retina.

E-G. Images acquired at Nyquist limit resolution by oversampling and processing by deconvolution (see Online Methods for software) show crossings of *Pcdhgrko/rko* SAC dendrites in single optical sections. Scale bars, 50 μm in **A-D**, 20 μm in **E**, and 5 μm in **F,G**.

* Asterisks denote non-SAC labeled neurons.

2.3 Results

We used a conditional mutant (*Pcdhg*^{fcon3}) (Lefebvre et al., 2008) to bypass the neonatal lethality of constitutive *Pcdhg* mutants and employed Cre drivers that delete *Pcdhg* genes from all or subsets of retinal cells. We visualized individual neurons by infection with recombinant adeno-associated virus (rAAV) expressing a fluorescent protein (XFP; **Figure 2.1D-E**), biolistic delivery of DNA encoding XFP, or intracellular injection of a fluorescent dye. We identified SACs, the sole cholinergic neurons in retina, with antibodies to choline acetyltransferase (ChAT), which also demonstrated the association of XFP-positive SAC dendrites with dendrites from other (XFP-negative) SACs (**Figures 2.2 and 2.3**).

2.3.1 Pcdhgs are required for self-avoidance of SAC dendrites

SAC morphology was profoundly altered in *Pcdhg* mutant retinas (*Pcdhg*$^{fcon3/fcon3}$*; retina-cre*, called *Pcdhg*$^{rko/rko}$ here; see Methods for genotypes). Dendrites arising from a single SAC frequently crossed each other and sometimes formed loose bundles (**Figure 2.1F-I and Figure 2.2**). Crossing frequency was increased several-fold in both proximal and distal regions of the arborization (**Figure 2.1J**). These defects were highly specific, in that the diameter of SAC arborizations, the number of dendritic termini, the laminar targeting of SAC dendrites, and the mosaic arrangement of SAC bodies were all unaffected in *Pcdhg*$^{rko/rko}$ mutants (**Figures 2.1K-L, 2.2, and 2.3**). Thus, Pcdhgs are dispensable for many aspects of SAC morphogenesis but are required for their self-avoidance.

In the absence of *Pcdhg* genes, neurons of many types die in elevated numbers during the period of naturally occurring cell death (Lefebvre et al., 2008; Prasad et al., 2008; Wang et al., 2002c; Weiner et al., 2005). Although SACs are largely spared in *Pcdhg* mutants (Lefebvre et al., 2008), their dendritic defects might be secondary to loss of other neurites with which they ordinarily interact. To test this possibility, we blocked apoptosis by deleting the *Bax* gene, which is required for naturally occurring and *Pcdhg*-dependent neuronal death (Lefebvre et al., 2008; Weiner et al., 2005; White et al., 1998). SAC morphology was normal in *Bax*$^{-/-}$ mice, but self-avoidance defects persisted in *Bax*$^{-/-}$; *Pcdhg*$^{rko/rko}$ double mutants (**Figure 2.4**).

Figure 2.3: Laminar targeting, density, and mosaic arrangement of SACs are unaffected in the absence of Pcdhgs

A-**B**. Cross-section of wild-type and *Pcdhg*$^{rko/rko}$ retina labeled with nuclear marker Popro1 and SAC marker ChAT. ChAT-positive SAC somata reside in INL (inner nuclear layer) and GCL (ganglion cell layer) and processes target and ramify in appropriate sublaminae in control (**A**) and in mutant *Pcdhg*$^{rko/rko}$ retina (**A**). Reduced INL and IPL in mutant are due to elevated loss of interneurons and RGCs (see Lefevbre et al., 2008).

C-F.In the INL and GCL, SACs stained with ChAT reveal mosaic arrangements of SAC somata in flatmount preparations of wild-type and *Pcdhgrko/rko* mutant retinas. Scale bars, 50 μm.

G. Mosaic spacing of SAC arrays in INL as measured by Density recovery profiles (DRPs). DRP graph shows the density of somata present in a ring of radius *x* from each cell. Dashed line is mean density for whole image and represents a random distribution. Mosaic spacing is marked by an exclusion zone, which is represented here as the distance between the observed and random distributions. DRPs do not differ between wild-type (black) and mutants (blue).

H-I. SAC density and packing factor (a regularity index ranging between 0 [a randomly distributed array] and 1 [a perfect hexagonal array]) in INL in mutants were indistinguishable from wild-type.

J-L. SAC DRPs (**J**), density (**K**) and packing factor (**L**) in GCL did not differ between mutants (blue) and wild-type (black). n.s., not significant, by Student's *t* test. All data are mean ± x s.e.m. WT, n=9 from 2 animals; mutant, n =14, 4 animals.

(Figure continues on next page)

Figure 2.3 (continued)

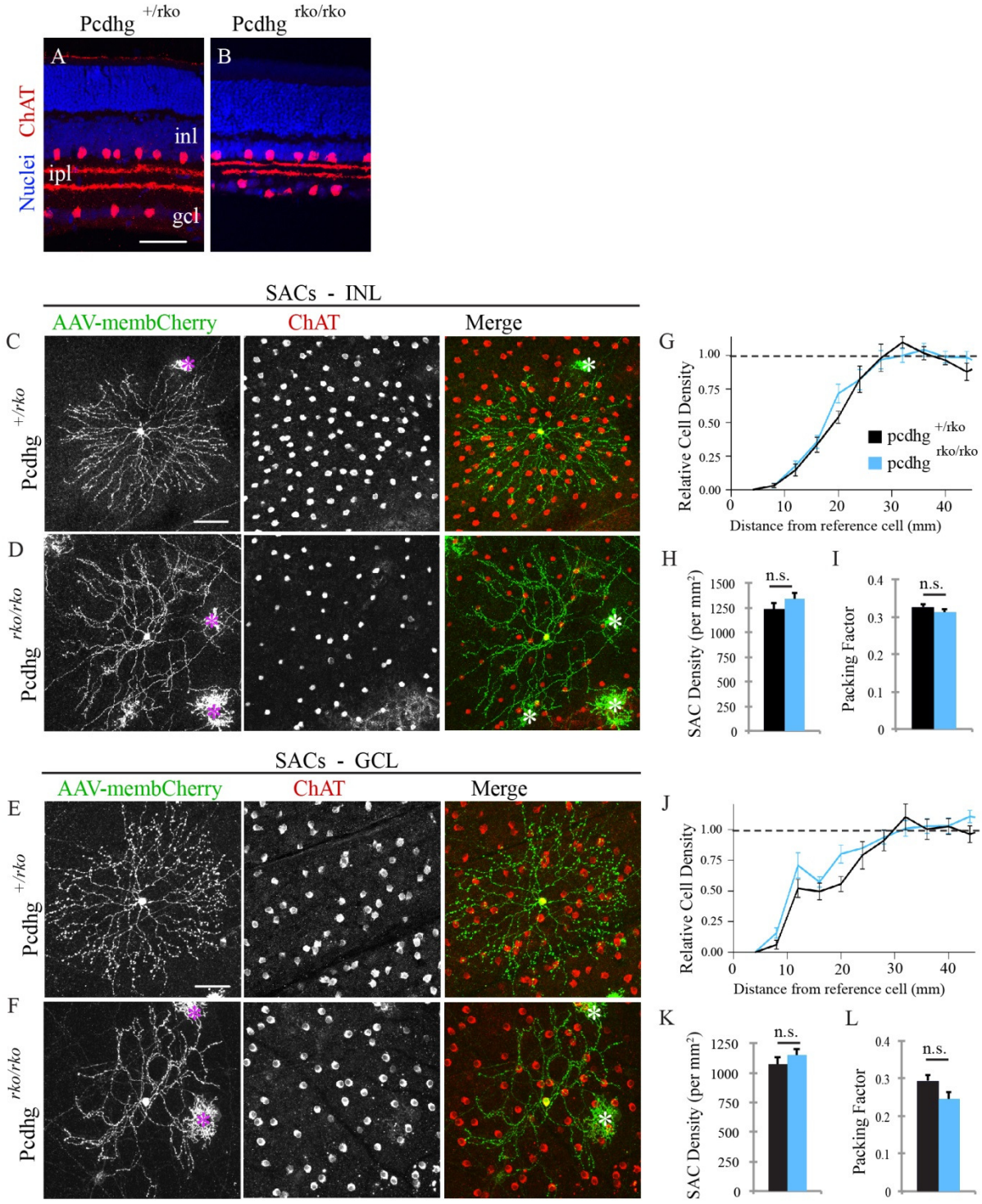

Figure 2.4: Self-avoidance defects persist in Pcdhg mutant SACs following genetic blockade of programmed cell death

A-C. Morphology of SACs in *Bax-/-* and *Pcdhg rko/rko; Bax-/-* double mutant retinas. Self-crossing and bundling defects of SAC dendrites are present in *Pcdhg rko/rko; Bax-/-* double mutants.

D-E. Higher magnification of SAC dendrite morphology of insets in wild-type (**A**) and mutant (**B**). Labeled dendrites (green) are confined to ChAT-labeled SAC plexus (red), and show dramatic crossings in double mutants. Scale bars, 50 μm.

F-I. Mosaic spacing and density of SACs in INL and GCL are indistinguishable in *Bax-/-* and *Pcdhg rko/rko; Bax-/-* double mutant retinas. DRP analysis as in Supplementary Figure 2.

N ≥12 from 3-4 animals per genotype.

(Figure continues on next page)

Figure 2.4 (continued)

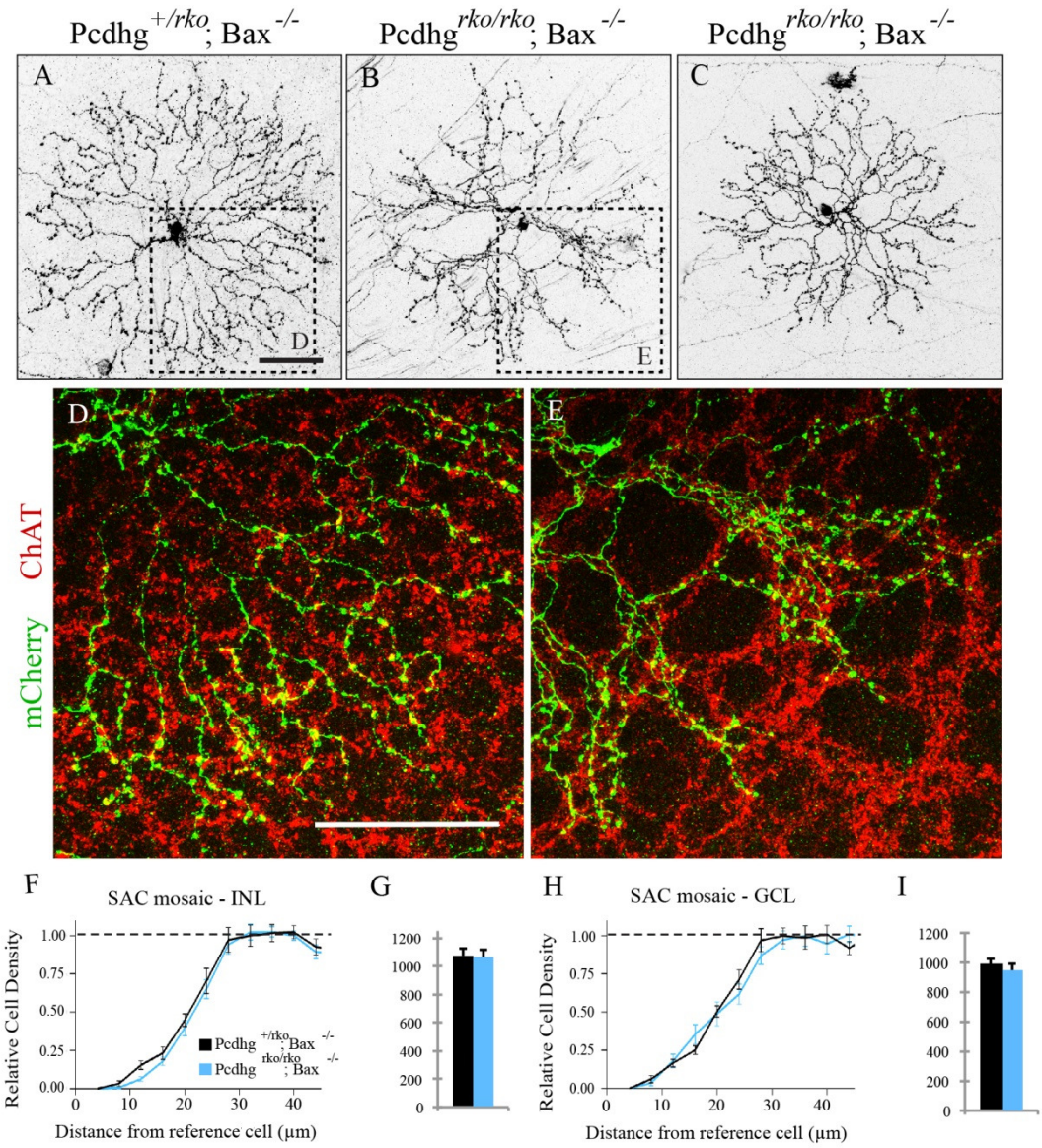

2.3.2 Pcdhgs pattern developing SAC dendrites in a cell autonomous manner

We next asked whether Pcdhgs are required for the development of SAC arborizations, or only for their maintenance. In wild-type neonates, SACs extended dendrites that branched profusely and contacted each other (**Figure 2.5A-C**). By postnatal day (P)12, however, excess neurites and isoneuronal contacts were eliminated, resulting in a radial arborization with evenly spaced branches (**Figure 2.5D**, and see Stacy and Wong, 2003). Thus, self-avoidance arises rapidly following a short period of isoneuronal 'sampling'. In *Pcdhg*$^{rko/rko}$ mice, SACs were clearly aberrant by P3, exhibiting excessive crossing and tangling of neurites (**Figure 2.5E-G**). Excess branches were subsequently eliminated, but whereas most crossing branches were eliminated in controls, many persisted in mutants (**Figure 2.5H**). Thus, Pcdhgs may lead to self-avoidance by mediating repulsive interactions that bias the rearrangement process to selectively eliminate contacts among isoneuronal branches.

To initiate analysis of the mechanism by which Pcdhgs mediate self-avoidance, we next asked whether they act cell-autonomously. We selectively removed *Pcdhg* genes from SACs using a *ChAT-Cre* line. In this case, *Pcdhg*-negative SACs were surrounded by *Pcdhg*-positive neurons of other types. We also deleted *Pcdhg* genes from individual SACs using a transgenic line that expressed tamoxifen-activated Cre recombinase in SACs; we activated Cre with a low dose of tamoxifen and introduced a Cre-dependent reporter to mark mutant SACs. In this case, *Pcdhg*-negative SACs were surrounded by *Pcdhg*-positive SACs. In both cases, SACs lacking *Pcdhg* genes exhibited striking self-avoidance defects (**Figure 2.6**). To test whether Pcdhgs can act in completely isolated SACs, we used fluorescence-activated cell sorting to purify SACs from a transgenic line in which they are selectively labelled by an orange fluorescent protein (*Thy1-OFP3*) and cultured them at low density. Isolated SACs extended dendrites that formed radial, web-like arborizations (**Figure 2.5I**), reminiscent of those observed at ~P5 *in vivo* (**Figure 2.5B**). In contrast, SACs from *Pcdhg*$^{rko/rko}$; *Thy1-OFP3* mice exhibited less symmetrical and unevenly spaced arborizations, reminiscent of those observed in *Pcdhg*$^{rko/rko}$ retinas at P5 (**Figures 2.5J and 2.7**). Analysis of the space-filling capacity of dendritic arborizations (Jelinek and Fernandez, 1998; Montague and Friedlander, 1989) (see Methods) revealed that defects *in vitro* were similar in magnitude

Figure 2.5: Pcdhgs pattern developing SAC dendrites in a cell-autonomous manner

A-H. SACs in developing wild-type and *Pcdhg* mutant retinas. Wild-type SACs extend fine, exuberant branches (P3, P5) that make transient intradendritic contacts (P5, P8); by P12, excess branches and isoneuronal contacts are eliminated. Dendrites of mutant SACs display excessive self-crossing and bundling by P3; by P12, excess branches are eliminated, but crossing dendrites remain.

I-J. Cultured *Pcdhg* mutant SACs exhibit loss of symmetric growth and uneven distribution of neurites.

K. Histogram of fractal dimensions (*Df,* metric for space-filling) for 47 wild-type (black) and 47 mutant (grey) SACs. Wild-type SAC in i has *Df* of 1.61 and mutant SAC in j has *Df* of 1.53.

L. Mean *Df* for cultured SACs (n=47 cells), SACs *in vivo* at P5 (n=6) and adult (n=9). *** *P<0.001*. Error bars, s.e.m. Scale bars, 50 μm except 20 μm in **I** and **J**.

(Figure continues on next page)

Figure 2.5 (continued)

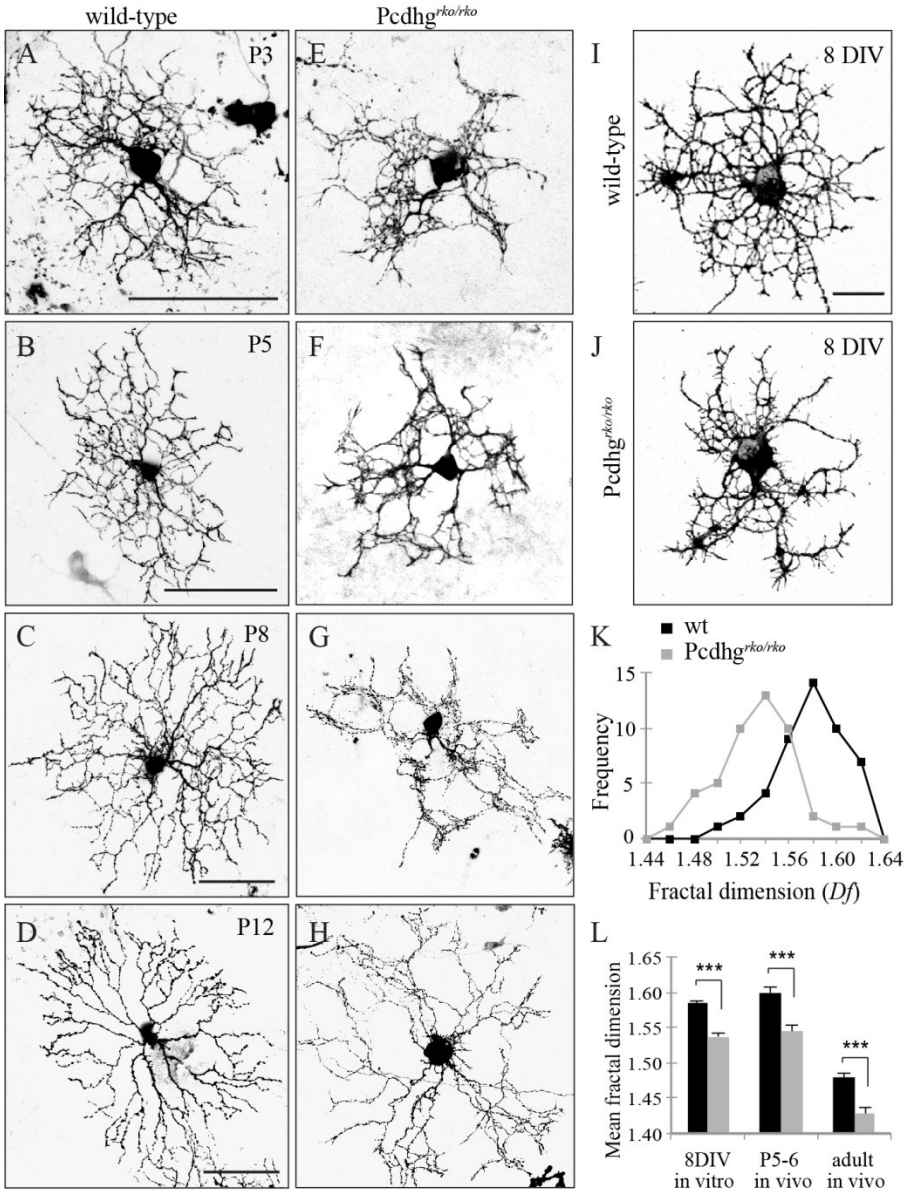

Figure 2.6: Selective removal of Pcdhgs in SAC population and in single SACs disrupts dendritic self-avoidance

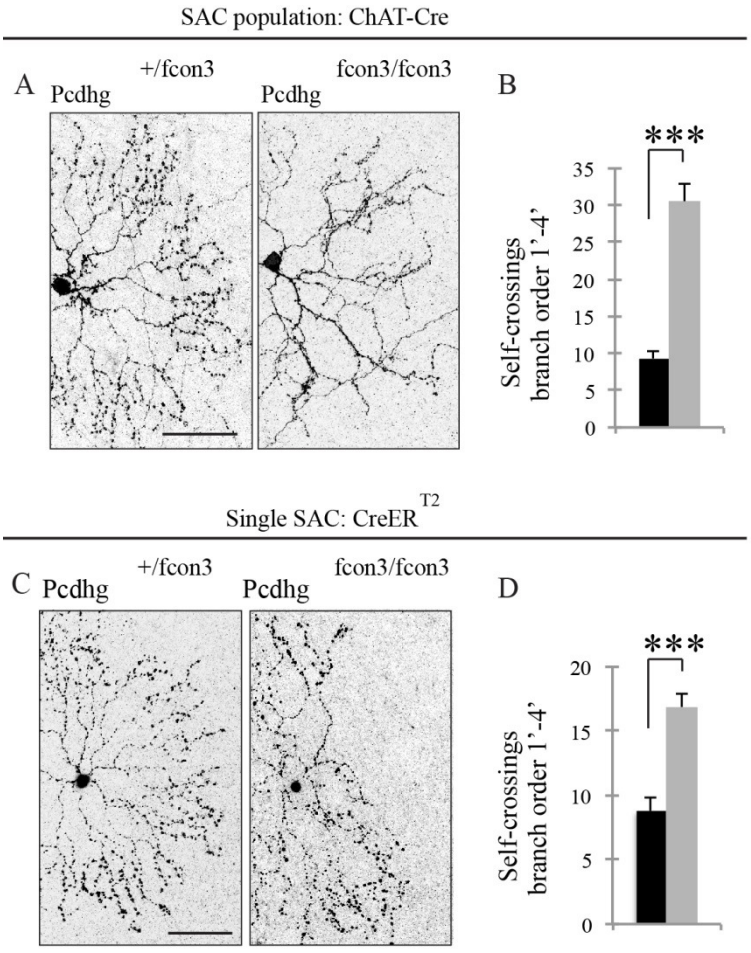

A, C. SAC self-avoidance defects are present following selective Pcdhg inactivation in SACs using ChAT-Cre (**A**, right panel) or in single mutant SACs generated by tamoxifen activation of CreER (**C**, right panel). SACs were labeled with AAV in **A** and with a Cre responsive reporter in **C**.

B, D. show increased self-crossings in 1st-4th order dendrites of mutant SACs (gray; n = 9 in **b** and n=20 in **d**) compared to controls (black; n=9, 11). Bars are mean ± s.e.m., *** *P<0.001.*

Scale bars, 50 μm.

Figure 2.7: Isolated SACs cultured in vitro show outgrowth defects

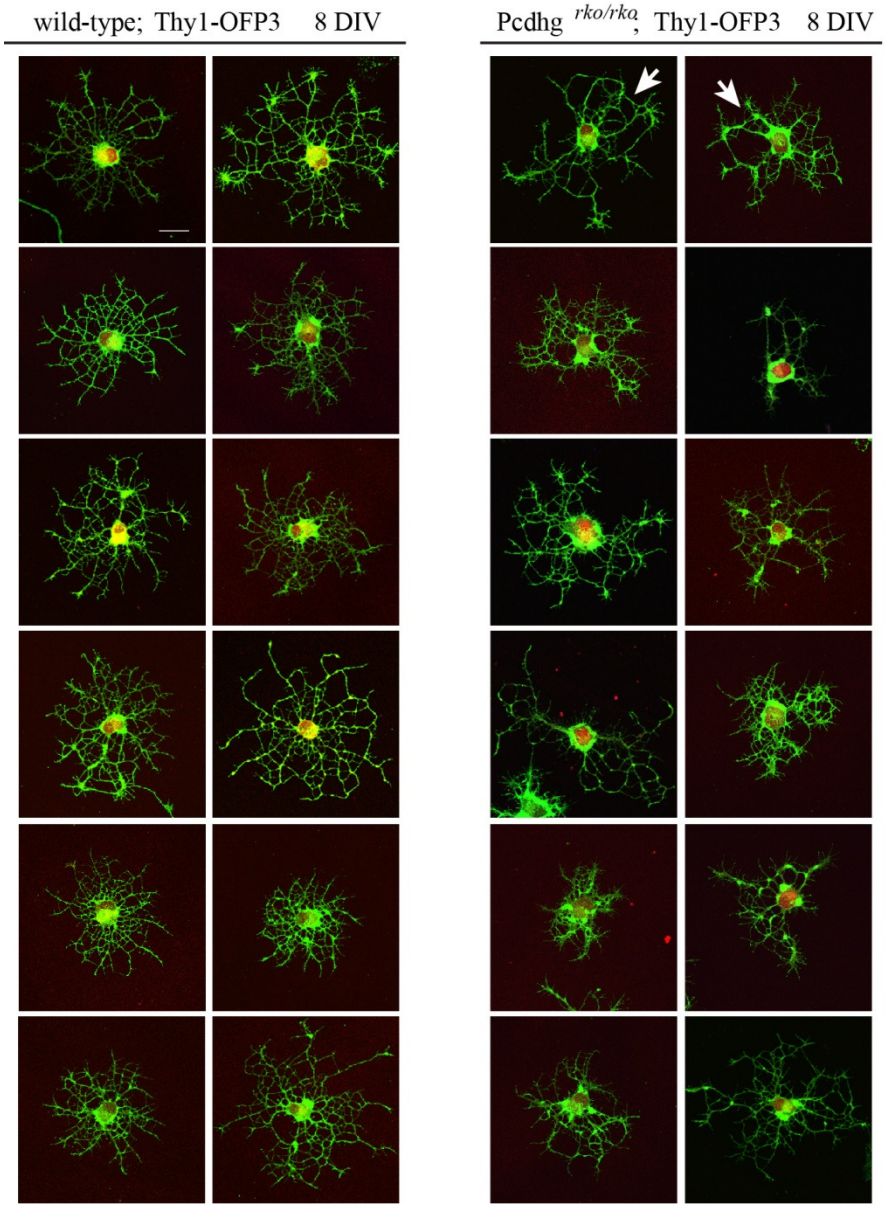

OFP+ SACs from dissociated retinas of Thy1-OFP3 transgenic P2 animals were isolated by FACS and cultured in vitro for 8 days. Isolated SACs are marked by OFP (red) and immunostained with syntaxin (green). Compared to the radial, web-like array of neurites of wild-type SACs (gallery on left), *Pcdhg* mutant SACs exhibit neurite outgrowth defects such as bundling (arrows) and loss of symmetric outgrowth (gallery on right). Scale bar, 20 μm.

to those *in vivo* (**Figure 2.5K-L**). Thus, Pcdhgs do not depend on intercellular interactions to promote self-avoidance.

2.3.3 No single Pcdhg isoform is necessary and any isoform is sufficient for dendritic self-avoidance

We next assessed the requirement for isoform diversity in Pcdhg-dependent self-avoidance. We used RT–PCR (PCR with reverse transcription) to survey expression of *Pcdhg* isoforms in whole retina, in amacrines generally and in SACs specifically. All 22 *Pcdhg* variants were expressed in each preparation, with no indication of decreased diversity in purified subpopulations (**Figure 2.8**). We then analyzed a targeted mouse mutant, $Pcdhg^{tcko}$, in which three contiguous *Pcdhg* variable exons, C3–C5, had been deleted. Expression of the remaining 19 *Pcdhg* isoforms is unperturbed in this allele (Chen et al., 2012). Because $Pcdhg^{tcko}$ homozygous mice die at birth (Chen et al., 2012), we generated transheterozygous animals ($Pcdhg^{tcko/fcon3}$*;retina-cre*) so that only retina lacks both copies of *Pcdhgc3-c5*. In these retinas, neuronal death was as prevalent as in those of $Pcdhg^{rko/rko}$ mice (Chen et al., 2012; Lefebvre et al., 2008), yet SACs exhibited normal self-avoidance (**Figure 2.9A,E**).

In a complementary approach, we generated a line in which the single PcdhgC3 isoform, fused to a fluorescent protein (mCherry), could be expressed in any cell in a Cre-dependent manner (*ROSA26-CAG::lox-Stop-lox-Pcdhgc3-mCherry* or *cC3-mCherry*). Thus, in *cC3-mCherry*; $Pcdhg^{rko/rko}$ mice, *Cre* both deletes all 22 endogenous *Pcdhg* genes and activates the single PcdhgC3-mCherry isoform throughout the retina. Analysis of mCherry fluorescence confirmed Cre-dependent expression of the transgene in all retinal cells and appropriate localization of the fusion protein to cell membranes and synaptic layers (**Figure 2.10**). Expression of *Pcdhgc3* alone rescued self-avoidance defects of *Pcdhg* mutants (**Figure 2.9B,E**).

To test the possibility that only some isoforms are dispensable for self-avoidance, we analyzed a second set of isoforms. We generated $Pcdhg^{tako}$, which lacks the *Pcdhga1-a3* variable exons (Chen et al., 2012), and a line that expresses *Pcdhga1-mCherry* in a Cre-dependent manner (*cA1-mCherry*). Results were similar to those for the C3–C5 group: self-avoidance persisted in the absence of PcdhgA1–A3 and

Figure 2.8: All 22 Pcdhg variable transcripts are expressed by SACs

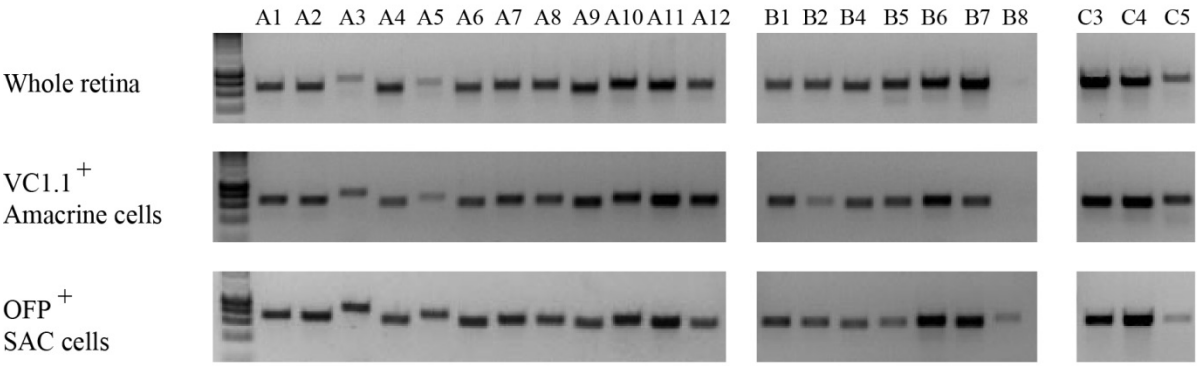

Expression profile of 22 Pcdhg variable transcripts by RT-PCR using isoform-specific primers. Whole retina, amacrine cells sorted by VC1.1+ expression, and OFP+ sorted SACs were isolated and profiled by RT-PCR. Purity of the sorted populations were confirmed by showing that markers of other cell types (*brn3a* and *brn3b* for RGCs, *trpm1* and *grm6* for bipolar cells, *rho* for rods) were expressed by whole retina but not SACs, whereas *chat* was expressed at many-fold higher levels by SACs than by whole retina (data not shown).

Figure 2.9: No single Pcdhg isoform is necessary and any isoform is sufficient for dendrite self-avoidance

A. SACs lacking *Pcdhgc3–c5* (*pcdhg*$^{tcko/fcon3}$*;retina-cre*) exhibit self-avoidance.

B. Replacement of all 22 Pcdhgs by the PcdhgC3 isoform, using the *RC::cC3-cherry* transgene, rescues SAC dendrite self-avoidance.

C. SACs lacking *Pcdhga1-a3* (*pcdhg*$^{tako/tako}$) exhibit self-avoidance.

D. Replacement of all 22 Pcdhgs by the PcdhgA1 isoform, using the *RC::cA1-cherry* transgene, rescues SAC dendrite self-avoidance.

E. Compared to mutants lacking all 22 isoforms, self-crossings of SACs in retinas expressing 19 or 1 isoforms are restored to control levels. ***$P < 0.001$; n.s., not significant. Data are mean ± s.e.m., from 7 SACs from*pcdhg*$^{tcko/fcon3}$*;retina-cre* retinas, 3 SACs from *pcdhg*$^{tako/tako}$, and 9 from remaining genotypes. Scale bar in **A**, 50 μm; applies to **B–D** also.

(Figure continues on next page)

Figure 2.9 (continued)

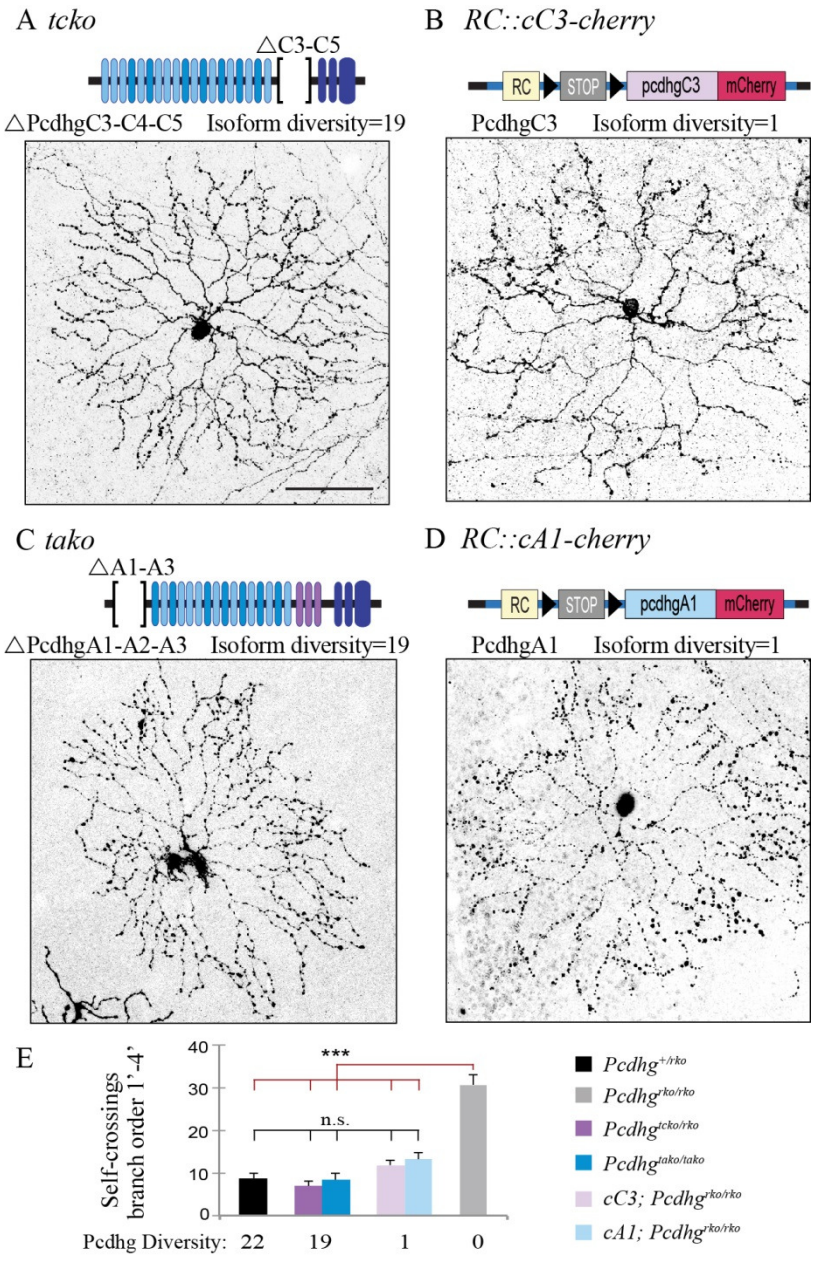

Figure 2.10: Single isoform 'rescue' strategy

A. Diagram of targeting strategy to insert a cassette encoding *Pcdhga1* or *Pcdhgc3* cDNA fused to mCherry at the C'terminus into the Rosa26 locus, between exons 1 and 2. See methods and Farley et al., 2000 for more details. Targeting construct also includes a CAG promoter (chicken β-actin promoter and CMV immediate-early enhancer), a LoxP flanked 'Stop'41, WPRE (woodchuck posttranslational response element)36, polyadenylation signal (pA), and a *Frt*-flanked Neomycin selection cassette. Arrows show location of primers used for genotyping.

B. Validation of *cC3- and cA1-mCherry* targeting by PCR from genomic DNA.

C-E. Cre-dependent expression and appropriate localization of PcdhgA1-mCherry and PcdhgC3-mCherry fusion proteins was confirmed by immunostaining of retina cross-sections with antibody against mCherry (red). In the absence of Cre, no mCherry was detected (**c**). With Chx10-Cre activity, PcdhgA1-mCherry and PcdhgC3-mCherry fusion proteins were present in the synaptic OPL and IPL, as well as in outer segment (os), Muller glia processes and endfeet (arrowheads) and RGC axonal layer (arrow). Overexpression of a Pcdhg isoform in wild-type retina does not disrupt laminar organization of cellular (blue) and synaptic layers.

F-H. Processes of ChAT-labeled SAC (green) and vGluT3-positive amacrine subsets (magenta) target appropriate sublaminae in IPL in wild-type retina overexpressing PcdhgA1-mCherry (**G**) or PcdhgC3-mCherry (**H**). Scale bars, 50 μm.

(Figure continues on next page)

Figure 2.10 (continued)

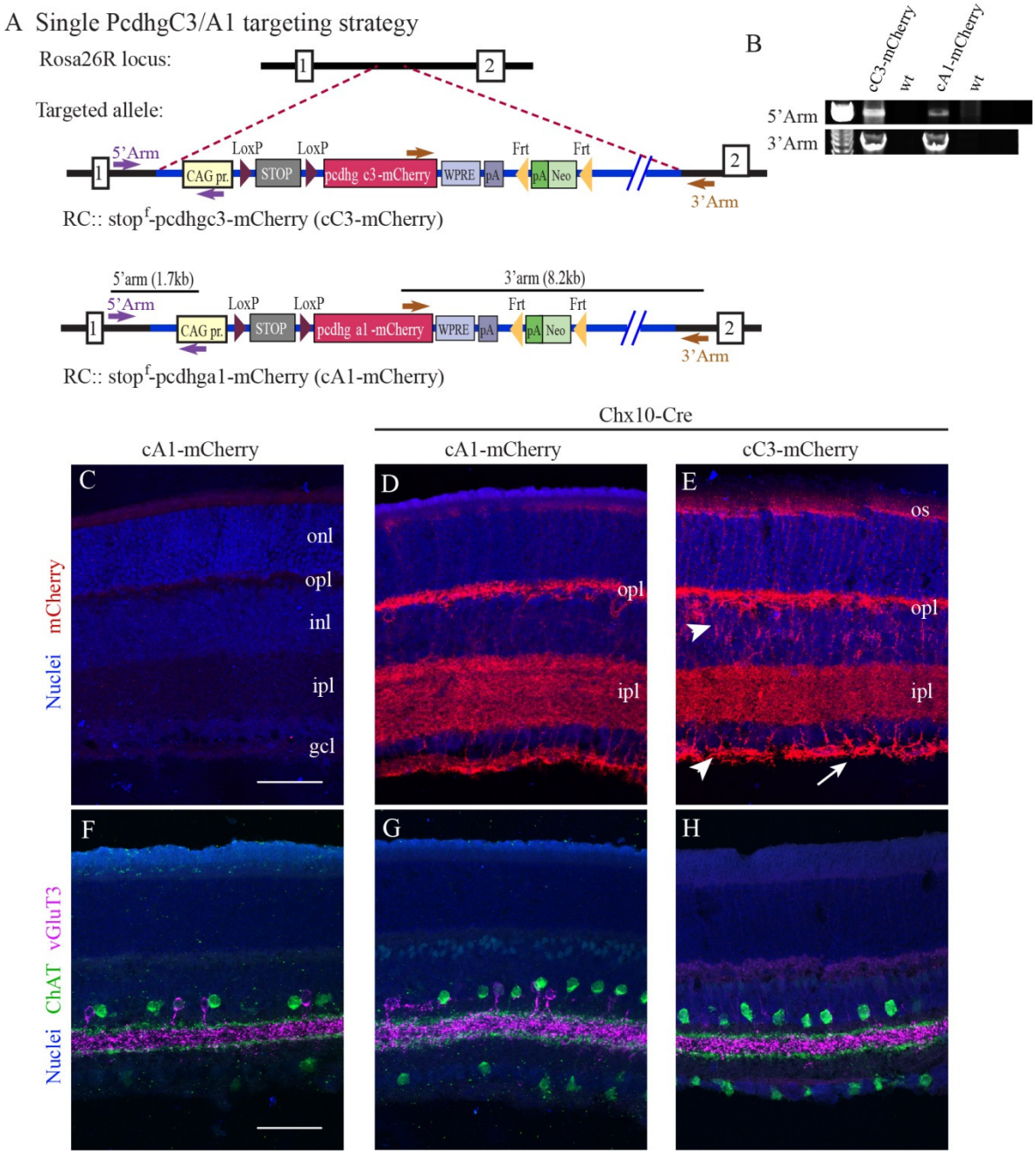

was rescued by replacement of all Pcdhg isoforms with PcdhgA1 alone (**Figure 2.9C-E and 2.10**). From these results, we conclude that no single Pcdhg isoform is necessary but any single isoform is sufficient for dendritic self-avoidance.

2.3.4 Reducing *Pcdhg* diversity disrupts heteroneuronal SAC interactions

Although Pcdhg isoform diversity is not required for isoneuronal self-avoidance, it may be required to ensure that dendrites of adjacent SACs do not avoid each other, which would prevent them from interacting. The ability to generate a SAC population expressing a single Pcdhg isoform (*Pcdhga1*or *Pcdhgc3*) enabled us to test this idea. We injected closely spaced pairs of SACs with different fluorophores (**Figure 2.11A**) and measured the extent to which their dendrites overlapped. To determine whether this method reliably revealed interactions among SACs, we rotated, flipped or rotated and flipped the image of one of the cells, and recalculated overlap. Only the real image showed an overlap greater than that of the manipulated images (**Figure 2.11B**). We then measured overlap for pairs of SACs from wild-type, mutant and single isoform-expressing mice, normalizing for intercellular distance by comparing overlap to the value calculated from the flipped image (**Figures 2.11C-E** and **12**). Overlap was equivalent in wild-type and mutant retina, but significantly decreased in retinas expressing a single isoform (**Figure 2.11F**); values for *Pcdhga1* and *Pcdhgc3* were similar (1.01 and 1.08). Likewise, the mean length of overlapping segments was greater than expected for random overlap in wild-type and mutant but not in single isoform-expressing pairs (**Figure 2.11G**). Thus, when all SACs express the same *Pcdhg* isoform, heteroneuronal dendrites avoid each other, just as isoneuronal dendrites do in control SACs. We conclude that isoform diversity enables SACs to distinguish isoneuronal from heteroneuronal dendrites.

Figure 2.11: Reducing *Pcdhg* diversity disrupts heteroneuronal SAC interactions

A. Two nearby SACs from a wild-type mouse injected with contrasting fluorescent dyes. Right panel shows image of the green SAC flipped vertically.

B. Overlap between red and green cells in **A**. First two bars are derived from the two panels in **A**. The green cell was rotated in 45° steps or flipped and then rotated (manipulations indicated by symbols beneath graph); third and fourth bars show mean overlap ± s.e.m. derived from these images ($n = 7$). All inversions and rotations decrease overlap, indicating that overlap in the real image is non-random.

C-E. Tracings of SAC pairs, and versions flipped as in **A**, from wild-type (**C**), $Pcdhg^{rko/rko}$ (**D**) and *cA1*;$Pcdhg^{rko/rko}$ (**E**) mice. Overlap shown in black.

F. Overlap between neighboring cells, expressed as ratio between overlap measured in real and flipped images. Bars show mean ± s.e.m. for 11, 9 and 8 pairs from wild-type, $Pcdhg^{rko/rko}$ and single isoform-expressing (*cA1;*$Pcdhg^{rko/rko}$ and*cC3;*$Pcdhg^{rko/rko}$) animals. Expression of a single isoform in neighboring SACs decreases their interaction.

G. Mean length of overlapping segments between SAC pairs. R, real image; F, flipped image. $*P = 0.05$; $**P < 0.05$; $***P < 0.01$. Error bars, s.e.m.; n as in **F**. Scale bar in **A**, 50 μm; applies to **C-E** also.

(Figure continues on next page)

Figure 2.11 (continued)

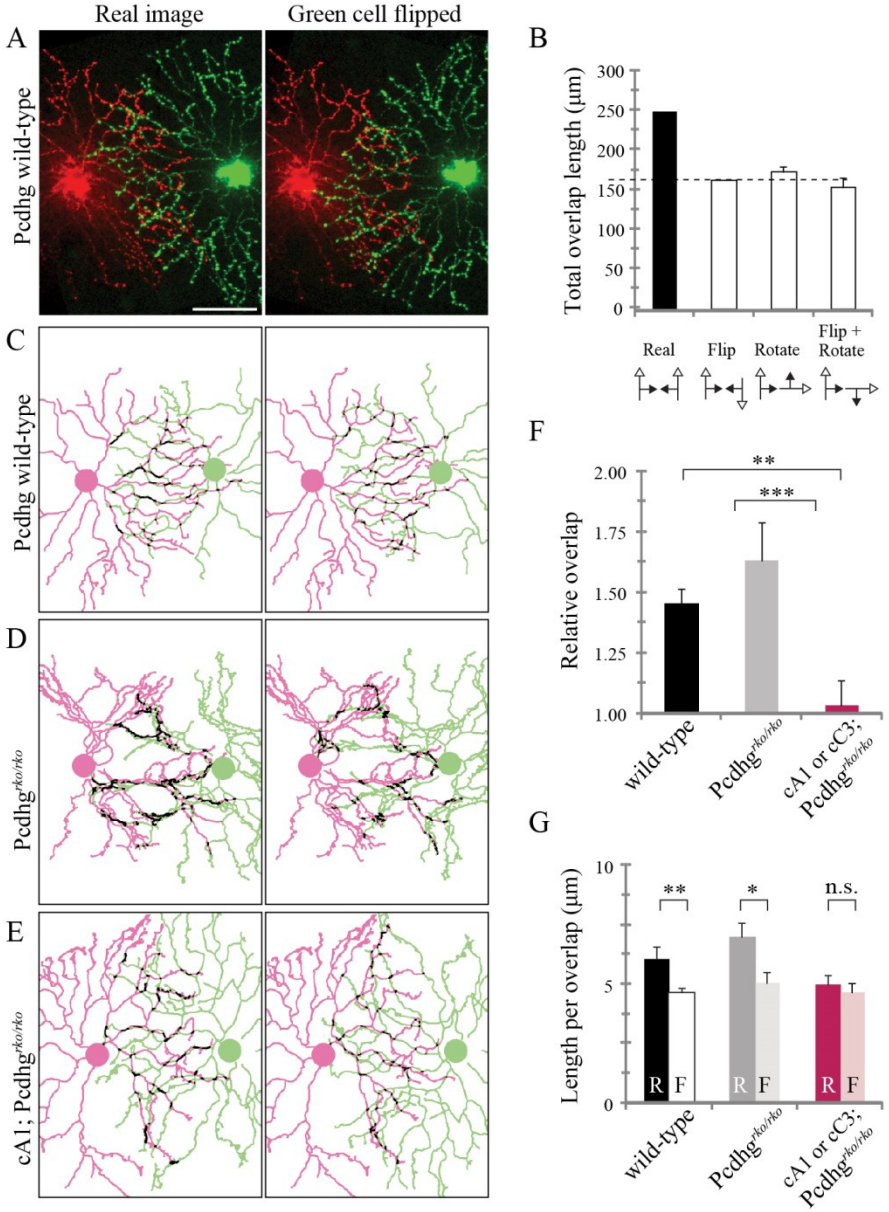

Figure 2.12: Requirement of Pcdhg diversity for heteroneuronal interactions of SACs

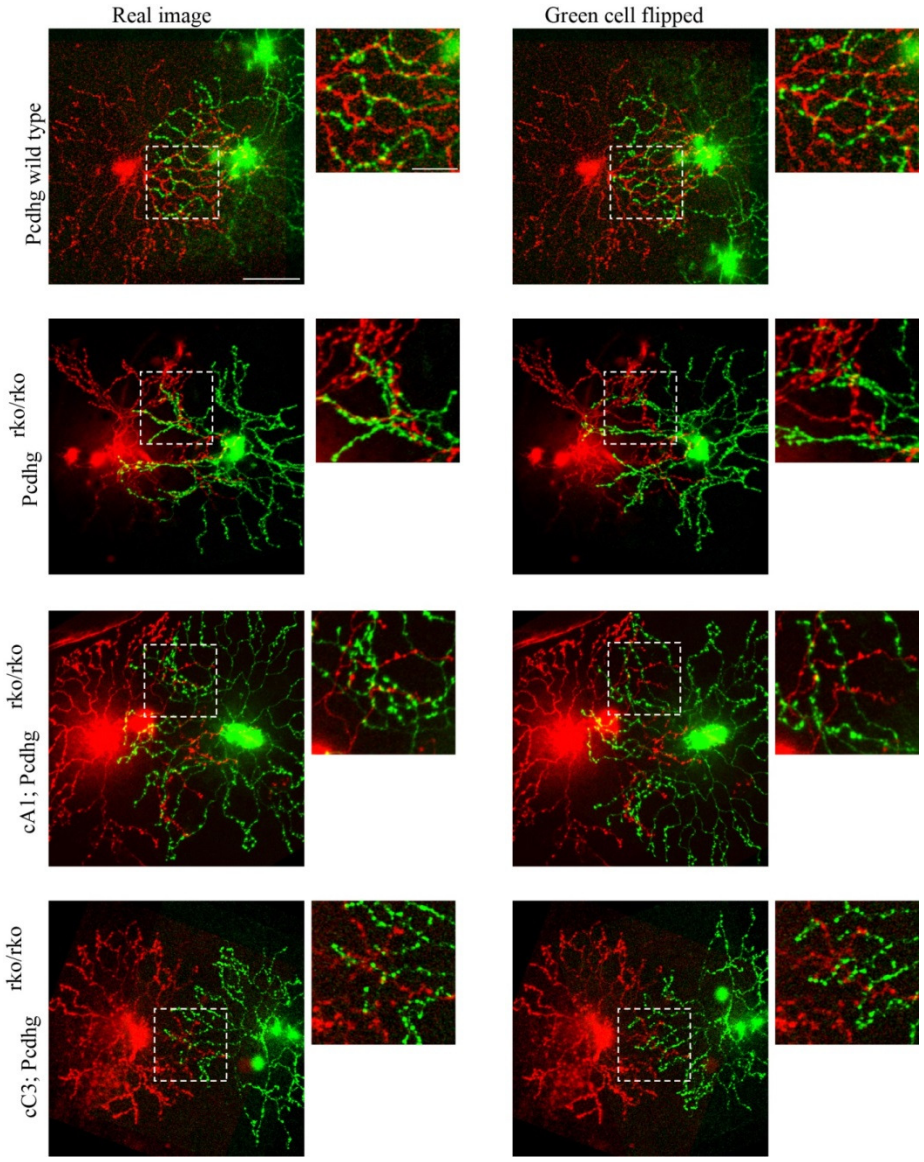

Two nearby SACs from mice of indicated genotypes were injected with contrasting fluorescent dyes. Magnifications of boxed insets of full sized images are shown right to the right of each image. The left column of images shows the real images of paired SAC fills. The right shows the same images, with the green cell digitally flipped and realigned to the center of the cell bodies. Quantitative data from these and other pairs are shown in **Figure 2.11F-G**. Scale bars, 50 μm for full sized images and 20 μm for insets.

2.3.5 Purkinje cell dendritic self-avoidance requires *Pcdhgs*

Finally, we asked whether Pcdhgs mediate self-avoidance in areas other than retina. We examined cerebellar Purkinje cells, which have elaborate, planar dendritic arborizations known to exhibit self-avoidance (Grueber and Sagasti, 2010) (**Figure 2.13A-C**). Importantly, stochastic and combinatorial expression, which underlies the ability of *Drosophila Dscam1* to mediate self-avoidance (Hattori et al., 2009; Hughes et al., 2007; Matthews et al., 2007; Neves et al., 2004; Soba et al., 2007; Wang et al., 2004; Zhan et al., 2004), has been documented for *Pcdhg* genes in Purkinje cells (Kaneko et al., 2006). We selectively deleted *Pcdhg* genes from Purkinje neurons using an *L7-cre* transgene, marked cells with a vector that expresses fluorescent proteins in a Cre-dependent manner, and examined them at P15, P21 and at P35, after arborizations have matured (Kaneko et al., 2011). Deletion of *Pcdhg* genes from Purkinje cells had no detectable effect on their survival, shape, size or branching pattern (**Figure 2.13D,E,H and 2.14**), but their arborizations were disorganized and dendrites often crossed over each other **(Figure 2.5F-G).** Use of a Cre-dependent reporter revealed that deletion remained incomplete at P8, at which time Purkinje dendrite growth was already advanced (**Figure 2.14**). It is therefore possible that earlier deletion of *Pcdhg* genes would lead to a more dramatic effect. Nonetheless, these results demonstrate a role for *Pcdhg* genes in Purkinje cell self-avoidance.

Figure 2.13: Purkinje cell dendrite self-avoidance requires *Pcdhgs*

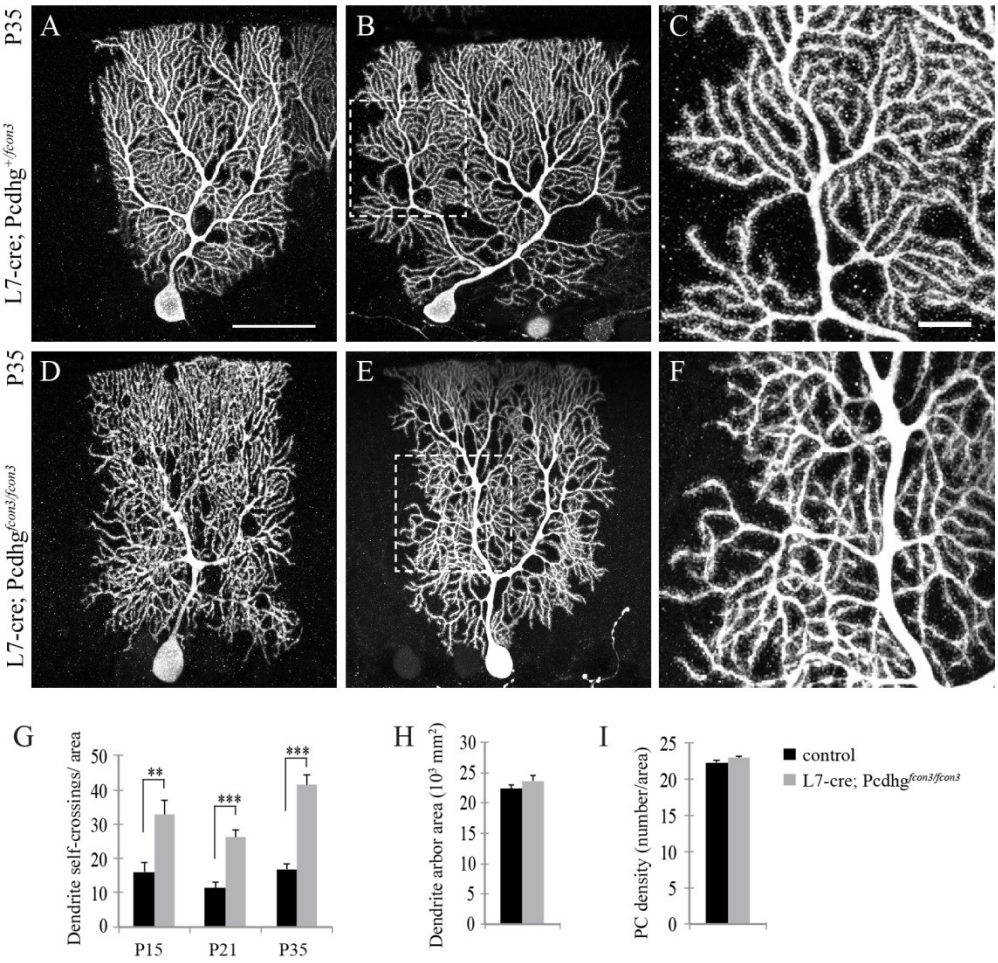

A-C. Control Purkinje cells (**A, B**) labelled with Cre-dependent AAV-XFP in *L7-cre* transgenic mouse. Self-avoidance is clear in high-magnification view in **C** (shows area boxed in **B**).

D-F. Purkinje cells lacking Pcdhgs and labelled as in **A-C** have disorganized arborizations marked by frequent self-crossing defects. Panel **F** shows area boxed in **E**.

G. Self-crossings detected in single confocal *z*-sections of 7,225 μm^2 unit area from controls and mutants. $^{**}P < 0.01$; $^{***}P < 0.001$; $n = 8$, 15 and 15 cells at P15, P21 and P35 from ≥3 mice per genotype.

H-I. Area of dendritic arborizations ($n = 20$ cells) and cell density (>40 regions) do not differ between control and mutant Purkinje cells. Data show mean ± s.e.m. Scale bars, 50 μm (**A**, **B**, **D**, **E**) and 10 μm (**C**, **F**).

Figure 2.14: L7/Pcp2-Bac::Cre recombination pattern in the developing cerebellum

A-B. Cross sections of control and *L7-cre; Pcdhgfcon3/fcon3* mice showing that overall cerebellar size is unchanged in the mutant. Because the size (here) and Purkinje cell number per unit length (Figure 5i) do not differ between mutants and controls, we believe that total Purkinje cell number is unaffected by Pcdhg deletion.

C-D. Dendrite self-crossing and disorganization is detected in developing PC arbor in Pcdhg mutants at P15.

E-I. Sagittal brain sections of L7-Cre; RC-Stopflox-tdTomato mice illustrate L7/Pcp2-Cre mediated recombination pattern marked by expression of td-Tomato in recombined Purkinje cells (red). Purkinje cells (PC) are labeled with anti-Calbindin (green) and nuclei with Neurotrace (blue). By P4, there are very sparse recombined PCs throughout the cerebellum, with increased numbers in the posterior lobules VII-IX (**E**).By P8, the number of recombined PCs (red) increases (**H, I**), but unrecombined cells are still present (asterisks) in **I**.

Scale bars, 1mm in **A-B**; 50 μm in **C-D** and **I**, and 200 μm in **E-H**.

(Figure continues on next page)

Figure 2.14 (continued)

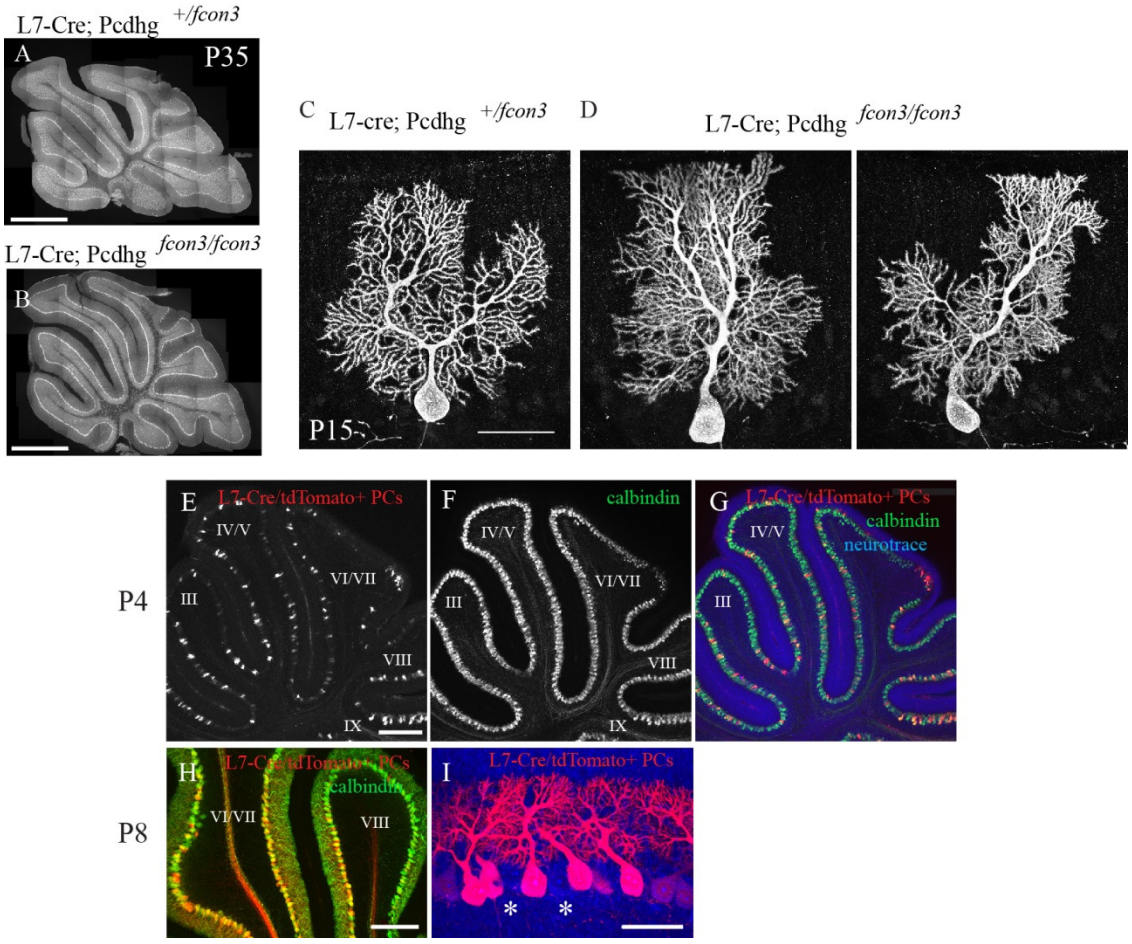

2.4 Discussion

In summary, although vertebrate *Pcdh* genes and *Drosophila Dscam1* are structurally unrelated, they have remarkable parallels: both encode numerous isoforms from a single locus, the isoforms are expressed stochastically and combinatorially, and the encoded proteins interact homophilically (Hattori et al., 2009; Kaneko et al., 2006; Schreiner and Weiner, 2010; Wojtowicz et al., 2004; Wu and Maniatis, 1999; Zhan et al., 2004; Zipursky and Sanes, 2010). We have now shown that in mammalian neurons, Pcdhgs, like Dscam1 (Hughes et al., 2007; Matthews et al., 2007; Soba et al., 2007; Zhan et al., 2004), promote self-avoidance during development by a cell-autonomous mechanism. In addition, for both *Dscam1* and *Pcdhg* genes, diversity appears to underlie self/non-self discrimination, presumably because neighboring neurons are unlikely to express the same isoforms and are therefore free to interact (Neves et al., 2004; Wang et al., 2004; Wojtowicz et al., 2004; Zhan et al., 2004; Zipursky and Sanes, 2010). Thus, two phyla appear to have recruited different molecules to mediate similar, complex strategies for self-recognition during formation of neuronal arborizations. These parallels raise the question of why vertebrate and invertebrate nervous systems have invested heavily in mechanisms that promote self-avoidance. In principle, self-avoidance allows neurons to cover their receptive or projective fields maximally while retaining the ability to overlap those of neighboring neurons (Grueber and Sagasti, 2010; Kramer and Kuwada, 1983; Montague and Friedlander, 1989). However, to our knowledge, the effect of perturbing self-avoidance on circuit function has yet to be assessed in any system. We can now address this issue by electrophysiological analysis of SACs, Purkinje cells, and their synaptic targets in *Pcdhg* mutant mice.

2.5 Methods

2.5.1 Mouse strains

The *Pcdhg*^{fcon3} conditional mutant allele, in which the third constant exon is flanked by loxP sequences and which generates a functionally null allele following Cre recombination, was described previously (Lefebvre et al., 2008; Prasad et al., 2008). Retina-specific *Chx10-cre* (Rowan and Cepko, 2004) and *Six3-cre* transgenic mice (Furuta et al., 2000) were provided by C. Cepko (Harvard) and W. Klein (M.D. Anderson Cancer Center), respectively. *Bax*$^{-/-}$ mutants (Knudson et al., 1995), Purkinje-specific *L7Bac-cre* transgenic mice (Zhang et al., 2004), *Chat-cre*, in which the Cre recombinase gene was targeted to the endogenous ChAT gene (Rossi et al., 2011), and Rosa-CAG-LoxP-STOP-LoxP-tdTomato-WPRE reporter mice (Madisen et al., 2010) were obtained from Jackson Laboratories. A line of BAC transgenic mice in which regulatory elements from the *fstl4* gene drive expression of CreER was generated as described in Kay et al., 2011. In this line, called line 1 to distinguish it from the line called 'BD' in Kay et al., 2011, CreER was expressed in SACs, as well as sparse other amacrine cells. We believe that expression reflects influences at the site of transgene integration rather than expression of *fstl4*. Thy1-OFP3 transgenic mice, in which Thy1 promoter and regulatory elements direct expression of Kusabira Orange (OFP) in SACs and subsets of retinal ganglion cells (RGCs), were described previously (Kay et al., 2011a). Pcdhg^{tcko} and Pcdhg^{tako} mice were generated using standard gene targeting techniques (Chen et al., 2012). Mice were maintained on a C57/B6J background. All experiments were carried out in accordance with protocols approved by the Harvard University Standing Committee on the Use of Animals in Research and Teaching.

2.5.2 Generation of single Pcdhg isoform conditional knock-in mice

Pcdhga1 and *pcdhgc3* full-length cDNAs were amplified from RNA isolated from P21 C57/BL6 mouse brain, and cloned in frame into pCMV-mCherry-N1 (Clontech). Linker sequence residing between the third constant exon and *gfp* in Pcdhg^{fusg} knock-in mice and shown to produce functional Pcdhg-GFP fusion proteins *in vivo* (Wang et al., 2002c) was subcloned into pCMV-pcdhga1/c3-mCherry-N1.

Targeting vector pRosa26-PAS (Srinivas et al., 1999) was modified as described in Yamagata and Sanes, 2012b to include a CAG cassette (chicken β-actin promoter and CMV immediate-early enhancer), a Gateway RfA destination site (Invitrogen), a WPRE fragment (woodchuck hepatitis virus posttranscriptional element), and a STOP sequence was cloned from pBS302 (Addgene plasmid 11925). LoxP-STOP-loxP-Pcdhga1/c3-mCherry was recombined into pROSA26-CAG-Rfa-WPRE-FNF-iSceI, creating pROSA26-CAG-loxP-STOP-loxP-Pcdhga1/c3-mCherry-WPRE-FNF-iSceI targeting vectors. The iSceI-linearized vectors were electroporated into 129/B6 F1 hybrid ES cell line V6.5. G418-resistant, targeted ES clones were identified by PCR: 1.7 kb fragment amplified by 5′-Rosa-F: GGCGGACTGGCGGGACTA and 5′-CAG-R: CCAGGCGGGCCATTTACCGTAAG; and 8.2 kb fragment amplified by 3′-CherryF: CTCCCACAACGAGGACTACACCATC and 3′-RosaR: GCATTTTAAAAGCATGAAACTACAAC. ES cell transfections and blastocyst injections were performed by the Genome Modification Facility, Harvard University. Following germ-line transmission, the FRT-neo-FRT cassette was excised by crossing to mice that express Flp recombinase ubiquitously (Farley et al., 2000). *Gt(ROSA)26Sor::CAG-loxP-STOP-loxP-Pcdhga1/c3-mCherry* conditional knock-in mice are called *cA1-mCherry* and *cC3-mCherry.*

2.5.3 Labelling of neurons

Plasmid encoding pAAV2/2-CAG-palmitoylation tag-mCherry-WPRE was used to generate recombinant AAV2/2 expressing membrane-tagged Cherry. To label SACs in retina expressing *cC3-mCherry* or *cA1-mCherry*, we used rAAV2/2-CBA-YC3.6-WPRE expressing a calcium sensor that includes cytosolic YFP and used here for visualization of neuronal morphology (Kuchibhotla et al., 2008). Recombinant AAV2/2-CAG-memb-mCherry and rAAV2/2-YC3.6 were prepared at the Harvard Gene Therapy Institute ((1–2) × 10^{12} genome copies per ml). Optimal titres of (1–2) × 10^{9} viral genome particles per ml for AAV2/2-CAG-memb-mCherry and 2 × 10^{10} viral genome particles per ml for rAAV2/2- YC3.6 were prepared in phosphate-buffered saline (PBS, pH = 7.4). rAAV2/9 expressing GFP

and mCherry were generated and provided by D. Cai and K. Cohen in our laboratory; high titer virus was produced at the University of Pennsylvania Vector Core.

To inject virus into eyes, adult mice were anaesthetized with ketamine/xylazine by intraperitoneal injection. A 30½G needle was used to make a small hole in the temporal eye, below the cornea, and 1.5 µl of rAAV virus was injected into the vitreous humor with a Hamilton syringe and 33G blunt-ended needle. Animals were killed and retinas were dissected 4–6 weeks following injection. For cerebellar virus infection, P1–P2 mice were anaesthetized with ice and a small puncture was made into the caudal-medial position of one cortical lobe; 1.5 µl of rAAV2/9-GFP; mCherry virus was injected with a Hamilton syringe and 33G blunt-ended needle. Mice were analyzed 12–35 days after infection.

For biolistic transfection of SACs, gold particles (1.0 µm diameter, Bio-Rad) were coated with plasmids encoding tdTomato driven by CMV promoter (Stacy and Wong, 2003). Live retinas were dissected, transected with four radial incisions, flattened with photoreceptor side down, and mounted onto a nitrocellulose filter (Millipore). Gold particles were delivered using a Biolistics Helios Gene gun device (Bio-Rad), and retinas were cultured in Ames medium (Sigma) in an oxygenated incubator heated to 37 °C for 12–16 h.

To assess interactions between dendrites of neighboring SACs, we injected pairs of cells with fluorescent dyes. Retinas from mice expressing OFP in SACs (Thy1-OFP3) were mounted RGC side up and perfused with Ames medium bubbled with 95%O_2/5%CO_2 at 25 °C. OFP^+ SACs were visualized with epifluorescence, and impaled with high resistance electrodes (50 MΩ) filled with a K^+ based intracellular recording solution supplemented with 50 µM Alexa Fluor 568 (for targeting) and 200 µM of Alexa Fluor 488 or 647 (for filling, Invitrogen). Square voltage pulses of ~3 V were applied to SACs at 50 Hz using a BK Precision Model 3011B function generator. After filling one SAC, the electrode was replaced with a second containing the contrasting dye and the second cell was filled. Images of labelled SAC pairs in live retinas were acquired at 40× on a Zeiss LSM 510 confocal microscope.

2.5.4 Tissue preparation and immunohistochemistry

Mice were killed with intraperitoneal injection of Nembutal, and either enucleated immediately or transcardially perfused with Ringer's solution followed by 4% paraformaldehyde (PFA) in PBS. Eye cups were removed and fixed in 4% PFA on ice for 1 h, followed by dissection and post-fixation of retinas for an additional 30 min, then rinsed with PBS. Brains were post-fixed in 4% PFA at 4 °C overnight. Animal procedures were in compliance with the US National Institutes of Health Guide for the Care and Use of Laboratory Animals and approved by the Animal and Care and Use Program at Harvard University.

Whole-mount preparations and cryosections of retinas were performed as described (Hong et al., 2011; Lefebvre et al., 2008). Briefly, whole retinas were incubated for 1–2 h in blocking buffer (0.4% Triton-X, 4% normal donkey serum in PBS), then incubated for 6 days at 4 °C with primary antibodies. Sagittal 80 μm sections of cerebellum were obtained with a vibratome (Leica), incubated in blocking buffer, and with primary antibodies for 2 days at 4 °C. Following washing, retinas and brain sections were incubated for 3 h at room temperature with Alexa-conjugated secondary antibodies (Invitrogen or Jackson ImmunoResearch). Whole retinas were flattened with photoreceptor side down onto nitrocellulose filters. Retina flat-mounts and brain sections were mounted onto glass slides, covered with Vectashield (Vector) or Fluoromount G (Southern Biotech), and imaged on an Olympus FV1000 scanning confocal microscope. Antibodies used were as follows: chick and rabbit anti-GFP (Aves and Millipore); rabbit anti-DsRed (Clontech); goat anti-choline acetyltransferase (Millipore); guinea pig anti-vGluT3 (Millipore); rabbit anti-Calbindin (Swant); mouse anti-syntaxin HPC1 clone (Sigma); rabbit anti-cleaved caspase3 (Cell Signaling Technology). Nuclei were labelled with DAPI, Po-pro1, or NeuroTrace Nissl 435/455 (Invitrogen).

2.5.5 SAC purification and culture

To isolate and culture wild-type and *Pcdhg* mutant SACs *in vitro,* we crossed the *Thy1-OFP3* transgene, which selectively directs expression of Kusabira Orange (OFP) in SACs and subset of RGCs (Kay et al., 2011a), into $Pcdhg^{fcon3}$*; Six3-cre* mice. Retinas from genotyped $Pcdhg^{fcon3/fcon3}$*; Six3-*

cre; Thy1-OFP3 mutant and control P2 mice were dissociated using papain (Lefebvre et al., 2008). OFP^+ SACs were isolated by fluorescence activated cell sorting (FACS, MoFlo), plated onto poly-L-lysine-coated glass coverslips (Warner) and cultured for 7–9 days in RGC growth media modified from Meyer-Franke (Meyer-Franke et al., 1995) in the following ways: (1) substitution of NS21 (Chen et al., 2008) for B27, (2) substitution of N2 (Invitrogen) for Sato stock, (3) addition of TGF-β1 and TGF-β2 (2.5 ng ml^{-1}; Peprotech), and (4) addition of mouse glia-conditioned medium (15%). One-third of media was exchanged with fresh media every three days. Cells were fixed with cold 4%PFA/4% sucrose for 15 min, and immunostained for syntaxin and calbindin to confirm SAC identity, and for GFP to confirm *Pcdhg*$^{-/-}$; GFP^- SACs from unrecombined Pcdhg-GFP^+ SACs due to variegated Six3-Cre activity in retina.

2.5.6 Image analysis

For best reproduction and clarity of SAC arborizations, maximized projections of confocal images were inverted and contrast-enhanced using Photoshop (Adobe Systems). For morphometric analysis of SACs, we used Fiji software and selected confocal image series of wild-type and *Pcdhg* mutant SACs situated in comparable retinal eccentricities. Self-crossings per dendritic branch order were quantified as number of branch overlaps detected in single confocal planes; crossings occurring distal to fifth branch order could not be quantified accurately owing to severity of defects in mutants. Dendritic field diameter was measured as the longest axis of arborization. In some cases, arborizations were re-imaged by oversampling using a 60× 1.45NA objective at *x*,*y*,*z* resolution of 47 × 47 × 131 µm and then subjected to deconvolution using Huygens software (http://www.svi.nl/HuygensProfessional).

For analysis of SAC density and mosaic regularity, confocal *z*-stacks of ChAT-labelled SACs through the GCL and INL were acquired at similar locations in central retina. Sample sizes were 4–5 areas (0.099 mm^2) per animal, 2–4 animals per genotype. For each field, *x*–*y* coordinates of SAC arrays were obtained by manually marking centers of cells using Fiji and used to compute SAC density (number

per mm^2), packing factor (Whitney et al., 2008), and density recovery profiles (DRP) (Rodieck, 1991) with WinDRP software (http://www.mpimf-heidelberg.mpg.de/~teuler/WinDRP/ReadMe.htm).

To compare the space-filling and complexity of control and mutant SAC arborizations, we computed fractal dimensions, *Df*, which provide a measure of how completely dendrites fill its area (Jelinek and Fernandez, 1998; Montague and Friedlander, 1989, 1991; Smith et al., 1996). To calculate D_f, we applied the box-counting method as implemented in the FracLac 2.5 plug-in for ImageJ software (http://rsb.info.nih.gov/ij/plugins/fraclac/FLHelp/Introduction.htm; NIH). Confocal images of cultured mutant and control SACs were obtained at equivalent laser scanning parameters with a 60× oil immersion lens, and maximum projections and thresholded, binary images were processed using Image J. Box counts using a series of progressively smaller box sizes (d) were scanned in a region of interest covering the SAC arborization, and the number of boxes intersected by pixels [$k(d)$] were analyzed; this computes D_f, which represents an inverse linear regression between $\log[k(d)]$ and $\log(d)$. D_f ranges from 1.0 (straight line with a dimension of 1) to 2.0 (plane with a dimension of 2); a difference of 0.1 represents a doubling of complexity (Jelinek and Fernandez, 1998).

For analysis of dendrite overlap between arborizations of neighboring SACs, pairs with somata separated by 80–160 µm were selected because their dendrites are known to interact (Lee and Zhou, 2006). Images were processed using Fiji or Photoshop software. To estimate the amount of dendritic overlap that would occur by chance if two SAC arborizations occupy the same territory, we flipped or rotated the image of one SAC, realigned cell body position, and merged images. This method was inspired by work on tiling of RGC dendrites (Wassle et al., 1981). We measured total overlapping pixels in real and flipped images, interpreting ratios of >1 (real/flipped) as indicating non-random interactions between SACs.

Purkinje cell dendrite self-crossings detected in single confocal planes were counted in a 7,225 μm^2 region of interest assigned to middle of arborization. Purkinje arborization areas were measured using the convex-hull selection in Fiji. Calbindin-labelled Purkinje somata residing along a 635 µm segment in lobules III–VI in single confocal planes were counted to measure Purkinje cell density.

Means were compared using the two-tailed Student's *t* test on condition of equivalent variances determined by *F*-test, or with the Mann–Whitney non-parametric test. Means of multiple samples were compared using ANOVA and posthoc Tukey test.

2.5.7 RT–PCR of dissociated retina cells

We used FACS to sort live cells from dissociated P7 whole retina, VC1.1^{+} amacrine cells, and OFP^{+}; Thy1.2^{-} SACs cells, as described previously (Kay et al., 2011a; Kay et al., 2011b). Amacrine cells were sorted from a live cell suspension of dissociated retinal cells using monoclonal VC1.1 antibody (200 μg ml^{-1}, Sigma) and an anti-IgM secondary conjugated to phycoerythrin-Cy7 (Southern). OFP^{+} SACs were sorted from OFP^{+} RGCs by negative selection of Thy1.2-PE-Cy7 labelled RGCs. In each condition, 2,000 cells were sorted directly into RNA lysis buffer (Qiagen); RNA was purified and first strand cDNAs were generated with Superscript RT III (Invitrogen). Primers that uniquely detect the 22 Pcdhg variable exon-constant exon spliced transcripts were adapted from Prasad et al., 2008, with modifications to avoid cross-hybridization. These primers, and others used to assess purity of the sorted population, are listed in **Table 2.1**. PCR program used is: 94 °C for 2 min; 30 cycles of 94 °C for 20 s, 56 °C for 30 s, 72 °C for 1 min; 72 °C for 7 min.

Table 2.1: Primers for RT-PCR

Primer Target/Name	Amplicon size	Primer sequence (5'-3')
Pcdhga1-F	**669**	**CTTGGTGCTCAAGCTGCGACA**
Pcdhga2-F	**658**	**GCTGAGGCGCTGGCATCTGT**
Pcdhga3-F	**795**	**CTGGGGGACCTGGAAAGCATC**
Pcdhga4-F	612	TGGGTTGTCATCCTTGCCTG
Pcdhga5-F	**622**	**CCACAGGCAGATTGGCCGAC**
Pcdhga6-F	600	GTCCACTTCACATTTCGTGG
Pcdhga7-F	628	GCTACAGGCTTCTTCAGGTG
Pcdhga8-F	**628**	**CCAGCTCCAGGGCTCCAGAA**
Pcdhga9-F	**584**	**GTGGGTGTGCATGGGGTTCAGA**
Pcdhga10-F	**654**	**GCGCTGGCACAAGTCTCACG**
Pcdhga11-F	**618**	**ATTGGCTGGTGTGCCTCCTTCG**
Pcdhga12-F	603	CGTTGCAGCCTCTCACTTTG
Pcdhgb1-F	594	CCTGAAGTCTCAACCTGTGG
Pcdhgb2-F	592	CTCTAACCTTGCGACTGGAG
Pcdhgb4-F	566	GCTTTCAGTCGGAAGTGGTG
Pcdhgb5-F	588	TCTAAGCCTGTGGTTTTCCC
Pcdhgb6-F	**618**	**TCAGTCTGGTCTTTGTTCTAAGGCT**
Pcdhgb7-F	590	CTAGACCAGTACTTCCACCC
Pcdhgb8-F	**663**	**CCTTCGCCTTCGACAGTCCC**
Pcdhgc3-F	612	GTGAGCTCCCTGTACCGAAC
Pcdhgc4-F	614	TCACCAGATCTCGGAGGAGG
Pcdhgc5-F	**649**	**GCAGGGGCCAGGACTCACC**
Pcdhg-conex3R		**CCATATTACTTCTTCTCTTTCTTGCCC**
		bold = modified from Prasad et al., 2008.
ChAT-F ChAT-R (SAC marker)	634	CTGGCAACTTCGTCGGAGGC TGGCTGTCCAGCAGAGCCTT
Brn3a-F Brn3a-R (RGC marker)	618	ATCTGCGACTCGGACACGGA CATGGGACTCCTGCCCCCAA
Brn3b-F Brn3b-R (RGC marker)	613	TAGCGGGAGACACAGGAGCG GGTAAGTGGCGTCCGGCTTG
Gad1 (amacrine marker)	102	CTGTGACTCGCTTAGCTGAAACCT GCACAGTGTGGGTTTCATGTCTTC
mGluR6-F mGluR6-R (bipolar marker)	527	CAAGGCCCGAGGTGTGCCAG GGCCAGCCTGCCCAGGAAAG
Trpm1-F Trpm1-R (bipolar marker)	367	GCGTGGTTCAATCAAGAGCTC CATGAGGTGGAGCAGGGAATCTG
Rhodopsin-F Rhodopsin-R (Rod photoreceptor marker)	370	CTACTTCGTCTTTGGGCCCACAG CCCATAGCAGAAGAAGATGACGATCA
Beta-actin-F Beta- actin-R	168	ACCAACTGGGACGACATGGAGAA CATGGCTGGGGTGTTGAAGGT

2.6 Acknowledgements

We thank members of our laboratory for providing advice and reagents, including D. Cai and K. Cohen (rAAV), I.-J. Kim (*fstl4*-line 1 mice) and M. Yamagata for modified Rosa-CAG targeting vector. We also thank B. Stevens (Children's Hospital) for advice on culture methods. This work was supported by grants from NIH to J.R.S. (R01NS029169 and R01EY022073) and T.M. (R01NS043915) and NARSAD Young Investigator Award to J.L.L.

Chapter 3: Protocadherin-dependent dendritic self-avoidance regulates neural connectivity and circuit function

Preface:

This chapter contains work that was not done in collaboration with anyone. I have performed all experiments and data analysis presented. This study was supervised by Josh Sanes.

3.1 Abstract

Dendritic and axonal arbors of many neuronal types exhibit self-avoidance, in which branches repel each other. In some cases, these neurites interact with those of neighboring neurons, a phenomenon called self/non-self discrimination. The functional roles of these processes remain unknown. Here, we used retinal starburst amacrine cells (SACs), critical components of a direction-selective circuit, to address this issue. In SACs, both processes are mediated by the gamma-protocadherins (Pcdhgs), a family of 22 recognition molecules. We manipulated Pcdhg expression in SACs and recorded from them and their targets, direction-selective ganglion cells (DSGCs). SACs form autapses when self-avoidance is disrupted and fail to form connections with other SACs when self/non-self discrimination is perturbed. Pcdhgs are also required to prune connections between closely spaced SACs. These alterations degrade the direction selectivity of DSGCs. Thus, self-avoidance, self/non-self discrimination, and synapse elimination are essential for proper function of a circuit that computes directional motion.

3.2 Introduction

The geometry of a neuron's dendritic and axonal arbors is a major determinant of the neuron's role within a circuit. In sensory systems, for example, the size and shape of a dendritic arbor determines the size and shape of the neuron's receptive field, and the degree of branching within the arbor determines how densely the field is sampled (Lefebvre et al., 2015). Similarly, the size and density of the axonal arbor are critical determinants of a neuron's projective field.

For many neurons, a major contributor to the patterning of arbors is a phenomenon called self-avoidance, in which sibling branches do not contact each other. Although not all neurons exhibit self-avoidance, this phenomenon has been observed in a variety of systems including sensory neurons of leech (in which the process was first described), Manduca sexta, Drosophila, C.elegans, and zebrafish (Grueber et al., 2001; Grueber et al., 2003b; Kramer and Kuwada, 1983; Kramer and Stent, 1985; Liu and Halloran, 2005; Nicholls and Baylor, 1968; Sagasti et al., 2005; Smith et al., 2012; Yau, 1976). Dendrites of olfactory projection neurons and axons of mushroom body neurons also exhibit self-avoidance in Drosophila (Hattori et al., 2007; Wang et al., 2002a; Zhan et al., 2004). In mammals, self-avoidance has been documented in cerebellar Purkinje cells and some types of retinal horizontal, bipolar, amacrine and ganglion cells (Lefebvre et al., 2012; Matsuoka et al., 2012; Montague and Friedlander, 1991; Wassle et al., 2009). Several cell-surface proteins have been implicated in self-avoidance, including Dscam1, Turtle, Flamingo, LAR-like receptor tyrosine phosphatase, Unc-5, Unc-6 (Netrin) and Unc-40 (DCC) in invertebrates (Baker and Macagno, 2000; Gao et al., 2000; Long et al., 2009; Matthews et al., 2007; Smith et al., 2012) and Dscam, DscamL1, Slit, Robo, Sema6A, PlexA4, PlexA2, and gamma-Protocadherins (Pcdhgs) in mice (Fuerst et al., 2009; Fuerst et al., 2008; Gibson et al., 2014; Lefebvre et al., 2012; Matsuoka et al., 2012; Sun et al., 2013). In each case, they appear to act through contact-dependent repellent mechanisms.

In some instances, processes of neurons that exhibit self-avoidance do not avoid other neurons of the same type; rather, they overlap extensively with and sometimes even form synapses on each other. Thus, these neurons appear to discriminate between their own processes, which they repel, and those of

their neighbors, with which they interact (**Figure 3.1A**). This puzzling observation suggests that processes of nominally identical neurons are immune to the repellent forces that act within each other's arbors, a phenomenon that has been called self/non-self discrimination (S/NSD) (Zipursky and Grueber, 2013). Of the molecules that mediate self-avoidance, two have also been shown to mediate S/NSD: fly Dscam1 and mouse Pcdhgs (Hattori et al., 2007; Hughes et al., 2007; Lefebvre et al., 2012; Matthews et al., 2007; Soba et al., 2007). While Dscam1 and Pcdhg proteins are not structurally related, they have three properties that allow them to mediate both self-avoidance and S/NSD. First, both are transmembrane recognition molecules with remarkable extracellular diversity. Alternative splicing of the Dscam1 transcripts and alternative promoter choice (**Figure 3.1B**) plus isoform multimerization of Pcdhgs lead to >10,000 recognition units (Murata et al., 2004; Schmucker et al., 2000; Schreiner and Weiner, 2010; Tasic et al., 2002; Thu et al., 2014). Second, each Dscam1 and Pcdhg isoform binds homophilically, but does not bind appreciably to other, closely related isoforms (Schreiner and Weiner, 2010; Thu et al., 2014; Wojtowicz et al., 2004; Wojtowicz et al., 2007). Finally, each neuron in a population expresses a small randomly selected subset of isoforms (Kaneko et al., 2006; Neves et al., 2004; Toyoda et al., 2014; Zhan et al., 2004), leading to molecular diversification. Together, these observations have led to a model for self-avoidance and S/NSD in which Dscam1- and Pcdhg-mediated homophilic interactions generate signals leading to repulsion. Because all dendrites (or axons) of a single neuron display the same set of Dscam1 or Pcdhg isoforms, they exhibit self-avoidance. On the other hand, any individual neuron is unlikely to encounter a neighbor that displays the same combination of isoforms, so the neurons do not repel each other, and thus display S/NSD.

These morphological and molecular analyses of self-avoidance and S/NSD have led to several hypotheses about roles they might play in the function of neurons and neuronal circuits. To our knowledge, however, none of these hypotheses has been tested experimentally. Here, we report such tests, focusing on starburst amacrine cells (SACs) of the mouse retina (**Figure 3.1C**). SACs have planar, radially symmetric dendritic arbors that exhibit striking self-avoidance (**Figure 3.1D**), but they fasciculate and form synapses with neighboring SACs (Lee and Zhou, 2006), and thus exhibit S/NSD. SACs also

provide the principal inhibitory input to ON and ON-OFF direction-selective retinal ganglion cells (DSGCs) and are essential for their direction selectivity (Yoshida et al., 2001). Elegant structural and functional studies have revealed the principal elements of the underlying mechanism: individual SAC dendrites are inhibitory direction-selective subunits that wire asymmetrically to DSGCs and inhibit these ganglion cells when visual motion is presented along their proximo-distal axis (Briggman et al., 2011; Euler et al., 2002; Fried et al., 2002; Vaney et al., 2012). Thus, the preferred direction of motion for the DSGC is opposite the preferred direction of motion for the SAC dendrites that innervate it (**Figure 3.1E**). In addition, SACs form inhibitory synapses onto each other, and it has been suggested that these connections sharpen the directional preference of SAC dendrites and thus the directional preference of the DSGCs that they innervate (Enciso et al., 2010; Lee and Zhou, 2006; Taylor and Smith, 2012).

We showed recently that Pcdhgs mediate self-avoidance and S/NSD in SACs (Lefebvre et al., 2012). Pcdhg-deficient SACs exhibit a dramatic loss of self-avoidance but maintain overlap with neighboring SACs, as if they mistake their own dendrites for those of their neighbors and fail to repel them. In contrast, forcing all SACs to express the same single Pcdhg isoform restores self-avoidance to individual cells but decreases the overlap between neighboring cells, as if they mistake dendrites of these neighbors for their own and repel them (**Figures 3.1F-H**). These results lead to three specific hypotheses about circuit function: (1) in the absence of self-avoidance, SACs will form synapses with themselves (autapses), (2) when S/NSD fails, SACs will form few synapses with each other, and (3) loss of self-avoidance or S/NSD will degrade the direction selectivity of DSGCs. Here, we present evidence in support of these hypotheses, thereby providing insights into the functional roles of self-avoidance and S/NSD. We also demonstrate an unexpected role of Pcdhgs in control of synapse elimination.

Figure 3.1: Pcdhg-dependent self-avoidance and self/non-self discrimination in SACs

A. Self-avoiding neurites lack isoneuronal contacts (repulsion, red), but adhere to and can form synapses with neurites of other cells of the same type, displaying self/non-self discrimination (adhesion, green).

B. Schematic of Pcdhg genomic locus and protein product. Distinct Pcdhg isoforms are assembled by splicing one of 22 variable exons, encoding the extracellular and transmembrane portions of the protein, to three constant exons, encoding the intracellular portion of the protein.

C. Vertical section of retina stained against ChAT to label all SACs (gray) overlaid with cartooned individual OFF and ON SACs (red). OFF SAC cell bodies reside in the inner nuclear layer (INL) and ON SAC cell bodies reside in the ganglion cell layer (GCL). SAC neurites reside in the inner plexiform layer (IPL).

D. *En face* view of individual dye-filled ON SAC in $Pcdhg^{22}$ retina.

E. Schematic of the retinal direction-selective circuit components and connections. PRs, photoreceptors; BCs, bipolar cells; SACs, starburst amacrine cells; DSGC, direction-selective ganglion cell. Gray stripes indicate OFF and ON direction-selective sublaminae (S2 and S4, respectively). Green and red arrows indicate directional preferences of DSGCs and SAC dendrites, respectively.

F-H. Schematic representation of the effects of changing Pcdhg expression in SACs (summary from Lefebvre et al., 2012). SACs from $Pcdhg^{22}$ retinas (**F**) are posited to express unique subsets of Pcdhgs and thus exhibit both self-avoidance and non-self adhesion. SACs from $Pcdhg^{0}$ retinas (**G**) express no Pcdhgs and thus do not exhibit self-avoidance. SACs from $Pcdhg^{1}$ retinas (**H**) all express the same Pcdhg and thus exhibit self-avoidance but not non-self adhesion.

Scale bar = 50 μm in **C** and **D**.

(Figure continues on next page)

Figure 3.1 (continued)

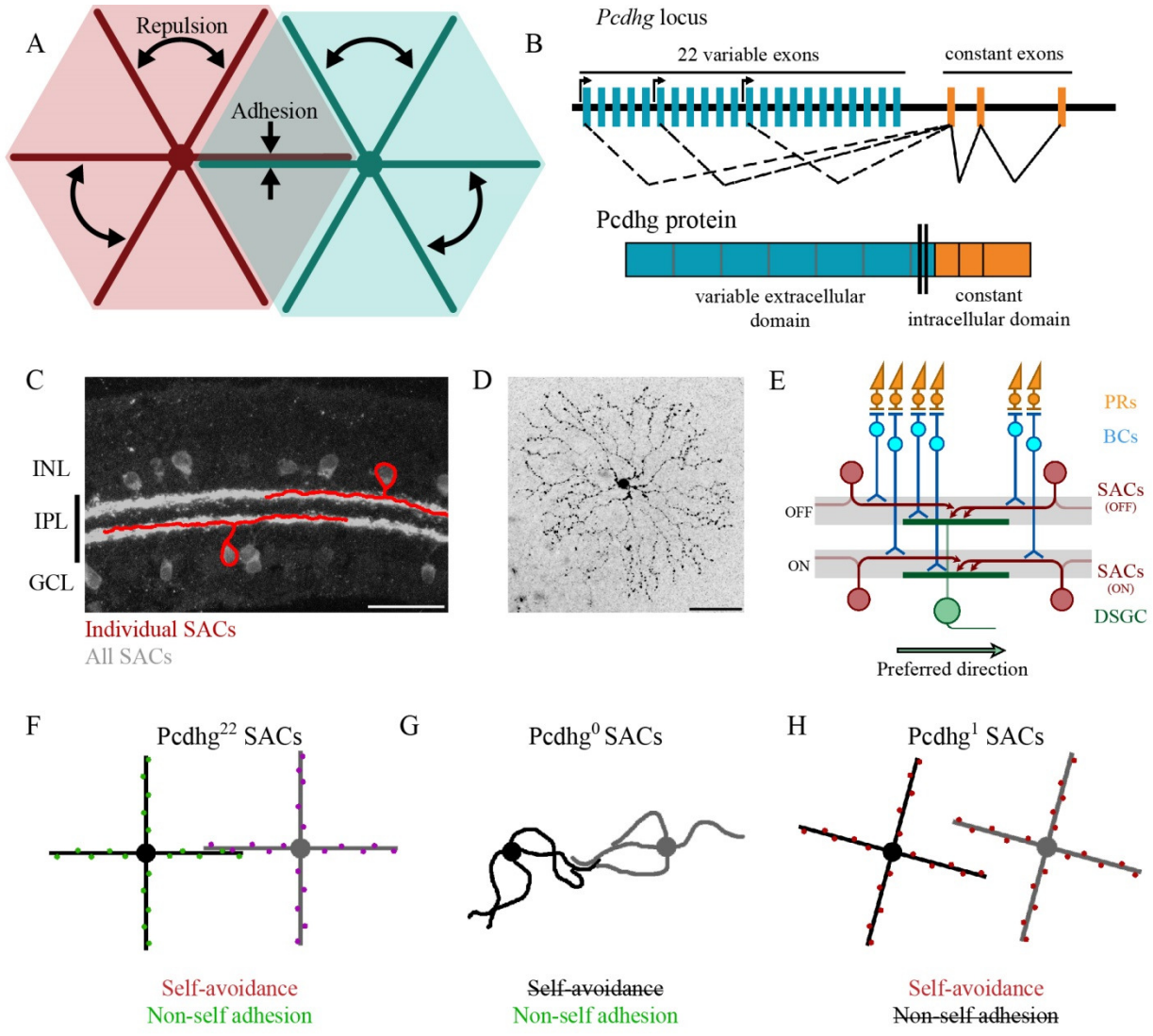

3.3 Results

3.3.1 SACs are connected by inhibitory synapses

Zheng et al. (2004) demonstrated the presence of GABAergic synapses between SACs shortly after eye-opening in rabbits. To begin this study, we confirmed that similar connections occur in young mice and asked whether they persist in adults. In addition to releasing GABA, SACs also release acetylcholine, the only retinal neuron to do so (Famiglietti, 1983; Hayden et al., 1980), so we used a line that expresses Cre recombinase from the choline acetyltransferase locus to mark and manipulate them selectively ($Chat^{cre}$; Rossi et al., 2011). We mated $Chat^{cre}$ mice to lines that express Cre-dependent fluorescent reporters (Buffelli et al., 2003; Madisen et al., 2010), identified SACs in explants, and recorded from pairs of ON SACs shortly after eye opening (postnatal day [P] 15-24; eye opening occurs at P14) and in young adults (P40-100) (**Figure 3.2A**). In each case, we tested pairs separated by distances varying from 35 to 175µm; the dendritic radius of SACs in living tissue is ~100µm, and varies little between P15 and P100 (**Figures 3.3A-B**). For each pair, we stepped presynaptic SACs from a holding potential (V_h) of -70 mV to +20 mV while holding postsynaptic SACs at +30 mV to record inhibitory currents. In the majority of cases, we obtained bidirectional recordings.

Stimulation of a SAC elicited an inhibitory current in a neighboring SAC in some but not all pairs tested at P15-24 and P40-100 (**Figures 3.2B-C**). Currents occurred with a latency of ~7ms and averaged ~15 pA in connected cells at both ages (**Figure 3.2J**). They were blocked by 50 µM picrotoxin and reversed at the chloride reversal potential for our recording solutions (~-70 mV), indicating that they were GABAergic and inhibitory (**Figures 3.4A-C**). Although SAC-SAC connections are both GABAergic and cholinergic synapses before eye-opening they exhibited no significant cholinergic component at the ages we tested (see also Zheng et al., 2004).

3.3.2 Synapses between closely spaced SACs are eliminated after eye-opening

The frequency with which SACs were interconnected varied systematically with the distance between their somata and with age. At P15-24, pairs were over twice as likely to be connected if they

Figure 3.2: SAC-SAC connections in Pcdhg^{22} and Pcdhg^{0} retinas

A. Paired recording configuration: SACs at various intercellular distances were targeted for recording in Pcdhg^{22} (left) and Pcdhg^{0} (right) retinas. Imaged are tracings of real SACs. Scale bar = 50 μm.

B-E. Presynaptic voltage steps from V_h = -70 to +20 mV (top), and examples of currents recorded from connected postsynaptic SACs (middle) and non-connected postsynaptic SACs (bottom) in juvenile Pcdhg^{22} retinas (**B**), adult Pcdhg^{22} retinas (**C**), juvenile Pcdhg^{0} retinas (**D**), and adult Pcdhg^{0} retinas (**E**).

F-I. Scatter plots of intercellular distance versus peak current size in juvenile Pcdhg^{22} retinas (**F**), adult Pcdhg^{22} retinas (**G**), juvenile Pcdhg^{0} retinas (**H**), and adult Pcdhg^{0} retinas (**I**). Number of connections tested = 34, 35, 37, and 39 in **F-I**, respectively.

J. Average peak current in connected SAC pairs at P15-24 (left) and P40-100 (right). Number of connections recorded = 21, 9, 23, and 20 in juvenile Pcdhg^{22} retinas, adult Pcdhg^{22} retinas, juvenile Pcdhg^{0} retinas, and adult Pcdhg^{0} retinas, respectively.

K. Distance dependence of SAC-SAC connectivity at in P15-24 animals (left) and P40-100 animals (right).

Data are shown as mean ± S.E.M. Statistics: n.s. = not significant, *P < .05, ** P < .01.

(Figure continues on next page)

Figure 3.2 (continued)

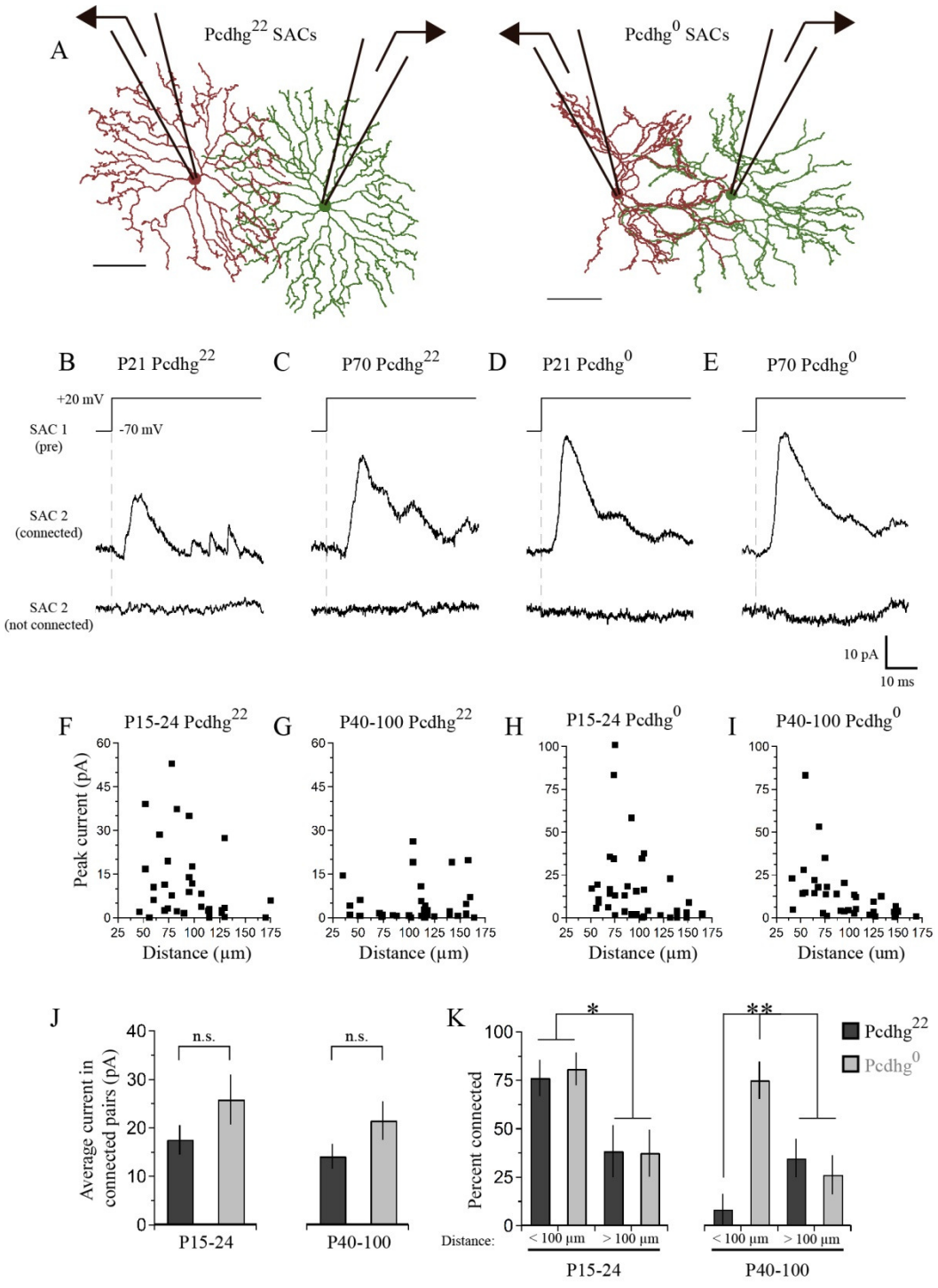

Figure 3.3: Recording distances and SAC dendritic radii

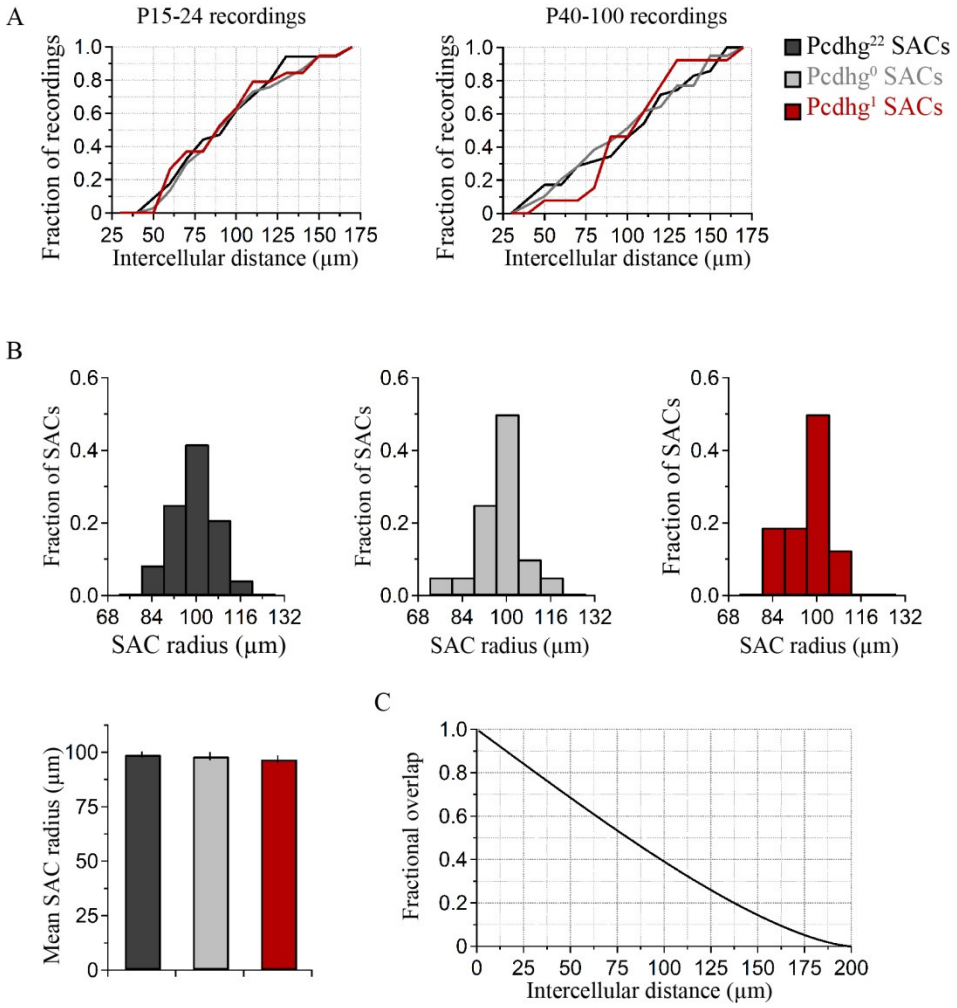

A. Cumulative histogram of intercellular distances of SAC connections that were tested in juvenile animals (left) and adult animals (right). Histogram range is 25-175 µm with bins of 10 µm. Number of connections tested = 34, 37, 19, 35, 39, and 13 for P15-24 Pcdhg^{22}, P15-24 Pcdhg^{0}, P15-24 Pcdhg^{1}, P40-100 Pcdhg^{22}, P40-100 Pcdhg^{0} SACs, and P40-100 Pcdhg^{1} SACs, respectively.

B. Top: Histograms of dendritic radii of Pcdhg^{22}, Pcdhg^{0}, and Pcdhg^{1} SACs. Bottom: Average dendritic radii across conditions. These measurements are from living retinas; following fixation, staining, and mounting, the dendritic radius of SACs is ~25% larger, as reported in many anatomical studies.

C. Relationship between intercellular distance and amount of dendritic overlap (SAC modeled as 100 µm radius circles).

Figure 3.4: Characterization of SAC-SAC synaptic connections

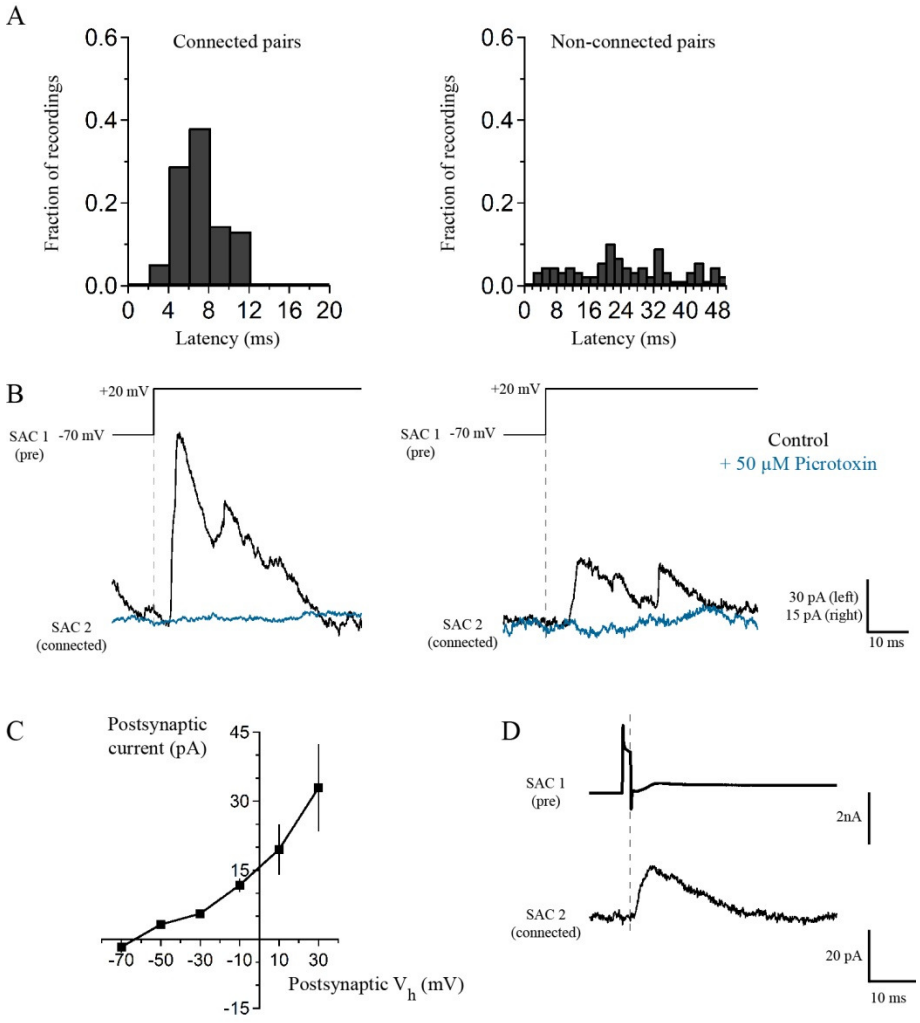

A. Left: Histogram of synaptic latencies in all connected cells. Histogram range is 0-20 ms after presynaptic depolarization, and bin size is 2 ms. Right: Same analysis performed on non-connected pairs with histogram range of 0-50 ms and bin size 2 ms.

B. Two examples of SAC paired recording showing that application of 50 µM Picrotoxin eliminates evoked transmission in these pairs and these currents are therefore GABAergic. Presynaptic cells were stepped from Vh = -70 to +20 mV. Postsynaptic cells were held at Vh = +30 mV.

C. Average current-voltage relationship of SAC-SAC connections, showing reversal at E_{Cl} (n = 3 pairs).

D. Example of paired recording using 'autaptic' voltage stimulus, showing that brief depolarization can evoke transmission in pairs of neurons, just as it does in single Pcdhg^0 SACs.

were separated by 35-100µm than if they were separated by 100-175µm (**Figures 3.2F and K, left**). This difference mirrors the inverse relationship of the distance between SACs and the overlap of their dendritic arbors (**Figure 3.3C**). In contrast, connections were seldom detectable between pairs separated by <100µm in adults. The frequency of connections between pairs >100µm apart did not change significantly with age (**Figures 3.2G and K, right**), indicating that the decline did not reflect decreased ability to detect connections in older mice. The most parsimonious explanation for this difference is that synapses between closely-spaced SACs are eliminated as SACs mature.

3.3.3 Pcdhgs drive elimination of connections between closely spaced SACs

Next, we asked whether Pcdhgs are required for formation of SAC-SAC synapses. For this purpose, we inactivated all 22 Pcdhgs in SACs using a conditional Pcdhg allele ($Pcdhg^{flox}$) (Lefebvre et al., 2008) and the $Chat^{cre}$ line. We refer to $Pcdhg^{flox/flox}$;$Chat^{cre}$ mice as $Pcdhg^{0}$ and controls ($Pcdhg^{flox/+}$ or $Pcdhg^{+/+}$; $Chat^{cre}$) as $Pcdhg^{22}$. Restricting the mutation to SACs allowed us to analyze roles of Pcdhgs in SACs without the complication of directly affecting other synaptic partners. Moreover, deletion of Pcdhgs leads to excessive cell death in many retinal neuronal populations, but not in SACs (Lefebvre et al., 2012; Lefebvre et al., 2008). As expected, we observed no alterations in the density of SACs or of other retinal cells in $Pcdhg^{0}$ retinas. We further verified that the laminar position and mosaic spacing of SACs, as well as overall retinal structure, did not differ detectably between $Pcdhg^{22}$ and $Pcdhg^{0}$ retinas (**Figures 3.5 and 3.6**).

At P15-24, the number and strength of SAC-SAC connections were similar in $Pcdhg^{22}$ and $Pcdhg^{0}$ retinas: in both genotypes, connections were over twice as common in closely spaced pairs than in pairs separated by >100µm and current sizes did not differ significantly between $Pcdhg^{22}$ and $Pcdhg^{0}$ retinas (**Figures 3.2D, H, and J**). Thus, Pcdhgs are dispensable for formation of SAC-SAC synapses. In adults, in contrast, the pattern of SAC-SAC connectivity differed between $Pcdhg^{22}$ and $Pcdhg^{0}$ mice. Synapses between closely spaced SACs were retained in mutants during the period that they were lost from controls (**Figures 3.2E, G, I, and K**). This loss of proximal connections was selective in that the frequency and

Figure 3.5: Lamination and spacing of SACs are normal in Pcdhg^{0}, and Pcdhg^{1} retinas

A. Vertical section of retina stained against ChAT to label all SACs in Pcdhg^{22}, Pcdhg^{0}, and Pcdhg^{1} retinas (left to right). Scale bar = 50 μm.

B. Top: En face view of OFF SACs in Pcdhg^{22}, Pcdhg^{0}, and Pcdhg^{1} retinas (left to right, respectively). Scale bar = 100 μm. Bottom: Density recovery profile of OFF SACs in Pcdhg^{22}, Pcdhg^{0}, and Pcdhg^{1} retinas (left) and total OFF SAC density.

C. Same as B but for ON SACs.

(Figure continues on next page)

Figure 3.5 (continued)

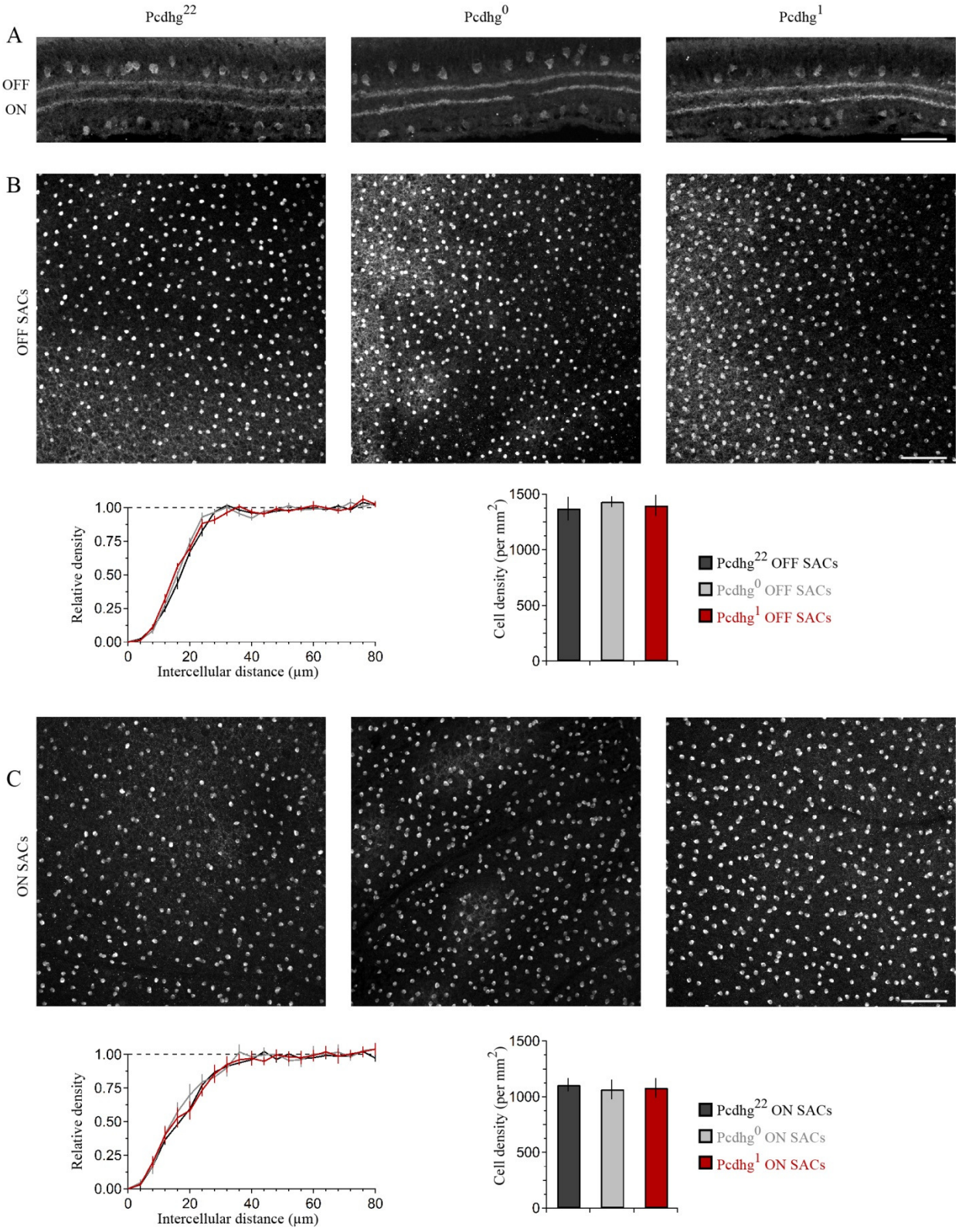

Figure 3.6: Normal retinal morphology in Pcdhg^{0}, and Pcdhg^{1} retinas

A. Nuclear label of all retinal neurons (TO-PRO3) showing retinal thickness is similar across conditions. The whole retinal thickness is shown.

B. Anti-Chx10 immunostaining to label bipolar cells. Image is cropped to just show inner nuclear layer.

C. Anti-AP2 immunostaining to label amacrine cells. Image is cropped to just show inner nuclear layer through ganglion cell layer. Some retinal blood vessels were also labeled because primary antibody is mouse monoclonal.

D. Anti-Brn3a immunostaining to label many retinal ganglion cells. Image is cropped to just show ganglion cell layer.

E. Anti-Calbindin immunostaining to label horizontal cells, some amacrine cells, and some retinal ganglion cells. Image is cropped to just show outer plexiform layer through ganglion cell layer.

All images show examples from P21 Pcdhg^{22}, Pcdhg^{0}, and Pcdhg^{1} vertical retinal sections in parallel (left to right, respectively). Scale bar = 50 μm in all panels. Images are oriented with photoreceptors towards the top and retinal ganglion cells toward the bottom of the page.

(Figure continues on next page)

Figure 3.6 (continued)

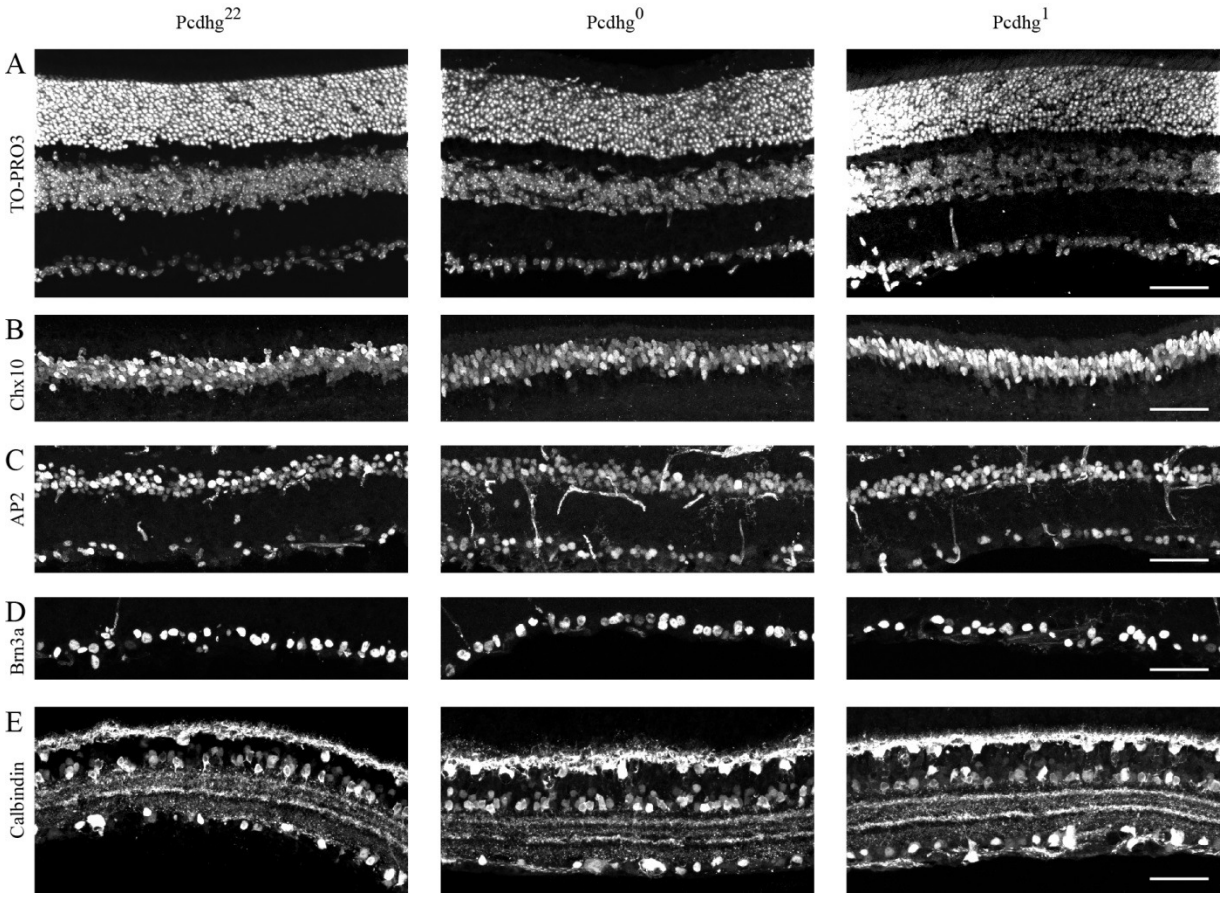

size of connections between SACs separated by >100µm did not differ significantly between $Pcdhg^{22}$ and $Pcdhg^{0}$ mice (**Figures 3.2J-K**). These results reveal a requirement of Pcdhgs for synapse elimination.

3.3.4 Pcdhgs prevent formation of SAC autapses

If $Pcdhg^{0}$ SAC dendrites treat other dendrites of the same SAC as if they are dendrites of other SACs, we wondered whether they would form autapses. To test this hypothesis, we adapted a protocol that had been used to elicit autaptic currents in cultured neurons and cortical slices (Bacci et al., 2003; Bekkers and Stevens, 1991). We stimulated SACs with brief voltage steps to very positive potentials (V = +60 mV, 2-4 ms), then returned to more negative potentials (V = -20 mV) (**Figures 3.4D and 3.7A**). These stimuli elicited autaptic currents in ~75% of $Pcdhg^{0}$ SACs at P21-24, but in no $Pcdhg^{22}$ SACs (**Figures 3.7B-C**). Autaptic currents resembled SAC-SAC connections in their latencies and rise times, were blockable by application of 50 µM picrotoxin, and averaged ~20pA in size (**Figures 3.7F-G**).

We also asked whether autapses are present in adult $Pcdhg^{0}$ SACs or whether, like synapses between closely-spaced SACs in wild-type retina (see previous section), they are progressively eliminated. Autapses persisted into adulthood in $Pcdhg^{0}$ SACs with sizes and frequency similar to those observed at P21-24 (**Figures 3.7D-G**). Thus, one role of Pcdhg-mediated self-avoidance is to prevent formation of autapses.

3.3.5 SACs that express the same Pcdhg isoform are seldom connected to each other

The proposed mechanism for Pcdhg-dependent S/NSD is that the stochastic expression of a subset of Pcdhg isoforms endows each SAC with a unique molecular identity that abrogates Pcdhg-dependent avoidance between neighboring SACs (Lefebvre et al., 2012). We hypothesized that if all SACs expressed the same Pcdhg isoform, they would treat dendrites of other SACs as if they were other dendrites of the same SAC, and form few SAC-SAC synapses. To test this idea, we used a mouse line in which a single Pcdhg isoform (PcdhgC3) can be expressed in any cell type in a Cre-dependent manner

Figure 3.7: Pcdhg^{0} SACs form autapses

A. SAC autaptic voltage stimulus (left). Single SAC recording configuration in Pcdhg^{22} (middle) and Pcdhg^{0} (right) retinas.

B-C. Example currents recorded from SACs in juvenile Pcdhg^{22} retinas (**B**) and juvenile Pcdhg^{0} retinas (**C**) in response to voltage stimulus shown in **A**. Arrowhead in **C** points to autaptic current in SAC from Pcdhg^{0} retina that was blockable by application of 50 μM picrotoxin (blue trace in **C**). Depolarization step to V_h = +60 mV was 2 ms in both **B** and **C**.

D-E. Example current recordings from SACs in adult Pcdhg^{22} retinas (**D**) and adult Pcdhg^{0} retinas (**E**) in response to voltage stimulus shown in **A**. Depolarization step to V_h = +60 mV was 4 ms in both **D** and **E**.

F. Peak outward currents measured during falling phase recorded current after initial voltage-step to +60 mV. Data points are staggered slightly for visual clarity.

G. Average peak autaptic currents evoked in SACs from Pcdhg^{0} retinas at P21-24 (left) and P40-100 (right) at V_h = -20 mV.

Upstroke of stimulus artifact (step to +60 mV) was removed from traces in **B**-**D** for visual clarity. Data are shown as mean ± S.E.M.

(Figure continues on next page)

Figure 3.7 (continued)

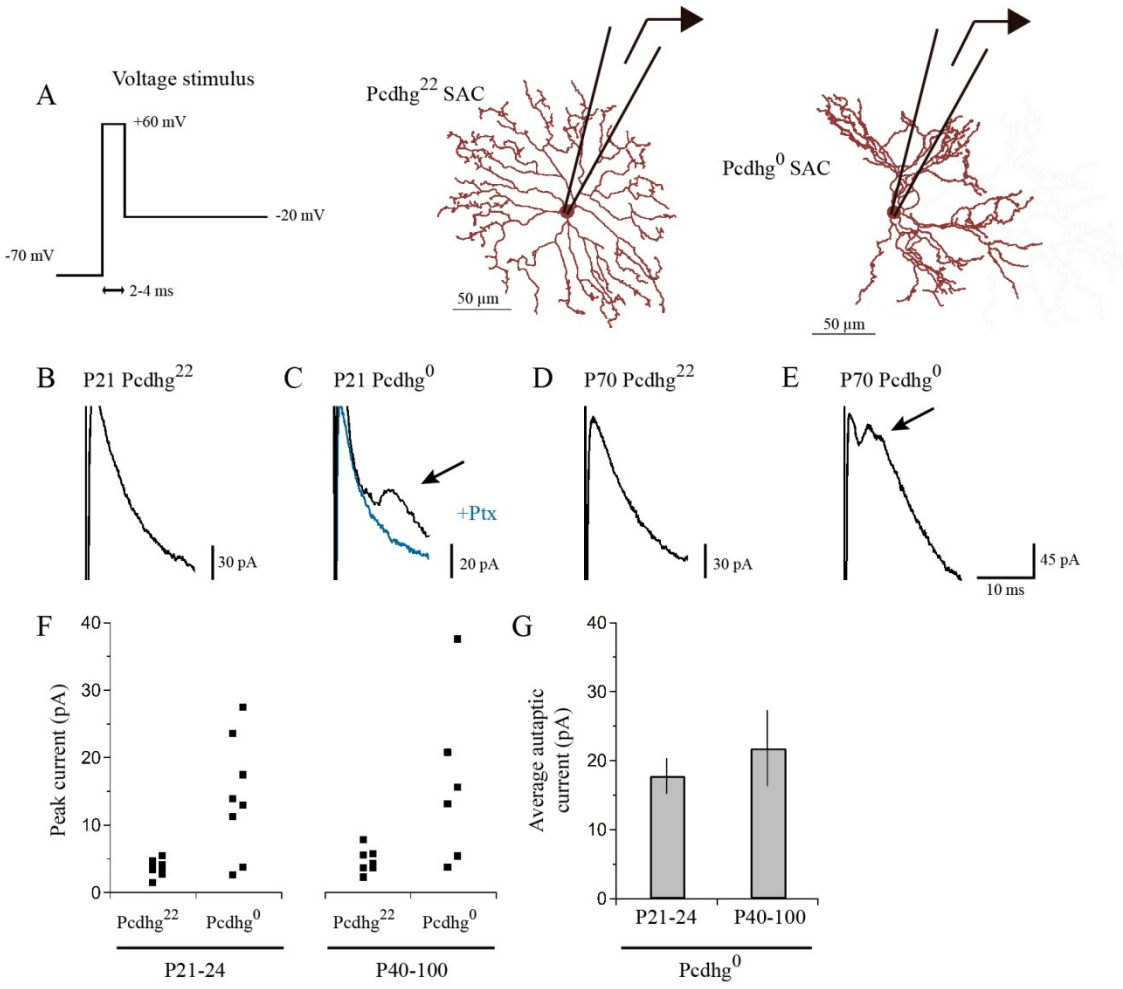

(Lefebvre et al., 2012). We call mice in which SACs expressed only this isoform $Pcdhg^{1}$ (Rosa-CAGS-lox-stop-lox-PcdhgC3-mCherry;$ChAT^{cre}$;$Pcdhg^{flox/flox}$).

The overall morphology, number, and spacing of SACs, as well as overall retina structure, were normal in $Pcdhg^{1}$ mice (**Figures 3.5, 3.6, and 3.8A**), and SAC dendrites formed a fine plexus within which they had ample opportunity to come into close proximity to each other (**Figure 3.8B**). We made paired recordings from SACs in $Pcdhg^{1}$ mice at P15-24 using methods described in Figure 2 (**Figures 3.8C-D**). The frequency of SAC-SAC connections in $Pcdhg^{1}$ mice was ~20% of that in $Pcdhg^{22}$ or $Pcdhg^{0}$ mice (**Figure 3.8F**). Similarly, currents in connected pairs were in $Pcdhg^{1}$ mice averaged ~40% of that in $Pcdhg^{22}$ or $Pcdhg^{0}$ mice (**Figure 3.8H**). Thus, forcing expression of the same Pcdhg isoform in all SACs decreased their connection strength to <10% (0.2 x 0.4) of controls. A similar decrease was observed in adult $Pcdhg^{1}$ retinas (**Figures 3.8E, G, and H**). We conclude that Pcdhg diversity is required for functional connectivity between neighboring SACs.

3.3.6 Pcdhgs are dispensable for connections of SACs with bipolar and ganglion cells

Having found that manipulation of Pcdhg expression affects the ability of SACs to form synapses on their own dendrites or those of other SACs, we asked whether such manipulations affect their ability to receive synapses from bipolar cells or form synapses onto DSGCs. We used visual stimuli based on previous findings that the main visually-evoked excitatory input to SACs is from bipolar cells, and that SACs provide the main inhibitory input to DSGCs (**Figure 3.9A**) (Helmstaedter et al., 2013; Hoggarth et al., 2015; Taylor and Wassle, 1995; Vaney et al., 2012).

To assess bipolar input to SACs, we recorded from ON SACs while holding the cells at V_h = -70 mV and presenting bright spot flashes centered on the soma of the recorded cell. SACs received strong excitatory inputs in $Pcdhg^{22}$, $Pcdhg^{0}$ and $Pcdhg^{1}$ mice, with no significant differences among them (**Figures 3.9B-C**).

Four populations of ON-OFF DSGCs have been described, each tuned to one of the cardinal directions: dorsal, ventral, nasal and temporal (Barlow and Hill, 1963; Elstrott et al., 2008; Oyster and

Figure 3.8: Decreased SAC-SAC connections in Pcdhg^{1} retinas

A. Replacement of all 22 Pcdhgs in SACs with a single Pcdhg isoform (top) rescues self-avoidance in individual SACs (bottom).

B. Plexus of all SAC dendrites (stained with anti-ChAT) in Pcdhg^{22} (left), Pcdhg^{0} (middle), and Pcdhg^{1} (right) retinas.

C. Presynaptic voltage steps from V_h = -70 to +20 mV (top), and examples of currents recorded from connected postsynaptic SACs (middle) and non-connected postsynaptic SACs (bottom) in juvenile Pcdhg^{1} retinas.

D-E. Scatter plots of intercellular distance versus peak current size in juvenile (**D**) and adult (**E**) Pcdhg^{1} retinas.

F. Percent of P15-24 recorded SAC pairs that were connected, irrespective of intercellular distance. Number of connections tested = 34, 37, and 19 in Pcdhg^{22}, Pcdhg^{0}, and Pcdhg^{1} retinas, respectively.

G. Same as **F** for adult retinas. Number of connections tested = 35, 39, and 13 in Pcdhg^{22}, Pcdhg^{0}, and Pcdhg^{1} retinas, respectively.

H. Average peak current in connected SAC pairs at all ages. Number of recorded connections = 30, 43, and 3 in Pcdhg^{22}, Pcdhg^{0}, and Pcdhg^{1} retinas, respectively.

Scale bar = 50 μm in **A** and 25 μm in **B**. Data are shown as mean ± S.E.M. Statistics: ** P < .01.

(Figure continues on next page)

Figure 3.8 (continued)

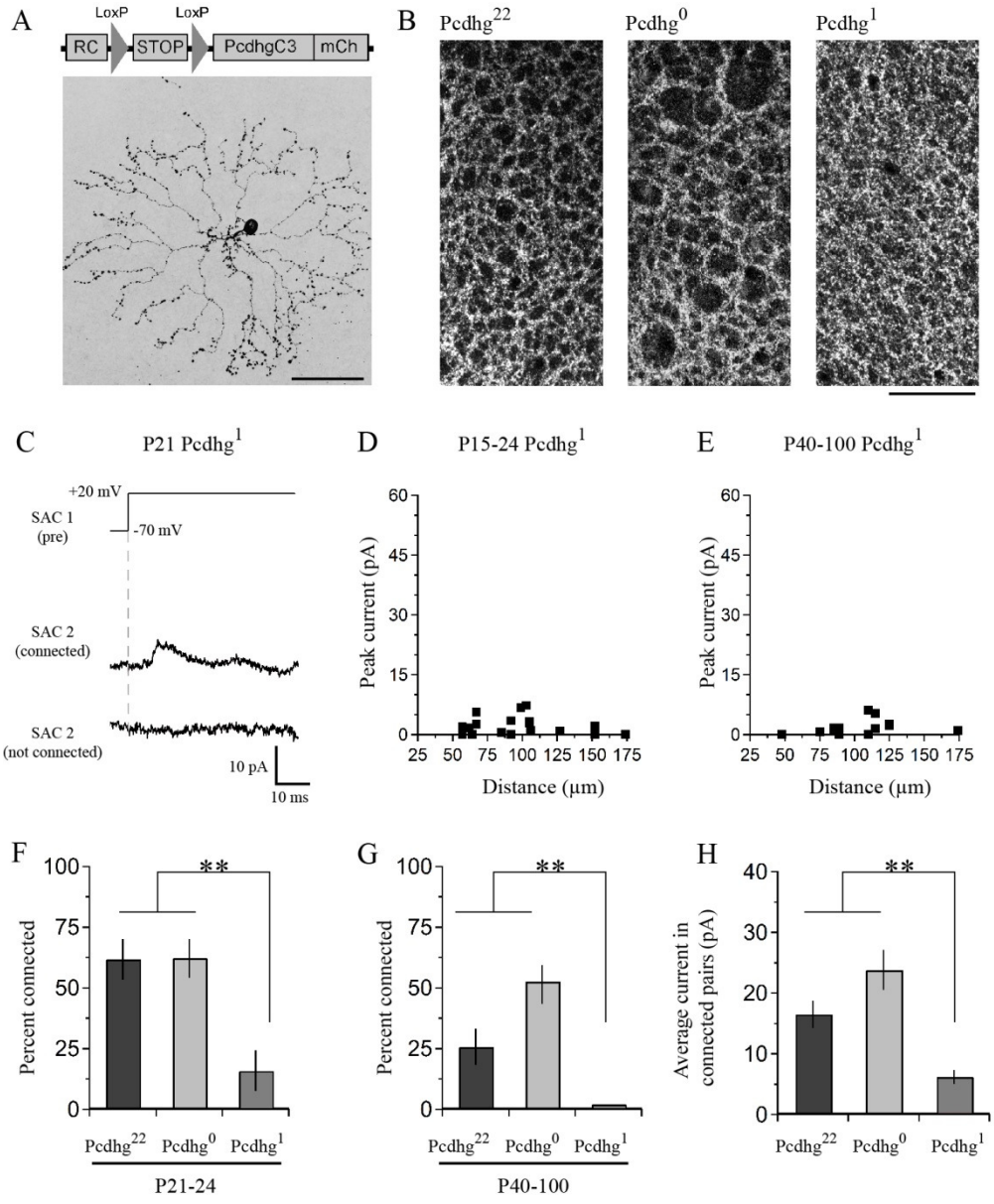

Figure 3.9: Integration of SACs into a direction-selective circuit is Pcdhg-independent

A. Schematic of excitatory and inhibitory synaptic inputs of retinal direction-selective circuit, showing bipolar inputs to SACs (measured in **B** and **C**), SAC inputs to DSGCs (measured in **D** and **E**), and bipolar inputs to DSGCs (measured in **F** and **G**).

B. Example excitatory currents (V_h = -70 mV) of ON SACs from $Pcdhg^{22}$ (black), $Pcdhg^{0}$ (gray), and $Pcdhg^{1}$ (red) retinas evoked by a 2 second bright spot flash.

C. Average peak current responses to the onset of flash stimulus. Number of SACs recorded is 8, 9, and 7 in $Pcdhg^{22}$, $Pcdhg^{0}$, and $Pcdhg^{1}$ retinas, respectively.

D. Example inhibitory currents (V_h = 0 mV) of vDSGCs from $Pcdhg^{22}$, $Pcdhg^{0}$, and $Pcdhg^{1}$ retinas evoked by a 2 second bright spot flash.

E. Average peak current responses to the onset (left) and offset (right) of flash stimulus. Number of vDSGCs recorded is 12, 13, and 10 in $Pcdhg^{22}$, $Pcdhg^{0}$, and $Pcdhg^{1}$ retinas, respectively.

F. Example excitatory currents (V_h = -70 mV) of vDSGCs from $Pcdhg^{22}$, $Pcdhg^{0}$, and $Pcdhg^{1}$ retinas evoked by a 2 second bright spot flash.

G. Average peak current responses to the onset (left) and offset (right) of flash stimulus. Number of vDSGCs recorded is 14, 11, and 13 in $Pcdhg^{22}$, $Pcdhg^{0}$, and $Pcdhg^{1}$ retinas, respectively.

H-J. Dye-filled vDSGCs with OFF and ON arborizations separated (top and middle, respectively) in $Pcdhg^{22}$ (**H**), $Pcdhg^{0}$ (**I**), and $Pcdhg^{1}$ (**J**) retinas. Bottom panels: Overlay of ON vDSGC dendrites (green) with ON SAC dendrites labeled with anti-ChAT antibody (red). Similar cofasciculation was seen for OFF dendrites. Scale bar = 50 μm.

Data are shown as mean ± S.E.M.

(Figure continues on next page)

Figure 3.9 (continued)

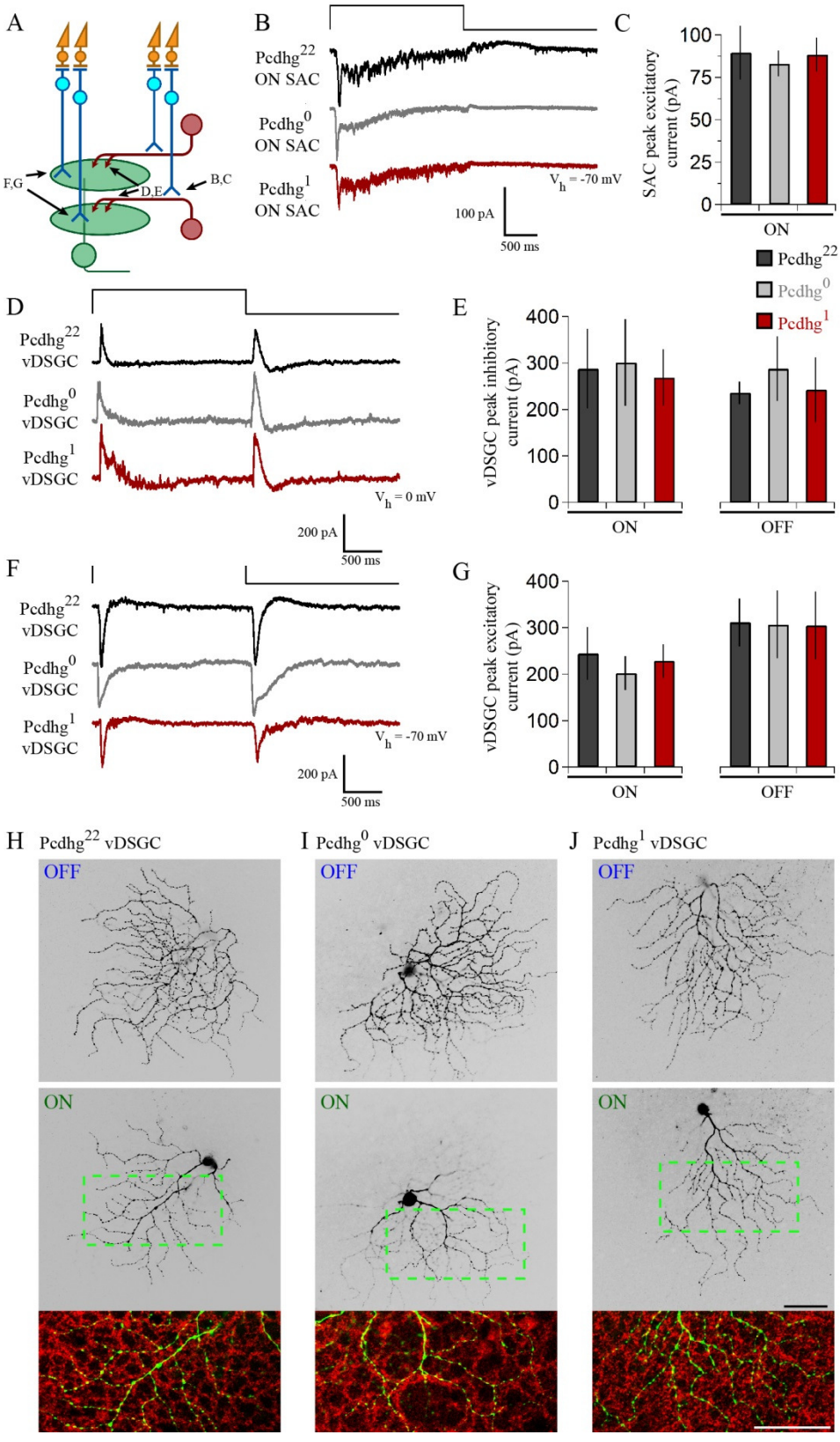

Barlow, 1967). Their physiological properties other than preferred direction are similar, but they exhibit molecular differences that allow them to be marked selectively (Kay et al., 2011a). To assess SAC input to DSGCs, we used a transgenic line in which DSGCs that prefer motion in the ventral direction express GFP (HB9-GFP; Trenholm et al., 2011). We introduced this transgene into the $Pcdhg^{22}$, $Pcdhg^{0}$ and $Pcdhg^{1}$ backgrounds, and recorded inhibitory currents (V_h= 0 mV) from GFP-labeled DSGCs, which we call vDSGCs here. Sizes of both ON and OFF inhibitory responses to spot flashes were indistinguishable across the three genotypes (**Figures 3.9D-E**). Similarly, excitatory spot flash responses in vDSGCs were unaffected by manipulation of Pcdhgs in SACs (**Figures 3.9F-G**). Thus, Pcdhg expression in SACs is dispensable for their ability to form and maintain synapses with other cell types.

We also assessed the structure of vDSGCs in $Pcdhg^{22}$, $Pcdhg^{0}$, and $Pcdhg^{1}$ mice. We filled single cells with fluorescent dye, stained SACs with antibodies to ChAT, and imaged the two cell types. In all conditions, the ON and OFF dendrites of these DSGCs stratified in the ON and OFF SAC plexus, fasciculated with SAC dendrites, and maintained their modest structural asymmetry (**Figures 3.9H-J**). Thus, altering Pcdhg expression in SACs had no detectable effect on the morphology of vDSGCs. We also validated that altering Pcdhg expression in SACs did not affect cell number, mosaic spacing, or expression patterns of vDSGCs (**Figure 3.10**).

3.3.7 Loss of SAC self-avoidance or S/NSD degrades direction selectivity of DSGCs

We next tested the hypothesis that loss of self-avoidance or S/NSD degrades the information-processing ability of SACs within the direction-selective circuit. To this end, we recorded spikes from vDSGCs while moving a bright bar over their receptive field in 8 different directions. Because vDSGCs are all tuned to a single direction in wild-type mice, we were able to ask whether manipulation of Pcdhgs affects preferred direction as well as the degree of direction selectivity.

vDSGCs in $Pcdhg^{22}$ mice exhibited strong ON and OFF directional responses (**Figures 3.11A**) as shown previously (Duan et al., 2014; Kim et al., 2010; Trenholm et al., 2011). We calculated a direction-selective index (DSI) for each vDSGC by computing the vector sum of the responses to different

Figure 3.10: Normal expression, spacing, and number of vDSGCs in Pcdhg^{0}, and Pcdhg^{1} retinas

A. Anti-GFP immunostaining in HB9-GFP positive retinas. Note that GFP signal is faint in dendrites by P21 but retained in cell body. Image is cropped to show inner nuclear layer through ganglion cell layer.

B. Anti-CART immunostaining same sections from A to label all populations of DSGCs.

C. Merge of panels **A** and **B** showing that HB9-GFP positive vDSGCs are positive for CART, but not the only CART positive cells in the ganglion cell layer. Note that CART antibody also labels Tyrosine hydroxylase-positive amacrine cells strongly in retinal sublamina 1.

D. Top: En face view of field of HB9-positive vDSGCs (inverted contrast). Bottom: Density recovery profile of HB9-GFP positive vDSGCs in Pcdhg^{22}, Pcdhg^{0}, and Pcdhg^{1} retinas (left) and total HB9-GFP positive vDSGC density.

All images show examples from P21 Pcdhg^{22}, Pcdhg^{0}, and Pcdhg^{1} retinas in parallel (left to right, respectively). Scale bar = 50 μm in panels **A-C** and 100 μm in panel **D**. Images in panels **A-C** are vertical retinal sections oriented such that photoreceptors are towards the top of the page.

(Figure continues on next page)

Figure 3.10 (continued)

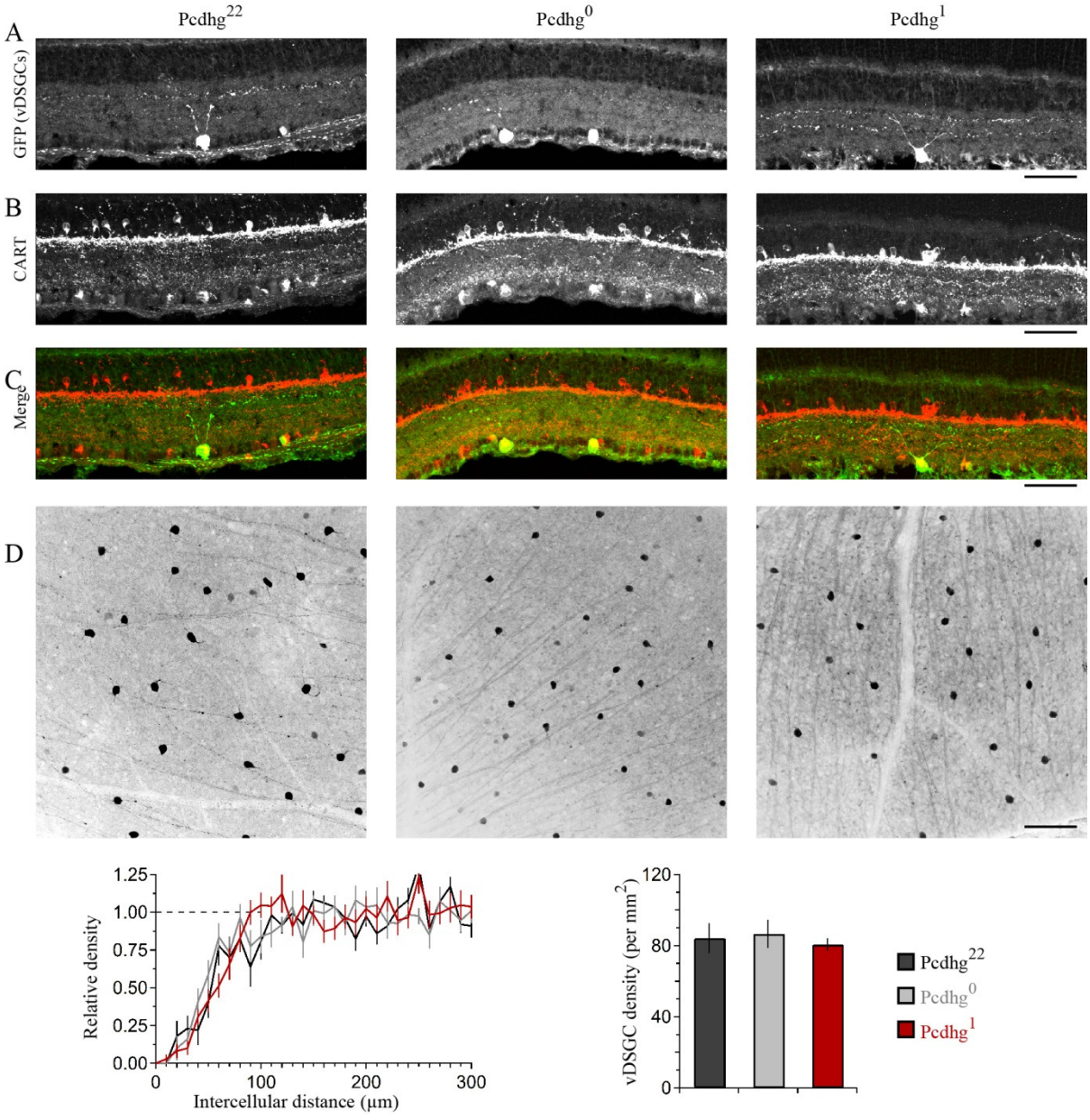

Figure 3.11: Alteration of Pcdhg expression degrades direction selectivity

A. Spiking responses of vDSGC from adult $Pcdhg^{22}$ retina to a bright moving bar moving in 8 directions. Polar plot is of peak firing rates in response to bar entering (ON, green) and exiting (OFF, blue) the receptive field center. Vectors represent vector sum direction-selective indices (DSIs) of ON and OFF responses. Surrounding central plot are spike histograms used to make polar plot and calculate DSIs and preferred directions.

B. ON (left, green) and OFF (right, blue) DSI vectors for all recorded DSGCs in $Pcdhg^{22}$ retina (n = 28 cells). Axes of retina are indicated with compass arrows: D, V, N, and T represent dorsal, ventral, nasal, and temporal.

C-D. Same as A and B but from adult $Pcdhg^{0}$ retinas (n = 28 cells).

E-F. Same as A and B but from adult $Pcdhg^{1}$ retinas (n = 19 cells).

G. Mean absolute DSI for all cells recorded, irrespective of which direction they preferred.

H. Mean angle deviated from ventral direction for all cells recorded.

I. Mean absolute difference between DSI (left) and angle of preference (right) for all recorded cells.

J. Plot of mean ventral projections of DSI vectors. For each recorded vDSGC, maximal ON and OFF firing rates in each direction were summed and used to generate a single DSI vector for each cell.

Data are shown as mean ± S.E.M. Statistics: n.s. = not significant, *P < .05, ** P < .01, *** P < .001.

(Figure continues on next page)

Figure 3.11 (continued)

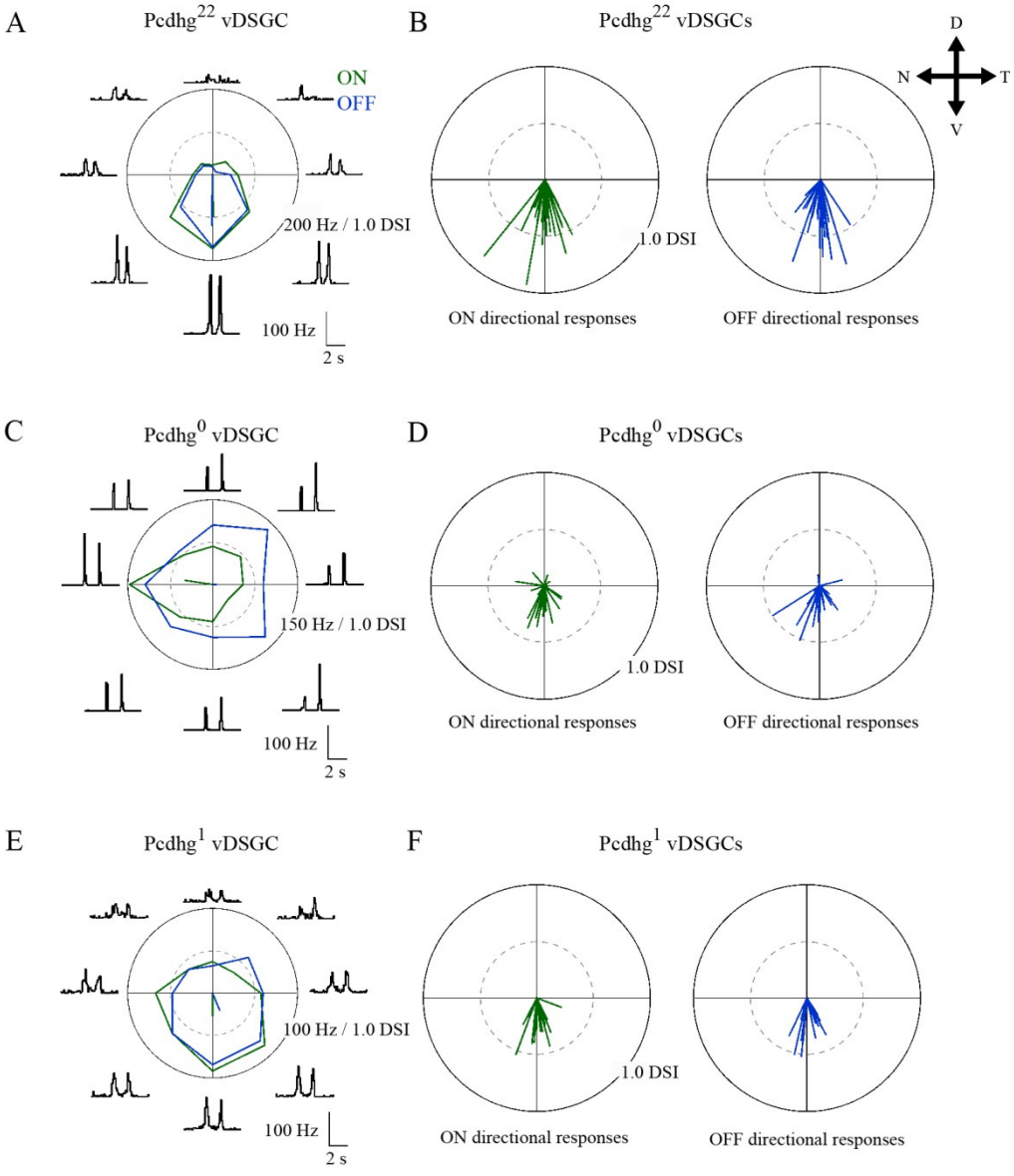

(Figure continues on next page)

Figure 3.11 (continued)

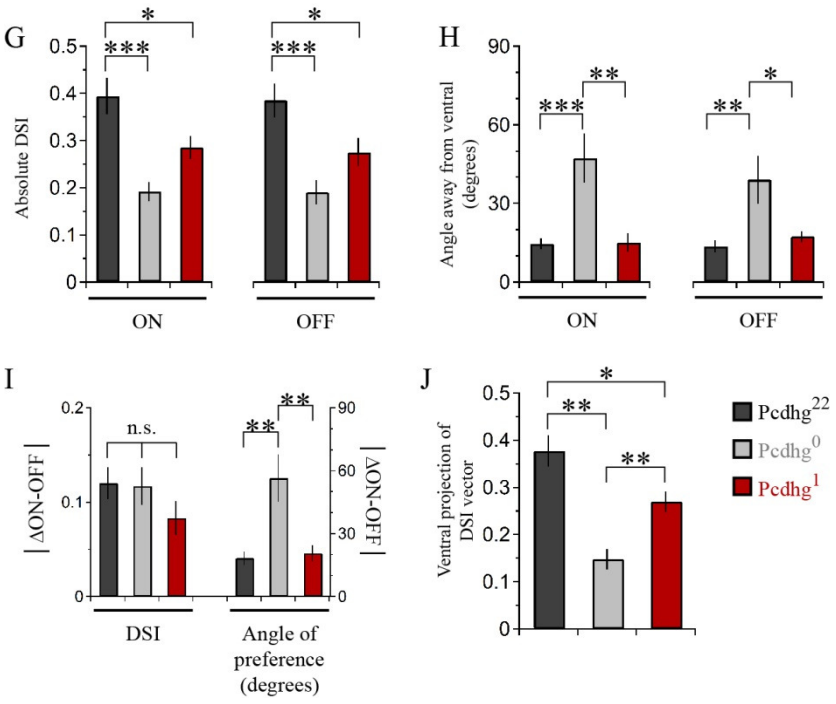

directions (Kim et al., 2008) and calculated both the magnitude of directional responses and the angle of preference (**Figure 3.11B**). Direction selectivity of vDSGCs was diminished in both $Pcdhg^{0}$ and $Pcdhg^{1}$ retinas, but in different ways. In both genotypes, the magnitude of the DSI vectors were significantly decreased with respect to controls (by ~50% in $Pcdhg^{0}$ and ~35% in $Pcdhg^{1}$; **Figures 3.11C-G**). In contrast, responses of vDSGCs in $Pcdhg^{0}$ retinas exhibited a significantly greater scatter around the ventral axis than those in wild-type retinas, whereas vDSGCs in $Pcdhg^{1}$ retinas were as precisely tuned to ventral motion as controls (**Figures 3.11C-F, H and 3.12**). This variance may reflect the contorted morphology of SAC dendrites in $Pcdhg^{0}$ but not $Pcdhg^{1}$ retinas. Likewise, the variation between the preferred direction of ON and OFF responses was greater in $Pcdhg^{0}$ retinas than in either $Pcdhg^{22}$ or $Pcdhg^{1}$ retinas, indicating that SAC morphology and connectivity are disrupted independently in the ON and OFF SAC layers (**Figure 3.11I**).

To obtain a single measure of how well vDSGCs reported on ventral motion, we projected the directional vectors onto the ventral axis. This gave us a ventral DSI that combined the degree of directional preference and the fidelity of ventral preference for ON and OFF responses together. vDSGCs in $Pcdhg^{22}$ (control) retinas were most ventrally selective, followed by those in $Pcdhg^{1}$ retinas; vDSGCs in $Pcdhg^{0}$ retinas were the least selective (**Figure 3.11J**). Together, these results demonstrate that manipulating Pcdhg expression in SACs, and thereby attenuating self-avoidance or S/NSD, degrades the direction selectivity of DSGCs.

Previous studies have shown that direction-selective responses are already present at eye opening in mice but become more selective with age (Chan and Chiao, 2013; Chen et al., 2014; Elstrott et al., 2008; Yonehara et al., 2011). We wondered whether this improvement of direction selectivity with age was related to the loss of proximal SAC-SAC connections. To assess this possibility, we recorded from direction-selective responses from vDSGCs at P15-24 in $Pcdhg^{0}$ mice, which do not go through a developmental change in SAC-SAC connectivity. We confirmed the improved age-dependent directional tuning of DSGCs in control retinas. In contrast, direction selectivity of vDSGCs did not improve in

Figure 3.12: ON and OFF direction responses of vDSGCs are similarly blunted when Pcdhg expression in SACs is altered

A. Cumulative histogram of ON and OFF direction-selective indices (top) and angle away from ventral (bottom) for all recorded vDSGCs in $Pcdhg^{22}$, $Pcdhg^{0}$, and $Pcdhg^{1}$ retinas (n = 28, 28, and 19, respectively). Histogram bins are .05 DSI units and 10 degrees for top and bottom panels, respectively.

B. Ratios of excitatory (left) and inhibitory (right) ON and OFF current sizes (ventral over dorsal motion) for all recorded cells in $Pcdhg^{22}$, $Pcdhg^{0}$, and $Pcdhg^{1}$ retinas (Excitatory n = 14, 10, and 10 ON and OFF each, respectively; Inhibitory n = 14, 10, and 13 ON and OFF each, respectively).

C. Relative timing of ON and OFF excitation compared to inhibition during ventral motion (left) and dorsal motion (right) for all recorded cells in $Pcdhg^{22}$, $Pcdhg^{0}$, and $Pcdhg^{1}$ retinas (n = 12, 8, and 8 ON and OFF each, respectively).

ON and OFF responses are shown in green and blue, respectively. Statistics: n.s. = not significant.

(Figure continues on next page)

Figure 3.12 (continued)

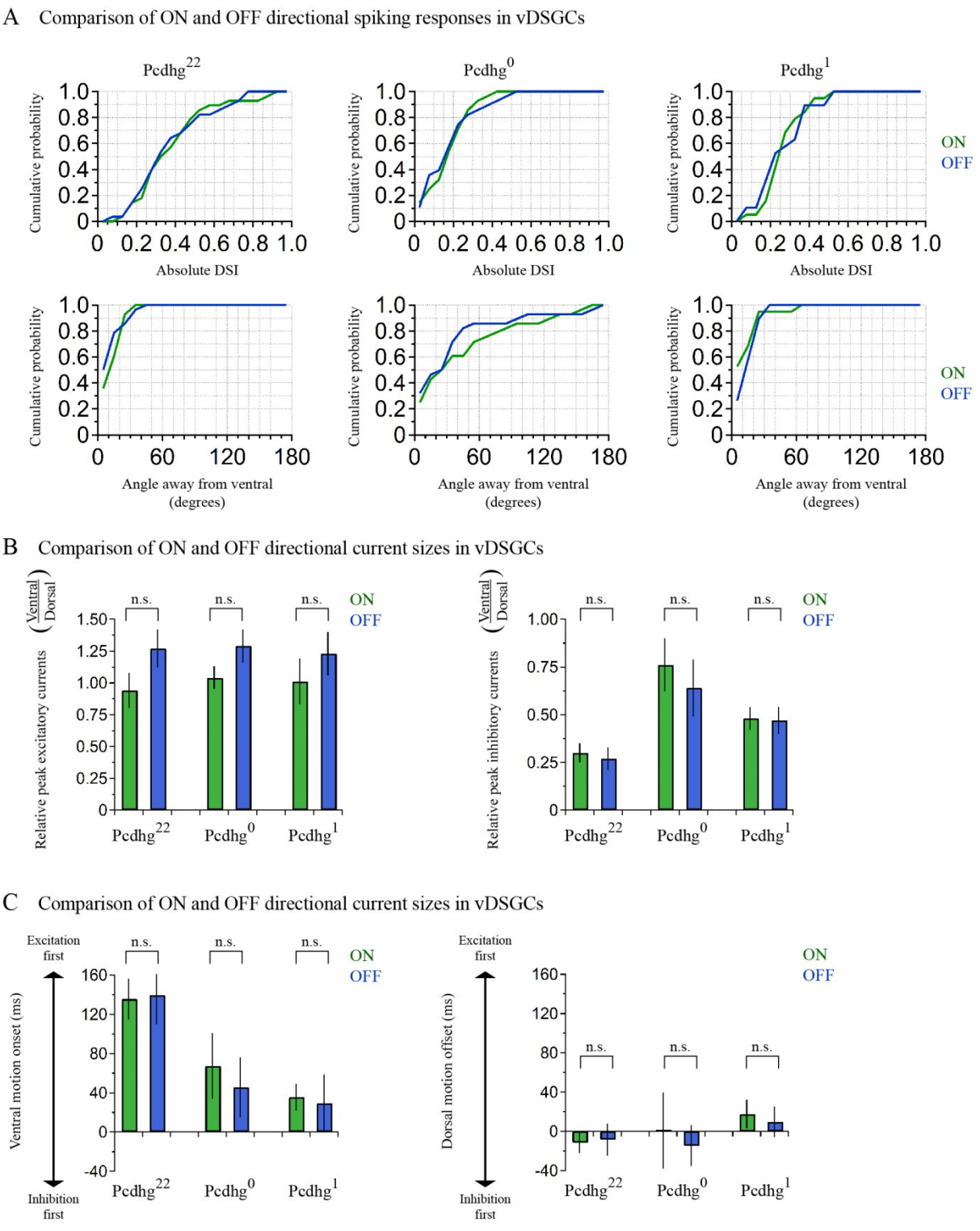

Pcdhg^{0} retinas (**Figure 3.13**). This result is consistent the idea that developmental refinement in SAC-SAC connectivity contributes to age-dependent improvement in direction selectivity.

3.3.8 Synaptic mechanisms underlying effects of Pcdhgs on direction selectivity

Finally, we sought to explain the degradation of directional selectivity of vDSGCs in Pcdhg^{0}, and Pcdhg^{1} retinas (**Figure 3.11**) in terms of alterations in SAC connectivity (**Figures 3.2, 3.7, and 3.8**). To this end, we recorded inhibitory and excitatory currents from vDSGCs in the three genotypes in response to bars moving in the null and preferred directions (dorsal and ventral, respectively). As noted previously, the inhibitory currents arise predominantly from SACs, which are genetically altered in mutants, while the excitatory currents arise predominantly from bipolar cells, which are not altered.

Studies in mice and rabbits have revealed two key aspects of SAC-DSGC connectivity that lead to direction selectivity (Fried et al., 2002; Park et al., 2014; Taylor and Vaney, 2002; Vaney et al., 2012; Yonehara et al., 2013), both of which we confirmed in vDSGCs from Pcdhg^{22} retinas. First, inhibitory input to DSGCs is greater for movement in the null direction (dorsal for vDSGCs) than for movement in the preferred direction (ventral for vDSGCs), whereas excitatory input is similar for movement in both directions (**Figures 3.14A, J, and K**). Second, excitatory and inhibitory currents recorded from DSGCs arise at the same time when motion is in the null direction, whereas inhibitory currents lag with respect to excitatory currents when motion is in the preferred direction (**Figures 3.14B, L, and M**). Together, these features allow inhibition to veto excitation in DSGCs more strongly for null motion than for preferred motion. Consequently, net depolarization in DSGCs is largest for motion in the preferred direction.

We found that both of these contributors to direction selectivity were blunted in Pcdhg^{0} and Pcdhg^{1} retinas (**Figures 3.12 and 3.14D-E, G-H**). First, inhibitory currents were larger for ventral motion and smaller for dorsal motion in Pcdhg^{0} and Pcdhg^{1} retinas than in Pcdhg^{22} retinas, with no significant change in excitation (**Figures 3.14J-K**). The difference from control values was greater for Pcdhg^{0} than for Pcdhg^{1} retinas but significant in both. Second, the delay of inhibition in response to preferred motion was less in Pcdhg^{0} and Pcdhg^{1} retinas than in Pcdhg^{22} retinas, with no significant change for movement in

Figure 3.13: Age-dependent improvement in direction selectivity of vDSGCs requires Pcdhgs

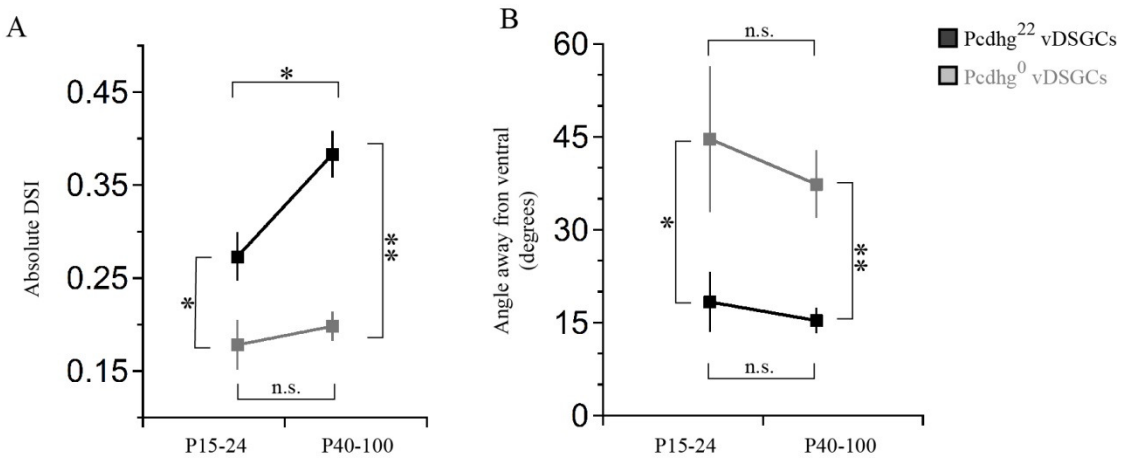

A. Comparison of DSI of juvenile and adult vDSGCs in $Pcdhg^{22}$ and $Pcdhg^{0}$ retinas.

B. Comparison of deviations from ventral of juvenile and adult vDSGCs $Pcdhg^{22}$ and $Pcdhg^{0}$ retinas. Statistics: n.s. = not significant, *P < .05, ** P < .0005. n = 10 and 6 for P15-24 $Pcdhg^{22}$ and $Pcdhg^{0}$ vDSGCs, respectively, and n = 28 and 28 for adult $Pcdhg^{22}$ and $Pcdhg^{0}$ vDSGCs, respectively. Leading edge (ON) and trailing edge (OFF) responses were measured for all cells and used as independent data points.

Figure 3.14: Synaptic basis of degraded direction selectivity in Pcdhg^{0}, and Pcdhg^{1} retinas

A. Example excitatory (black, V_h = -70 mV) and inhibitory (gray, V_h = 0 mV) currents evoked by leading edge (ON response) of bar moving in ventral (left) and dorsal (right) directions in vDSGC from Pcdhg^{22} retina.

B. Examples of relative timing of excitation and inhibition in same cell from panel **A**.

C. Schematic of inhibitory input to vDSGCs in Pcdhg^{22} retinas. vDSGCs receive inhibitory input from SAC dendrites with predominately dorsal orientations and directional preferences, setting the null direction of vDSGCs. These SAC dendrites, in turn, receive inhibitory input from SAC dendrites with predominately ventral orientation and preference, suppressing inhibition to vDSGCs during ventral motion through inhibition of inhibition.

D-E. Same as **A-B** but in Pcdhg^{0} retina.

F. Schematic of inhibitory input to vDSGCs in Pcdhg^{0} retinas. vDSGCs receive inhibitory input from curvilinear SAC dendrites with disrupted orientations and directional preferences, diminishing their ability to set the null direction of vDSGCs. These SAC dendrites, in turn, receive inhibitory input from both parallel and antiparallel SAC dendrites.

G-H. Same as **A-B** but for trailing edge (OFF response) in Pcdhg^{1} retina.

I. Schematic of inhibitory input to vDSGCs in Pcdhg^{1} retinas. vDSGCs receive inhibitory input from SAC dendrites with predominately dorsal orientations and directional preferences, setting the null direction of vDSGCs. These SAC dendrites, however, are no longer inhibited by SAC dendrites with predominately ventral orientation and preference, so their input to vDSGCs during ventral motion is not suppressed.

J. Ratio of peak excitatory current sizes evoked in vDSGCs by ventral versus dorsal motion in Pcdhg^{22} (black), Pcdhg^{0} (gray), and Pcdhg^{1} (red) retinas.

K. Same as **J** but for inhibitory currents.

(Figure continues on next page)

Figure 3.14 (continued)

L. Relative timing of onset of excitation compared to inhibition during ventral motion in $Pcdhg^{22}$ (black), $Pcdhg^{0}$ (gray), and $Pcdhg^{1}$ (red) retinas.

M. Same as **L** but during dorsal motion.

Data are shown as mean ± S.E.M. Number of recorded vDSGCs = 14, 10, and 13 in $Pcdhg^{22}$, $Pcdhg^{0}$, and $Pcdhg^{1}$ retinas. Leading edge (ON) and trailing edge (OFF) responses were measured for all cells and used as independent data points for quantification (see Figure S6). Statistics: n.s. = not significant, *P < .05, ** P < .001.

(Figure continues on next page)

Figure 3.14 (continued)

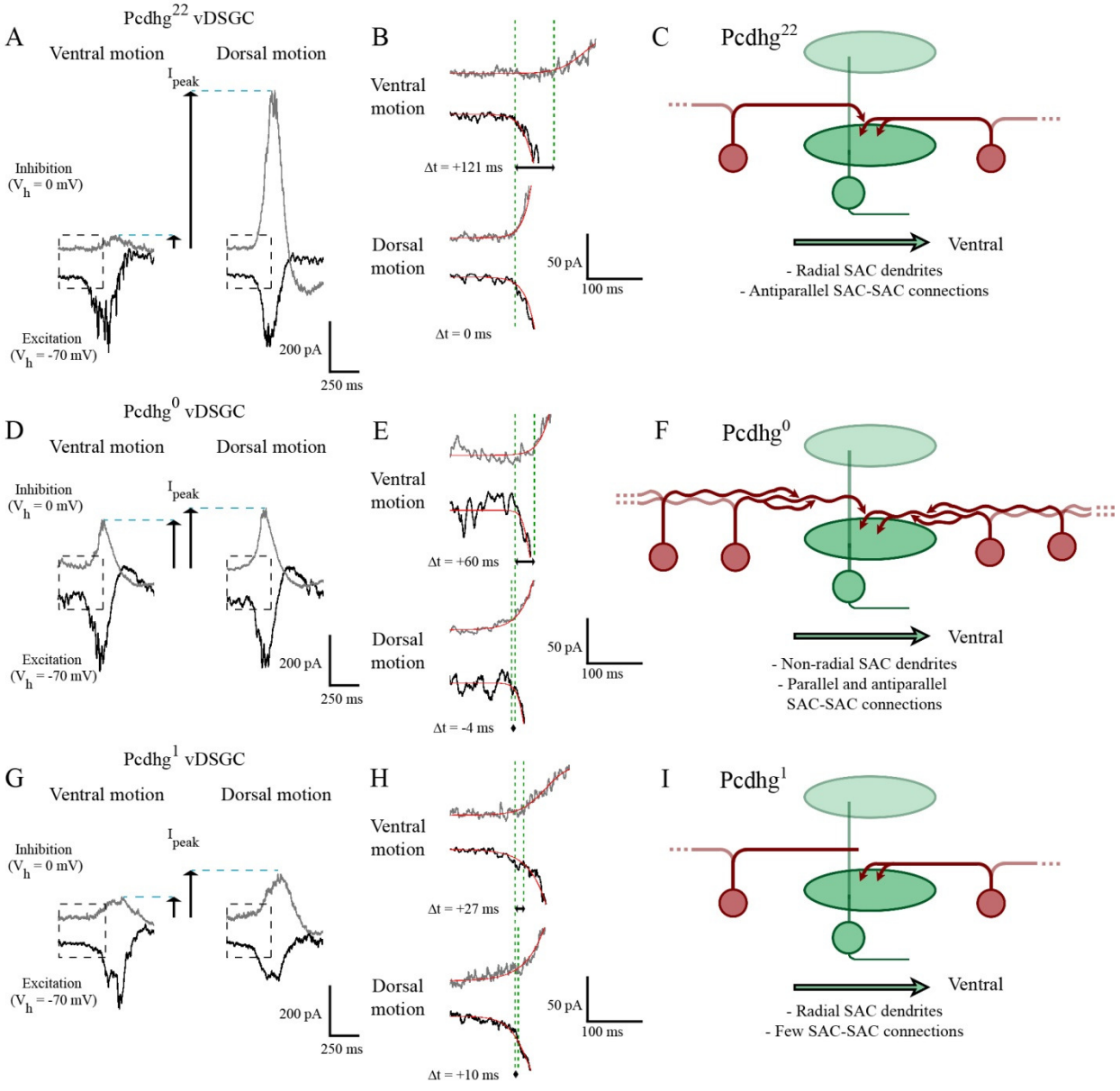

(Figure continues on next page)

Figure 3.14 (continued)

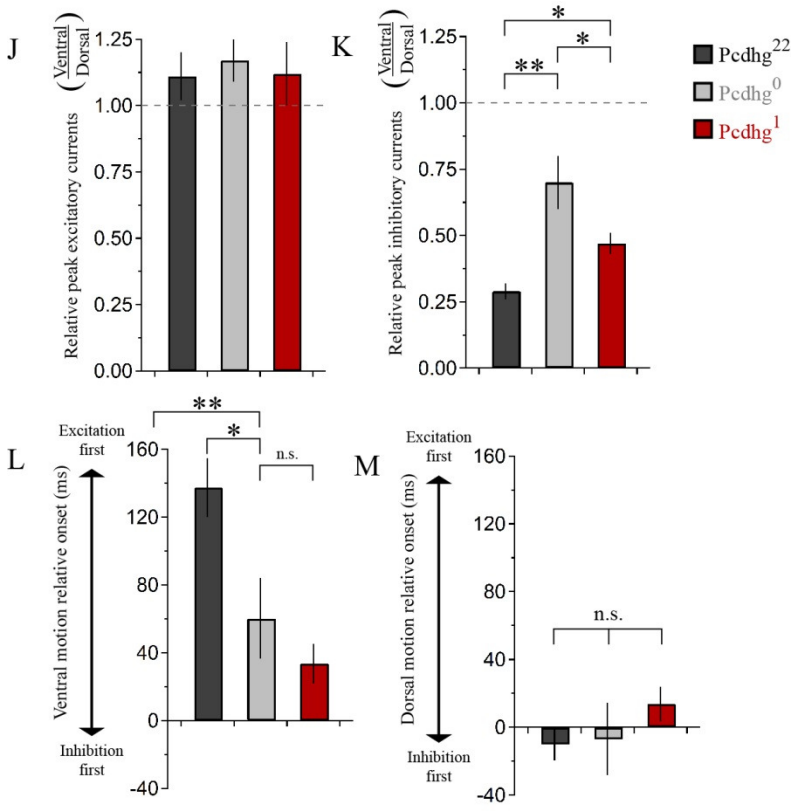

the null direction; in this case, Pcdhg^{0} and Pcdhg^{1} retinas were equally affected (**Figures 3.14L-M**). Thus, the ability of inhibition to veto excitation for preferred motion was greater in Pcdhg^{0} and Pcdhg^{1} retinas than in Pcdhg^{22} retinas. It is likely that the differences in the size and timing of inhibitory currents in vDSGCs from Pcdhg^{0} and Pcdhg^{1} retinas result in the changes in spiking observed in Figure 6. In the Discussion, we suggest a possible explanation for these alterations in terms of perturbations in SAC self-avoidance, S/NSD, and synapse elimination.

3.4 Discussion

Dendritic arbors of many neuronal types in both vertebrates and invertebrates exhibit self-avoidance and S/NSD (references in Introduction). In this study, we used SACs to assess the functional consequences of perturbing these processes. SACs were uniquely suited for this study for several reasons. First, they exhibit robust self-avoidance and S/NSD. Second, Pcdhgs are necessary for both processes, providing a means to manipulate them. Moreover, our genetic methods allowed us to manipulate Pcdhgs selectively in SACs, without directly affecting other neuronal types to which they connect. Third, removal or replacement of Pcdhgs in SACs allowed us to perturb self-avoidance and S/NSD independently. Finally, the role of SACs in retinal circuit function is remarkably well understood. By exploiting these features, we elucidated roles of self-avoidance and S/NSD in SAC connectivity, discovered a previously undescribed phase of synapse elimination between SACs, and showed that alterations in these processes decrease the ability of the retina to compute direction of motion.

3.4.1 Linking Pcdhg expression to SAC connectivity

Loss of Pcdhgs has been shown to have several effects on developing neurons including decreased neuronal survival in retina and spinal cord, decreased synaptic maintenance in spinal cord, decreased dendritic branching in neocortex, and decreased self-avoidance in retina and cerebellum (Garrett et al., 2012; Lefebvre et al., 2012; Lefebvre et al., 2008; Prasad et al., 2008; Wang et al., 2002c; Weiner et al., 2005). Any of these phenotypes would complicate our attempt to assess roles of self-

avoidance and S/NSD in SAC and circuit function. We therefore manipulated Pcdhg expression selectively in SACs and performed a variety of control experiments to assess whether our manipulations affected other aspects of retinal development or function. Our results are as follows:

First, SACs are unusual among retinal neurons in that their survival does not depend on Pcdhg expression (Lefebvre et al., 2012), and we confirmed that SAC number was unaltered in $Pcdhg^{0}$ and $Pcdhg^{1}$ retina. Second, we confirmed (Lefebvre et al., 2012) that alteration of Pcdhg expression in SACs had no effect on their dendritic length or mosaic spacing. Third, basic electrical properties (resting membrane potential and input resistance) of SACs were preserved in $Pcdhg^{0}$ and $Pcdhg^{1}$ retinas. Fourth, manipulation of Pcdhgs in SACs had no detectable effect on the strength of the inputs they receive from bipolar cells or deliver to DSGCs. Fifth, removing or replacing Pcdhgs in SACs had no detectable effect on cell number or general organization of the retina. Finally, we detected no alteration in the number, spacing, dendritic arbors, molecular markers or electrical properties of DSGCs. Thus, although we cannot completely exclude the possibility that Pcdhg manipulation had additional effects, we favor the explanation that alterations in SAC connectivity and circuit function documented here result from perturbation of Pcdhg-dependent self-avoidance, S/NSD and synapse elimination.

3.4.2 Self-avoidance, self/non-self discrimination and SAC connectivity

Morphological studies led to the idea that self-avoidance serves to optimize coverage of a receptive field by a dendritic arbor, minimizing gaps and clumps (Grueber and Sagasti, 2010; Kramer and Kuwada, 1983; Kramer and Stent, 1985). Our physiological studies revealed an additional role of self-avoidance in SACs: it prevents formation of autapses (**Figure 3.7**). In many neuronal types, autapses cannot form because pre- and postsynaptic machinery are confined to axons and dendrites, respectively, which are physically segregated. SACs, in contrast, form dendro-dendritic synapses, and therefore have pre- and postsynaptic specializations intermingled. This situation is not uncommon in the retina and elsewhere in the central nervous system, such as the olfactory bulb (Murthy, 2011). We suggest that self-avoidance may play similar roles in other such cells.

S/NSD is generally viewed as a means of limiting inter-dendritic repulsion to sibling processes, so that neurons of a single type can share territory (Grueber and Sagasti, 2010; Lefebvre et al., 2015; Zipursky and Grueber, 2013). In the retina, it additionally allows formation of synapses between SACs. Several types of neurons have been shown to form homotypic connections in cortex and cerebellum (Pfeffer et al., 2013; Rieubland et al., 2014). Since most molecules described to date that mediate self-avoidance are ill-suited to mediate S/NSD, additional mechanisms likely remain to be discovered. In addition, some cell types that connect homotypically may lack robust mechanisms for self-avoidance. Indeed, cortical fast-spiking interneurons, which form homotypic connections, also form autapses (Bacci et al., 2003). It is unclear whether these autapses are beneficial to the circuit or whether they are an acceptable cost of homotypic connectivity.

3.4.3 Age- and distance-dependent elimination of SAC-SAC connections

Zhou and colleagues previously demonstrated inhibitory SAC-SAC synaptic connections in rabbit retina soon after eye opening, a result we confirmed here for mouse (Lee and Zhou, 2006; Zheng et al., 2004). We also discovered two additional features of these connections. First, in mature retina (>P40), SACs separated by less than 100µm seldom formed synapses with each other, whereas SACs separated by >100µm were connected frequently. Since dendritic overlap is inversely proportional to the distance between SACs, this distance-dependence is not a passive consequence of proximity but instead implies spatial selectivity to SAC-SAC connections. Second, we found that this distance-dependence was absent in immature retinas (P15-24; eye opening occurs at P14). Thus, connections between closely-spaced SACs are selectively eliminated as the retina matures.

We view the loss of proximal SAC-SAC connections as synapse elimination, a process that occurs in many and perhaps most neuronal types (Kano and Hashimoto, 2009), but has not previously been described for SACs. In most cases, synapse elimination was first described physiologically (Crepel et al., 1976; Purves and Lichtman, 1980; Redfern, 1970) as we have done here. For these cases, morphological confirmation was obtained many years later. We expect this will be the case for SACs as

well. Such demonstration will be difficult, however, because SAC dendrites are so thin and densely packed that it is infeasible to map synapses on them by light microscopic methods. Ultrastructural studies using genetic tags or extensive reconstruction at several developmental time points will therefore be needed to decide this issue.

Why might connections between closely-spaced SACs be counterproductive? Inhibitory connections between nearby SACs would frequently be made between dendrites with similar directional preferences. The ability of a SAC dendrite to respond to centrifugal motion along its dendrite would thereby decrease, because this motion would lead to inhibition of the dendrite by other SACs. This, in turn, would degrade the direction selectivity of DSGCs (Taylor and Smith, 2012). In contrast, connections of distant SACs will most frequently be made between dendrites with opposite directional preference; as discussed in the next section, this enhances directional computation.

Conversely, might there be a role for connections between closely-spaced SACs early in development? In fact, strong SAC-SAC connectivity is critical for the developing visual system, because it underlies propagation of the retinal waves that pattern the segregation of binocular input in retinorecipient areas such as the superior colliculus and lateral geniculate nucleus (Ackman and Crair, 2014; Burbridge et al., 2014). Because waves occur before eye-opening, directional selectivity is unimportant. Thus, we suggest that postponing distance-dependent elimination of SAC-SAC connections until after eye-opening allows both the dense connectivity needed for wave propagation and the selective anti-parallel connectivity needed for direction selectivity. Consistent with this view, the direction selectivity of DSGCs increases during the period in which connections between closely-spaced SACs are being eliminated.

We also found that connections between closely-spaced SACs are not eliminated in the absence of Pcdhgs, revealing a novel role for these molecules in neural development. The mechanism of this effect remains to be determined. One attractive possibility is that an uneven distribution of Pcdhgs within SACs might confine synapses to distal portions of dendrites.

3.4.4 Roles of SAC-SAC inhibition in directional computation

We have argued that alterations in SAC connectivity in $Pcdhg^0$ and $Pcdhg^1$ retinas documented in the first part of this study (**Figures 3.2, 3.7, and 3.8**) result from defects in self-avoidance, S/NSD and synapse elimination. We now argue that these defects largely explain the degradation in direction selectivity in vDSGCs documented in the second part (**Figures 3.11 and 3.14**).

As described above, SACs contribute to the direction selectivity of DSCGs in two ways. First, inhibitory currents are larger during null motion than preferred motion. The difference in inhibitory currents arises in large part from the geometric arrangement of SAC-DSGC connections: vDGSCs, for example, receive most SAC input from dendrites that respond preferentially to dorsal (null) motion (Briggman et al., 2011). In addition, anti-parallel inhibitory connections between SACs decrease the currents that these dendrites would otherwise provide during preferred motion (**Figure 3.14C**). Together, these processes result in greater net depolarization and therefore spiking for preferred motion than null motion. The number of SAC-SAC connections is markedly decreased in $Pcdhg^1$ retinas (**Figure 3.14I**). These connections persist in $Pcdhg^0$ retinas, but their efficacy is decreased because parallel SAC dendrites remain connected and inhibit each other, resulting in decreased inhibitory input from SACs to DSCGs for null motion and decreased antiparallel SAC-SAC inhibition (and thus increased SAC-DSCG inhibition) for preferred motion (**Figure 3.14F**). The autapses in $Pcdhg^0$ retina would act similarly to synapses between parallel dendrites, since autapsing dendrites are likely to point in similar directions (see $Pcdhg^0$ SAC image in **Figure 3.7**).

Second, inhibitory and excitatory currents in DSGCs are nearly simultaneous during null motion, allowing inhibition to veto excitation, whereas inhibition is delayed with respect to excitation during preferred motion, decreasing the power of the veto. A recent computational model argues that the delayed inhibition for preferred motion arises in part because anti-parallel SAC-SAC connections transiently suppress transmitter release from SACs to DSGCs (Taylor and Smith, 2012). Decreased inhibition, from loss of SAC-SAC connections in $Pcdhg^1$ retinas and decreased efficacy of SAC-SAC synapses $Pcdhg^0$ retinas would thus be expected to decrease the delay, thereby blunting the response to preferred motion.

In summary, the spatial organization of SAC-SAC inhibition and SAC-DSGC inhibition work together to generate a direction-selective output from the retina. When self-avoidance, S/NSD, or synapse elimination is perturbed, SAC-SAC inhibition is rendered less effective and direction selectivity is degraded. Thus, our results demonstrate roles for these Pcdhg-dependent processes in computation of direction selectivity and provide new evidence in support of the hypothesis (Enciso et al., 2010; Lee and Zhou, 2006; Taylor and Smith, 2012; Vaney et al., 2012) that SAC-SAC connections play important roles in this computation.

3.5 Methods

3.5.1 Animals

Animals were used in accordance with NIH guidelines and protocols approved by Institutional Animal Use and Care Committee at Harvard University. All mice were maintained on a C57BL/6 background. The lines used were reported previously: $Pcdhg^{fcon3}$ (Lefebvre et al., 2012; Lefebvre et al., 2008; Prasad et al., 2008), $ChAT^{Cre}$ (Rossi et al., 2011), Thy1-stop-YFP line #15 (Buffelli et al., 2003), Hb9-GFP (Trenholm et al., 2011), RC-stop-tdTomato (Madisen et al., 2010), and RC-stop-PcdhgC3-mCherry (Lefebvre et al., 2012). We generally used $ChAT^{Cre}$ mice as homozygotes, because we found that this gave earlier and more even Cre activity at P1, when SAC dendrites are beginning to elaborate.

3.5.2 Electrophysiology

Mice were dark adapted for at least 2 hours prior to euthanasia. Retinas were rapidly dissected under infrared illumination into room temperature, oxygenated (95% O_2, 5% CO_2) Ames medium and placed in a recording chamber on the stage of a custom built electrophysiology set up. Recordings were carried out in same medium heated to 32-34^oC. Fluorescent cells were identified with a brief (<40 ms) LED flash, overlaid onto infrared images, and targeted with electrodes. Recordings were made from SACs and vDSGCs using patch electrodes with resistance of 6-8 MΩ and 4-6 MΩ, respectively. For loose patch recordings, electrodes were filled with Ames medium. For intracellular recordings, electrodes were filled with intracellular solution containing the following (in mM): 120 Cs-Methanesulfonate, 10 Na-Acetate, 0.2 $CaCl_2$, 1 $MgCl_2$, 10 EGTA, 5 CsCl, 2 Mg-GTP, and 0.5 Na_2-GTP (pH 7.3). Intracellular recording solutions were supplemented with 5mM QX314-Br for vDSGC voltage clamp recordings and 5mM TEA-Br for SAC autapse recordings.

3.5.3 Visual stimuli

Light stimuli were presented using a modified DLP projector (Dell) suspended underneath the microscope stage with a custom substage lens system focused onto the retinal photoreceptors.

Monochrome light was used (wavelength peak = 405 nm) at a background intensity 5 x 10^2 R*/rod/s set using neutral density filters. Visual stimuli were presented at 100:1 positive contrast and patterns generated using Psychophysics Toolbox in MATLAB (Mathworks). All stimuli were centered on the cell body of recorded neurons. Spot flash stimuli were 300 μm-diameter circles. Moving bars were 1000-1500 μm long and 300 μm wide, travelled at 1000 μm/s, presented moving along their long axis in 8 directions, and rotated by 135^o with each presentation. At the speeds we used for our visual stimuli, nonlinear dendritic processes contributing to directional tuning are not observed in HB9-GFP vDSGCs (Trenholm et al., 2011). A minimum of 4 repetitions were presented for each stimulus.

3.5.4 SAC and DSGC fills and histology

SACs and DSGCs were filled through patch electrodes using methods described above. Alexa Fluor 488 hydrazide (200 μM) was added to the intracellular recording solution, and recordings were maintained for ~20 minutes in current-clamp mode while maintaining a negative holding potential (<-60mV). After individual cells were filled, retinas were either imaged live (to measure SAC dendritic radius) or immediately placed in fixative and processed for histology.

Mice used exclusively for histology were euthanized by intraperitoneal injection of pentobarbital or euthasol and either enucleated immediately or transcardially perfused with Ringer's solution followed by 4% paraformaldehyde (PFA) in PBS. Eye cups were removed and fixed in 4% PFA in PBS on ice for one hour then rinsed with PBS. Retinas were analyzed as whole mounts or cryosections as described (Lefebvre et al., 2012). Whole retinas were in blocking buffer (0.5% Triton-X-100, 5% normal donkey serum in PBS for 1-2 hours), then incubated for 5-7 days at 4^{o}C with primary antibodies. For cryosections, fixed retinas were incubated with 30% sucrose/PBS for >2 hours (until they lost buoyancy), frozen, and sectioned at 20 μm in a cryostat. Sections were blocked with 5% donkey serum/0.5% Triton X-100/PBS for 1-2 hours, with primary antibodies overnight at 4^{o}C, and with secondary antibodies for 2 hours at room temperature. Whole mount retinas or sections were mounted onto glass slides using Fluoromount G (Southern Biotech). The following primary antibodies were used: chick anti-GFP (1:500,

Abcam); rabbit anti-DsRed (1:1000, Clontech); goat anti-choline acetyltransferase (ChAT) (1:400, Millipore); goat anti-VAChT (1:1000, Promega); rabbit anti-Calbindin (1:2500, Swant); rabbit anti-CART (1:1000, Phoenix); mouse anti-Brn3a (1:1000, Millipore); goat anti-Chx10 (1:200, Santa Cruz); and mouse anti-AP2 (1:1000, DSHB). Nuclei were labeled with TO-PRO3 (1:3000, Invitrogen). Secondary antibodies were conjugated to Alexa Fluor 488, Alexa Fluor 568 (Invitrogen), or DyLight 649 (Jackson ImmunoResearch) and used at 1:1000.

3.5.5 Imaging

Immunofluorescence samples were imaged using Olympus FV1000 confocal microscope using 488, 568, and 647 lasers with a z-step size of 1.0 µm. FIJI (NIH) was used to analyze confocal stacks and generate maximum intensity projections. ON and OFF dendrites of DSGCs were separated using depths in the IPL and corresponding SAC bands. Retinal orientations were maintained throughout.

3.5.6 Data acquisition and analysis

Electrophysiological recordings were acquired using a Multiclamp 700B Amplifier (Molecular Devices) at 20 kHz. Acquisition was controlled by custom LabView software (National Instruments). Data were analyzed using custom written MATLAB software (Mathworks) and displayed in IgorPro (Wavemetrics). All statistics were calculated in MATLAB. Pairwise comparisons were made using two-tailed t-test, and multiple samples were compared using one-way analysis of variance (ANOVA). Errors on connection probability were calculated using the variance of the binomial distribution.

3.6 Acknowledgements

We thank members of the Sanes lab (official and adopted) for useful discussions and comments on this manuscript, J. Lefebvre for guidance during initial stages of the project and comments on this manuscript, E. Soucy and J. Greenwood for assistance in construction of electrophysiology set-up, M. Do for advice on physiological methods, T. Dunn for assistance with data analysis software, and R. Helmiss for assistance with illustration. Funding was provided by NIH grants T32 EY007110 and F31 NS078893 (D.K.) and RO1 EY022073 (J.R.S.).

Chapter 4: Combinatorial analysis of alpha- and gamma-Protocadherin gene clusters

Preface:

The work presented in this chapter is a collaboration that started between Julie Lefebvre and me before she left the Sanes laboratory as an effort to expand our studies of the Protocadherin-gamma to include the alpha subcluster. Julie performed the initial CRISPR validation experiments in heterologous cells and generated the targeting construct for injection. Subsequently, I have screened the resulting animals, characterized their mutations, and begun to analyze the anatomical and functional defects in Protocadherin-alpha/gamma double mutants.

4.1 Abstract

The combinatorial role of recognition molecules has been an elusive problem in developmental neuroscience. Such molecules are often part of related families that have both overlapping and distinct functions in neural circuit assembly. One daunting problem for studying such combinatorial problems is that cumbersome generation of generating and analyzing the role of these combinations. One such family is the mammalian clustered Protocadherins (Pcdhs), comprised of three subfamilies (alpha, beta, and gamma) contain 14, 22, and 22 family members in mice, respectively. Subsets of these molecules have distinct roles in dendritic self-avoidance, neuronal survival, and axon targeting; however, the proximity of these subclusters to each other has precluded the level of redundancy in their function. Recent technological developments in the field of genome editing have made addressing such issues much more feasible. Here, I present our initial efforts to understand the combinatorial roles of the multiple subfamilies of the clustered Pcdhs. Using the CRISPR/Cas9 system, we have generated Pcdh-alpha/Pcdh-gamma double mutants. We are now in the process of analyzing these double mutants to test the hypothesis that they have combinatorial roles in developing neural circuits.

4.2 Introduction

Neural circuit assembly relies of combinations of decisions made by neurons to elaborate axons and dendrites, reach appropriate target locations, and make functional synaptic connections with appropriate partners. Many of these processes require that neurons communicate with cues in their environment, including interaction with their own processes and the processes of neighboring neurons. Understanding the molecular mediators of these functions is a fundamental focus of developmental neuroscience. To date, most of these studies have focused on analysis of single molecules or pairs of interacting molecules that accomplish such tasks; however, it is clear that circuit assembly relies on expression of combinations of such molecules.

The clustered Protocadherins (Pcdhs) are a large family of related recognition molecules that, in mice, are comprised of 58 members divided into 14 alpha (Pcdha), 22 beta (Pcdhbs), and 22 gamma (Pcdhg) isoforms that are tandemly arrayed in the genome (**Figure 4.1A**) (Kohmura et al., 1998; Wu and Maniatis, 1999; Wu et al., 2001). Each *Pcdh* gene encodes a protein with six extracellular cadherin-like (EC) repeats, a transmembrane domain, and an intracellular domain that is common to each subcluster (except Pcdhbs, which have no intracellular domain). Each extracellular and transmembrane domain are encoded by a single exon that is spliced to the three common constant exons for Pcdh-α (Pcdha) and Pcdhg.

These molecules are expressed throughout the nervous system – in the retina, hippocampus, cortex, cerebellum, and spinal cord (Esumi et al., 2005; Hirano et al., 2012; Kaneko et al., 2006; Katori et al., 2009; Kohmura et al., 1998; Wang et al., 2002c). In many but not all of these regions, members of multiple subclusters are expressed. Furthermore, biochemical and expression studies have shown that individual isoforms, which normally exhibit homophilic recognition, can change their binding specificity when expressed in combination (Murata et al., 2004; Schreiner and Weiner, 2010; Thu et al., 2014). Thus, *cis* interactions among members, both within and across subcluster, may have important functions *in vivo*.

The functional roles of the Pcdhs are many. Pcdhas are important for proper innervation of the olfactory bulb by olfactory sensory neurons, of the lateral geniculate nucleus by retinal ganglion cell

axons, and of various brain regions by serotonergic neurons (Hasegawa et al., 2008; Katori et al., 2009; Meguro et al., 2015). The roles of Pcdhbs remain poorly understood. The best studied of the Pcdh clusters are the Pcdhgs. These functions of these molecules in the nervous system are many. Initial studies demonstrated their importance for survival of developing neurons in the spinal cord and retina (Lefebvre et al., 2008; Prasad et al., 2008; Wang et al., 2002c; Weiner et al., 2005). More recently, Pcdhgs have been shown to mediate dendritic self-avoidance and self/non-self discrimination in retinal starburst amacrine cells and cerebellar Purkinje cells (Lefebvre et al., 2012; see chapter 2). A working model of how Pcdhgs mediate this process is that individual neurons express distinct subsets of these molecules and present them on their surface to generate individual neuronal identities, generating self-recognition units that lead to repulsion. Neighboring neurons are unlikely to express the same complement of isoforms, so their dendrites do not repel each other.

While expression studies of Pcdhgs in starburst amacrine cells have not been demonstrated, these studies have been done in Purkinje cells. Indeed, individual Purkinje cells express distinct subsets of Pcdhgs (Kaneko et al., 2006). Interestingly, Purkinje cells also express Pcdhas and Pcdhbs differentially, suggesting that these molecules may be used in tandem to generate neuronal individuality (Esumi et al., 2005; Hirano et al., 2012). However, the genomic proximity of the three Pcdh subclusters (the whole locus is about one megabase long) has made generation of mice with mutations in multiple subclusters from existing single-clusters through homologous recombination unlikely.

The advent of the CRISPR/Cas9 genome editing technology has rendered this problem obsolete (Deltcheva et al., 2011; Mali et al., 2013; Sander and Joung, 2014). Here, I present the development of mice in which we will be able to analyze the combinatorial role of Pcdhas and Pcdhgs. Mutations of the Pcdha subcluster were targeted on a Pcdhg-conditional mutant background, and we have now generated these mice and are beginning to analyze them. Our preliminary results indicate that these double mutant mice exhibit phenotypes that are not present in either single mutant, suggesting that Pcdhas and Pcdhgs work together to pattern neural circuits.

Figure 4.1: Strategy for the generation of Pcdha/Pcdhg conditional double mutants

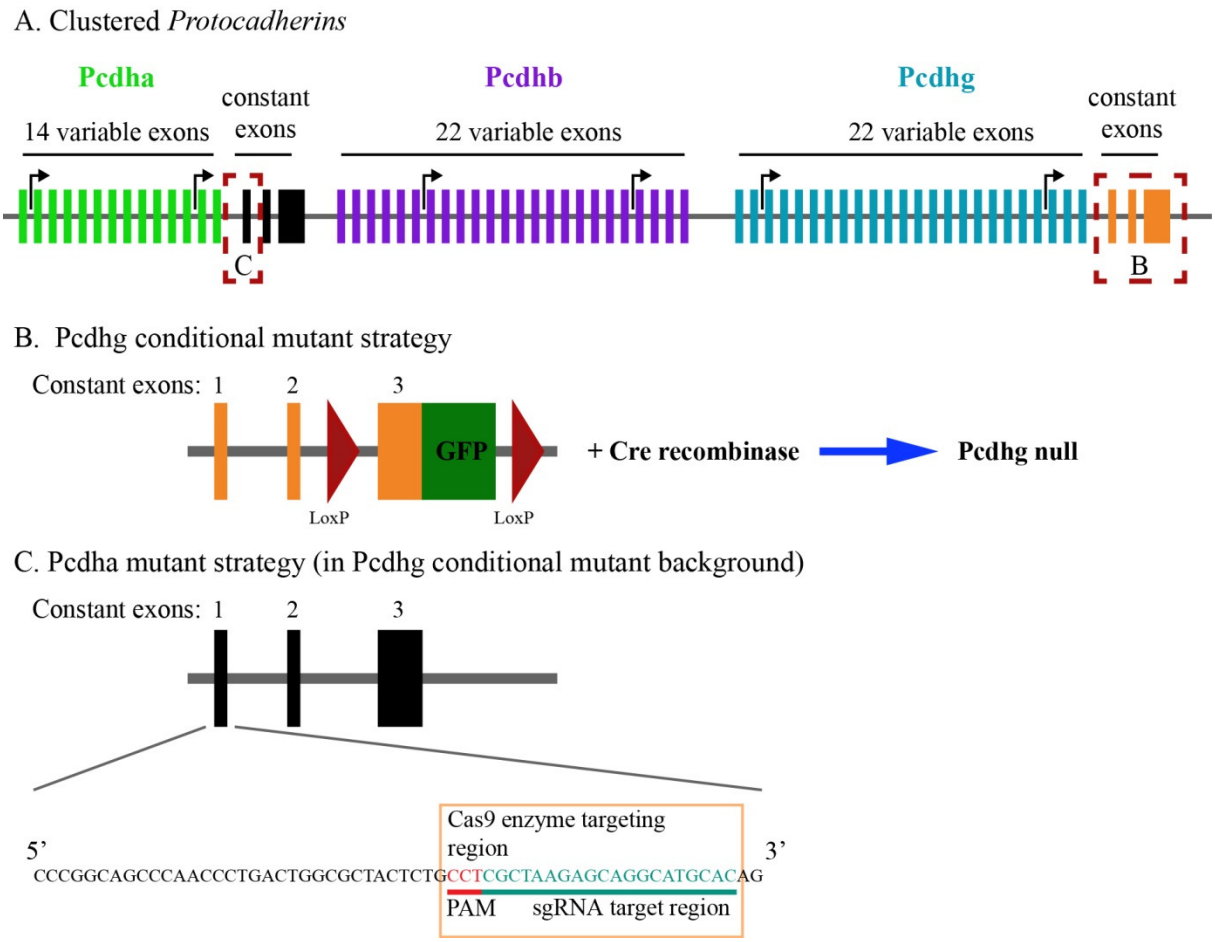

A. The clustered Protocadherin locus is shown. Variable exons of Pcdhas, Pcdhbs, and Pcdhgs are shown in green, purple, and cyan, respectively. The constant exons of Pcdhas and Pcdhgs are shown in black and orange, respectively.

B. The conditional Pcdhg mutant allele (described in Lefebvre et al., 2008 and Prasad et al., 2008).

C. Mutation strategy for the generation of Pcdha mutant/Pcdhg conditional mutant mice. Pcdhg conditional heterozygote embryos were injected with Cas9 enzyme and guide RNA targeting the antisense strand of the 3' end of the first constant exon of the Pcdha subcluster (bottom). The reverse complement of the PAM sequence and sgRNA targeting region are shown in red and cyan, respectively.

4.3 Methods and Results

4.3.1 Targeting strategy for *Pcdha* disruption

In seeking a rapid way to generate Pcdha/Pcdhg double mutant animals, we sought to introduce a mutation in the Pcdha locus in mice that already had conditional mutations in the Pcdhg locus. To this end, we took advantage of the emerging CRISPR/Cas9 genome editing technique (**ref)**. Briefly, this technique involves using a guiding RNA molecule to direction a nuclease, Cas9, to specific genomic locations, where this enzyme cleaves DNA and can potentially cause genomic disruptions when this cleaved location is repaired by cells. We targeted the constant exons common to all *Pcdhas*, because previous studied indicated that removing a constant exon of *Pcdhgs* creates a null mutation (**Figure 4.1A-B**) (Lefebvre et al., 2012; Lefebvre et al., 2008; Prasad et al., 2008). Specifically, we designed a guide RNA targeting construct against the 3' end of the first constant exon of *Pcdha* (**Figure 4.1C**). The antisense DNA strand at this location contains a specific primer-like region followed protospacer-adjacent motif (PAM) that are required to target the Cas9 enzyme to specific DNA sequences (Deltcheva et al., 2011). We first sought to confirm that our single guide RNA (sgRNA) was capable of creating disruptions of Pcdhas in heterologous cells. To this end, we transfected cells with a GFP construct and RFP-tagged Pcdha construct, then with the Cas9 nuclease and sgRNA. We then looked for reduction in red fluorescence and maintenance of green fluorescence. As expected, our sgRNA was able to knock down expression of Pcdha.

4.3.2 Screening of Pcdha/Pcdhg double mutants

We next sought to create Pcdha-mutant/Pcdhg-conditional mutant (from now on referred to as PRAG) mice by using the reagents described above. We injected fertilized embryos from Pcdhg wild type-Pcdhg conditional homozygote parents with sgRNA and Cas9 nuclease constructs and obtained 16 viable offspring from 4 litters (**Figure 4.2A**). Of these 16 animals, all of which were Pcdhg condition heterozygotes, 6 showed large disruptions in constant exon 1 of the *Pcdha* locus. More detailed analysis showed that more than half of the 32 total alleles had some sort of disruption. We have now propagated four of the founder lines with large deletions (#4, 6, 9, and 13) after confirming that the Pcdha deletion

Figure 4.2: Screening of potential mutations

A. Initial PCR of *Pcdha* constant exon 1 and surrounding introns revealed 6 alterations to this genomic region (animals 4, 6, 7, 9, 10, 13). Wild type band is 750 bp long. None of the 16 animals showed large disruptions on both chromosomes, but subsequent restriction digests revealed several other mutations that were unresolved by gel electrophoresis, including some animals where both alleles were mutated.

B. Sequencing of CRISPR-induced deletions were consistent with initial PCR and demonstrated deletions in and around target sequence specified by protospacer-adjacent motif (PAM) and single guide RNA (sgRNA).

C. Outcrossing to wild type mice revealed that the four mutations to *Pcdha* constant exon 1 were in *cis* with (on the same chromosome as) our Pcdhg conditional mutation. The genotyping resulting from the outcross of animal 9 is shown. Similar results were obtained in founder lines 4, 6, and 13.

(Figure continues on next page)

Figure 4.2 (continued)

A. Screening of Pcdha mutants

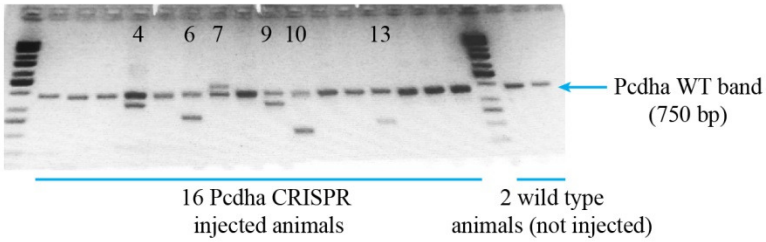

B. Characterization of mutations

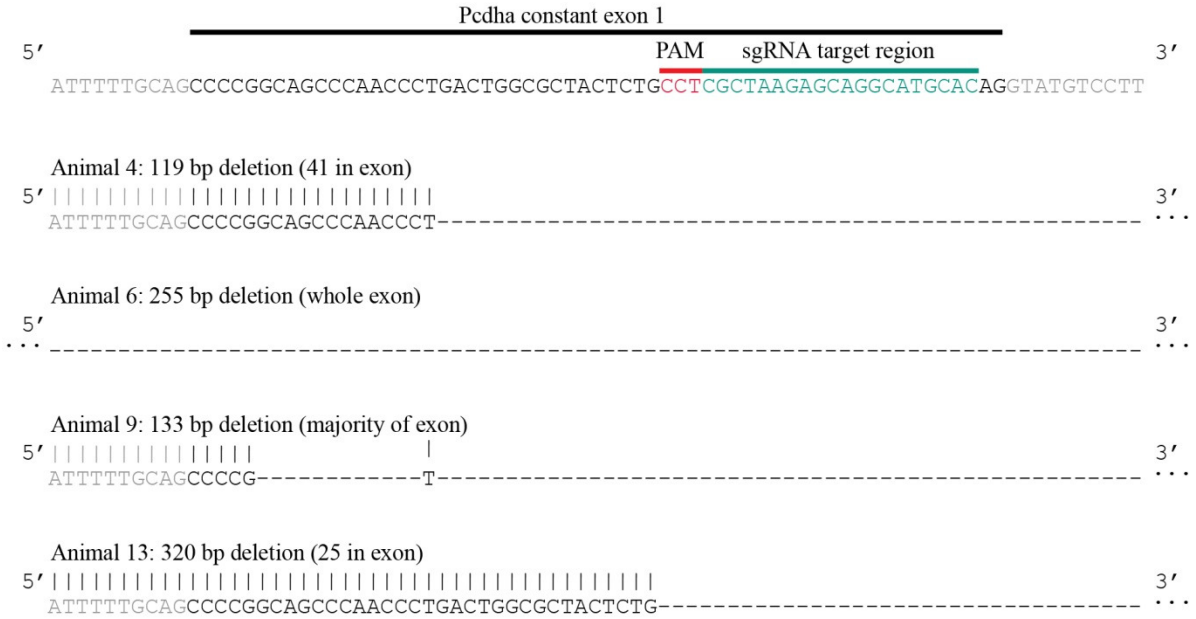

C. *Cis* transmission of mutations

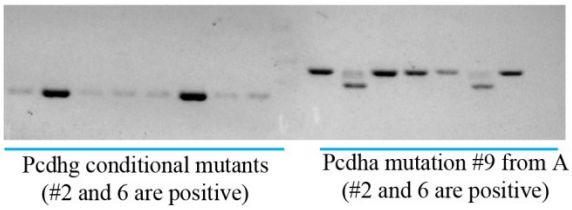

was in *cis* and therefore transmitted with the Pcdhg conditional mutation by outcrossing these animals to wild type mice (**Figure 4.2B-C**). Because off target effects are a concern when using the CRISPR/Cas9 system (Fu et al., 2013), we outcrossed our Pcdha/Pcdhg double mutant mice to wild type mice before crossing them to Cre lines and each other to obtain specific disruption of both Pcdha and Pcdhg in the brain.

4.3.3 Initial characterization of Pcdha/Pcdhg double mutant viability

Our initial efforts to obtain homozygous PRAG animals were unsuccessful. Genotyping of juvenile heterozygote-heterozygote crosses revealed that wild type, heterozygote, and mutant mice were present in a 1:2:0 ratio. However, we noticed that these litters often had pups that died at birth. Genotyping of these animals showed that they were homozygous double mutants and revealed that these animals could come to term but were unable to survive after birth. This is very reminiscent of global disrupts of Pcdhgs, which cause neuronal death in many places in the nervous system including the spinal cord and render these animals unviable (Wang et al., 2002c).

This observation was puzzling since without Cre activity, our PRAG mice should just be Pcdha mutants, which are viable (Hasegawa et al., 2008; Katori et al., 2009; Meguro et al., 2015). However, this may be explained by the additional DNA elements contained in the Pcdhg conditional mutant locus, which render this allele slightly hypomorphic. In an attempt to overcome this lethality, we have performed several round of outcrossing of these animals to CD1 mice, which are not inbred like the C57/B6J animals that we normally maintain. Two additional round of outcrossing rescued the neonatal lethality in these animals (**Figure 4.3**), and we now have viable conditional mutants that we have crossed to Cre lines in order to study the roles of these molecules in the development of neural circuits.

4.3.4 Analysis of retinal defects in Pcdha/Pcdhg double mutant mice

We began by crossing PRAG mice to Six3-Cre, which is expressed in the retina (Furuta et al., 2000). Pcdhgs are known to have several roles in the retina. They are necessary for postnatal survival of many bipolar, amacrine, and ganglion cells, but dispensable for the survival of horizontal cells and photoreceptors (Lefebvre et al., 2008). As documented in chapter 2 of this thesis, they are also necessary

Figure 4.3: Viable PRAG mutant mice

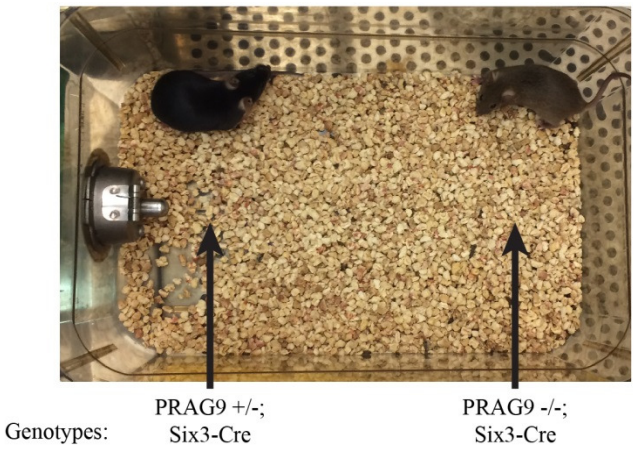

Several rounds of outcrossing before incrossing led to generation of viable Pcdha mutant/Pcdhg conditional mutant animals from several of the founder lines, including line 9 (PRAG9). Single P70 PRAG9 heterozygote and homozygote animals are shown on left and right, respectively. Both these animals also express Six3-Cre, a retina specific Cre line.

to promote dendritic self-avoidance of starburst amacrine cells (Lefebvre et al., 2012). The roles of Pcdhas in the retina are unclear; however, they are expressed by retinal neurons, and a recent study has documented the role of these molecules in the proper development of retinogeniculate axon terminals (Meguro et al., 2015). Here, I present our initial description of retinal histology in PRAG mutants as it relates to wild type mice.

Similar to Pcdhg mutants alone, I observed a substantial reduction in cell number in retinal PRAG mutants (**Figure 4.4A**). However, this phenotype was substantially worse in PRAG mutants than in Pcdhg mutants alone. Thus, it appears that removing Pcdhgs unmasks a role for Pcdhas in promoting neuronal survival in the retina, and that the role of the different Pcdh subfamilies is, in this case, redundant. It is important to note however, that Pcdha mutants alone shown no cell death phenotype, so they require the presence of Pcdhgs to perform this function.

I next asked what cell types were susceptible to cell death. Similarly to Pcdhg mutants alone, photoreceptors and horizontal cells were spared in PRAG mutant retinas (**Figure 4.4A-B**). However, the number of bipolar cells, amacrine cells, and retinal ganglion cells was decreased substantially in PRAG mutants (**Figure 4.4C-D**). Furthermore, the inner plexiform layer, which is normally about 100 µm in vertical sections of retina, was almost nonexistent in PRAG mutant mice **(Figure 4A**). This led to a lack of distinct laminae in the inner plexiform layer as determined by Calbindin immunostaining, which labels many amacrine and ganglion cell processes and normally shows a triplet banding pattern in the IPL, as well as Syt2 staining., which normally labels the axon terminals of a single OFF (type 2) and a single ON (type 6) type of bipolar cells (**Figure 4.5**) (Wassle et al., 2009). Laminar circuit formation is largely intact in Pcdhg mutants, despite the absence of approximately half of interneurons and retinal ganglion cells (Lefebvre et al., 2008), as well as Pcdha mutants. Therefore, Pcdhas and Pcdhgs may have roles in retinal circuit formation that have previously eluded researchers due to the inability to study multiple families of cellular recognition molecules.

Figure 4.4: Enhanced cell death in PRAG9 mutant retinas

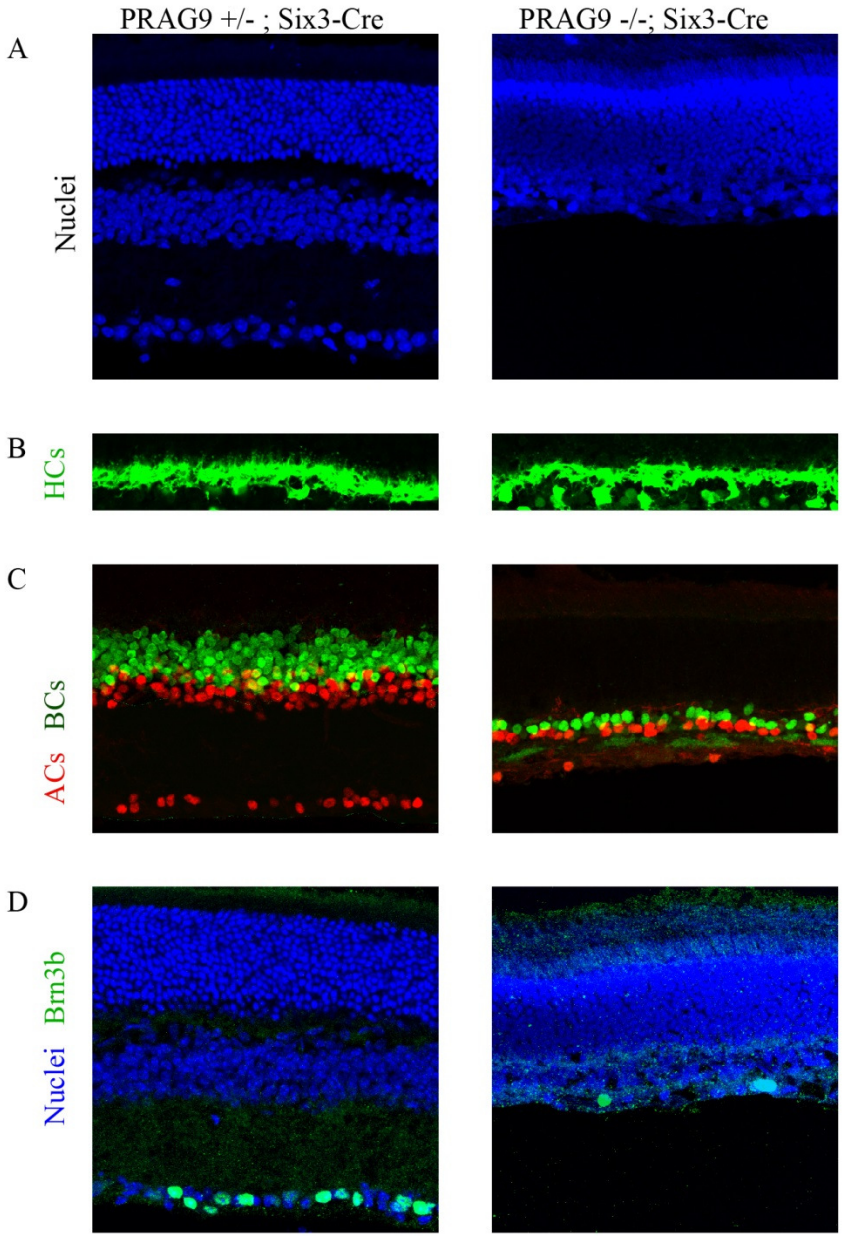

A. Nuclear stain of vertical retinal section showing 3 nuclear layers in heterozygotes (left) but lack of distinct layers in PRAG9 retinal mutants.

B. Horizontal cells are spared in PRAG9 mutants.

C. Bipolar cells (green) and amacrines cell (red) exhibit cell death in PRAG9 mutants.

A. Retinal ganglion cells (green) exhibit cell death in PRAG9 mutants.

Figure 4.5: Lack of distinct synaptic laminae in the IPL of PRAG9 mutants

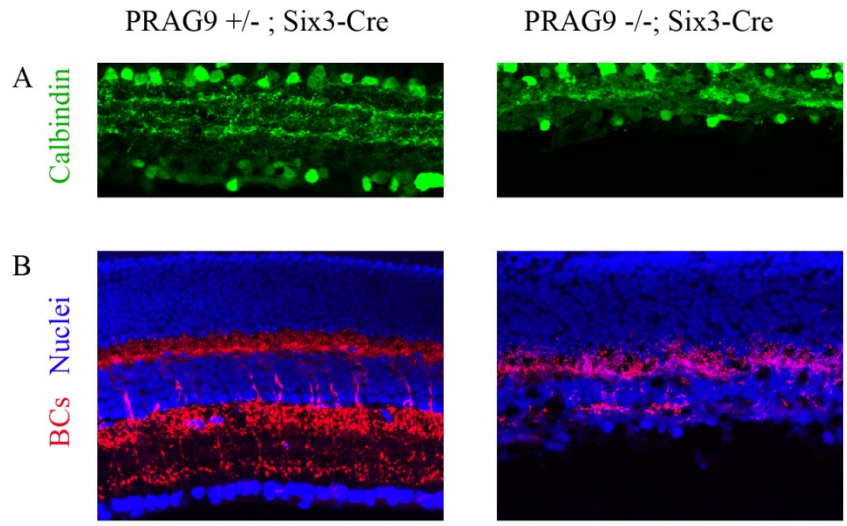

A. Calbindin immunostaining in the inner plexiform layer (IPL) reveals lack of distinct sublaminae in PRAG9 mutants. Note that in wild type mice, the upper and lower of the three staining bands in the IPL represent the dendrites of starburst amacrine cells, and that these processes have failed to segregate and show large gaps in PRAG9 mutants.

B. Syt2 immunostaining for type 2 and type 6 bipolar cells reveals lack of segregation of the processes of these cells and a reduction in their cell number.

4.4 Discussion

In this chapter, I have presented our initial attempts to use novel genome editing technologies to study the combinatorial role of multiple Pcdh subclusters in neural circuit function. Using the CRISPR/Cas9 system was essential for these studies mainly due to the genomic proximity of the *Pcdha* and *Pcdhg* loci in the genome. The characterization of these new mutants is ongoing, as we have just obtained viable mutants. The next and most important course of action will be to confirm that the disruptions we have made to the *Pcdha* locus in the Pcdhg conditional mutant background are indeed null mutations. We will do this by RT-PCR of Pcdha transcript and immunoblotting of Pcdha protein in homozygous mutant animals.

4.4.1 Studies of the retina

We began by looking in the retina, where we have a good sense of the histological signatures of Pcdha mutants (no noticeable phenotypes) and Pcdhg mutants (accentuated cell death and self-avoidance defects). Remarkably, it appears that Pcdha/Pcdhg double mutants exhibit cell of bipolar, amacrine, and ganglion cells that is substantially worse than that seen in Pcdhg mutants alone. While the cells that do not die in Pcdhg mutants alone still form laminar circuits that are functional (Lefebvre et al., 2008), Pcdha/Pcdhg double mutants fail to form distinguishable sublaminae in the inner plexiform layer and likely have substantial physiological defects. Furthermore, staining of the processes of starburst amacrine cells, which exhibit striking self-avoidance defects in Pcdhg mutant retinas, revealed that the processes of these cells fail to segregate into their OFF and ON strata. Whole mount staining of the starburst amacrine cell dendritic plexus and single cell labeling will give us a better sense of whether self-avoidance defects are more severe than in Pcdhg mutants alone. It also remains to be determined whether starburst amacrine cells exhibit cell death in Pcdha/Pcdhg double mutants, since they do not exhibit such death in Pcdhg mutants alone (Lefebvre et al., 2012). These studies would also benefit from retinal subtype-specific deletions as I have done in chapter 3 of this thesis in order to minimize non-autonomous effects of cell death. Finally, it would be great to understand the functional implications of these retinal phenotypes.

This could either be done in a low-throughput but sensitive manner using patch-clamp electrophysiology or on a population level using calcium imaging.

4.4.2 Looking elsewhere in the brain

The power of cell type and tissue-specific Cre drivers will give us an opportunity to study the combinatorial roles of the Pcdha and Pcdhg families throughout the brain. One logical place to start is in the cerebellum, focusing on Purkinje cells. These cells exhibit striking self-avoidance, express all subclusters of the Pcdh locus (Esumi et al., 2005; Hirano et al., 2012; Kaneko et al., 2006; Lefebvre et al., 2012). Furthermore, Purkinje cells lacking Pcdhgs exhibit self-avoidance defects (Lefebvre et al., 2012); however, this phenotype was somewhat mild compared to the defects we observed in retinal starburst amacrine cells. It is possible that this is due to redundancy in the function of Pcdh subcluster in mediating dendritic self-avoidance, and we will be able to address this issue directly by studying Purkinje cells lacking both Pcdhas and Pcdhgs.

Pcdhs are not only important for the patterning of retinal and cerebellar circuits; they have important developmental functions throughout the brain, such as spinal cord, hippocampus, olfactory bulb, and cerebral cortex (Garrett et al., 2012; Hasegawa et al., 2008; Katori et al., 2009; Wang et al., 2002c; Weiner et al., 2005). The toolkit that we have generated here will allow us to study how different Pcdh families interact in all of these regions.

Chapter 5: Conclusion and future directions

The present work has sought to address a fundamental problem in neuroscience – the relationship between the structure and function of neural circuits. The many distinct shapes and size of neurons dictate the roles that these components will play within a circuit, and the developmental assembly of these circuits underlies our ability to perform complex mental tasks and behaviors as adults. Without the diversity of such circuits, it would be impossible for animals to perform daily tasks such as feeding and courtship, but also to create culture, make art, play sports, and do science. In short, understanding how the brain is wired will help us understand what makes us who we are as humans.

In the studies presented in this thesis, I have sought to tackle a small piece of this enormous puzzle. My colleagues and I have identified the molecular mediators and functional significance of a particular dendritic patterning strategy – self-avoidance combined with self/non-self discrimination – that is generally used by many neuronal classes throughout the animal kingdom. In sensory neurons, dendritic self-avoidance is thought to ensure that individual neurons can sample from their whole receptive fields uniformly but not redundantly. In higher processing centers of the brain, where the notion of receptive fields is less clear, self-avoidance likely ensures an economical strategy used by dendrites to capture a maximal number of different synaptic partners while minimizing the resources needed to grow large arbors. In this chapter, I will summarize the findings described in this thesis and possible future directions of study that have been uncovered by the studies herein.

5.1 Molecular mechanisms of dendritic self-avoidance and self/non-self discrimination in the mammalian nervous system

5.1.1 Summary of present studies

In Chapter 2, we have demonstrated that dendritic self-avoidance and self/non-self discrimination in mammalian neurons requires a diverse family of cellular recognition molecules – the clustered gamma-Protocadherins (Pcdhgs). Our studies have focused on two cell types that normally exhibit dendritic self-avoidance: retinal starburst amacrine cells (SACs) and cerebellar Purkinje cells. In the absence of Pcdhgs, both of these cell classes exhibit striking abnormalities in their dendritic patterning, forming crossed and clumped dendritic branches. Remarkably, these defects are confined to the relative position of individual dendrites, as the total number of branches, branch length, and maximal dendritic arbor size is unchanged in Pcdhg mutant SACs and Purkinje cells. Focusing on SACs, we have gained several mechanistic insights into how dendritic self-avoidance is established in these cells.

First, we asked how SACs acquire their mature self-avoiding dendritic geometry. As SACs extend dendrites during early postnatal development, sister branches from the same cell are often in close proximity to each other, meaning these cells do not initially exhibit self-avoidance. However, in the days prior to eye-opening, postnatal day 14 in mice, SACs preferentially eliminate sister branches that are overlapping, yield a mature, self-avoiding dendritic morphology. SACs lacking self-avoidance still go through a similar pruning of excessive branches, but they do not show any preference for elimination of branches that cross, and therefore exhibit self-avoidance defects at maturity.

Next, we asked whether require the presence of other cells, SACs or other retinal neurons, to for proper dendritic patterning. Sparsely cultured SACs from Pcdhg wild type mice established radially symmetric dendritic arbors that looked similar to juvenile SACs *in vivo*, while similarly cultured neurons from Pcdhg mutant mice did not. Thus, individual SACs do not require the presence of their neighbors to form self-avoiding arbors. Furthermore, removing Pcdhg from either the whole population of SACs or individual SACs (as opposed to the whole retina) prevented the ability of these cells to form self-avoiding

dendrites. Together, these findings demonstrated that SAC self-avoidance is accomplished in a cell-autonomous manner.

Our next experiments addressed the requirement of Pcdhg diversity for SAC dendritic self-avoidance. The *Pcdhg* locus encodes 22 distinct protein isoforms that have extracellular diversity and homophilic recognition, but conserved intracellular signaling domains. We therefore hypothesized that these different isoforms may serve a redundant function in promoting self-avoidance. To test this directly, we reduced Pcdhg diversity in two different ways. First, we labeled SACs in Pcdhg mutants that had 19 rather than 22 Pcdhgs and showed that self-avoidance is normal in these SACs. Next, we used a replacement strategy to reduce Pcdhg diversity to a single isoform In this case, SACs self-avoidance was also not perturbed. Thus, we concluded that self-avoidance of SAC dendrites does not require Pcdhg diversity.

If self-avoidance does not require Pcdhg diversity, then why has evolution created such a diverse genomic locus? The answer to this question was revealed from our studies of neighboring SACs. Individual SACs overlap extensively with their neighbors; a given cell's dendrites can potentially come into contact with over 100 other SACs. We reasoned that diversity may be required to allow SACs to avoid their own dendritic branches, but not those of their neighbors. To test this directly, we filled pairs of SACs with different colored dyes and measured the overlap between these neighbors. We found that when all SACs express the same Pcdhg, they repel the dendrites of their neighbors, just as they do their own.

These studies led us to propose a model for Pcdhg-mediate self-avoidance and self-non-self discrimination in SACs. Individual SACs express subsets of Pcdhgs differentially and display them on their surface. In this way, SAC dendrites can repel their own sister dendrites, which display the same cohort of Pcdhgs, but they are immune to the repellent forces in the dendrites of their neighbors, which are unlikely to express the same combination of isoforms. Importantly, differential, stochastic expression of Pcdhgs has been demonstrated in Purkinje cells, which also use these molecules for dendritic self-avoidance. This model is very similar to the *Dscam1*-mediated process proposed for self-avoidance and

self/non-self discrimination in Drosophila. Remarkably, *Dscam1* and *Pcdhgs* are unrelated families of recognition molecules. However, it seems that stochastically-expressed, molecularly diverse families of repulsive cellular recognition molecules are an evolutionarily-conserved strategy for adopting self-avoiding and self/non-self discriminating neuronal arbors.

5.1.2 Future directions

The studies described in Chapter 2 have left several open questions regarding Pcdhgs and self-avoidance. First, one major question how self-avoidance is used by neurons to shape their function within a neural circuit. This is actually still an open question in Drosophila, but we have addressed it directly in SACs in chapter 3 of this thesis. Another open question was the interplay between the different subclusters of Pcdh isoforms. In chapter 4, I have described our initial attempts to tackle this problem as well. Finally, we still have not tested all of the predictions made by our model of Pcdhg-mediated self-avoidance and self/non-self discrimination.

We still have a poor understanding of the structural elements of Pcdhgs that are required to mediate self-avoidance and the downstream actuators that alter dendritic morphology in response to Pcdhg homophilic binding. The former question could be done using detailed examination of fluorescently-tagged Pcdhs. Biochemical studies and binding assays in heterologous cells have predicted that Pcdhs form *cis* tetramers that increase the diversity and binding specificity of these molecules, but whether these assemblies are used by neurons is unclear. This question could be answered by employing subunit counting methods that have been used to understand the assembly of glutamate receptor subunits (Ulbrich and Isacoff, 2007, 2008). The latter question would require an expression system in which we can deliver mutated Pcdhg constructs to developing SACs and track their dendritic development. This has been possible in Drosophila larvae (Wu et al., 2012), which are transparent, but it is more difficult in the retina for several reasons. First, intact retinas, and especially retinal ganglion cells, survive poorly *in vitro*, likely due to lack of trophic factors derived from their axonal targets. Recent studies have shown that a possible way to overcome this problem, at least partially, is to maintain retinal explant on co-culture of

superior colliculus neurons (Barkis et al., 2010). The survival rates of ganglion cells and general retinal structure are much improved in this condition, so this could be a useful approach. In pilot experiments not described in this thesis, I have used this strategy to watch the dendritic development of SAC in early postnatal development (**Figure 5.1**), and I believe this approach could open up a wealth of possibilities to ask about structure-function relationships in the extracellular domains of Pcdhgs used for *trans* binding, as well as signaling mechanisms downstream of homophilic recognition and activation.

Another prediction of our model that we have yet to address is whether SACs express distinct Pcdhg subsets. Traditional expression profiling techniques such as single cell RT-PCR have demonstrated that this is the case in Purkinje cells, which are large and provide a lot of genetic material, but it is more difficult in SACs, which are much smaller. In fact, our efforts to repeat the Purkinje cell experiments of Yagi and colleagues (Esumi et al., 2006) were a failure. However, the emerging field of single-cell sequencing could provide a method to profile expression of all Pcdhs in many individual SACs (Zeisel et al., 2015).

More generally, it would be great to develop more quantitative approaches to determine the extent to which different neuronal types exhibit self-avoidance and self/non-self discrimination. So far, the studies of these phenomena have been confined to neurons with two-dimensional arbors, likely due to ease of phenotypic quantification. Improved morphometric analysis and visualization tools of neuronal arborizations would be very useful tools for the study of these phenomena in the future.

Figure 5.1: Time-lapse imaging of developing SACs

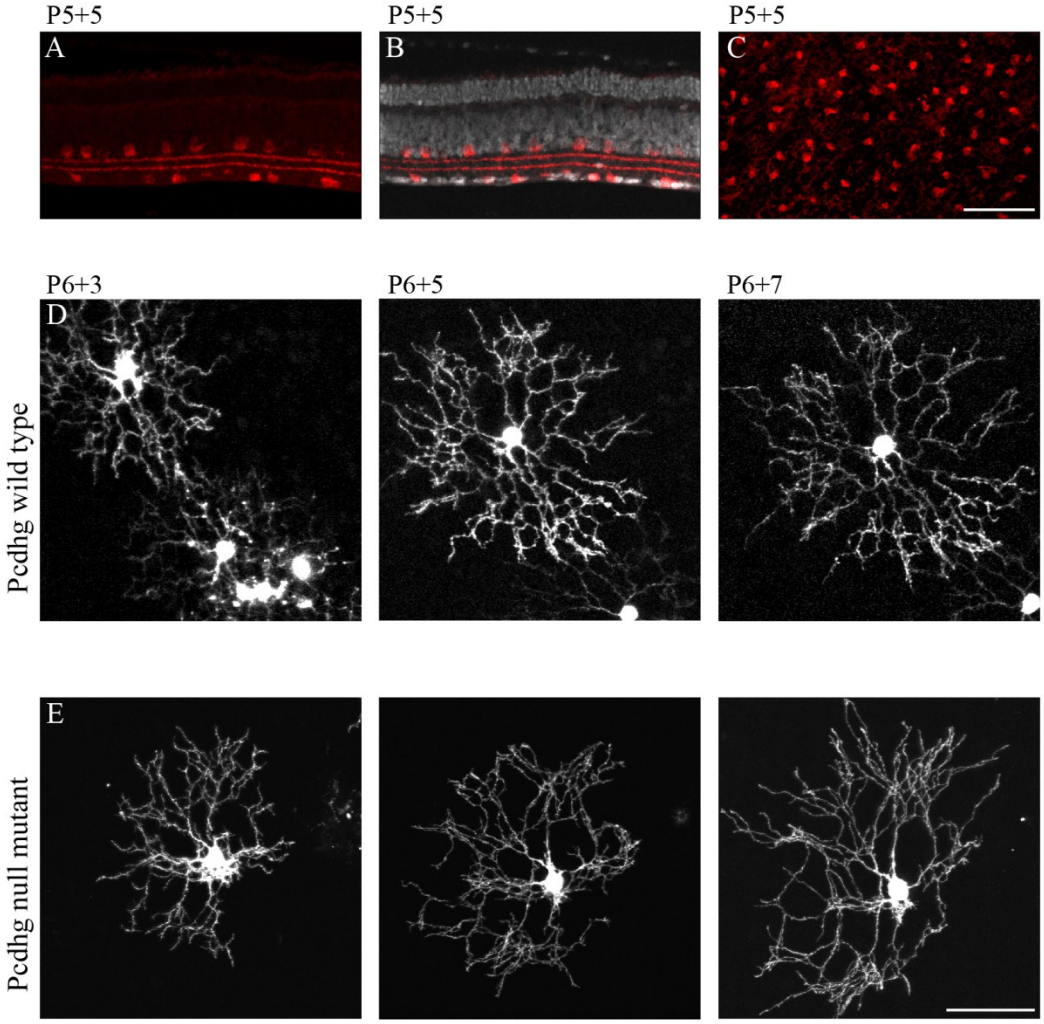

A. Vertical section of retina explanted at postnatal day (P) 5 and kept in culture for 5 days (P5+5) that has been stained with against ChAT (red) to label all SACs.

B. Same section from panel **A** with nuclear stain overlaid (gray).

C. Whole mounted retina (P5+5 DIV) showing regular arrangement of SAC cell bodies

D. SAC labeled with biolistics from Pcdhg wild type retina explanted at P6 and maged after 3 days (left), 5 days (middle), and 7 days (right) in culture.

E. Same as **D** form Pcdhg null mutant retina

Scale bar = 50 µm. Same magnification is shown for panels **A-C** and for panels **D-E**.

5.2 Roles of self-avoidance and self/non-self discrimination in circuit function

5.2.1 Summary of present studies

In Chapter 3 of this thesis, I have directly addressed the utility of dendritic self-avoidance and self/non-self discrimination in circuit function. Focusing on starburst amacrine cells and the direction-selective circuit, I have shown that both self-avoidance and self/non-self discrimination are necessary for strong computation of directional motion. This circuit provided an excellent platform to study the roles of self-avoidance and self/non-self discrimination because we know a lot about the synaptic mechanisms of this computation. SACs provide the main inhibitory input to direction-selective retinal ganglion cells (DSGCs) and are essential for their direction selectivity (Fried et al., 2002; Yoshida et al., 2001). Each dendrite of a SAC is an independent direction-selective subunit responds preferentially to motion along its proximo-distal axis (Euler et al., 2002). SAC dendrites of similar orientations wire to the same classes of DSGCs and inhibit them when motion is presented along the aforementioned axis (Briggman et al., 2011). Thus, the directional preference of a given class of DSGCs is opposite the preferred direction of the SAC dendrites that innervate it. SACs are also known to form inhibitory connections with each other as well, providing a second level of directional inhibition presynaptic to DSGCs (Lee and Zhou, 2006). From these studies, it has been predicted that radially symmetric, self-avoiding dendritic arbors of SACs and mutual SAC-SAC inhibition are both necessary for proper directional computation by DSGCs; however, prior to the studies in this thesis, a direct test of these predictions was lacking.

We began our studies by characterizing SAC-SAC synaptic connections in wild type mice and mice where we removed Pcdhgs selectively from SACs. Analysis of wild type mice revealed an unexpected developmental progression and geometric specificity of these connections. At eye-opening, the probability that a pair of SACs will be connected is predicted well by the extent that their dendrites overlap, meaning closely spaced SACs are more often connected than far away SACs. In adults, meanwhile, the connections between such closely-spaced SACs are preferentially eliminated, so the majority of connections are made between SAC dendrites with opposing directional preferences. Juvenile Pcdhg mutant SACs showed similar connection probabilities as wild types, despite a reduced radial

dendritic coverage caused by a lack of self-avoidance. Surprisingly, when we repeated these experiments in adult Pcdhg mutant SACs, we found no such developmental progression to their connectivity. Closely spaced SACs were still connected in at the same frequency as juvenile SAC pairs. Thus, we have demonstrated an unexpected role of Pcdhgs in synapse elimination in SACs. The mechanism of this elimination is still unclear (see next section); however, the geometric orientation of these connections has strong functional implications. Connections between SACs with parallel dendrites (nearby pairs) would tend to reduce the direction-selectivity of individual SAC dendrites, since processes computing the same direction would inhibit each other. Connections between SACs with antiparallel dendrites (far away but overlapping pairs) would tend to improve the directional responses of any individual dendrites, since it would be inhibited during visual motion in its non-preferred (null) direction.

We next asked whether the disruption of Pcdhg-mediated self-avoidance in Pcdhg null mutants and self/non-self discrimination in SACs expressing the same Pcdhg isoform is reflected in the synaptic connectivity within and between SACs. Giving brief depolarizing steps to SACs that lacked self-avoidance caused outward currents in these cells that had synaptic latencies and were eliminated by the application of blockers of inhibitory neurotransmission. Therefore, one purpose of dendritic self-avoidance in SACs is to prevent the formation of autapses. In parallel experiments, we recorded from pairs of SACs expressing the same Pcdhg isoform. In this case, we found these SACs formed few connections with each other both in juvenile animals and in adults. From these SAC recordings, we concluded that dendritic self-avoidance is not only necessary to establish the morphological geometry of SAC dendrites but also specifies the synaptic connectivity of the inhibitory SAC network. Functionally, we believe that autaptic SAC connections would be analogous to parallel connections between nearby SACs, since overlapping dendrites from a given SAC would tend to grow in the same direction and have similar directional preferences.

Finally, we probed the significance of SAC self-avoidance, self/non-self discrimination, and synapses elimination for directional computation by DSGCs. To begin our studies, we confirmed that alterations of Pcdhg expression in SACs did not alter the ability of these cells and DSGCs form synaptic

connections generally. We recorded excitatory currents in response to static flashing spots from SACs across all conditions and found no difference in the total drive to these cells, consistent with the finding that Pcdhgs do not affect number and outgrowth of SAC dendrites. We also recorded excitatory and inhibitory currents from DSGCs in retinas where Pcdhg expression was altered in SACs alone and found no difference in the responses of these cells to static visual stimuli. Finally, we filled DSGCs with fluorescent dye and assessed whether alterations of Pcdhg expression in SACs altered the ability of these ganglion cells to laminate and fasciculate with the plexus of SAC dendrites. As expected from our functional studies, we found no noteworthy differences across conditions.

With the confidence that altering Pcdhg expression in SACs did not affect retinal function generally, we proceeded to recording responses of DSGCs to moving visual stimuli, the trigger feature of choice for these neurons. Our first set of experiments involved recording action potential firing from DSGCs in response to moving visual stimuli. We found that the loss of self-avoidance and self/non-self discrimination altered the ability of DSGCs to compute direction of motion in distinct ways. When SAC radially morphology and synapse elimination was disrupted in Pcdhg null mutants, DSGCs had much less direction-selective responses and showed a scattering of preferred directions, consistent with an inability of SACs to compute a single direction strongly. Alternatively, DSGCs in retinas where SACs expressed a single Pcdhg isoform, which resulted in normal single cell morphology but reduced connections between SACs, showed weaker directional responses but no alterations in the direction of preference.

To uncover the synaptic basis of these altered spiking responses, we measured excitatory and inhibitory responses of DSGCs in response to visual motion across our three genetic conditions. We found that across these different conditions, excitation onto DSGCs was not altered. However, we found two features – the relative size and the relative timing – of inhibitory currents were altered in both conditions when Pcdhg expression was altered in SACs. In wild type retinas, DSGCs receive strong inhibition from SACs in response to visual motion in their null direction that is coincident in time with excitation. Motion in the preferred direction of a DSGCs causes a relatively small inhibitory current that lags in time relative to excitation. Together, the difference in magnitude and timing of these currents

allow inhibition to veto excitation more strongly in the null direction, preventing depolarization and spiking. We found that the relative size and timing of this inhibition were blunted in both conditions where we altered Pcdhg expression in SACs. The size of inhibition was less asymmetric in retinas where SACs expressed either zero or one Pcdhg isoform, but the effects were more severe in Pcdhg null mutants, explaining why the spiking responses of DSGCs were more severely affected in this condition. The delay of the onset of inhibition in response to preferred motion was also blunted in our two manipulated conditions, this time to a similar degree. Our interpretation of this finding is that normally, antiparallel SAC-SAC inhibition suppresses inhibition onto DSGCs through inhibition of inhibition. When SAC-SAC inhibition is altered, either because of parallel connectivity and autapses in Pcdhg null mutants or because of mutual repulsion between SACs in Pcdhg single isoform mutants, the suppressive effect of antiparallel SAC-SAC inhibition is perturbed similarly.

Thus, self-avoidance and self/non-self discrimination regulate the ability of SAC dendrites to compute directional motion by establishing their radial morphology and specifying their interconnections. To our knowledge, this is the first functional description of the role of these phenomena in a neural circuit. However, there still remain open questions about how other circuits may require dendritic self-avoidance and self/non-self discrimination and what role the computations of these circuits may have in driving behavior.

5.3.2 Future directions

5.3.2.1 Follow-up studies of retinal direction selectivity

The approach we have taken to study the function role of self-avoidance and self/non-self discrimination in the direction-selective circuit by manipulating Pcdhg expression exclusively in SACs has allowed us to isolate these pheonomena from other roles that Pcdhgs play in neural development, like promoting neuronal survival. Harnessing this power of mouse genetics, it would be possible to ask how the alterations in retinal direction-selective computation are used by downstream brain areas.

It is known that this retinal computation is required for the optokinetic reflex (Simpson, 1984; Yoshida et al., 2001), so a straightforward first set of experiments might be to test this reflex in mice where we have manipulated Pcdhg expression in SACs and altered the ability of DSGCs to compute directional motion. While it is known that ablating SACs destroys this reflex, it remains to be seen how our more subtle manipulation of retinal direction-selective computation will do. It will be interesting to see how the intermediate phenotype of direction-selective responses that we observed when we diminished SAC-SAC connections will be affected in this behavioral paradigm. This will allow us to ask how much retinal direction selectivity is enough to drive this reflex, and whether there is enough robustness built into this system to overcome subtle differences in retinal input. It is very important, however, that these behavioral experiments are done with great care, since the Cre line that we have used to remove selectively in retinal SACs (ChAT-Cre) is also expressed in all motor neurons, which are cholinergic. It would be crucially important to be sure that any alterations we observe are due to perturbations of the sensory stream from the retina and not due to motor defects. This could be done by ensuring that our mice have normal motor behaviors by doing motor-specific behavioral tasks in parallel with the optokinetic reflex tests.

Another line of study might be to ask how retinal direction-selective computation relates to direction-selectivity elsewhere in the visual stream. Based on its presence at eye opening, some studies have argued that direction-selectivity in primary visual cortex in mice is inherited from the retina (Cruz-Martin et al., 2014; Rochefort et al., 2011), so it would be great to assess how cortical responses to directional stimuli are affected by our retinal manipulations. Furthermore, recent studies have called into question exactly how retinal input is processed by subsequent brain regions (Feinberg and Meister, 2015), and the best way to probe this directly is by manipulating retinal inputs to these regions. Lastly, studying higher brain regions in the context of motion detection would also provide access to studying learned visual behaviors and higher brain functions.

5.3.2.2 Studying self-avoidance elsewhere in the brain

Another brain region where the functional role of dendritic self-avoidance may be addressed is the cerebellum. Like starburst amacrine cells, cerebellar Purkinje cells use Pcdhgs for dendritic self-avoidance. The cerebellar circuit has been studied extensively has been studied extensively and is critically important for sensory processing, motor coordination, and motor learning (Chadderton et al., 2014; Marr, 1969; Wolpert et al., 1998). Importantly, we have very specific tools to manipulate gene expression selectively in Purkinje cells without affecting most other cells in the brain – our L7-Cre line is expressed only in cerebellar Purkinje cells and retinal rod bipolar cells, whose function can be diminished by doing *in vivo* experiments in photopic conditions.

These studies would follow two streams. First, it would be interesting to ask whether self-avoidance of Purkinje cells is necessary for the development of the cerebellum. During the first three postnatal weeks, Purkinje cells eliminate all but one of their excitatory climbing fiber inputs, and this elimination is required for proper motor behavior (Ichise et al., 2000; Kano and Hashimoto, 2009). How perturbing dendritic self-avoidance would alter this process is unclear, but easily testable. The other source of excitation to Purkinje cells comes from parallel fibers, the axons of cerebellar granule cells. These synapses are a major site of synaptic plasticity (long term depression or LTD) in the brain, and this plasticity is thought to be crucial for motor learning. Studying whether parallel fiber to Purkinje cell LTD is affect when self-avoidance is perturbed would also be a straightforward set of studies. Ultimately, we would like to know how these cellular processes relate to animal behavior. The cerebellum is involved in both reflexive and learned behaviors, and testing the behavioral consequences of perturbing Purkinje cell self-avoidance, and the circuit mechanisms underlying these changes is possible. These studies would be done best by using a closed loop behavior system where researchers can present sensory stimuli, monitor motor behavior, and recording functional activity, either electrically or optically. Imaging is possible at a whole-brain level in larval zebrafish (Ahrens et al., 2012), and in single brain regions in mice (Dombeck et al., 2007; Harvey et al., 2009). Adapting these systems to cerebellum is possible, because it is a superficial brain structure.

Interestingly, there is already some evidence that self-avoidance in Purkinje cells is important for the function of the cerebellum. Purkinje cells use multiple mechanisms for dendritic self-avoidance. In addition to the role of Pcdhgs that we have documented, these neurons require Slit/Robo signaling for dendritic self-avoidance, through a mechanism that works in parallel with Pcdhgs (Gibson et al., 2014). Mice with perturbed Slit/Robo signaling show alterations in their gait, highlighting necessity of Purkinje cell self-avoidance in neural function. How these changes in gait relate to more interesting motor programs is still an open question.

5.3 Combinatorial analysis of alpha- and gamma-Protocadherins

The studies I have described in Chapter 4 of this thesis are extremely preliminary. We have only just begun to get viable alpha/gamma-Protocadherin (PRAG) mutants. To obtain these double mutants, we have leveraged a new technology that has made generating mutations in mice much more straightforward. The CRISPR/Cas9 system allows for targeting mutations to particular genomic locations that is no more difficult than designing a PCR primer (Mali et al., 2013). The ease of this approach made it possible to rapidly create a mutation in the *Pcdha* locus that is only one megabase away from the *Pcdhg* locus. Generating this mutant through homologous recombination of our Pcdhg conditional mutants and existing Pcdha mutant mice would have taken a very long time due to the low likelihood of a recombination even between these two locations. Ultimately, it will be possible to make conditional mutants for both alpha- and gamma-Protocadherins together, but using CRISPR/Cas9 to make knock-in mice was not a viable strategy when we designed these studies. Furthermore, we will eventually be able to incorporate the third subcluster of Pcdhs, the betas, into our analysis.

Our preliminary analysis of these mutants in the retina has revealed redundant roles of alpha- and gamma-Protocadherins in neuronal survival. The defects in PRAG double mutants are much more severe than the previously documented defects in Pcdhg mutants, which results in approximately half of interneurons and ganglion cells dying (Lefebvre et al., 2008), and the complete lack of cell death in Pcdha mutants. Thus, the preliminary description of the defects in PRAG mutants has already unmasked an additive role of the double mutants relative to either mutation alone.

Immunostaining of laminar markers in these PRAG mutants has revealed that distinct synaptic laminae are lacking when many cells die. It would be interesting to examine this process in more detail, because this study may directly address a longstanding hypothesis about the

development of laminar circuits in early visual systems – the so called 'self-assembly' hypothesis (Baier, 2013; Lefebvre et al., 2015; Sanes and Zipursky, 2010). This idea states that the processes of retinal neurons that laminate in the inner plexiform layer (IPL) early may set the scaffold for neurons that laminate later. Conversely, the laminate of later neurons may drive the formation of additional synaptic layers in between exist laminae, forcing the processes of the existing neurons apart. Interestingly, calbindin staining of retinal sections, which normally labels three laminae in the IPL – the OFF SAC band, the ON SAC band, and a third intermediate band – appears as a single band in PRAG mutants. Thus, a preliminary but testable hypothesis is that neurons that normally laminate between the SAC bands arrive later and force the SAC bands apart. A direct test of this may be obtained by performing the sorts of live imaging experiments that I described in the first section of this conclusion.

A more specific question about the roles combinatorial roles of alpha- and gamma-Protocadherins may be to ask how self-avoidance of SACs and Purkinje cells is affected in these double mutants. Clearly, it will be difficult to assess this process for SAC using a retina-wide Cre line like we have done for our preliminary analysis, but using a SAC-specific Cre line, like we did for our studies in Chapter 3, may facilitate these studies. As described previously, we also have specific genetic access to Purkinje cells, so analysis of their morphology and function in these double mutants will be possible.

Lastly, it will be interesting to probe the roles of Pcdhs more generally in the brain. These molecules are expressed throughout the nervous system, where they have roles in axonal patterning, synapse formation, and dendritic morphogenesis. How specific these different phenotypes are to individual Pcdh subclusters is an open question but will be possible by comparing mutants of individual Pcdh subclusters to mutants of multiple subclusters. As

mentioned above, the CRISPR/Cas9 system will eventually make it possible to study the six combinations of alpha-, beta-, and gamma-Protocadherins individually and together.

References

Ackman, J.B., and Crair, M.C. (2014). Role of emergent neural activity in visual map development. Current opinion in neurobiology *24*, 166-175.

Ahrens, M.B., Li, J.M., Orger, M.B., Robson, D.N., Schier, A.F., Engert, F., and Portugues, R. (2012). Brain-wide neuronal dynamics during motor adaptation in zebrafish. Nature *485*, 471-477.

Amthor, F.R., Oyster, C.W., and Takahashi, E.S. (1984). Morphology of on-off direction-selective ganglion cells in the rabbit retina. Brain Research *298*, 187-190.

Baas, P.W., Deitch, J.S., Black, M.M., and Banker, G. (1988). Polarity orientation of microtubules in hippocampal neurons: Uniformity in the axon and nonuniformity in the dendrite. Proceedings of the National Academy of Sciences of the United States of America *85*, 8335-8339.

Bacci, A., Huguenard, J.R., and Prince, D.A. (2003). Functional autaptic neurotransmission in fast-spiking interneurons: a novel form of feedback inhibition in the neocortex. The Journal of neuroscience : the official journal of the Society for Neuroscience *23*, 859-866.

Badea, T.C., Cahill, H., Ecker, J., Hattar, S., and Nathans, J. (2009). Distinct roles of transcription factors brn3a and brn3b in controlling the development, morphology, and function of retinal ganglion cells. Neuron *61*, 852-864.

Baden, T., Berens, P., Bethge, M., and Euler, T. (2013). Spikes in mammalian bipolar cells support temporal layering of the inner retina. Current biology : CB *23*, 48-52.

Baier, H. (2013). Synaptic laminae in the visual system: molecular mechanisms forming layers of perception. Annu Rev Cell Dev Biol *29*, 385-416.

Baker, M.W., and Macagno, E.R. (2000). The role of a LAR-like receptor tyrosine phosphatase in growth cone collapse and mutual-avoidance by sibling processes. J Neurobio *44*, 194-203.

Barkis, W.B., Ford, K.J., and Feller, M.B. (2010). Non-cell-autonomous factor induces the transition from excitatory to inhibitory GABA signaling in retina independent of activity. Proceedings of the National Academy of Sciences of the United States of America *107*, 22302-22307.

Barlow, H.B., and Hill, R.M. (1963). Selective sensitivity to direction of movement in ganglion cells of the rabbit retina. Science *139*, 412-414.

Barlow, H.B., Hill, R.M., and Levick, W.R. (1964). Retinal ganglion cells responding selectively to direction and speed of image motion in the rabbit. J Physiol *173*, 377-407.

Barlow, H.B., and Levick, W.R. (1965). The mechanism of directionally selective units in rabbit's retina. J Physiol *178*, 477-504.

Barnes, A.P., and Polleux, F. (2009). Establishment of axon-dendrite polarity in developing neurons. Annual review of neuroscience *32*, 347-381.

Bekkers, J.M., and Stevens, C.F. (1991). Excitatory and inhibitory autaptic currents in isolated hippocampal neurons maintained in cell culture. Proceedings of the National Academy of Sciences of the United States of America *88*, 7834-7838.

Berson, D. (2003). Strange vision: ganglion cells as circadian photoreceptors. Trends in Neurosciences *26*, 314-320.

Blackshaw, S.E., Nicholls, J.G., and Parnas, I. (1982). Expanded receptive fields of cutaneous mechanoreceptor cells after single neuron deletion in leech central nervous system. J Physiol *326*, 261-268.

Bleckert, A., Schwartz, G.W., Turner, M.H., Rieke, F., and Wong, R.O. (2014). Visual space is represented by nonmatching topographies of distinct mouse retinal ganglion cell types. Current biology : CB *24*, 310-315.

Borst, A., and Euler, T. (2011). Seeing things in motion: models, circuits, and mechanisms. Neuron *71*, 974-994.

Branco, T., Clark, B.A., and Hausser, M. (2010). Dendritic discrimination of temporal input sequences in cortical neurons. Science *329*, 1671-1675.

Branco, T., and Hausser, M. (2010). The single dendritic branch as a fundamental functional unit in the nervous system. Current opinion in neurobiology *20*, 494-502.

Briggman, K.L., Helmstaedter, M., and Denk, W. (2011). Wiring specificity in the direction-selectivity circuit of the retina. Nature *471*, 183-188.

Buffelli, M., Burgess, R.W., Feng, G., Lobe, C.G., Lichtman, J.W., and Sanes, J.R. (2003). Genetic evidence that relative synaptic efficacy biases the outcome of synaptic competition. Nature *424*, 430-434.

Burbridge, T.J., Xu, H.P., Ackman, J.B., Ge, X., Zhang, Y., Ye, M.J., Zhou, Z.J., Xu, J., Contractor, A., and Crair, M.C. (2014). Visual circuit development requires patterned activity mediated by retinal acetylcholine receptors. Neuron *84*, 1049-1064.

Chadderton, P., Schaefer, A.T., Williams, S.R., and Margrie, T.W. (2014). Sensory-evoked synaptic integration in cerebellar and cerebral cortical neurons. Nature reviews Neuroscience *15*, 71-83.

Chan, Y.C., and Chiao, C.C. (2013). The distribution of the preferred directions of the ON-OFF direction selective ganglion cells in the rabbit retina requires refinement after eye opening. Physiological reports *1*, e00013.

Chen, H., Liu, X., and Tian, N. (2014). Subtype-dependent postnatal development of direction- and orientation-selective retinal ganglion cells in mice. Journal of neurophysiology *112*, 2092-2101.

Chen, W.V., Alvarez, F.J., Lefebvre, J.L., Friedman, B., Nwakeze, C., Geiman, E., Smith, C., Thu, C.A., Tapia, J.C., Tasic, B.*, et al.* (2012). Functional significance of isoform diversification in the protocadherin gamma gene cluster. Neuron *75*, 402-409.

Chen, Y., Stevens, B., Chang, J., Milbrandt, J., Barres, B.A., and Hell, J.W. (2008). NS21: re-defined and modified supplement B27 for neuronal cultures. J Neurosci Methods *171*, 239-247.

Cheng, P.L., and Poo, M.M. (2012). Early events in axon/dendrite polarization. Annual review of neuroscience *35*, 181-201.

Chiao, C.C., and Masland, R.H. (2002). Starburst cells nondirectionally facilitate the responses of direction-selective retinal ganglion cells. The Journal of neuroscience *22*, 10509-10513.

Choi, J.H., Law, M.Y., Chien, C.B., Link, B.A., and Wong, R.O. (2010). In vivo development of dendritic orientation in wild-type and mislocalized retinal ganglion cells. Neural development *5*, 29.

Cline, H., and Haas, K. (2008). The regulation of dendritic arbor development and plasticity by glutamatergic synaptic input: a review of the synaptotrophic hypothesis. J Physiol *586*, 1509-1517.

Conde, C., and Caceres, A. (2009). Microtubule assembly, organization and dynamics in axons and dendrites. Nature reviews Neuroscience *10*, 319-332.

Craig, A.M., and Banker, G. (1994). Neuronal polarity. Annual review of neuroscience *17*, 267-310.

Crepel, F., Mariani, J., and Delhaye-Bouchard, N. (1976). Evidence for a multiple innervation of Purkinje cells by climbing fibers in the immature rat cerebellum. J Neurobio *7*, 567-578.

Cruz-Martin, A., El-Danaf, R.N., Osakada, F., Sriram, B., Dhande, O.S., Nguyen, P.L., Callaway, E.M., Ghosh, A., and Huberman, A.D. (2014). A dedicated circuit links direction-selective retinal ganglion cells to the primary visual cortex. Nature *507*, 358-361.

Cubelos, B., Sebastian-Serrano, A., Beccari, L., Calcagnotto, M.E., Cisneros, E., Kim, S., Dopazo, A., Alvarez-Dolado, M., Redondo, J.M., Bovolenta, P.*, et al.* (2010). Cux1 and Cux2 regulate dendritic branching, spine morphology, and synapses of the upper layer neurons of the cortex. Neuron *66*, 523-535.

Cui-Wang, T., Hanus, C., Cui, T., Helton, T., Bourne, J., Watson, D., Harris, K.M., and Ehlers, M.D. (2012). Local zones of endoplasmic reticulum complexity confine cargo in neuronal dendrites. Cell *148*, 309-321.

Deans, M.R., Krol, A., Abraira, V.E., Copley, C.O., Tucker, A.F., and Goodrich, L.V. (2011). Control of neuronal morphology by the atypical cadherin Fat3. Neuron *71*, 820-832.

Deltcheva, E., Chylinski, K., Sharma, C.M., Gonzales, K., Chao, Y., Pirzada, Z.A., Eckert, M.R., Vogel, J., and Charpentier, E. (2011). CRISPR RNA maturation by trans-encoded small RNA and host factor RNase III. Nature *471*, 602-607.

Dickson, B.J. (2002). Molecular mechanisms of axon guidance. Science *298*, 1959-1964.

Dombeck, D.A., Khabbaz, A.N., Collman, F., Adelman, T.L., and Tank, D.W. (2007). Imaging large-scale neural activity with cellular resolution in awake, mobile mice. Neuron *56*, 43-57.

Dong, X., Liu, O.W., Howell, A.S., and Shen, K. (2013). An extracellular adhesion molecule complex patterns dendritic branching and morphogenesis. Cell *155*, 296-307.

Duan, X., Krishnaswamy, A., De la Huerta, I., and Sanes, J.R. (2014). Type II cadherins guide assembly of a direction-selective retinal circuit. Cell *158*, 793-807.

Elstrott, J., Anishchenko, A., Greschner, M., Sher, A., Litke, A.M., Chichilnisky, E.J., and Feller, M.B. (2008). Direction selectivity in the retina is established independent of visual experience and cholinergic retinal waves. Neuron *58*, 499-506.

Enciso, G.A., Rempe, M., Dmitriev, A.V., Gavrikov, K.E., Terman, D., and Mangel, S.C. (2010). A model of direction selectivity in the starburst amacrine cell network. Journal of computational neuroscience *28*, 567-578.

Esumi, S., Kakazu, N., Taguchi, Y., Hirayama, T., Sasaki, A., Hirabayashi, T., Koide, T., Kitsukawa, T., Hamada, S., and Yagi, T. (2005). Monoallelic yet combinatorial expression of variable exons of the protocadherin-alpha gene cluster in single neurons. Nature genetics *37*, 171-176.

Esumi, S., Kaneko, R., Kawamura, Y., and Yagi, T. (2006). Split single-cell RT-PCR analysis of Purkinje cells. Nature protocols *1*, 2143-2151.

Euler, T., and Denk, W. (2001). Dendritic processing. Current Opinions in Neurobiology *11*, 415-422.

Euler, T., Detwiler, P.B., and Denk, W. (2002). Directionally selective calcium signals in dendrites of starburst amacrine cells. Nature *418*, 845-852.

Famiglietti, E.V. (1983). 'Starburst' amacrine cells and cholinergic neurons: mirror-symmetric ON and OFF amacrine cells of rabbit retina. Brain Research *261*, 138-144.

Famiglietti, E.V. (1987). Starburst amacrine cells in cat retina are associated with bistratified, presumably directionally selective, ganglion cells. Brain Research *413*, 404-408.

Famiglietti, E.V. (1991). Synaptic organization of starburst amacrine cells in rabbit retina: Analysis of serial thin sections by electron microscopy and graphic reconstruction. The Journal of comparative neurology *209*, 40-70.

Famiglietti, E.V. (1992). Dendritic co-stratification of ON and ON-OFF directionally selective ganglion cells with starburst amacrine cells in rabbit retina. The Journal of comparative neurology *324*, 322-335.

Famiglietti, E.V., and Kolb, H. (1976). Structural basis for ON-and OFF-center responses in retinal ganglion cells. Science *194*, 193-195.

Farajian, R., Raven, M.A., Cusato, K., and Reese, B.E. (2004). Cellular positioning and dendritic field size of cholinergic amacrine cells are impervious to early ablation of neighboring cells in the mouse retina. Visual neuroscience *21*, 13-22.

Farley, F.W., Soriano, P., Steffen, L.S., and Dymecki, S.M. (2000). Widespread recombinase expression using FLPeR (Flipper) mice. Genesis *28*, 106-110.

Feinberg, E.H., and Meister, M. (2015). Orientation columns in the mouse superior colliculus. Nature *519*, 229-232.

Feller, M.B., Wellis, D.P., Stellwagen, D., Werblin, F.S., and Shatz, C.J. (1996). Requirement for cholinergic synaptic transmission in the propagation of spontaneous retinal waves. Science *272*, 1182.

Fried, S.I., Munch, T.A., and Werblin, F.S. (2002). Mechanisms and circuitry underlying directional selectivity in the retina. Nature *420*, 411-414.

Fu, Y., Foden, J.A., Khayter, C., Maeder, M.L., Reyon, D., Joung, J.K., and Sander, J.D. (2013). High-frequency off-target mutagenesis induced by CRISPR-Cas nucleases in human cells. Nature biotechnology *31*, 822-826.

Fuerst, P.G., Bruce, F., Tian, M., Wei, W., Elstrott, J., Feller, M.B., Erskine, L., Singer, J.H., and Burgess, R.W. (2009). DSCAM and DSCAML1 function in self-avoidance in multiple cell types in the developing mouse retina. Neuron *64*, 484-497.

Fuerst, P.G., Koizumi, A., Masland, R.H., and Burgess, R.W. (2008). Neurite arborization and mosaic spacing in the mouse retina require DSCAM. Nature *451*, 470-474.

Furuta, Y., Lagutin, O., Hogan, B.L.M., and Oliver, G.C. (2000). Retina- and ventral forebrain-specific cre recombinase activity in transgenic mice. Genesis *26*, 130-132.

Galli-Resta, L. (2000). Local, possibly contact-mediated signalling restricted to homotypic neurons controls the regular spacing of cells within the cholinergic arrays in the developing rodent retina. Development *127*, 1509-1516.

Galli-Resta, L., Novelli, E., and Viegi, A. (2002). Dynamic microtubule-dependent interactions position homotypic neurones in regular monolayered arrays during development. Development *129*, 3803-3814.

Gao, F.-B., Kohwi, M., Brenman, J.E., Jan, L.Y., and Jan, Y.N. (2000). Control of dendritic formation in Drosophila: The roles of Flamingo and competition between homologous neurons. Neuron *28*, 91-101.

Garrett, A.M., Schreiner, D., Lobas, M.A., and Weiner, J.A. (2012). gamma-protocadherins control cortical dendrite arborization by regulating the activity of a FAK/PKC/MARCKS signaling pathway. Neuron *74*, 269-276.

Gavrikov, K.E., Nilson, J.E., Dmitriev, A.V., Zucker, C.L., and Mangel, S.C. (2006). Dendritic compartmentalization of chloride cotransporters underlies directional responses of starburst amacrine cells in retina. Proceedings of the National Academy of Sciences of the United States of America *103*, 18793-18798.

Gibson, D.A., Tymanskyj, S., Yuan, R.C., Leung, H.C., Lefebvre, J.L., Sanes, J.R., Chedotal, A., and Ma, L. (2014). Dendrite self-avoidance requires cell-autonomous slit/robo signaling in cerebellar purkinje cells. Neuron *81*, 1040-1056.

Gidon, A., and Segev, I. (2012). Principles governing the operation of synaptic inhibition in dendrites. Neuron *75*, 330-341.

Godinho, L., Mumm, J.S., Williams, P.R., Schroeter, E.H., Koerber, A., Park, S.W., Leach, S.D., and Wong, R.O. (2005). Targeting of amacrine cell neurites to appropriate synaptic laminae in the developing zebrafish retina. Development *132*, 5069-5079.

Gollisch, T., and Meister, M. (2010). Eye smarter than scientists believed: Neural computations in circuits of the retina. Neuron *65*, 150-164.

Grueber, W.B., Graubard, K., and TRuman, J.W. (2001). Tiling of the body wall by multidendritic sensory neurons in Manduca sexta. 2001 *440*, 271-283.

Grueber, W.B., Jan, L.Y., and Jan, Y.N. (2002). Tiling of the Drosophila epidermis by multidendritic sensory neurons. Development *129*, 2867-2878.

Grueber, W.B., Jan, L.Y., and Jan, Y.N. (2003a). Different levels of the homeodomain protein Cut regulate distinct dendrite branching patterns of Drosophila multidendritic neurons. Cell *112*, 805-818.

Grueber, W.B., and Sagasti, A. (2010). Self-avoidance and tiling: Mechanisms of dendrite and axon spacing. Cold Spring Harbor perspectives in biology *2*, a001750.

Grueber, W.B., and Truman, J.W. (1999). Development and organization of a nitric-oxide-sensitive peripheral neural plexus in larvae of the moth, Manduca sexta. The Journal of comparative neurology *199*.

Grueber, W.B., Ye, B., Moore, A.W., Jan, L.Y., and Jan, Y.N. (2003b). Dendrites of distinct classes of Drosophila sensory neurons show different capacities of homotypic repulsion. Current biology : CB *13*, 618-626.

Gundersen, R.W., and Barrett, J.N. (1979). Neuronal chemotaxis: Chick dorsal-root axons turn toward high concentrations of nerve growth factor. Science *206*, 1079-1080.

Han, C., Wang, D., Soba, P., Zhu, S., Lin, X., Jan, L.Y., and Jan, Y.N. (2012). Integrins regulate repulsion-mediated dendritic patterning of drosophila sensory neurons by restricting dendrites in a 2D space. Neuron *73*, 64-78.

Hartline, H.K. (1938). The response of single optic nerve fibers of the vertebrate eye to illumination of the retina. American Journal of Physiology *121*, 400-415.

Harvey, C.D., Collman, F., Dombeck, D.A., and Tank, D.W. (2009). Intracellular dynamics of hippocampal place cells during virtual navigation. Nature *461*, 941-946.

Hasegawa, S., Hamada, S., Kumode, Y., Esumi, S., Katori, S., Fukuda, E., Uchiyama, Y., Hirabayashi, T., Mombaerts, P., and Yagi, T. (2008). The protocadherin-alpha family is involved in axonal coalescence of olfactory sensory neurons into glomeruli of the olfactory bulb in mouse. Molecular and cellular neurosciences *38*, 66-79.

Hattori, D., Chen, Y., Matthews, B.J., Salwinski, L., Sabatti, C., Grueber, W.B., and Zipursky, S.L. (2009). Robust discrimination between self and non-self neurites requires thousands of Dscam1 isoforms. Nature *461*, 644-648.

Hattori, D., Demir, E., Kim, H.W., Viragh, E., Zipursky, S.L., and Dickson, B.J. (2007). Dscam diversity is essential for neuronal wiring and self-recognition. Nature *449*, 223-227.

Hausselt, S.E., Euler, T., Detwiler, P.B., and Denk, W. (2007). A dendrite-autonomous mechanism for direction selectivity in retinal starburst amacrine cells. PLoS biology *5*, e185.

Hayden, S.A., Mills, J.W., and Masland, R.H. (1980). Acetylcholine synthesis by displaced amacrine cells. Science *210*, 435-437.

Helmstaedter, M., Briggman, K.L., Turaga, S.C., Jain, V., Seung, H.S., and Denk, W. (2013). Connectomic reconstruction of the inner plexiform layer in the mouse retina. Nature *500*, 168-174.

Hinds, J.W., and Hinds, P.L. (1978). Early development of amacrine cells in the mouse retina: An electron microscopic, serial section analysis. The Journal of comparative neurology *179*, 277-300.

Hirano, K., Kaneko, R., Izawa, T., Kawaguchi, M., Kitsukawa, T., and Yagi, T. (2012). Single-neuron diversity generated by Protocadherin-beta cluster in mouse central and peripheral nervous systems. Frontiers in molecular neuroscience *5*, 90.

Hoggarth, A., McLaughlin, A.J., Ronellenfitch, K., Trenholm, S., Vasandani, R., Sethuramanujam, S., Schwab, D., Briggman, K.L., and Awatramani, G.B. (2015). Specific wiring of distinct amacrine cells in the directionally selective retinal circuit permit independent encoding of direction and size. Neuron *86*, 1-16.

Hong, W., Mosca, T.J., and Luo, L. (2012). Teneurins instruct synaptic partner matching in an olfactory map. Nature *484*, 201-207.

Hong, W., Zhu, H., Potter, C.J., Barsh, G., Kurusu, M., Zinn, K., and Luo, L. (2009). Leucine-rich repeat transmembrane proteins instruct discrete dendrite targeting in an olfactory map. Nature neuroscience *12*, 1542-1550.

Hong, Y.K., Kim, I.J., and Sanes, J.R. (2011). Stereotyped axonal arbors of retinal ganglion cell subsets in the mouse superior colliculus. The Journal of comparative neurology *519*, 1691-1711.

Horton, A.C., Racz, B., Monson, E.E., Lin, A.L., Weinberg, R.J., and Ehlers, M.D. (2005). Polarized secretory trafficking directs cargo for asymmetric dendrite growth and morphogenesis. Neuron *48*, 757-771.

Huang, C.F., and Banker, G. (2012). The translocation selectivity of the kinesins that mediate neuronal organelle transport. Traffic *13*, 549-564.

Hubel, D.H., and Wiesel, T.N. (1962). Receptive fields, binocular interaction, and functional architecture in the cat's visual cortex. Journal of physiology *160*, 106-154.

Huckfeldt, R.M., Schubert, T., Morgan, J.L., Godinho, L., Di Cristo, G., Huang, Z.J., and Wong, R.O. (2009). Transient neurites of retinal horizontal cells exhibit columnar tiling via homotypic interactions. Nature neuroscience *12*, 35-43.

Hughes, M.E., Bortnick, R., Tsubouchi, A., Baumer, P., Kondo, M., Uemura, T., and Schmucker, D. (2007). Homophilic Dscam interactions control complex dendrite morphogenesis. Neuron *54*, 417-427.

Ichise, T., Kano, M., Hashimoto, K., Yanagihara, D., Nakao, K., Shigemoto, R., Katsuki, M., and Aiba, A. (2000). mGluR1 in cerebellar Purkinje cells essential for long-term depression, synapse elimination, and motor coordination. Science *288*, 1832-1835.

Jefferis, G.S., Vyas, R.M., Berdnik, D., Ramaekers, A., Stocker, R.F., Tanaka, N.K., Ito, K., and Luo, L. (2004). Developmental origin of wiring specificity in the olfactory system of Drosophila. Development *131*, 117-130.

Jefferis, G.S.X.E., Marin, E.C., Stocker, R.F., and Luo, L. (2001). Target neuron prespecification in the olfactory map of Drosophila. Nature *414*, 204-208.

Jelinek, H.F., and Fernandez, E. (1998). Neurons and fractals: how reliable and useful are calculations of fractal dimensions? Journal of Neuroscience Methods *81*, 9-18.

Jinushi-Nakao, S., Arvind, R., Amikura, R., Kinameri, E., Liu, A.W., and Moore, A.W. (2007). Knot/Collier and cut control different aspects of dendrite cytoskeleton and synergize to define final arbor shape. Neuron *56*, 963-978.

Joo, W., Hippenmeyer, S., and Luo, L. (2014). Dendritic morphogenesis depends on relative levels of NT-3/TrkC signaling. Science *346*, 626-629.

Kaneko, M., Yamaguchi, K., Eiraku, M., Sato, M., Takata, N., Kiyohara, Y., Mishina, M., Hirase, H., Hashikawa, T., and Kengaku, M. (2011). Remodeling of monoplanar Purkinje cell dendrites during cerebellar circuit formation. PloS one *6*, e20108.

Kaneko, R., Kato, H., Kawamura, Y., Esumi, S., Hirayama, T., Hirabayashi, T., and Yagi, T. (2006). Allelic gene regulation of Pcdh-alpha and Pcdh-gamma clusters involving both monoallelic and biallelic expression in single Purkinje cells. The Journal of biological chemistry *281*, 30551-30560.

Kano, M., and Hashimoto, K. (2009). Synapse elimination in the central nervous system. Current opinion in neurobiology *19*, 154-161.

Katori, S., Hamada, S., Noguchi, Y., Fukuda, E., Yamamoto, T., Yamamoto, H., Hasegawa, S., and Yagi, T. (2009). Protocadherin-alpha family is required for serotonergic projections to appropriately innervate target brain areas. The Journal of neuroscience : the official journal of the Society for Neuroscience *29*, 9137-9147.

Kay, J.N., Chu, M.W., and Sanes, J.R. (2012). MEGF10 and MEGF11 mediate homotypic interactions required for mosaic spacing of retinal neurons. Nature *483*, 465-469.

Kay, J.N., De la Huerta, I., Kim, I.J., Zhang, Y., Yamagata, M., Chu, M.W., Meister, M., and Sanes, J.R. (2011a). Retinal ganglion cells with distinct directional preferences differ in molecular identity, structure, and central projections. The Journal of neuroscience : the official journal of the Society for Neuroscience *31*, 7753-7762.

Kay, J.N., Roeser, T., Mumm, J.S., Godinho, L., Mrejeru, A., Wong, R.O., and Baier, H. (2004). Transient requirement for ganglion cells during assembly of retinal synaptic layers. Development *131*, 1331-1342.

Kay, J.N., Voinescu, P.E., Chu, M.W., and Sanes, J.R. (2011b). Neurod6 expression defines new retinal amacrine cell subtypes and regulates their fate. Nature neuroscience *14*, 965-972.

Kerschensteiner, D., Morgan, J.L., Parker, E.D., Lewis, R.M., and Wong, R.O. (2009). Neurotransmission selectively regulates synapse formation in parallel circuits in vivo. Nature *460*, 1016-1020.

Kim, I.J., Zhang, Y., Meister, M., and Sanes, J.R. (2010). Laminar restriction of retinal ganglion cell dendrites and axons: subtype-specific developmental patterns revealed with transgenic markers. The Journal of neuroscience : the official journal of the Society for Neuroscience *30*, 1452-1462.

Kim, I.J., Zhang, Y., Yamagata, M., Meister, M., and Sanes, J.R. (2008). Molecular identification of a retinal cell type that responds to upward motion. Nature *452*, 478-482.

Kim, J.S., Greene, M.J., Zlateski, A., Lee, K., Richardson, M., Turaga, S.C., Purcaro, M., Balkam, M., Robinson, A., Behabadi, B.F.*, et al.* (2014). Space-time wiring specificity supports direction selectivity in the retina. Nature *509*, 331-336.

Kim, M.E., Shrestha, B.R., Blazeski, R., Mason, C.A., and Grueber, W.B. (2012). Integrins establish dendrite-substrate relationships that promote dendritic self-avoidance and patterning in drosophila sensory neurons. Neuron *73*, 79-91.

Kittila, C.A., and Massey, S.C. (1995). Effect of ON pathway blockade on directional selectivity in the rabbit retina. Journal of neurophysiology *73*, 703-712.

Knudson, C.M., Tung, K.S.K., Tourtellotte, W.G., Brown, G.A.J., and Korsmeyer, S.J. (1995). Bax-deficient mice with lymphoid hyperplasia and male germ cell death. Science *270*, 96.

Kohmura, N., Senzaki, K., Hamada, S., Kai, N., Yasuda, R., Watanabe, M., Ishii, H., Yasuda, M., Mishina, M., and Yagi, T. (1998). Diversity revealed by a novel family of cadherins expressed in neurons at a synaptic complex. Neuron *20*, 1137-1151.

Komiyama, T., Johnson, W.A., Luo, L., and Jefferis, G.S.X.E. (2003). From lineage to wiring specificity: POU domain transcription factors control precise connections of Drosophila olfactory projection neurons. Cell *112*, 157-167.

Komiyama, T., Sweeney, L.B., Schuldiner, O., Garcia, K.C., and Luo, L. (2007). Graded expression of semaphorin-1a cell-autonomously directs dendritic targeting of olfactory projection neurons. Cell *128*, 399-410.

Kramer, A.P., and Kuwada, J.Y. (1983). Formation of receptive fields of leech mechanosensory neurons during embryonic development. The Journal of neuroscience : the official journal of the Society for Neuroscience *3*, 2474-2486.

Kramer, A.P., and Stent, G.S. (1985). Developmental arborization of sensory neurons in the leech Haementeria ghilianii. II. Experimentally induced variations in the branching pattern. The Journal of neuroscience : the official journal of the Society for Neuroscience *5*, 768-775.

Kuchibhotla, K.V., Goldman, S.T., Lattarulo, C.R., Wu, H.Y., Hyman, B.T., and Bacskai, B.J. (2008). Abeta plaques lead to aberrant regulation of calcium homeostasis in vivo resulting in structural and functional disruption of neuronal networks. Neuron *59*, 214-225.

Kuffler, S.W. (1953). Discharge patterns and functional organization of the mammalian retina. Journal of neurophysiology *16*, 37-68.

Kuo, R.I., and Wu, G.K. (2012). The generation of direction selectivity in the auditory system. Neuron *73*, 1016-1027.

Lah, G.J., Li, J.S., and Millard, S.S. (2014). Cell-specific alternative splicing of Drosophila Dscam2 is crucial for proper neuronal wiring. Neuron *83*, 1376-1388.

Ledderose, J., Dieter, S., and Schwarz, M.K. (2013). Maturation of postnatally generated olfactory bulb granule cells depends on functional gamma-protocadherin expression. Scientific reports *3*, 1514.

Lee, S., Kim, K., and Zhou, Z.J. (2010). Role of ACh-GABA cotransmission in detecting image motion and motion direction. Neuron *68*, 1159-1172.

Lee, S., and Zhou, Z.J. (2006). The synaptic mechanism of direction selectivity in distal processes of starburst amacrine cells. Neuron *51*, 787-799.

Lefebvre, J.L., Kostadinov, D., Chen, W.V., Maniatis, T., and Sanes, J.R. (2012). Protocadherins mediate dendritic self-avoidance in the mammalian nervous system. Nature *488*, 517-521.

Lefebvre, J.L., Sanes, J.R., and Kay, J.N. (2015). Development of dendritic form and function. Annu Rev Cell Dev Biol *in press*.

Lefebvre, J.L., Zhang, Y., Meister, M., Wang, X., and Sanes, J.R. (2008). gamma-Protocadherins regulate neuronal survival but are dispensable for circuit formation in retina. Development *135*, 4141-4151.

Li, W., Wang, F., Menut, L., and Gao, F.B. (2004). BTB/POZ-zinc finger protein abrupt suppresses dendritic branching in a neuronal subtype-specific and dosage-dependent manner. Neuron *43*, 823-834.

Liu, Y., and Halloran, M.C. (2005). Central and peripheral axon branches from one neuron are guided differentially by Semaphorin3D and transient axonal glycoprotein-1. The Journal of neuroscience : the official journal of the Society for Neuroscience *25*, 10556-10563.

Lohmann, C., and Wong, R.O. (2001). Cell-type specific dendritic contacts between retinal ganglion cells during development. J Neurobio *48*, 150-162.

Lom, B., and Cohen-Cory, S. (1999). Brain-derived neurotrophic factor differentially regulates retinal ganglion cell dendritic and axonal arborization in vivo. The Journal of neuroscience *19*, 9928-9938.

London, M., and Hausser, M. (2005). Dendritic computation. Annual review of neuroscience *28*, 503-532.

Long, H., Ou, Y., Rao, Y., and van Meyel, D.J. (2009). Dendrite branching and self-avoidance are controlled by Turtle, a conserved IgSF protein in Drosophila. Development *136*, 3475-3484.

Madisen, L., Zwingman, T.A., Sunkin, S.M., Oh, S.W., Zariwala, H.A., Gu, H., Ng, L.L., Palmiter, R.D., Hawrylycz, M.J., Jones, A.R.*, et al.* (2010). A robust and high-throughput Cre reporting and characterization system for the whole mouse brain. Nature neuroscience *13*, 133-140.

Makita, T., Sucov, H.M., Gariepy, C.E., Yanagisawa, M., and Ginty, D.D. (2008). Endothelins are vascular-derived axonal guidance cues for developing sympathetic neurons. Nature *452*, 759-763.

Mali, P., Esvelt, K.M., and Church, G.M. (2013). Cas9 as a versatile tool for engineering biology. Nature methods *10*, 957-963.

Marr, D. (1969). A theory of cerebellar cortex. J Physiol *202*, 437-470.

Masland, R.H. (2012). The tasks of amacrine cells. Visual neuroscience *29*, 3-9.

Masland, R.H., Mills, J.W., and Cassidy, C. (1984a). The function of acetylcholine in the rabbit retina. Proceedings of the Royal Society Series B-Biological Sciences *223*, 121-139.

Masland, R.H., Mills, J.W., and Hayden, S.A. (1984b). Acetylcholine-synthesizing amacrine cells: Identification and selective staining using radioautography and fluorescent markers. Proceedings of the Royal Society Series B-Biological Sciences *223*, 79-100.

Matsuoka, R.L., Chivatakarn, O., Badea, T.C., Samuels, I.S., Cahill, H., Katayama, K., Kumar, S.R., Suto, F., Chedotal, A., Peachey, N.S.*, et al.* (2011a). Class 5 transmembrane semaphorins control selective Mammalian retinal lamination and function. Neuron *71*, 460-473.

Matsuoka, R.L., Jiang, Z., Samuels, I.S., Nguyen-Ba-Charvet, K.T., Sun, L.O., Peachey, N.S., Chedotal, A., Yau, K.W., and Kolodkin, A.L. (2012). Guidance-cue control of horizontal cell morphology,

lamination, and synapse formation in the mammalian outer retina. The Journal of neuroscience : the official journal of the Society for Neuroscience *32*, 6859-6868.

Matsuoka, R.L., Nguyen-Ba-Charvet, K.T., Parray, A., Badea, T.C., Chedotal, A., and Kolodkin, A.L. (2011b). Transmembrane semaphorin signalling controls laminar stratification in the mammalian retina. Nature *470*, 259-263.

Matthews, B.J., Kim, M.E., Flanagan, J.J., Hattori, D., Clemens, J.C., Zipursky, S.L., and Grueber, W.B. (2007). Dendrite self-avoidance is controlled by Dscam. Cell *129*, 593-604.

Maunsell, J.H.R., and Newsome, W.T. (1987). Visual processing in monkey extrastriate cortex. Annual review of neuroscience *10*, 363-401.

McAllister, A.K., Katz, L.C., and Lo, D.C. (1996). Neurotrophin regulation of cortical dendritic growth requires activity. Neuron *17*, 1057-1064.

McAllister, A.K., Lo, D.C., and Katz, L.C. (1995). Neurotrophins regulate dendritic growth in developing visual cortex. Neuron *15*, 791-803.

McLaughlin, T., and O'Leary, D.D.M. (2005). Molecular gradients and development of retinotopic maps. Annual review of neuroscience *28*, 327-355.

Meguro, R., Hishida, R., Tsukano, H., Yoshitake, K., Imamura, R., Tohmi, M., Kitsukawa, T., Hirabayashi, T., Yagi, T., Takebayashi, H*., et al.* (2015). Impaired clustered protocadherin-alpha leads to aggregated retinogeniculate terminals and impaired visual acuity in mice. Journal of neurochemistry *133*, 66-72.

Meijers, R., Puettmann-Holgado, R., Skiniotis, G., Liu, J.H., Walz, T., Wang, J.H., and Schmucker, D. (2007). Structural basis of Dscam isoform specificity. Nature *449*, 487-491.

Meyer-Franke, A., Kaplan, M.R., Pfrieger, F.W., and Barres, B.A. (1995). Characterization of the signaling interactions that promote the survival and growth of developing retinal ganglion cells in culture. Neuron *15*, 805-819.

Miura, S.K., Martins, A., Zhang, K.X., Graveley, B.R., and Zipursky, S.L. (2013). Probabilistic splicing of Dscam1 establishes identity at the level of single neurons. Cell *155*, 1166-1177.

Montague, P.R., and Friedlander, M.J. (1989). Expression of intrinsic growth strategies by mammalian retinal neurons. Proceedings of the National Academy of Sciences of the United States of America *86*, 7223-7227.

Montague, P.R., and Friedlander, M.J. (1991). Morphogenesis and territorial coverage by isolated mammalian retinal ganglion cells. The Journal of neuroscience : the official journal of the Society for Neuroscience *11*, 1440-1457.

Morgan, J.L., Dhingra, A., Vardi, N., and Wong, R.O. (2006). Axons and dendrites originate from neuroepithelial-like processes of retinal bipolar cells. Nature neuroscience *9*, 85-92.

Mountcastle, V.B. (1957). Modality and topographic properties of single neurons of cat's somatic sensory cortex. Journal of neurophysiology *20*, 408-434.

Mumm, J.S., Williams, P.R., Godinho, L., Koerber, A., Pittman, A.J., Roeser, T., Chien, C.B., Baier, H., and Wong, R.O. (2006). In vivo imaging reveals dendritic targeting of laminated afferents by zebrafish retinal ganglion cells. Neuron *52*, 609-621.

Murata, Y., Hamada, S., Morishita, H., Mutoh, T., and Yagi, T. (2004). Interaction with protocadherin-gamma regulates the cell surface expression of protocadherin-alpha. The Journal of biological chemistry *279*, 49508-49516.

Murthy, V.N. (2011). Olfactory maps in the brain. Annual review of neuroscience *34*, 233-258.

Nagae, S., Tanoue, T., and Takeichi, M. (2007). Temporal and spatial expression profiles of the Fat3 protein, a giant cadherin molecule, during mouse development. Developmental dynamics : an official publication of the American Association of Anatomists *236*, 534-543.

Neves, G., Zucker, J., Daly, M., and Chess, A. (2004). Stochastic yet biased expression of multiple Dscam splice variants by individual cells. Nature genetics *36*, 240-246.

Nicholls, J.G., and Baylor, D.A. (1968). Specific modalities and receptive fields of sensory neurons in the CNS of the leech. Journal of neurophysiology *31*, 740-756.

O'Malley, D.M., and Masland, R.H. (1989). Co-release of acetylcholine and gamma-aminobutyric acid by a retinal neuron. Proceedings of the National Academy of Sciences of the United States of America *86*, 3414-3418.

O'Malley, D.M., Sandell, J.H., and Masland, R.H. (1992). Co-release of acetylcholine and GABA by the starburst amacrine cells. The Journal of neuroscience *12*, 1394-1408.

Oesch, N., Euler, T., and Taylor, W.R. (2005). Direction-selective dendritic action potentials in rabbit retina. Neuron *47*, 739-750.

Oesch, N.W., and Taylor, W.R. (2010). Tetrodotoxin-resistant sodium channels contribute to directional responses in starburst amacrine cells. PloS one *5*, e12447.

Ohki, K., and Reid, R.C. (2007). Specificity and randomness in the visual cortex. Current opinion in neurobiology *17*, 401-407.

Okawa, H., Della Santina, L., Schwartz, G.W., Rieke, F., and Wong, R.O. (2014). Interplay of cell-autonomous and nonautonomous mechanisms tailors synaptic connectivity of converging axons in vivo. Neuron *82*, 125-137.

Oyster, C.W. (1968). The analysis of image motion by the rabbit retina. J Physiol *199*, 613-635.

Oyster, C.W., and Barlow, H.B. (1967). Direction-selective units in rabbit retina: distribution of preferred directions. Science *155*, 841-842.

Ozaita, A., Petit-Jacques, J., Volgyi, B., Ho, C.S., Joho, R.H., Bloomfield, S.A., and Rudy, B. (2004). A unique role for Kv3 voltage-gated potassium channels in starburst amacrine cell signaling in mouse retina. The Journal of neuroscience : the official journal of the Society for Neuroscience *24*, 7335-7343.

Park, S.J., Kim, I.J., Looger, L.L., Demb, J.B., and Borghuis, B.G. (2014). Excitatory synaptic inputs to mouse on-off direction-selective retinal ganglion cells lack direction tuning. The Journal of neuroscience : the official journal of the Society for Neuroscience *34*, 3976-3981.

Parrish, J.Z., Kim, M.D., Jan, L.Y., and Jan, Y.N. (2006). Genome-wide analyses identify transcription factors required for proper morphogenesis of Drosophila sensory neuron dendrites. Genes & development *20*, 820-835.

Perry, V.H., and Linden, R. (1982). Evidence for dendritic competition in the developing retina. Nature *297*, 683-685.

Pfeffer, C.K., Xue, M., He, M., Huang, Z.J., and Scanziani, M. (2013). Inhibition of inhibition in visual cortex: the logic of connections between molecularly distinct interneurons. Nature neuroscience *16*, 1068-1076.

Poche, R.A., Raven, M.A., Kwan, K.M., Furuta, Y., Behringer, R.R., and Reese, B.E. (2008). Somal positioning and dendritic growth of horizontal cells are regulated by interactions with homotypic neighbors. The European journal of neuroscience *27*, 1607-1614.

Polleux, F., Morrow, T., and Ghosh, A. (2000). Semaphorin 3A is an chemoattractant for cortical apical dendrites. Nature *404*, 567-573.

Prasad, T., Wang, X., Gray, P.A., and Weiner, J.A. (2008). A differential developmental pattern of spinal interneuron apoptosis during synaptogenesis: insights from genetic analyses of the protocadherin-gamma gene cluster. Development *135*, 4153-4164.

Puram, S.V., and Bonni, A. (2013). Cell-intrinsic drivers of dendrite morphogenesis. Development *140*, 4657-4671.

Purves, D., and Lichtman, J.W. (1980). Elimination of synapses in the developing nervous system. Science *210*, 153-157.

Purves, D., Snider, W.D., and Voyvodic, J.T. (1988). Trophic regulation of nerve cell morphology and innervation in the autonomic nervous system. Nature *336*, 123-128.

Randlett, O., Poggi, L., Zolessi, F.R., and Harris, W.A. (2011). The oriented emergence of axons from retinal ganglion cells is directed by laminin contact in vivo. Neuron *70*, 266-280.

Redfern, P.A. (1970). Neuromuscular transmission in new-born rats. J Physiol *209*, 701-709.

Riccomagno, M.M., Sun, L.O., Brady, C.M., Alexandropoulos, K., Seo, S., Kurokawa, M., and Kolodkin, A.L. (2014). Cas adaptor proteins organize the retinal ganglion cell layer downstream of integrin signaling. Neuron *81*, 779-786.

Rieubland, S., Roth, A., and Hausser, M. (2014). Structured connectivity in cerebellar inhibitory networks. Neuron *81*, 913-929.

Rivlin-Etzion, M., Zhou, K., Wei, W., Elstrott, J., Nguyen, P.L., Barres, B.A., Huberman, A.D., and Feller, M.B. (2011). Transgenic mice reveal unexpected diversity of on-off direction-selective retinal ganglion cell subtypes and brain structures involved in motion processing. The Journal of neuroscience : the official journal of the Society for Neuroscience *31*, 8760-8769.

Rochefort, N.L., Narushima, M., Grienberger, C., Marandi, N., Hill, D.N., and Konnerth, A. (2011). Development of direction selectivity in mouse cortical neurons. Neuron *71*, 425-432.

Rodieck, R.W. (1991). The density recovery profile: A method for the analysis of points in the plane applicable to retinal studies. Visual neuroscience *6*, 95-111.

Rossi, J., Balthasar, N., Olson, D., Scott, M., Berglund, E., Lee, C.E., Choi, M.J., Lauzon, D., Lowell, B.B., and Elmquist, J.K. (2011). Melanocortin-4 receptors expressed by cholinergic neurons regulate energy balance and glucose homeostasis. Cell metabolism *13*, 195-204.

Rowan, S., and Cepko, C.L. (2004). Genetic analysis of the homeodomain transcription factor Chx10 in the retina using a novel multifunctional BAC transgenic mouse reporter. Developmental biology *271*, 388-402.

Rutlin, M., Ho, C.Y., Abraira, V.E., Cassidy, C., Bai, L., Woodbury, C.J., and Ginty, D.D. (2014). The cellular and molecular basis of direction selectivity of Adelta-LTMRs. Cell *159*, 1640-1651.

Sagasti, A., Guido, M.R., Raible, D.W., and Schier, A.F. (2005). Repulsive interactions shape the morphologies and functional arrangement of zebrafish peripheral sensory arbors. Current biology : CB *15*, 804-814.

Sander, J.D., and Joung, J.K. (2014). CRISPR-Cas systems for editing, regulating and targeting genomes. Nature biotechnology *32*, 347-355.

Sanes, J.R., and Yamagata, M. (2009). Many paths to synaptic specificity. Annu Rev Cell Dev Biol *25*, 161-195.

Sanes, J.R., and Zipursky, S.L. (2010). Design principles of insect and vertebrate visual systems. Neuron *66*, 15-36.

Sawaya, M.R., Wojtowicz, W.M., Andre, I., Qian, B., Wu, W., Baker, D., Eisenberg, D., and Zipursky, S.L. (2008). A double S shape provides the structural basis for the extraordinary binding specificity of Dscam isoforms. Cell *134*, 1007-1018.

Schmucker, D., Clemens, J.E., Shu, H., Worby, C.A., Xiao, J., and Zipursky, S.L. (2000). Drosophila Dscam is an axon guidance receptor exhibiting extraordinary molecular diversity. Cell *101*, 671-684.

Schreiner, D., and Weiner, J.A. (2010). Combinatorial homophilic interaction between gamma-protocadherin multimers greatly expands the molecular diversity of cell adhesion. Proceedings of the National Academy of Sciences of the United States of America *107*, 14893-14898.

Shen, W., Da Silva, J.S., He, H., and Cline, H.T. (2009). Type A GABA-receptor-dependent synaptic transmission sculpts dendritic arbor structure in Xenopus tadpoles in vivo. The Journal of neuroscience : the official journal of the Society for Neuroscience *29*, 5032-5043.

Simpson, J.I. (1984). The accessory optic system. Annual review of neuroscience *7*, 13-41.

Sivyer, B., and Williams, S.R. (2013). Direction selectivity is computed by active dendritic integration in retinal ganglion cells. Nature neuroscience *16*, 1848-1856.

Smith, C.J., Watson, J.D., VanHoven, M.K., Colon-Ramos, D.A., and Miller, D.M., 3rd (2012). Netrin (UNC-6) mediates dendritic self-avoidance. Nature neuroscience *15*, 731-737.

Smith, T.G., Lange, G.D., and Marks, W.B. (1996). Fractal methods and results in cellular morphology - dimensions, lacunarity, and multifractals. Journal of Neuroscience Methods *69*, 123-136.

Snider, W.D. (1988). Nerve growth factor enhances dendritic arborization of sympathetic ganglion cells in developing mammals. The Journal of neuroscience *8*, 2628-2634.

Soba, P., Zhu, S., Emoto, K., Younger, S., Yang, S.J., Yu, H.H., Lee, T., Jan, L.Y., and Jan, Y.N. (2007). Drosophila sensory neurons require Dscam for dendritic self-avoidance and proper dendritic field organization. Neuron *54*, 403-416.

Spruston, N. (2008). Pyramidal neurons: dendritic structure and synaptic integration. Nature reviews Neuroscience *9*, 206-221.

Srinivas, S., Goldberg, M.R., Watanabe, T., D'Agati, V., Al-Awqati, Q., and Constantini, F. (1999). Expression of green fluorescent protein in the ureteric bud of transgenic mice: A new tool for the analysis of ureteric bud morphogenesis. Developmental Genetics *24*, 241-251.

Stacy, R.C., and Wong, R.O. (2003). Developmental relationship between cholinergic amacrine cell processes and ganglion cell dendrites of the mouse retina. The Journal of comparative neurology *456*, 154-166.

Sugimura, K., Satoh, D., Estes, P., Crews, S., and Uemura, T. (2004). Development of morphological diversity of dendrites in Drosophila by the BTB-zinc finger protein abrupt. Neuron *43*, 809-822.

Sun, L.O., Jiang, Z., Rivlin-Etzion, M., Hand, R., Brady, C.M., Matsuoka, R.L., Yau, K.W., Feller, M.B., and Kolodkin, A.L. (2013). On and off retinal circuit assembly by divergent molecular mechanisms. Science *342*, 1241974.

Sweeney, L.B., Chou, Y.H., Wu, Z., Joo, W., Komiyama, T., Potter, C.J., Kolodkin, A.L., Garcia, K.C., and Luo, L. (2011). Secreted semaphorins from degenerating larval ORN axons direct adult projection neuron dendrite targeting. Neuron *72*, 734-747.

Tasic, B., Nabholz, C.E., Baldwin, K.K., Kim, Y., Rueckert, E.H., Ribich, S.A., Cramer, P., Wu, Q., Axel, R., and Maniatis, T. (2002). Promoter choice determines splice site selection in Protocadherin alpha and gamma pre-mRNA splicing. Molecular Cell *10*, 21-33.

Tauchi, M., and Masland, R.H. (1985). Local order among the dendrites of an amacrine cell population. The Journal of neuroscience *5*, 2494-2501.

Taylor, W.R., and Smith, R.G. (2012). The role of starburst amacrine cells in visual signal processing. Visual neuroscience *29*, 73-81.

Taylor, W.R., and Vaney, D.I. (2002). Diverse synaptic mechanisms generate direction selectivity in the rabbit retina. The Journal of neuroscience : the official journal of the Society for Neuroscience *22*, 7712-7720.

Taylor, W.R., and Wassle, H. (1995). Receptive field properties of starburst cholinergic amacrine cells in the rabbit retina. European Journal of Neuroscience *7*, 2308-2321.

Tessier-Lavigne, M., and Goodman, C.S. (1996). The molecular biology of axon guidance. Science *274*, 1123-1133.

Thu, C.A., Chen, W.V., Rubinstein, R., Chevee, M., Wolcott, H.N., Felsovalyi, K.O., Tapia, J.C., Shapiro, L., Honig, B., and Maniatis, T. (2014). Single-cell identity generated by combinatorial homophilic interactions between alpha, beta, and gamma protocadherins. Cell *158*, 1045-1059.

Toyoda, S., Kawaguchi, M., Kobayashi, T., Tarusawa, E., Toyama, T., Okano, M., Oda, M., Nakauchi, H., Yoshimura, Y., Sanbo, M.*, et al.* (2014). Developmental epigenetic modification regulates stochastic expression of clustered protocadherin genes, generating single neuron diversity. Neuron *82*, 94-108.

Trenholm, S., Johnson, K., Li, X., Smith, R.G., and Awatramani, G.B. (2011). Parallel mechanisms encode direction in the retina. Neuron *71*, 683-694.

Ulbrich, M.H., and Isacoff, E.Y. (2007). Subunit counting in membrane-bound proteins. Nature methods *4*, 319-321.

Ulbrich, M.H., and Isacoff, E.Y. (2008). Rules of engagement for NMDA receptor subunits. Proceedings of the National Academy of Sciences of the United States of America *105*, 14163-14168.

Vaney, D.I. (1984). 'Coronate' amacrine cells in the rabbit retina have the 'starburst' dendritic morphology. Proceedings of the Royal Society Series B-Biological Sciences *220*, 501-508.

Vaney, D.I., Peichl, L., and Boycott, B.B. (1981). Matching populations of amacrine cells in the inner nuclear and ganglion cell layers of the rabbit retina. The Journal of comparative neurology *199*, 373-391.

Vaney, D.I., and Pow, D.V. (2000). The dendritic architecture of the cholinergic plexus in the rabbit retina: selective labeling by glycine accumulation in the presence of sarcosine. The Journal of comparative neurology *421*, 1-13.

Vaney, D.I., Sivyer, B., and Taylor, W.R. (2012). Direction selectivity in the retina: symmetry and asymmetry in structure and function. Nature reviews Neuroscience *13*, 194-208.

Vetter, P., Roth, A., and Hausser, M. (2001). Propagation of action potentials in dendrites depends on dendritic morphology. Journal of neurophysiology *85*, 926-937.

Volgyi, B., Xin, D., Amarillo, Y., and Bloomfield, S.A. (2001). Morphology and physiology of the polyaxonal amacrine cells in the rabbit retina. The Journal of comparative neurology *440*, 109-125.

Wang, J., Ma, X., Yang, J.S., Zheng, X., Zugates, C.T., Lee, C.H., and Lee, T. (2004). Transmembrane/juxtamembrane domain-dependent Dscam distribution and function during mushroom body neuronal morphogenesis. Neuron *43*, 663-672.

Wang, J., Zugates, C.T., Liang, I.H., Lee, C.-H.J., and Lee, T. (2002a). Drosophila Dscam is required for divergent segregation of sister branches and suppresses ectopic bifurcation of axons. Neuron *33*, 559-571.

Wang, X., Su, H., and Bradley, A. (2002b). Molecular mechanisms governing Pcdh-gamma gene expression: Evidence for a multiple promoter and cis-alternative splicing model. Genome research *16*, 1890-1905.

Wang, X., Weiner, J.A., Levi, S., Craig, A.M., Bradley, A., and Sanes, J.R. (2002c). Gamma Protocadherins are required for survival of spinal interneurons. Neuron *36*, 843-854.

Wassle, H., Peichl, L., and Boycott, B.B. (1981). Dendritic territories of cat retinal ganglion cells. Nature *292*, 344-345.

Wassle, H., Puller, C., Muller, F., and Haverkamp, S. (2009). Cone contacts, mosaics, and territories of bipolar cells in the mouse retina. The Journal of neuroscience : the official journal of the Society for Neuroscience *29*, 106-117.

Wassle, H., and Riemann, H.J. (1978). Mosaics of nerve-cells in mammalian retina. Proceedings of the Royal Society Series B-Biological Sciences *200*, 441-461.

Wei, W., Hamby, A.M., Zhou, K., and Feller, M.B. (2011). Development of asymmetric inhibition underlying direction selectivity in the retina. Nature *469*, 402-406.

Weiner, J.A., Wang, X., Tapia, J.C., and Sanes, J.R. (2005). Gamma protocadherins are required for synaptic development in the spinal cord. Proceedings of the National Academy of Sciences of the United States of America *102*, 8-14.

Werblin, F.S. (2011). The retinal hypercircuit: a repeating synaptic interactive motif underlying visual function. J Physiol *589*, 3691-3702.

Werblin, F.S., and Dowling, J.E. (1969). Organization of the retina of the mudpuppy, Necturus maculosus. II. Intracellular recording. Journal of neurophysiology *32*, 339-355.

White, F.A., Keller-Peck, C.R., Knudson, C.M., Korsmeyer, S.J., and Snider, W.D. (1998). Widespread elimination of naturally occuring neuronal death in Bax-deficient mice. The Journal of neuroscience *18*, 1428-1439.

Whitney, I.E., Keeley, P.W., Raven, M.A., and Reese, B.E. (2008). Spatial patterning of cholinergic amacrine cells in the mouse retina. The Journal of comparative neurology *508*, 1-12.

Wojtowicz, W.M., Flanagan, J.J., Millard, S.S., Zipursky, S.L., and Clemens, J.C. (2004). Alternative splicing of Drosophila Dscam generates axon guidance receptors that exhibit isoform-specific homophilic binding. Cell *118*, 619-633.

Wojtowicz, W.M., Wu, W., Andre, I., Qian, B., Baker, D., and Zipursky, S.L. (2007). A vast repertoire of Dscam binding specificities arises from modular interactions of variable Ig domains. Cell *130*, 1134-1145.

Wolpert, D., Miall, R., and Kawato, M. (1998). Internal models in the cerebellum. Trends in Cognitive Science *2*, 338-347.

Wu, Q., and Maniatis, T. (1999). A striking organization of a large family of human neuron cadherin-like cell adhesion genes. Cell metabolism *97*, 779-790.

Wu, Q., Zhang, T., Cheng, J.-F., Kim, Y., Grimwood, J., Schmutz, J., Dickson, M., Noonan, J.P., Zhang, M.Q., Myers, R.M.*, et al.* (2001). Comparative DNA sequence analysis of mouse and human Protocadherin gene clusters. Genome research *11*, 389-404.

Wu, W., Ahlsen, G., Baker, D., Shapiro, L., and Zipursky, S.L. (2012). Complementary chimeric isoforms reveal Dscam1 binding specificity in vivo. Neuron *74*, 261-268.

Wu, Y., Helt, J.C., Wexler, E., Petrova, I.M., Noordermeer, J.N., Fradkin, L.G., and Hing, H. (2014). Wnt5 and drl/ryk gradients pattern the Drosophila olfactory dendritic map. The Journal of neuroscience : the official journal of the Society for Neuroscience *34*, 14961-14972.

Wyatt, H.J., and Daw, N.W. (1975). Directionally sensitive ganglion cells in the rabbit retina: specificity for stimulus direction, size, and speed. Journal of neurophysiology *38*, 613-626.

Xu, N.L., Harnett, M.T., Williams, S.R., Huber, D., O'Connor, D.H., Svoboda, K., and Magee, J.C. (2012). Nonlinear dendritic integration of sensory and motor input during an active sensing task. Nature *492*, 247-251.

Yamagata, M., and Sanes, J.R. (2008). Dscam and Sidekick proteins direct lamina-specific synaptic connections in vertebrate retina. Nature *451*, 465-469.

Yamagata, M., and Sanes, J.R. (2012a). Expanding the Ig superfamily code for laminar specificity in retina: expression and role of contactins. The Journal of neuroscience : the official journal of the Society for Neuroscience *32*, 14402-14414.

Yamagata, M., and Sanes, J.R. (2012b). Transgenic strategy for identifying synaptic connections in mice by fluorescence complementation (GRASP). Frontiers in molecular neuroscience *5*, 18.

Yamagata, M., Weiner, J.A., and Sanes, J.R. (2002). Sidekicks: Synaptic adhesion molecules that promote lamina-specific connectivity in the retina. Cell *110*, 649-660.

Yau, K.-W. (1976). Receptive fields, geometry and conduction block of sensory neurones in the central nervous system of the leech. Journal of physiology *263*, 513-538.

Yonehara, K., Balint, K., Noda, M., Nagel, G., Bamberg, E., and Roska, B. (2011). Spatially asymmetric reorganization of inhibition establishes a motion-sensitive circuit. Nature *469*, 407-410.

Yonehara, K., Farrow, K., Ghanem, A., Hillier, D., Balint, K., Teixeira, M., Juttner, J., Noda, M., Neve, R.L., Conzelmann, K.K.*, et al.* (2013). The first stage of cardinal direction selectivity is localized to the dendrites of retinal ganglion cells. Neuron *79*, 1078-1085.

Yonehara, K., Ishikane, H., Sakuta, H., Shintani, T., Nakamura-Yonehara, K., Kamiji, N.L., Usui, S., and Noda, M. (2009). Identification of retinal ganglion cells and their projections involved in central transmission of information about upward and downward image motion. PloS one *4*, e4320.

Yoshida, K., Watanabe, D., Ishikane, K., Tachibana, M., Pastan, I., and Nakanishi, S. (2001). A key role of starburst amacrine cells in originating retina directional selectivity and optokinetic eye movement. Neuron *30*, 771-780.

Zeisel, A., Muñoz-Manchado, A., Codeluppi, S., Lonnerberg, P., La Manno, G., Jureus, A., Marques, S., S, M., He, L., Betsholtz, C.*, et al.* (2015). Cell types in the mouse cortex and hippocampus revealedby sing-cell RNA-seq. Science *347*, 1138-1142.

Zhan, X.L., Clemens, J.C., Neves, G., Hattori, D., Flanagan, J.J., Hummel, T., Vasconcelos, M.L., Chess, A., and Zipursky, S.L. (2004). Analysis of Dscam diversity in regulating axon guidance in Drosophila mushroom bodies. Neuron *43*, 673-686.

Zhang, X.M., Ng, A.H., Tanner, J.A., Wu, W.T., Copeland, N.G., Jenkins, N.A., and Huang, J.D. (2004). Highly restricted expression of Cre recombinase in cerebellar Purkinje cells. Genesis *40*, 45-51.

Zheng, J., Lee, S., and Zhou, Z.J. (2006). A transient network of intrinsically bursting starburst cells underlies the generation of retinal waves. Nature neuroscience *9*, 363-371.

Zheng, J.J., Lee, S., and Zhou, Z.J. (2004). A developmental switch in the excitability and function of the starburst network in the mammalian retina. Neuron *44*, 851-864.

Zheng, Y., Wildonger, J., Ye, B., Zhang, Y., Kita, A., Younger, S.H., Zimmerman, S., Jan, L.Y., and Jan, Y.N. (2008). Dynein is required for polarized dendritic transport and uniform microtubule orientation in axons. Nature cell biology *10*, 1172-1180.

Zipursky, S.L., and Grueber, W.B. (2013). The molecular basis of self-avoidance. Annual review of neuroscience *36*, 547-568.

Zipursky, S.L., and Sanes, J.R. (2010). Chemoaffinity revisited: dscams, protocadherins, and neural circuit assembly. Cell *143*, 343-353.

Zolessi, F.R., Poggi, L., Wilkinson, C.J., Chien, C.-B., and Harris, W.A. (2006). Polarization and orientation of retinal ganglion cells in vivo. Neural development *1*.